Reviews of Geophysics

REVIEW ARTICLE
10.1029/2019RG000663

The Sensitivity of the Antarctic Ice Sheet to a Changing Climate: Past, Present, and Future

T. L. Noble[1], E. J. Rohling[2,3], A. R. A. Aitken[4], H. C. Bostock[5], Z. Chase[1], N. Gomez[6], L. M. Jong[7,8], M. A. King[9], A. N. Mackintosh[10], F. S. McCormack[10], R. M. McKay[11], L. Menviel[12], S. J. Phipps[1], M. E. Weber[13], C. J. Fogwill[14], B. Gayen[15], N. R. Golledge[11], D. E. Gwyther[1], A. McC. Hogg[2,16], Y. M. Martos[17,18], B. Pena-Molino[8,19], J. Roberts[7,8], T. van de Flierdt[20], and T. Williams[21]

[1]Institute for Marine and Antarctic Studies, University of Tasmania, Hobart, Tasmania, Australia, [2]Research School of Earth Sciences, Australian National University, Canberra, ACT, Australia, [3]Ocean and Earth Science, University of Southampton, National Oceanography Centre, Southampton, UK, [4]School of Earth Sciences, University of Western Australia, Perth, Western Australia, Australia, [5]School of Earth and Environmental Sciences, University of Queensland, Brisbane, Queensland, Australia, [6]Department of Earth and Planetary Sciences, McGill University, Montreal, Quebec, Canada, [7]Australian Antarctic Division, Department of Agriculture, Water and Environment, Kingston, Tasmania, Australia, [8]Australian Antarctic Program Partnership, Institute of Marine and Antarctic Studies, University of Tasmania, Hobart, Tasmania, Australia, [9]School of Technology, Environments and Design, University of Tasmania, Hobart, Tasmania, Australia, [10]School of Earth, Atmosphere and Environment, Monash University, Melbourne, Victoria, Australia, [11]Antarctic Research Centre, Victoria University of Wellington, Wellington, New Zealand, [12]Climate Change Research Centre, PANGEA, University of New South Wales, Sydney, New South Wales, Australia, [13]Steinmann Institute, University of Bonn, Bonn, Germany, [14]Geography, Geology and the Environment, Keele University, Staffordshire, UK, [15]Department of Mechanical Engineering, University of Melbourne, Melbourne, Victoria, Australia, [16]ARC Centre of Excellence for Climate System Science, Sydney, New South Wales, Australia, [17]Department of Astronomy, University of Maryland, College Park, MD, USA, [18]Planetary Magnetospheres Laboratory, NASA Goddard Space Flight Center, Greenbelt, MD, USA, [19]Ocean and Atmosphere, Commonwealth Scientific and Industrial Research Organization, Hobart, Tasmania, Australia, [20]Department of Earth Science and Engineering, Imperial College London, London, UK, [21]International Ocean Discovery Program, Texas A&M University, College Station, TX, USA

Key Points:
- The AIS is a highly dynamic component of the Earth system, evolving on a broad range of temporal and spatial scales
- Paleoenvironmental evidence highlights the centennial to millennial response time scales of the AIS to atmospheric-ocean forcing
- Coupling feedbacks in Earth system components are required to reduce the uncertainty in AIS's contribution to past and future sea level rise

Correspondence to:
T. L. Noble,
taryn.noble@utas.edu.au

Citation:
Noble, T. L., Rohling, E. J., Aitken, A. R. A., Bostock, H. C., Chase, Z., Gomez, N., et al. (2020). The Sensitivity of the Antarctic Ice Sheet to a Changing Climate: Past, Present, and Future. *Reviews of Geophysics*, *58*, e2019RG000663. https://doi.org/10.1029/2019RG000663

Received 21 JUN 2019
Accepted 11 AUG 2020
Accepted article online 15 AUG 2020

©2020. The Authors.
This is an open access article under the terms of the Creative Commons Attribution License, which permits use, distribution and reproduction in any medium, provided the original work is properly cited.

Abstract The Antarctic Ice Sheet (AIS) is out of equilibrium with the current anthropogenic-enhanced climate forcing. Paleoenvironmental records and ice sheet models reveal that the AIS has been tightly coupled to the climate system during the past and indicate the potential for accelerated and sustained Antarctic ice mass loss into the future. Modern observations by contrast suggest that the AIS has only just started to respond to climate change in recent decades. The maximum projected sea level contribution from Antarctica to 2100 has increased significantly since the Intergovernmental Panel on Climate Change (IPCC) 5th Assessment Report, although estimates continue to evolve with new observational and theoretical advances. This review brings together recent literature highlighting the progress made on the known processes and feedbacks that influence the stability of the AIS. Reducing the uncertainty in the magnitude and timing of the future sea level response to AIS change requires a multidisciplinary approach that integrates knowledge of the interactions between the ice sheet, solid Earth, atmosphere, and ocean systems and across time scales of days to millennia. We start by reviewing the processes affecting AIS mass change, from atmospheric and oceanic processes acting on short time scales (days to decades), through to ice processes acting on intermediate time scales (decades to centuries) and the response to solid Earth interactions over longer time scales (decades to millennia). We then review the evidence of AIS changes from the Pliocene to the present and consider the projections of global sea level rise and their consequences. We highlight priority research areas required to improve our understanding of the processes and feedbacks governing AIS change.

Plain Language Summary The Antarctic Ice Sheet (AIS) is an important component of the global climate system. Human activities have caused the atmosphere and especially the oceans to warm. However, the full effect of human caused climate change on the AIS has not currently been realized because the ice sheet responds on a range of time scales and to many different Earth processes. Modern observations show that West Antarctica has been melting at an accelerating rate since the 2000s, while the data for East Antarctica are less clear. Environmental records preserve the history of the climate

and AIS, which extend beyond the instrumental record and reveal how the AIS responded to past climate warming. Estimates of how much the AIS will contribute to sea level rise by the Year 2100 have changed as a result of new information on how the AIS evolved in the past and research into the interactions between the ice sheet, solid Earth atmosphere, and ocean systems. This review brings together our knowledge of the major processes and feedbacks affecting the AIS and the evidence for how the ice sheet changed since the Pliocene. We consider the future estimates and consequences of global sea level rise from melting of the AIS and highlight priority research areas.

1. Introduction and Motivation

The Antarctic Ice Sheet (AIS) is the largest potential source of and most uncertain contributor to global sea level rise (Oppenheimer et al., 2019). The marine-based sectors of Antarctica, meaning the portion of the AIS that lies below global mean sea level (GMSL), contain enough fresh water to raise GMSL by approximately 25 m (BEDMAP 2: Fretwell et al., 2013, Figure 1). The response of the AIS to anthropogenic climate warming in terms of the time scales of ice loss and where the ice loss occurs will depend on the extent of climate warming and interactions between the ice sheet and the atmosphere, ocean, and the solid Earth.

Observations during the satellite era show the AIS have been losing mass at an accelerating rate (Rignot et al., 2019). Continent-wide observations show a net acceleration of grounding line retreat between 2010 and 2016, driven by ice shelf thinning (Konrad et al., 2018). Differences in ice discharge from glaciers have been observed between West and East Antarctica. Mass loss of -214 ± 51 Gt yr^{-1} (2008–2015; Gardner et al., 2018) in the West Antarctic Ice Sheet (WAIS) has been driven predominantly by ocean-forced ice shelf melt in the Amundsen and Bellingshausen Sea sectors (Turner et al., 2017). Ice mass loss from WAIS has dramatically increased over the past two decades (Rignot et al., 2019; Shepherd et al., 2019). Increased ice velocity and glacier terminus retreat have been observed for outflows of the East Antarctic Ice Sheet (EAIS) in Wilkes Land, in response to warming ocean temperatures (Li et al., 2016; Miles et al., 2016; Shen et al., 2018). However, EAIS mass change has been difficult to quantify and remains uncertain. For example, previous assessments have suggested that the EAIS has remained close to mass balance through increased snow accumulation (Boening et al., 2012; King et al., 2012; The IMBIE Team et al., 2018), but the large uncertainty on these estimates has made it difficult to determine whether the EAIS has lost or gained mass (Gardner et al., 2018; Rignot et al., 2019; The IMBIE Team et al., 2018).

Uncertainties in the future contribution of the AIS to sea level rise are associated with unknowns in future climate change and in the processes and feedbacks governing the response of the AIS to warming of the atmosphere and ocean (Bamber et al., 2019; Nowicki & Seroussi, 2018; Schlegel et al., 2018). The Intergovernmental Panel on Climate Change (IPCC) Fifth Assessment Report (AR5) estimated that the AIS is likely to contribute only −0.08 to 0.14 m to sea level rise by 2100, even under the most extreme emissions scenario (Church et al., 2013), where projected ice mass loss is compensated by surface mass gains in the EAIS. Further assessments of global and regional sea level projections to 2100 have since been developed based on new ice dynamic feedbacks not explicitly considered in the IPCC AR5. For example, atmospheric-driven melting that causes hydrofracturing and leads to ice cliff failure has been proposed as a mechanism for triggering major, rapid mass loss from the AIS. A model incorporating ice cliff failure estimated an Antarctic contribution to global sea level rise of 1.05 ± 0.30 m by 2100 under the high-end Representative Concentration Pathway 8.5 (RCP8.5) climate scenario, increasing to 15.65 ± 2.00 m by 2500 (DeConto & Pollard, 2016). However, this mechanism has not been directly observed in polar ice sheets and glaciers. Edwards et al. (2019) revisited the projections of DeConto and Pollard (2016) and explored the uncertainties in ice sheet model projections of sea level rise to 2100. They suggested that under the RCP8.5 scenario the AIS is most likely to contribute 0.45 m to global sea level rise if the mechanism of DeConto and Pollard (2016) is true, but only 0.15 m otherwise. The expert judgment assessment of Bamber et al. (2019) for a high-temperature scenario, estimated "likely" (17–83%) sea level contributions of 0.03 to 0.46 m from WAIS and −0.04 to 0.11 m from EAIS by 2100, increasing to 0.07 to 2.28 m (WAIS) and −0.14 to 0.51 m (EAIS) by 2300.

Observations and modeling evidence indicates that the AIS can respond to disequilibria between the ice sheet and the atmosphere, ocean, and solid Earth on a range of time scales; from hours to decades (e.g.,

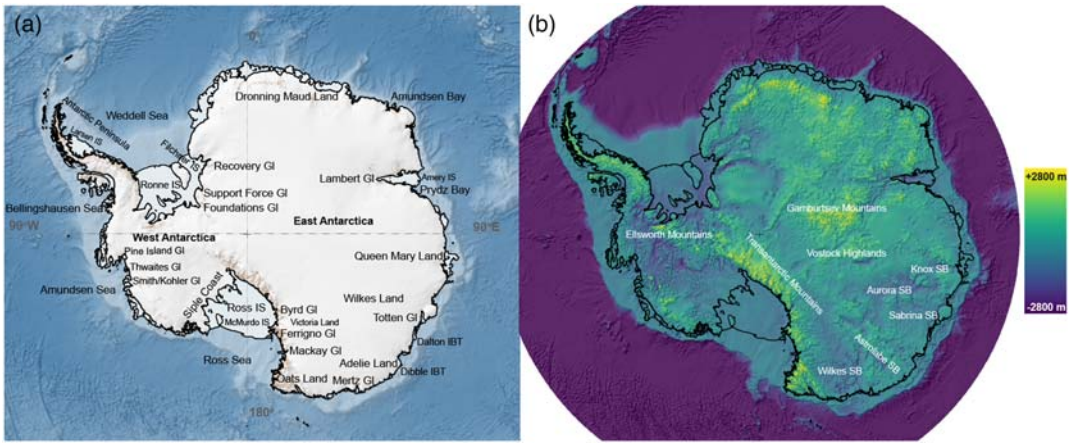


Figure 1. Map of Antarctica showing (a) the regions, glaciers (Gl), ice shelves (IS), and iceberg tongues (IBT) mentioned in the text and (b) the subglacial basins (SB) and mountainous features of the Antarctic continent (BEDMAP 2; Fretwell et al., 2013). Note that the Antarctic Peninsula is geographically and geologically part of West Antarctica, but the Antarctic Peninsula Ice Sheet is glaciologically distinct from the WAIS. Source: Quantarctica and the Norwegian Polar Institute.

Padman et al., 2018) and hundreds (MacAyeal, 1992a) to thousands of years (Warrick & Oerlemans, 1990). The need to develop a better understanding of AIS sensitivity to climate forcing is driving multidisciplinary research, as noted by the many recent publications on feedbacks with sea level and the solid Earth (e.g., de Boer et al., 2017; Whitehouse et al., 2019) and evolution of continental shelf bathymetry (Colleoni et al., 2018). Other recent reviews have focused on the processes governing AIS stability and ice sheet dynamic processes, including the role of ice shelf buttressing and marine ice sheet instability (MISI) (e.g., Pattyn, 2018; Pattyn et al., 2017). Sea ice (see Hobbs et al., 2016) and ice shelves have been shown to provide stability to the past and present AIS through buttressing (Hughes et al., 2017) and through dampening ocean swell (Massom et al., 2018). The role of ocean processes on AIS stability has also been reviewed. This includes ice shelf-ocean processes (Galton-Fenzi et al., 2016; Rintoul, 2018) and the influence of the Antarctic Slope Current on ocean heat flux to the Antarctic margin (Thompson et al., 2018), processes driving ice retreat in the Amundsen Sea Sector (Turner et al., 2017), and the role of tides (Padman et al., 2018), in ice sheet mass balance and dynamics.

We focus on new knowledge from the past 5 years, identifying gaps and priorities for future research. The paper is structured as follows: in section 2 new insights into AIS-Southern Ocean interactions are discussed, in particular the mechanism for oceanic heat transport to the Antarctic margin. In section 3, we highlight the ice dynamical processes governing the AIS response to the climate and solid Earth. In section 4, we review the current understanding of solid Earth interactions and processes over a range of time scales that affect the ice sheet directly or indirectly. Evidence for ice sheet changes from the observational record for the present climate-AIS state, and times in the past are reviewed in section 5. Finally, in section 6, the consequences of a more dynamic AIS are discussed in terms of our current understanding of sea level and wider effects on Southern Ocean and global climate processes.

An interdisciplinary perspective of AIS change is required if we are to make progress in Antarctic research (Figure 2). The motivation of this review was to provide a resource to engage and bring together the different fields of Antarctic science and thereby improve our understanding of the science and gaps in our knowledge. A summary is presented of the current knowledge about processes that govern AIS stability across the range of disciplines included in this review, and we offer a list of research priorities for understanding AIS behavior and hence for reducing uncertainty in its response to, and role in, future climate perturbations.

2. Ice-Ocean-Atmosphere Interactions

The atmosphere and ocean act together to induce changes in the AIS. Understanding how these systems interact and the associated feedbacks that arise from the AIS are key to quantifying the nature and time scales of the ice sheet response to a changing climate. Atmosphere and ocean processes impacting the ice sheet are expressed differently in East and West Antarctica. Variability in atmospheric circulation has

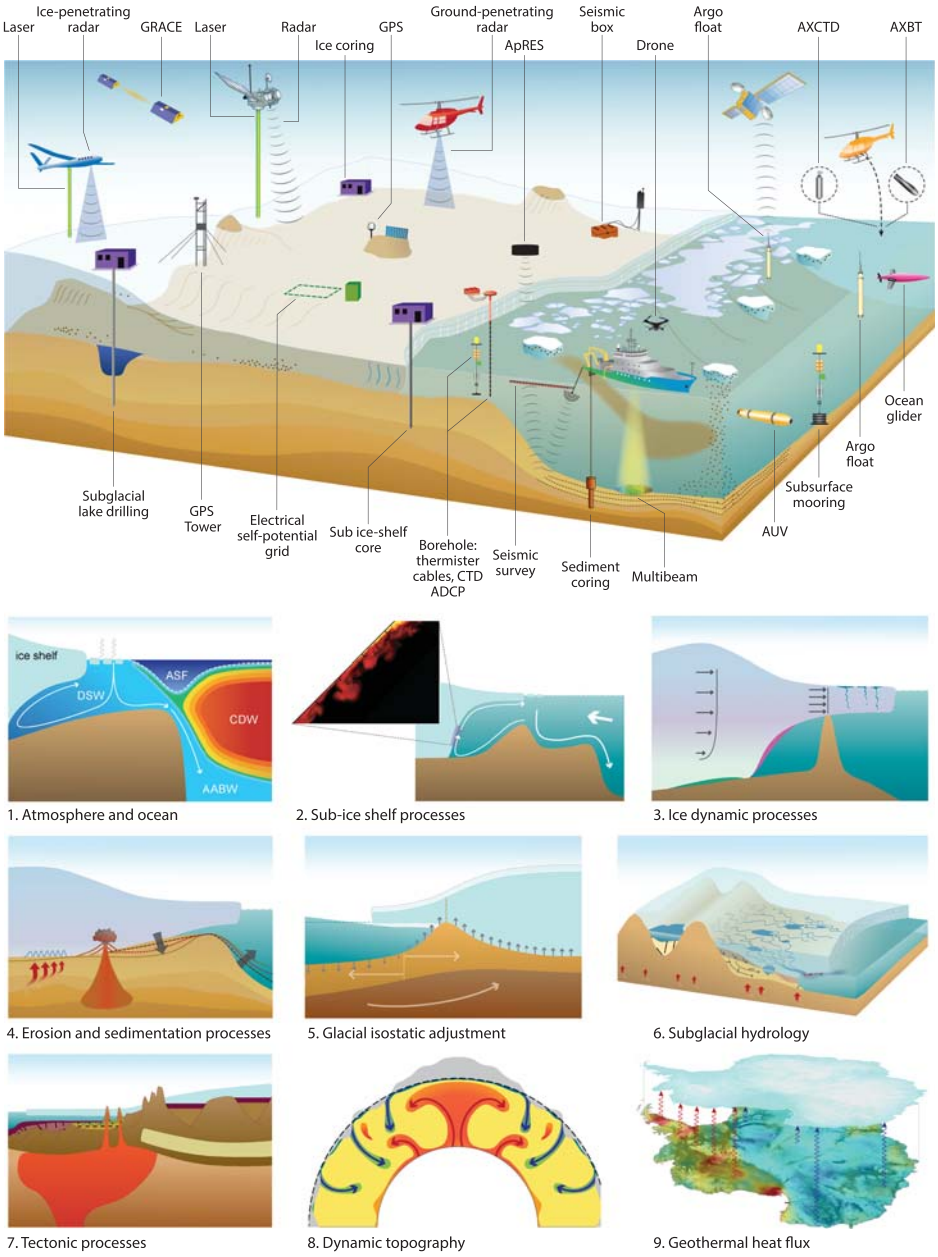


Figure 2. The upper panel shows current available methods for observations on the ice and in the ocean. ApRes: Autonomous Phase-Sensitive Radio echosounder can be mounted on aircraft or pulled by a snowmobile; AXCTD: Airborne eXpendable Conductivity Temperature Depth probe; ADCP: acoustic Doppler current profiler; AXBT: Airborne EXpendable BathyThermograph. The lower multipanels show an overview of the processes and feedbacks discussed in this review that affect AIS dynamics. Our understanding of these processes is underpinned by direct observations of the atmosphere, ocean, ice sheet, and solid Earth and the past reconstructions from ice, sub-ice, and marine sediment cores.

contributed to an increase in the mass loss of the WAIS (section 2.1). For both EAIS and WAIS, mass loss has been enhanced by intrusions of relatively warm water onto the Antarctic continental shelf (section 2.2), driven by changes in ocean currents, tides, and variability in surface winds and by feedbacks associated with increased freshwater flux around the Antarctic margin. The global oceans have absorbed 90% of the excess heat resulting from anthropogenic emissions, with 75 ± 22% heat uptake occurring in the Southern Ocean (Frölicher et al., 2015). Understanding how this heat is redistributed and the resulting changes in ocean circulation will impact on projections of sea level change.

2.1. Atmospheric Processes Driving AIS Mass Changes

The AIS mass balance is driven by atmospheric circulation, via its effects on near-surface air temperature and precipitation (and therefore snowfall and surface melt), and particularly through its influence on ocean forcing. The major climate drivers of atmospheric conditions include teleconnection modes such as the Southern Annular Mode (SAM), Pacific Decadal Oscillation (PDO), and El Niño–Southern Oscillation (ENSO) and the presence and strength of low-pressure systems such as the Amundsen Sea Low. These low-frequency coupled ocean-atmosphere interactions have a range of impacts, including altering rates of snowfall, air temperatures, and sea ice conditions and extent. Changes to surface wind patterns can also alter the degree of upwelling of relatively warm deep-water masses, such as Circumpolar Deep Water (CDW) and, as a result, melting of the underside of floating glacier ice.

SAM is a measure of the pressure gradient between the middle and high latitudes and describes the north-south position and strength of westerly winds circling Antarctica. A positive phase indicates a negative high-latitude and positive midlatitude pressure gradient, which leads to a southward shift in the storm tracks toward the Antarctica and a strengthening of the westerly winds (Thompson et al., 2000). Stronger and poleward shifted westerlies (positive SAM) have caused enhanced precipitation across much of West Antarctica and in the western Antarctic Peninsula over the past 50 years (Goodwin et al., 2016). However, the enhanced westerly winds cause an orographic "precipitation shadow" on the eastern side of the Antarctic Peninsula and reduce the relatively small amounts of precipitation over East Antarctica (Marshall et al., 2017). Ice core records reveal the complex relationship between SAM and other climate oscillators (e.g., PDO) in multidecadal analyses (Goodwin et al., 2016). Over the past millennia ice core records show that SAM has evolved toward a more positive state since CE 1480 (Abram et al., 2014; Dätwyler et al., 2018). This intensified and poleward-shifted atmospheric circulation likely results from a combination of stratospheric ozone depletion and increased greenhouse gas concentrations (Arblaster et al., 2014). In Dronning Maud Land, increased accumulation between 2009 and 2011 was driven by anomalous large-scale atmospheric conditions that enhanced the poleward transport of moisture via atmospheric rivers, long narrow bands of enhanced water vapor that stretched from subtropical latitudes to the Antarctic coast (Gorodetskaya et al., 2014). Although ice core records indicate that such accumulation events have occurred previously, climate models show that they are increasingly likely in a warming climate (Lenaerts et al., 2013).

There is mounting evidence that ENSO drives Antarctic mass balance changes primarily via its influence on ocean heat transport. Variability in ENSO has been linked to interannual variations in ice shelf melt rates at a regional scale (Paolo et al., 2018). Prevailing La Niña conditions in 2011 resulted in reduced rates of sub ice shelf melting at Pine Island Glacier (Dutrieux et al., 2014). A strong El Niño in the 1940s may have triggered the twentieth century retreat of Pine Island Glacier (Smith, Andersen, et al., 2017). Similarly, the warming trend observed over West Antarctica (Schneider & Steig, 2008; Steig et al., 2013) is likely linked to natural variability associated with high-latitude teleconnections from the ENSO (Smith & Polvani, 2017). A surface melt event in 2016 over the Ross Ice Shelf and extending to more than 1,000 m above sea level in West Antarctica was also likely favored by prevailing El Niño conditions (Nicolas et al., 2017). The linkage between ENSO and mass balance in West Antarctica occurs either directly via wind forcing of ocean currents and/or indirectly via effects on polynya formation and sea ice (St-Laurent et al., 2015; Webber et al., 2017).

Internal variability of the regional atmospheric circulation has a profound influence on Antarctic climate, primarily by affecting the distribution and strength of cyclones and anticyclones around the continent (e.g., Raphael, 2004). For example, the warming trend on the Antarctic Peninsula from the mid-1950s to the late 1990s (Turner et al., 2005) has now reversed, likely due to stronger cyclonic conditions in the northern Weddell Sea, bringing temperature trends on the Peninsula within bounds of natural variability (Turner et al., 2016). Given the large magnitude of natural variability, long observational periods are required to establish true statistical significance in interannual to decadal variability (Stevenson et al., 2010). However, recent modeling and observations of Holland et al. (2019) have shown how the regional retreat of glaciers and melting of ice shelves in the Amundsen Sea can be attributed to anthropogenic forcing (e.g., greenhouse gas increase). Their results demonstrated that increasing twentieth century anthropogenic greenhouse gases changed the shelf break winds in the Amundsen Sea, resulting in increased ice loss induced by enhanced ocean forcing.

Future projection experiments performed with CMIP5 models suggest that increased greenhouse gas content over the coming century could lead to a positive trend in the SAM (Zheng et al., 2013). Improved estimates of future changes in near-Antarctic winds, and their intrinsic variability, is a high priority for predicting heat fluxes onto the continental shelf, especially in the Amundsen-Bellingshausen sector, as well as studies on more extreme ENSO events (Cai et al., 2015) on Antarctic shelf subsurface temperatures.

2.2. Oceanic Processes Driving AIS Changes

Oceanic processes that drive changes to the floating parts of the AIS influence its evolution predominantly through changes in buttressing (De Angelis & Skvarca, 2003; Dupont & Alley, 2005a; Gudmundsson, 2013) (section 3.1.1). The ice shelves that have grounding lines below sea level are vulnerable to ocean forcing and MISI (section 3.1.2). Ocean-driven ice shelf mass loss has long been known to occur primarily through melting at the underside of ice shelves (~67%), but recent observations of iceberg calving have shown that this process also contributes significantly to mass loss (Depoorter et al., 2013; Liu et al., 2015; Rignot et al., 2013). Over the last decade, evidence for a significant role of intrusions of relatively warm CDW in driving sub-ice shelf melting of the AIS has increased (e.g., A. J. Cook et al., 2016; Dutrieux et al., 2014; Jacobs et al., 2011; Pritchard et al., 2012; Rintoul et al., 2016; Silvano et al., 2018). However, as the observational record grows it has become evident that the processes that allow this warm water to be delivered to the ice shelf vary in space and time. Additional observations and modeling studies are required to better understand the processes leading to CDW intrusions on the Antarctic shelf and to quantify their impact on slow and rapid changes in ice sheet evolution. In this section, CDW is used sensu lato; that is, CDW comprises the CDW sensu stricto, as well as all the deep-water masses that derive from it such as modified CDW (mCDW), and Warm Deep Water in the Weddell Sea (Nicholls et al., 2009; Vernet et al., 2019). Processes driving melt include those that deliver warmer offshore water onto the continental shelf (section 2.2.1), interaction of warmer water with ice shelves and icebergs (section 2.2.2), and microscale dynamics of sub-ice shelf melting (Jenkins et al., 2016; Schmidtko et al., 2014) (section 2.2.3).

2.2.1. Processes Across the Shelf Break: Winds, Eddies, and Waves

Ocean processes can significantly impact the AIS by transporting heat to the Antarctic coastline and so control the magnitude and distribution of basal melting under ice shelves. Factors involved in controlling the oceanic heat supply across the continental shelf to the AIS include (1) the topography of the continental shelf and slope (St-Laurent et al., 2013), (2) the presence and location of the Antarctic Slope Front (ASF) (Schmidtko et al., 2014), (3) the micromesoscale eddy field (Stewart & Thompson, 2015), and (4) atmospheric processes relating to changes in the strength and position of the westerly winds (Heywood et al., 2016; Jenkins et al., 2016). In areas where the clockwise Antarctic Circumpolar Current (ACC) takes a southerly path and comes close to the continental shelf, warmer off-shelf water such as CDW is more readily available, transferring heat across the continental slope (Figure 3). However, the combination of the continental slope, the ASF, and its associated westward current provides a barrier to heat transport around much of the continent. Where the ASF is weak (e.g., Amundsen Sea, West Antarctic Peninsula; Whitworth II et al.,1998; Thompson et al., 2018), this barrier is less effective and heat can more easily access the continental shelf (Schmidtko et al., 2014) (Figure 3b). But even where a strong ASF is present, the barrier is broken in key locations by processes such as eddy transport, overturning circulation and changes in the position and strength of the westerly winds. Once on the continental shelf the effect of the heat input by CDW transport is primarily controlled by the salinity budget. The balance between sea ice formation and melt, precipitation minus evaporation (E − P), lateral advection and freshwater input from melting ice shelves controls the stratification and the buoyancy-driven circulation, which in turn regulates the amount of heat that is available to further promote melting of ice shelves. While the notion that oceanic heat supply across the continental shelf drives AIS melt is well known (Jacobs et al., 1996), new research has been defining what these processes are, and their relative contribution to cross-shelf heat transport.

Foremost among these processes is the role of mesoscale eddies (size of order 4 to 40 km) in transporting warm and saline CDW from the open Southern Ocean onto the Antarctic continental shelf (Heywood et al., 2016; Stewart & Thompson, 2013). These eddies are relatively small on the Antarctic continental shelf, due to the combination of a strong Coriolis parameter and weak stratification, meaning that most regular ocean models are unable to resolve the eddy fluxes (Stewart & Thompson, 2013). However, the increase in computing power over the last decade has allowed for eddy resolving simulations to be run

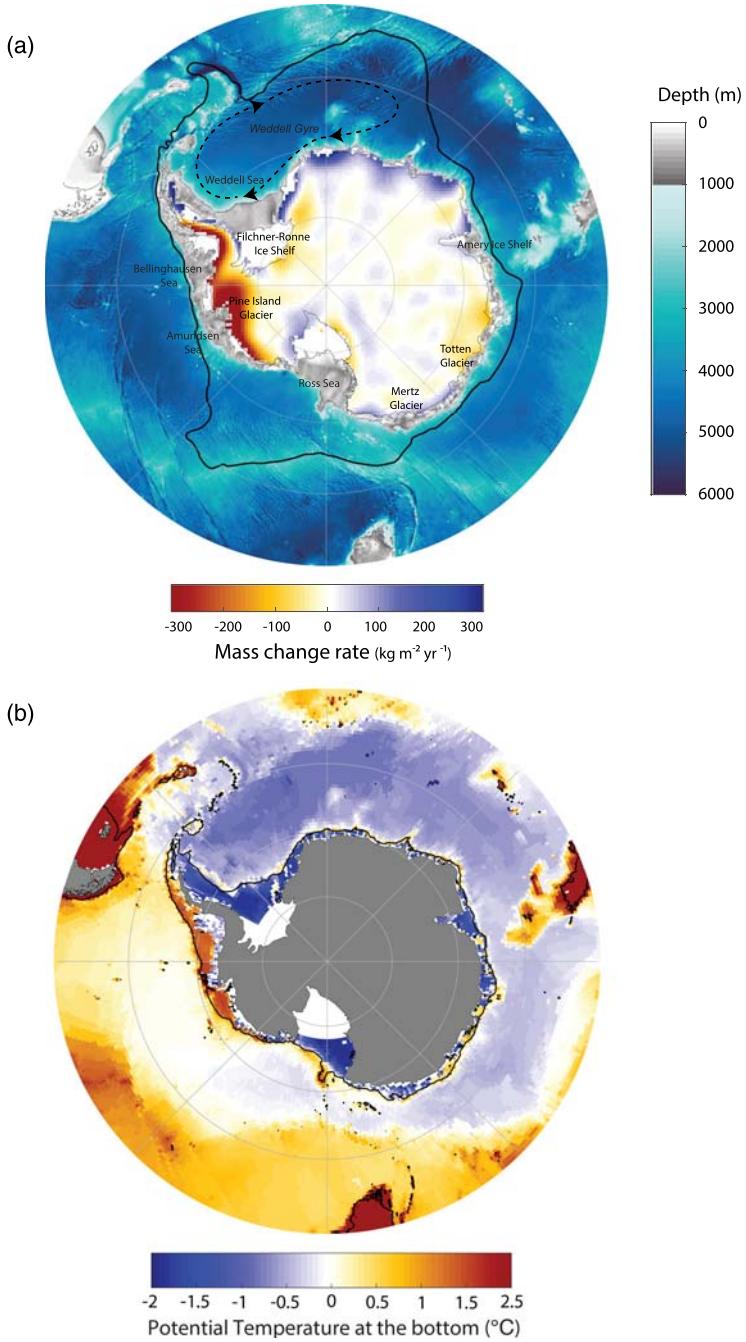


Figure 3. The connection between Antarctic ice mass loss and ocean forcing. (a) The black line shows the southern boundary of the ACC defined as the southernmost extent of the upper CDW. Gravimetric Mass Balance data for 2002–2016 shows ice mass changes across the continent (Groh et al., 2019), which is highest in West Antarctica where the Antarctic continental shelf and southern boundary of the ACC are in close proximity. (b) Map of the Southern Ocean bottom potential temperature highlights the presences of warmer waters along the West Antarctic margin, based on the WOCE global hydrographic climatology. The black line shows the 1,000 m bathymetry contour.

(e.g., Mack et al., 2019), even over regions as large as the Southern Ocean. Variations in topography are known to localize eddy fluxes (Couto et al., 2017; Moffat et al., 2009). Recent modeling work suggests that both eddies and tides are important for cross-slope heat transport, where eddy heat flux is the dominant driver of heat transport, and this is modulated by tides and wind-driven Ekman transport (Stewart

et al., 2018). More observations and high-resolution circum-Antarctic models are required to constrain uncertainty in the exact processes that move heat on to the shelf and the magnitude of their impact.

The cross-shelf transport of heat may also be related to the larger-scale ocean overturning circulation through the formation of Antarctic Bottom Water (AABW). AABW is one of the main water masses that comprise the global meridional overturning circulation (MOC) and is derived from dense shelf water (DSW) that is formed on the Antarctic continental shelf by brine rejection. During sea ice formation, brine rejection increases the density of very cold near-surface shelf waters, which sink and form DSW. This dense water flows off the continental shelf, then sinks along the continental slope, mixing with ambient waters, and is subsequently exported northward as AABW at the bottom of the Pacific and Atlantic basins (Orsi et al., 1999; Van Sebille et al., 2013). In the Weddell Sea, sea ice formation over the continental shelf leads to the formation of High Salinity Shelf Water (HSSW). In austral winter, the HSSW flows beneath the Filchner-Ronne Ice-Shelf, and because of the greater pressure at depth, HSSW melts the ice beneath the ice shelf and produces Ice Shelf Water (ISW). The HSSW and ISW then flow down the continental slope to produce an AABW precursor (Nicholls & Østerhus, 2004). A variety of processes can facilitate or inhibit relatively warm CDW incursions onto the shelf, which in turn influence the rate of DSW production and thus AABW formation. A reduction in AABW formation has been shown through modeling experiments to lead to decreases in the oceanic meridional heat transport to high southern latitudes, increased stratification, and ultimately increased warming in the subsurface ocean (Menviel et al., 2010) that can potentially drive increased sub-ice shelf melting of the AIS (Golledge et al., 2014). The feedbacks associated with AIS meltwater-driven suppression of AABW formation, as a consequence of AIS melt to the ocean, are reviewed in section 6.2.

A negative feedback mechanism relating to cross-shelf heat transport has been proposed by modeling work that resolves DSW formation on the Antarctic shelf (Snow et al., 2016). The negative feedback mechanism is based on the balance between off-shelf dense water transport and on-shelf flux, which is composed of fresh cold AABW and warm saline CDW, respectively. In the model configured by Snow, Hogg, et al. (2016), reductions in DSW formation and export were balanced by reduced on-shelf transport of CDW. However, improved understanding of the interaction between DSW formation and CDW incursions is required. This should be addressed in the coming years by gathering observational data and by performing sensitivity experiments using high-resolution ocean/sea ice models.

The strength and position of the southern hemispheric westerly and/or easterly winds can also impact heat transport to the shelf through their influence on the oceanic circulation changes and influence subsurface temperatures on the Antarctic shelf. Large-scale wind forcing affects the amount of heat available on the shelf through changes in thermocline depth that modulate access of CDW onto the shelf (Dutrieux et al., 2014; Galton-Fenzi et al., 2016; Jacobs et al., 2013; Schmidtko et al., 2014; Spence et al., 2014). At smaller scales, reductions in easterly wind stress near the Antarctic coastline act to alter the sea surface height, with internal adjustments transporting heat onto the shelf (Spence et al., 2014). This process is an expression of wider influences, with East Antarctic wind perturbations focusing their activity onto the western side of the Antarctic Peninsula via barotropic Kelvin waves (Spence et al., 2017), due to the steep bathymetry and strong offshore temperature gradients at that location. Overall, the complex interactions between eddies, topographic variations, winds, and dense water formation each act to modify the balance of heat flux onto the Antarctic shelf. Given the potential importance of these interactions in the future, such processes require urgent research to improve projections of AIS variability.

2.2.2. Processes Influencing the Heat Content Beneath Ice Shelves

Ice shelves around Antarctica can be broadly classified into two types (Jacobs et al., 1992): cold cavity ice shelves, which are characterized by considerable areas with basal freeze-on of marine ice, such as the Ross Ice Shelf and Filchner-Ronne Ice Shelf, and warm cavity ice shelves, where little or no DSW is formed and CDW is ubiquitous across the shelf, such as Pine Island Glacier Ice Shelf, and the West Antarctic Peninsula ice shelves (e.g., Bernales et al., 2017) (Figure 4). While sub-ice shelf melting occurs in both cold cavity and warm cavity ice shelves, the largest melt rates are observed in warm cavity ice shelves, due to the much higher heat content of CDW (e.g., Paolo et al., 2015; Pritchard et al., 2012). The particular water mass that drives melting below each ice shelf results from a complex variety of processes, such as atmospheric forcing (sea ice formation and melt, precipitation and evaporation, and variation in wind direction and

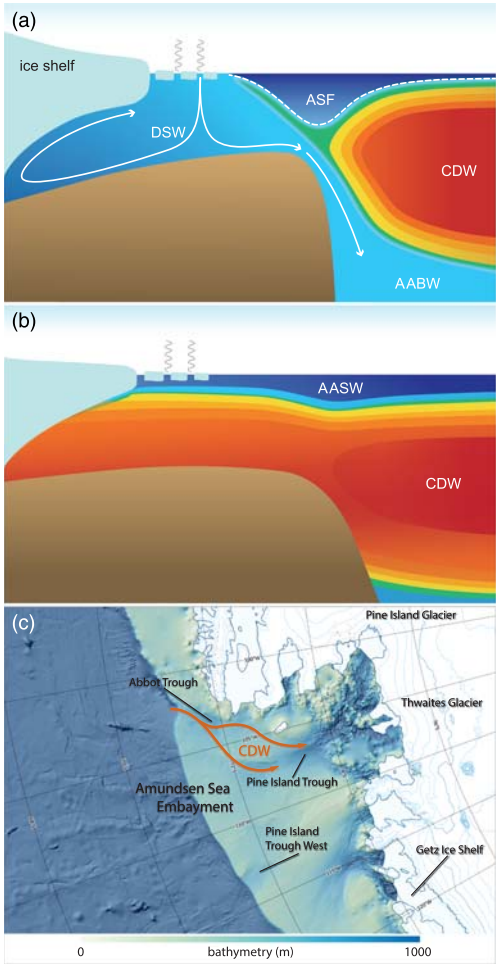


Figure 4. Cross-shelf exchange and basal melt. (a) Cold cavity ice shelf: A sharp ASF prevents the access of CDW onto the shelf. Moderate (e.g., Ross Sea) to large (e.g., George V-Adelie Land) buoyancy fluxes at the surface result in the formation of DSW, which drives low basal melt rates (after Jenkins et al., 2016; Petty et al., 2014; Schmidtko et al., 2014; Thompson et al., 2018). (b) Warm cavity ice shelf: Weak or absent ASF allows CDW to spread onto the continental shelf. DSW formation does not occur and CDW drives high basal melt rates. (c) Troughs and depressions at the shelf break can also facilitate access of oceanic heat on to the continental shelf and further to the coast, such as at Pine Island Glacier. Here, in the Amundsen Sea Embayment bathymetric troughs and depressions facilitate the exchange of CDW onto the shelf and toward the grounding line of the ice shelves (e.g., Thoma et al., 2008). The presence of CDW on the shelf drives melting of the nearby ice shelves (e.g., Jacobs et al., 2011), with freshwater release potentially leading to a shutdown of DSW formation where such dense waters are produced (e.g., Silvano et al., 2018; Williams et al., 2016). With DSW no longer exported across the shelf break in former areas DSW production the ASF weakens further promoting CDW access to the shelf (e.g., Thompson et al., 2018). Large, recurrent polynyas exist on the Amundsen Sea Embayment shelf; however, no DSW is produced there probably as a consequence of CDW presence. Panels (a) and (b) based on Jacobs et al. (1992).

strength), bathymetry, meltwater outflows, and tides. These processes control stratification and the buoyancy-driven circulation, which in turn regulate the amount of heat that is available to melt ice shelves. Ice shelf-ocean models are critical for researching these processes, as the coastal and sub-ice shelf region is typically very difficult to access. However, there is a lack of understanding of the boundary conditions, namely, the seafloor bathymetry. While recent efforts have significantly improved understanding of the geometry of some ice shelf cavities (e.g., Arndt et al., 2013; Fretwell et al., 2013; Timmermann et al., 2010), much of the Antarctic continental shelf and most ice shelf cavities remain very poorly constrained. As a result, the ability of models to simulate melting beneath ice shelves is hampered, particularly where that melting is heavily influenced by bathymetric-controlled flows. As more observations are available and models become more realistic, it has become clear that the relative contributions of the many processes influencing melting, and the interactions between them, vary around Antarctica. Such variation is responsible for the observed heterogeneity in the thinning response of Antarctic ice shelves.

Atmospheric forcing explains a large portion of observed variability in the temperature and salinity properties of Antarctic shelf waters and sea ice production (Petty et al., 2013, 2014). At the regional scale, offshore directed winds, such as katabatic winds advect ice away from the coast, resulting in large heat fluxes from the ocean to the atmosphere. This wind-driven and buoyancy flux process maintains high sea ice production rates in many Antarctic coastal polynyas (Tamura et al., 2016) and results in the production of cold DSW, which can reduce basal melting near the front of the ice shelf (St-Laurent et al., 2015). At the Mertz Glacier Tongue, prior to its break off in 2010 (Giles, 2017), increased basal melting of floating ice occurred during periods when the nearby polynya was much weaker (Cougnon et al., 2013; Holland et al., 2015). Changes to the local icescape, in particular the positioning of grounded icebergs, for example, after the calving of the Mertz Glacier Tongue (Kusahara et al., 2011), have been shown to play a role in defining the properties of the shelf waters and the rate of ice shelf basal melting (Cougnon et al., 2017).

In other locations where cold shelf waters are observed, upstream preconditioning of shelf waters, in particular freshening due to ocean-driven melting, is an important process controlling the properties of Antarctic shelf waters (Kusahara et al., 2017; Williams et al., 2016), as well as deep ocean properties through the reduction of AABW export (Hellmer, 2004). Along the Sabrina Coast, East Antarctica, where DSW does not result in the formation of AABW, the high glacier flow speed of the Totten Glacier has been linked to basal melting, driven by a pool of warm water on the continental shelf (Rintoul et al., 2016; Silvano et al., 2017). Observations and models suggest that the magnitude of basal melting of the Totten Glacier is modulated by the properties of DSW formed in the nearby Dalton Ice Tongue polynya (Gwyther et al., 2014; Khazendar et al., 2013). Even in very active polynyas, the freshening caused by the input of meltwater from upstream can partially offset the density contribution from brine released during sea ice formation, preventing top-to-bottom convection and further promoting access of warm water to the glacier cavity, as found in the Dalton Ice Tongue and Amundsen polynyas (Silvano et al., 2017).

There is increasing evidence that the continental shelf bathymetry, in particular submarine troughs and depressions (Figure 4c), is key in allowing the warm water to reach the ice front. For example, flow inertia has been shown to initiate exchange of along-slope currents onto the shelf when in the presence of a trough that crosscuts an offshore curving shelf break (Dinniman & Klinck, 2004; Klinck & Dinniman, 2010). Cross-shelf exchange has also been shown to result from interaction between an off shelf-sourced Rossby wave and the topography of a shelf breakthrough (St-Laurent et al., 2013). Conversely, seabed ridges can also block the deepest warmest waters from reaching the grounding line (De Rydt et al., 2014; Dutrieux et al., 2014; Jenkins et al., 2010; Muto et al., 2016). The local circulation on the shelf, whether wind (Dinniman et al., 2015; Stewart & Thompson, 2015) or buoyancy driven (Snow et al., 2016), also plays a role in delivering heat to the ice shelf front. A cyclonic gyre on the continental shelf helps to transport warm water from the shelf break to the ice shelf front both at the Amery Ice Shelf in East Antarctica (Galton-Fenzi et al., 2012; Herraiz-Borreguero et al., 2016; Liu et al., 2017), and in the Bellingshausen Sea (Zhang et al., 2016). However, the role of the gyre located in Pine Island Bay (Thurnherr et al., 2014) in delivering water to the Pine Island and Thwaites Glaciers is unknown (Heywood et al., 2016). Along the Western Antarctic Peninsula, a projected increase in westerly wind strength could increase mixing (Brearley et al., 2017), thus enhancing the heat content in shallower water, leading to decreased melting below deep ice shelves and increased melting below shallow ice shelves (Dinniman et al., 2012).

The meltwater outflows from warm cavity ice shelves can impact melting. Fine-resolution observations (~0.5 km spacing between conductivity temperature depth (CTD) stations) collected along the Pine Island Ice shelf front have recently shown that as these buoyant meltwater outflows rise they can mix laterally via centrifugal and gravitational instabilities (Naveira Garabato et al., 2017) and eventually spread at the base of the winter mixed layer. Adding freshwater to the surface of the ocean has the potential to increase sea ice formation by raising the freezing point; however, it is the suppression of convective overturning that is important. These outflows contribute to the preconditioning of polynyas by increasing the near-surface stratification and reducing the penetration of the deep convection that forms DSW (Williams et al., 2016). Weaker deep convection leads to less heat loss from the ocean to the atmosphere and can lead to warmer waters accessing the ice shelf cavity, possibly further accelerating the mass loss from the ice sheet.

Sub-ice shelf melting responds to the amount of heat flux present at the ice-ocean interface, which is in turn a function of cavity circulation and turbulent mixing. For higher ocean temperatures, stronger melting releases more buoyant meltwater, thus increasing the overturning circulation within the ice shelf cavity (Gwyther et al., 2016; Holland et al., 2008). As stronger circulation increases turbulent heat transfer to the ice shelf, tides also impact melt rate. This occurs through both tidal rectification, where the tidal current varies as a function of Earth's rotation and the topography above the continental slope, as the periodic oscillation of tidal currents leads to greater mean circulation strength (Padman et al., 2018), and through increased turbulence, which results in stronger mixing of heat and salt across the ice-ocean boundary layer (Mueller et al., 2012). The net impact of tides on basal melting is to increase the total basal mass loss and to change the spatial distribution of melting (Gwyther et al., 2016). On a broader scale, the rate at which the cavity is flushed and reventilated affects the heat budget within the cavity and thus the magnitude of basal melting (Holland, 2017).

Around Antarctica, basal melting contributes nearly twice as much to the total mass loss as iceberg calving (Liu et al., 2015). However, ice shelves that are currently thinning have an approximately even mass loss contribution from basal melting and calving, as a result of more frequent calving events. The filling of preexisting crevasses with surface meltwater is suggested to have led to the fragmentation and collapse of the Larsen A and B ice shelves (Scambos et al., 2004). The loss of these ice shelves has been linked to subsequent acceleration of tributary glaciers (Scambos et al., 2004). However, the loss of floating ice shelf area does not necessarily lead to increased glacier velocities. There is an area of the ice shelf known as the "passive ice shelf" (Fürst et al., 2016) that can be removed without damaging the integrity of the remaining ice shelf (see section 3.1.3). However, ice shelves in the Amundsen and Bellingshausen Seas were shown to not be protected by a band of passive ice. The role of a sea ice buffer and fast ice buttressing in maintaining the structural integrity of the frontal ice shelf region is relatively underexplored. Recent research suggests that the seasonal absence of sea ice can remove the buffer from ocean swell and allow increased wave-induced ice

shelf flexure, which likely contributed to the disintegration of Larsen A, B, and Wilkins Ice Shelves (Massom et al., 2018). The mechanical buttressing of landfast sea ice upon the front of ice shelves has been shown to be the primary contributor for controlling seasonal ice shelf velocity within 50 km of the calving front (Greene et al., 2018).

There is a strong effort to assess the role of atmospheric-driven processes, such as hydrofracturing, in driving grounding line retreat (see section 3.1.3), as demonstrated by the development of models of ice shelf rifting and calving (Benn et al., 2017) and of iceberg evolution (Stern et al., 2017). The formation of icebergs through rifting and fracturing processes is still poorly understood and difficult to model, particularly on larger spatial scales and longer time scales. As a result, this process is often excluded from global climate models, although it may be a very important process, in particular for achieving high rates of sea level rise not observed in the present but recorded during past deglaciations (e.g., Meltwater Pulse 1A) and warm climate periods (e.g., Last Interglacial (LIG) period) (see sections 4.2.2 and 4.2.3).

Low-frequency intrinsic ocean variability, generated internal to the ocean and in response to stochastic forcing, also has the potential to drive complex changes in ocean conditions (Leroux et al., 2018; O'Kane et al., 2013). Flushing and ventilation of the ice shelf cavity by periodic changes in ocean conditions such as thermocline depth, resulting from climate teleconnection modes (Holland et al., 2019; Jenkins et al., 2018) or intrinsic ocean variability (Gwyther et al., 2018; Huneke et al., 2019), will influence ice shelf mass loss. This has been demonstrated in a realistic model of the Totten Ice Shelf (Gwyther et al., 2018) and idealized models (Holland, 2017; Snow et al., 2017). While assessments of future mass loss from ice shelves can be conducted (e.g., Hellmer et al., 2012), intrinsic ocean variability and low-frequency climate models present a challenge for accurately simulating present day mass balance trends (e.g., Christianson et al., 2016) and projecting the future response of the AIS to anthropogenic climate forcing.

2.2.3. Microscale Interactions

The accelerated mass loss around Antarctica (see section 5.1) has been largely attributed to the intrusion of warm and salty CDW under ice shelf cavities and interaction with ice shelves through the ice-ocean boundary layer (Jacobs et al., 2012; Jenkins et al., 2016, 2018; Khazendar et al., 2013; Payne et al., 2004; Picard et al., 2012; Swingedouw et al., 2009). Understanding the processes that control melting at the smaller scale is important for accurate modeling and prediction of ice shelf basal melting; however, in situ investigation of the ice/ocean interface is limited (Jenkins et al., 2010; Stanton et al., 2013) due to logistical difficulties (Galton-Fenzi et al., 2016). As a result, models and laboratory experiments are critical in investigating the key processes that control microscale interactions: turbulence and convection.

The underlying microscale dynamics of ice melting involve the transport of both heat and salt in a thin boundary layer at the ice face (Gayen et al., 2016; Kerr & McConnochie, 2015; Mondal et al., 2019; Wells & Worster, 2011). Ocean modeling studies can only resolve the flow field at scales in the order of 100 m and must rely on parameterizations to represent small-scale boundary layer processes to infer the melt rate. The conditions inside ice shelf cavities change the melt rate by controlling ocean-ice interactions. The seawater temperatures inside ice shelf cavities vary from the freezing point temperature of seawater at the location (i.e., −2.3°C to −1.7°C for a cold cavity) to 0°C (for a warm cavity), with the salinity around 34 practical salinity unit (PSU) (Dutrieux et al., 2014; Jacobs et al., 2013, 2011, 2012; Jenkins et al., 2010; Nicholls et al., 2009; Payne et al., 2004). At these low temperatures, the primary transfer of solute to the ice lowers the melting point of the ice and enhances the heat transfer across the ice-ocean interface. This process is more accurately described by dissolution (Wells & Worster, 2011; Woods, 1992), meaning that both heat and salt fluxes must be considered in estimating the rate of ice shelf mass loss.

Heat and salt transfer occur through multiple ocean layers against the ice face. Diffusive fluxes dominate at the ice-ocean interface, with the flux controlled by diffusive boundary layers on the order of 1 mm thick. The thickness of the salinity layer is an order of magnitude smaller than the thermal boundary width due to the large differences in molecular diffusivity between heat and salt (Josberger, 1983; McPhee, 1981). Because of the small spatial extent of the layer dominated by diffusive fluxes, it is not possible to make direct measurements of these fluxes in the field. Therefore, we often rely on model simulations or parameterizations to estimate these fluxes.

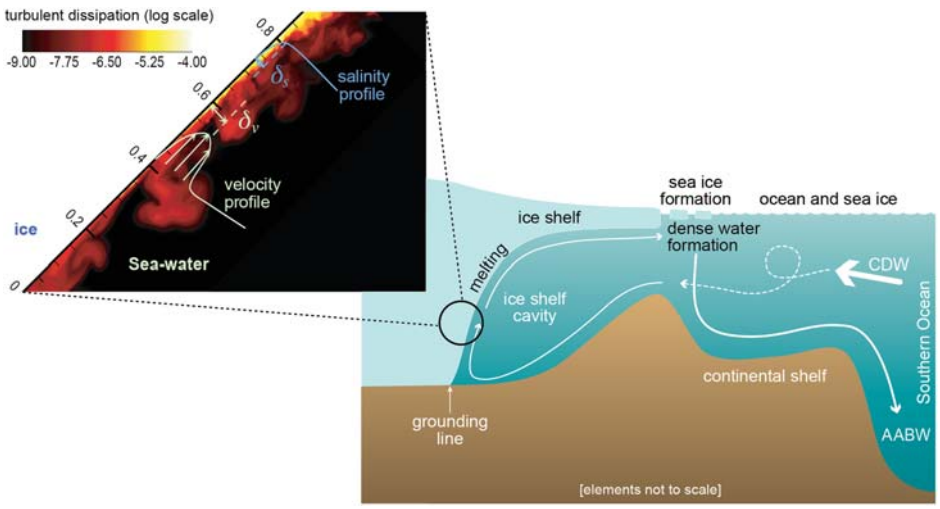


Figure 5. Schematic of microscale circulation processes on the Antarctic continental shelf. Grounded ice sheets are buttressed by floating ice shelves. Their basal melting is driven by the supply of salinity and heat from the Southern Ocean via CDW and its derivatives and influences the formation of deep-water masses and Antarctic Bottom Water (AABW). Zoomed view of boundary layer processes by showing snapshot of simulated turbulent dissipation (log scale) field underneath a sloping ice shelf base (Mondal et al., 2019).

Beyond the diffusive layer (further away from the ice interface), fluxes are usually dominated by turbulent processes in the outer layer which has a thickness in the order of 10 m. The turbulence is due to a combination of natural convection from buoyant melt water, strong shear ambient flows, internal waves, and ocean tides (Cenedese & Gatto, 2016; Gayen et al., 2016; Keitzl et al., 2016). Next to the ice face, meltwater is positively buoyant compared to the ambient seawater and forms a convective plume. This plume is turbulent and acts to amplify melting by transferring heat to the ice surface from the surrounding ocean (Figure 5) (Gayen et al., 2016; Kerr & McConnochie, 2015; McConnochie & Kerr, 2017; Mondal et al., 2019; Slater et al., 2016). Such convection-driven melting is not considered in present parameterizations used for ocean modeling (McConnochie & Kerr, 2017) and represents a key challenge in future models of the ice melting process. Future improvements in model parameterizations need to include stratification in the cavity water, which can impact the melt boundary layer in a complex way by forming of double-diffusive layers and enhancing the rate of mixing of melt water with the surrounding salty water (Gayen et al., 2015; Huppert et al., 1980; Huppert & Turner, 1978, 1980). In addition, turbulent heat transport across the ice-ocean boundary layer is significantly enhanced by roughness of the ice shelf bottom surface, usually caused by the small ice crystal accretion (frazil) (Robinson et al., 2017), as well as channels at the underside of an ice shelf formed by oceanic melting (Alley et al., 2016; Bindschadler et al., 2011; Mankoff et al., 2012) and possibly initiated by channelized subglacial meltwater outflow (Le Brocq et al., 2013), significantly enhances turbulent heat transport across the ice-ocean boundary layer (see section 4.2.3 for more on sub ice shelf channels). This can influence the distribution of melting and freezing (Gwyther et al., 2015; Le Brocq et al., 2013; Stanton et al., 2013; Vaughan et al., 2012) and even ice shelf stability (Alley et al., 2016). Estimates of turbulent-driven mixing and the magnitude of sub-ice shelf melt are currently limited by our lack of understanding of basal friction. Improving this understanding principally depends on measurements of basal roughness and the impact on adjacent flow beneath ice shelves.

The complex interactions inside the boundary layer, including ice surface morphology, strongly influence heat transport across the ice-ocean interface and the rate of basal melting. Thus better understanding and representation of these processes in ocean-climate models are necessary to increase accuracy in the prediction of future AIS evolution.

3. Ice Dynamic Processes

The AIS was traditionally viewed as a slowly evolving and passive component of the Earth system (Warrick & Oerlemans, 1990). However, recent evidence indicates that the AIS responds to forcings on time scales of

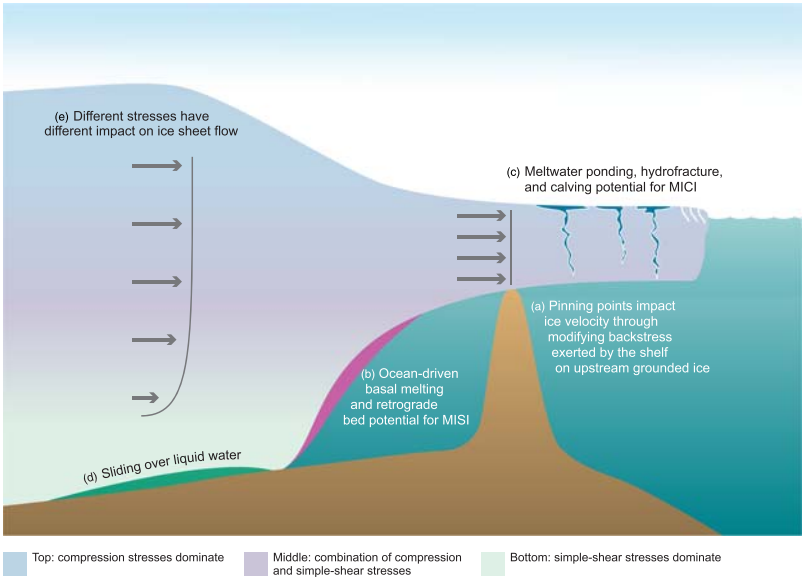


Figure 6. Ice sheet dynamic processes. (a) Friction from topographic pinning points or ice shelves impacts ice speeds. (b) Marine ice sheet instability (MISI). The geometry of the bed topography plays a critical role in ice flow and ice sheet stability. Specifically, a retrograde bed sloping downward into the interior of the continent can lead to unstable grounding line retreat when combined with melting of the base of the ice shelf from relatively warm ocean waters. (c) Marine ice cliff instability (MICI). Ice cliffs can collapse forming icebergs as a result of rapid ice shelf disintegration caused by meltwater ponding at the ice shelf surface and hydrofracturing. (d) Basal sliding, in the presence of subglacial meltwater, is one of the main processes by which ice flows from the interior of the continent to the oceans. (e) Ice deformation is the movement within and between ice crystals, which is a function of the different stress configurations within the ice sheet.

hours (e.g., tides) to millennia (e.g., glacial cycles) (Davis et al., 2018; Pattyn et al., 2018) and with significant spatial variations, even within ice sheet drainage sectors (e.g., Konrad et al., 2017). In this section, we review the shift in perspective of the AIS's dynamic interaction with other components of the Earth system in the context of processes that drive ice discharge from the AIS. We discuss processes that have been proposed to reconcile the evidence of past AIS change and sea level rise inferred from paleostudies, as well as grounding line controls, including ice shelf buttressing and the marine ice sheet and ice cliff instabilities (Figure 6). Ice flow processes, particularly basal sliding and ice deformation, that influence the ice mass flux over the grounding line, are also discussed. We highlight advances in observational capabilities and the development of numerical ice sheet models that improve understanding and prediction of the dynamic AIS evolution and stability.

3.1. Grounding Line Controls

The grounding line (or zone) is the interface between the grounded ice sheet and floating ice shelves and is a key control on ice discharge from the AIS (Weertman, 1974).

Grounding lines have been retreating since the last glacial period when they were near their peak extent (The RAISED Consortium et al., 2014). Satellite evidence points to accelerated retreat in key sectors over the last few decades. For example, Konrad et al. (2018) mapped grounding line migration for the AIS from 2010 to 2016 by combining surface elevation and mismatches in the surface elevation above mean sea level, breaks in the ice sheet surface elevation slope, and the effect of tides. While much of the continent's grounding lines showed no discernible change over this period, 3.3% of East Antarctic, 21.7% of West Antarctic, and 9.5% of Antarctic Peninsula grounding lines retreated. Grounding line retreat was found to be largest in the Amundsen and Bellingshausen Sea sectors (Christie et al., 2016; Parizek et al., 2013; Rignot et al., 2014), which are regions of significant ice sheet thinning and fast flow. Observations since the 1970s confirm long-term retreat in basins of West Antarctica and the Antarctic Peninsula (Mouginot et al., 2014), with 35 km retreat of Smith/Kohler Glaciers, 31 km retreat of Pine Island Glacier, and 14 km retreat of Thwaites Glacier over the period 1992–2011 (Rignot et al., 2014).

Grounding lines migrate in response to various forcing mechanisms. On long (centennial to millennial) time scales, grounding lines migrate in response to glacial isostatic adjustment (GIA) due to ice loading (section 4.2.2), and subglacial hydrology (section 4.2.4), long-term fluctuations in climate forcings and sea levels, and internal ice sheet dynamics. On time scales of hours to centuries, the ocean and atmosphere drive grounding line migration predominantly through ice sheet and shelf melting that modifies ice shelf buttressing, and may induce marine ice sheet and ice cliff instabilities.

3.1.1. Ice Shelf Buttressing

Ice shelves can stabilize the position of the grounding line, and ice mass flux across it, by applying a back stress on the upstream ice through interaction with topographic pinning points, or interaction with topography at basal or lateral boundaries—a process known as ice shelf buttressing (Doake et al., 1998; Dupont & Alley, 2005a, 2005b; MacAyeal, 1987; Rignot et al., 2004; Scambos et al., 2004). Buttressing can alternately act to slow ice flow (Gladstone et al., 2012; Humbert & Steinhage, 2011; Jenkins et al., 2010; Schmeltz et al., 2001) or generate a highly localized flow regime, particularly in the case of basal topographic pinning points (Favier et al., 2016). Several regional and idealized modeling studies (e.g., Berger et al., 2016; Favier et al., 2012, 2016; Goldberg et al., 2009) have found that grounding line dynamics are strongly sensitive to the buttressing provided by topographic pinning points.

Ice shelf buttressing is impacted by changes in ice shelf thickness and extent: With the thinning or calving of floating ice, the buttressing effect is diminished. Past ice shelf recession and collapse has been linked to a reduced buttressing effect, leading to increased mass flux. For example, the collapse of Larsen B ice shelf in the Antarctic Peninsula in 2002 led to increased ice shelf flow and ice front retreat in the subsequent decade, as well as acceleration of the tributary Leppard and Flask Glaciers (Khazendar et al., 2015). Ice shelf thinning and the reduction in buttressing effect that occurred in Larsen B was potentially sparked by the earlier collapse of the neighboring Larsen A ice shelf in 1995 (Albrecht & Levermann, 2014).

Recent work has highlighted the importance of the ice shelf buttressing effect in determining AIS stability (Fürst et al., 2016). In their analysis, Fürst et al. (2016) delineated regions of ice shelves that control buttressing from regions where the ice shelf could be removed without impacting flow—the latter denoted "passive" portions of the ice shelf. A total of only 13.4% of Antarctica's total ice shelf area could be removed without impact to the grounding line position and ice mass flux across it. Glaciers and ice streams in the Amundsen and Bellingshausen Sea sectors are particularly vulnerable to dynamic changes in the event of ice shelf thinning or calving, having passive ice shelf areas of only 7.9% and 5.3%, respectively.

A regional modeling study on the Lazarev and Roi Baudouin Ice Shelves in East Antarctica investigated the potential for future sea level rise as a result of ice discharge from these ice shelves (Favier et al., 2016). The study found that the buttressing effect of pinning points beneath the ice shelves led to an overall decrease of 10% in sea level rise from ice discharge compared with when the pinning point was removed. The results highlight the importance of high-resolution bed topography in numerical modeling, given that ice shelf stability can be controlled by kilometer-scale pinning points.

Ocean-driven melt of ice shelves is responsible for more than half of Antarctic ice shelf mass loss (Depoorter et al., 2013; Liu et al., 2015; Paolo et al., 2015; Rignot et al., 2013) and is a strong driver of changes in the buttressing effect. Reese, Gudmundsson, et al. (2018) diagnosed the dynamic response of grounded ice and particularly the corresponding mass flux across the grounding line, to specific spatial patterns of ice shelf mass loss. Their results highlighted a potential for "tele-buttressing," whereby relatively small changes to ice shelf thickness can initiate an ice dynamic response far upstream of the thickness perturbation. The ice shelves most vulnerable to change have ice-ocean fronts close to the continental shelf or in regions prone to intrusion of warm ocean waters (see section 2.2.1).

Recent observations of the Totten Glacier in East Antarctica suggest that ice shelves work in concert with ocean forcing to modify the ice flow regime and surface elevation through back stress generated from topographic pinning points Roberts et al., 2018). Specifically, when the seawater in contact with the ice shelf base is cool, a reduction in melting leads to ice shelf thickening, increased back stress at the pinning point, and an overall decrease in ice velocity. The converse is true when the ocean-forced melting is high. In studies of ice sheet retreat, topographic pinning points have also been found to play a leading role in stabilizing the grounding line position (e.g., Seroussi et al., 2017; Schlegel et al., 2018), highlighting the importance of buttressing and back-stress processes to ice shelf stability.

Numerical model studies estimating the potential future contribution of the AIS to sea level rise will benefit from continued improvement in the spatial and temporal resolution of topographic data beneath the ice sheet and shelves (e.g., Morlighem et al., 2020). The advent of high-resolution ice surface elevation data, such as the submeter resolution satellite imagery used in the construction of the Reference Elevation Model of Antarctica (REMA, Howat et al., 2018), may aid in identifying or characterizing pinning points, where they have a surface expression (see e.g., Budd & Carter, 1971; J. Roberts et al., 2018).

3.1.2. MISI

MISI (Figure 6) is an important process in evolution of the AIS. It describes the susceptibility of a marine-based ice sheet with a bed that slopes in an upstream direction (retrograde bed slope) to grounding line retreat especially under a warming climate (Mercer, 1978; Thomas, 1979; Weertman, 1974). Specifically, MISI occurs when the grounding line of a glacier flowing over a retrograde bed slope retreats, which acts to reduce the ice shelf buttressing effect and results in further grounding line retreat and accelerated ice discharge. If the ice thickness at the grounding line increases when the grounding line retreats, then the ice discharge will also increase, and the grounding line has to retreat further upstream, thereby also reducing the glacier's catchment area and thus the area of snow/ice accumulation. Schoof (2007, 2011) used analytical methods to verify MISI, demonstrating that for an ice sheet/ice shelf system that is not confined by an embayment, ice discharge at the grounding line is extremely sensitive to ice thickness at the grounding line, proportional to approximately its fifth power. For an ice sheet fringed by an embayed ice shelf, modeling shows this relationship is expected to be less strong due to the buttressing effect from interaction of ice with topography at the lateral boundaries (Goldberg et al., 2009).

MISI is triggered by an initial retreat of the grounding line, which can be activated by a variety of processes, for example, ice shelf thinning, sea level rise due to thermal expansion of seawater, or the sea level fingerprint from melting glaciers in the middle to low latitudes and high latitudes of the Northern Hemisphere. The grounding line retreat leads to a run-away effect (e.g., see Joughin & Alley, 2011; Vaughan & Arthern, 2007) associated with accelerated ice discharge (Pollard & DeConto, 2009, 2012). Several WAIS glaciers that satisfy the geometric requirements of MISI are potentially already undergoing MISI (Favier et al., 2012; Joughin et al., 2014).

In the Amundsen and Bellingshausen Sea sectors, MISI is believed to be driven by incursions of CDW onto the continental shelf (Holland et al., 2010; Jacobs et al., 2011; Jenkins et al., 2018; Nakayama et al., 2013), potentially as a result of broader changes in patterns of wind forcing (Thoma et al., 2008). In the event that CDW incursions decrease in the future, glaciers already undergoing MISI might continue to experience grounding line retreat even after the forcing is removed, as recently inferred from numerical modeling by Waibel et al. (2018). However, sustained retreat of MISI-prone glaciers is not guaranteed and depends on complex interactions and feedbacks between the ice sheet and other Earth and climate systems. For instance, the response time scales vary widely depending on the subglacial setting (Levermann & Feldmann, 2019) and ice-ocean interactions such as the magnitude of ocean-driven melting and the supply of warm ocean waters to the grounding line (Joughin et al., 2014; Seroussi et al., 2017). Furthermore, grounding line retreat is highly sensitive to, and can even be stabilized by, ice-solid Earth interactions such as the effect of significant topography, pinning points, or lateral buttressing (Gudmundsson, 2013; Jamieson et al., 2012; Schlegel et al., 2018; Seroussi et al., 2017; Thomas, 1979) or the bed slope and depth below sea level (Golledge, 2014), as well as the negative feedbacks from solid Earth rebound and sea level rise (Larour et al., 2019).

Challenges remain in using numerical models to predict the timing and magnitude of potential collapse of marine-based parts of the AIS as a result of MISI. One challenge is the treatment of ocean melt rates that drive MISI. These are often parameterized in ice sheet models as a function of the ice shelf draft, accounting for greater melt rates near the grounding line than at the ice-ocean front (Asay-Davis et al., 2016; Walker et al., 2008). Options exist that allow for a more sophisticated treatment of sub-ice shelf melt rates, such as that provided by the Potsdam Ice-shelf Cavity mOdel (PICO) (Reese, Albrecht, et al., 2018), which simulates the vertical overturning circulation in ice shelf cavities, using temperature and salinity fields to calculate sub-ice shelf melt rates. Plume models of shelf meltwater (e.g., Jenkins, 2016), may also provide realistic melt rate parameterizations by accurately representing melting in the ice shelf cavity. A combination of

PICO with a plume model (Pelle et al., 2019) has been shown to capture ocean melt rate patterns and magnitudes that agree well with observations.

Sub-shelf melt rate estimates from ocean models are continually improving due to the addition of new physical processes (e.g., Galton-Fenzi et al., 2012), improved boundary conditions, and model capabilities (e.g., Gwyther et al., 2014; Nakayama et al., 2019) and may be directly incorporated as the ocean forcing in ice sheet models. However, stand-alone ocean models are limited in their ability to account for changes in the geometry of the ice shelf cavity and moving grounding lines and thus cannot provide estimates of the timing and magnitude of collapse of the marine-based AIS. The effect of these issues is being explored in efforts such as the Marine Ice Sheet-Ocean Model Intercomparison Project (MISOMIP) (Asay-Davis et al., 2016), which aims to improve understanding of ocean-ice shelf interaction for the eventual inclusion in general circulation models, using coordinated modeling experiments across both standalone ocean and ice sheet models and coupled ice sheet-ocean modeling frameworks.

An alternative to parameterizing ocean melt rates in ice sheet models is coupling between ice sheet and ocean models, which enables accurate treatment of the ice-ocean boundary interactions and feedbacks that drive MISI. Recent developments have been made in asynchronous ice sheet-ocean model coupling, where each component model is run independently for short periods of time, and the outputs (e.g., geometry, melt rates, temperature, and salinity) are updated between models (Asay-Davis et al., 2016; De Rydt & Gudmundsson, 2016; Seroussi et al., 2017). Asynchronous coupling has the advantage of being relatively computationally inexpensive as it does not require each component model to be solved at the same time step where the time scales of evolution vary considerably (e.g., Goldberg et al., 2012). Nevertheless, this may come at the expense of accurately representing the full spectrum of coupling time scales relevant to each model component (Snow et al., 2017).

Synchronous high-resolution coupling of an ice-ocean model has also recently been undertaken (Jordan, Holland, et al., 2018). Snow et al. (2017) used synchronous coupling to show that the ice sheet responds most strongly to long ocean forcing time scales, and the ice volume above floatation changes in response to different ocean forcing periods that are generally shorter for the coupled model than for the uncoupled parameterizations. In addition to modifying the time scales of the ice sheet response, using a synchronous approach over an asynchronous one has the advantage of conserving heat, salinity, and mass, allowing for tidal deflections to be resolved.

Ice sheet models using a combination of the shallow ice approximation (SIA) and shallow shelf approximation (SSA) (De Rydt & Gudmundsson, 2016; Goldberg et al., 2012; Seroussi et al., 2017; Thoma et al., 2015) coupled to ocean models have been used in experiments to assess the sensitivity of the ice sheet to changing ocean temperatures and circulations. These studies consistently predict an enhanced ice sheet response (e.g., grounding line retreat or volume above floatation) in the absence of coupling between the ice and ocean model components. This suggests that projections of the AIS response to climate change and susceptibility to MISI require that spatial and temporal patterns in ocean melt rates as predicted by ocean models, and coupled feedbacks between the ice and ocean systems, are sufficiently resolved.

A challenge in predicting the impact of MISI on the AIS is the treatment of grounding line dynamics and migration. Recent developments in ice sheet model physics, parameterization of physical mechanisms, and mesh resolution have driven improvements in grounding line dynamics (Nowicki & Seroussi, 2018). For example, accurately resolving fine-scale migrations of the grounding line in numerical model simulations requires very fine mesh elements near the grounding line, which comes at a large computational cost for the time scales typical of ice sheet dynamic evolution. New approaches have accounted for this problem through subgrid parameterizations of friction or ocean melting (Feldmann et al., 2014; Gladstone et al., 2010; Leguy et al., 2014; Seroussi & Morlighem, 2018; Seroussi et al., 2014) or adaptive mesh refinement (Durand et al., 2009; Gladstone et al., 2010). High-resolution full Stokes models of the grounding zone are more accurate than models with simplified stress balance approximations (e.g., the SIA; Hutter, 1982) in yielding large short-term variations in the grounding line position (Drouet et al., 2013; Seddik et al., 2017). Models with sliding relations that incorporate a dependency on the effective pressure have been able to smooth the transition between grounded and floating ice (Brondex et al., 2017; Gladstone et al., 2017; Jong et al., 2018; Robel et al., 2016; Tsai et al., 2015), a problem that arises in models with less physically motivated sliding relations (see section 3.2.1).

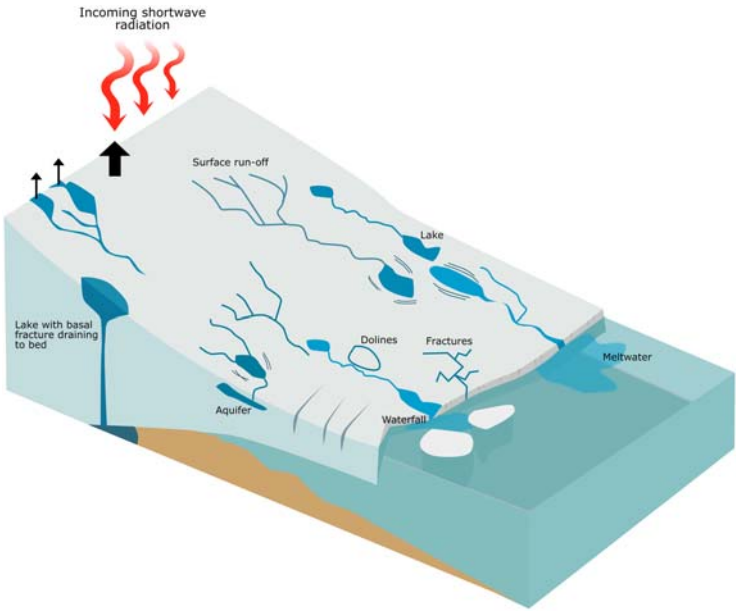


Figure 7. Schematic of Antarctic surface hydrology features that can influence AIS dynamics. Surface melting is enhanced due to reduced surface albedo, resulting in a positive melt feedback. Basal hydrology is impacted when the surface meltwater reaches the subglacial environment through fractures. Fracturing develops through surface lake and firn aquifer drainage. Hydrofracturing of the ice shelf can arise due to the loading and unloading of lakes. Direct surface runoff into the ocean can change seawater density properties and potentially result in stratification that can trap warming in the subsurface, enhancing basal melting of the ice shelf. Adapted from Bell et al. (2018).

3.1.3. Surface Melt and MICI

Surface meltwater in the form of supraglacial lakes, subsurface lakes, surface streams, and rivers (Bell et al., 2018) (Figure 7) can potentially impact AIS mass loss directly by accelerating ice shelf disintegration, which reduces buttressing back stresses and increases ice flow to the ocean (Scambos et al., 2004). Summer melting in Antarctica is generally confined to the ice sheet edge (Tedesco & Monaghan, 2009) and is most intense and widespread on the Antarctic Peninsula (Cook & Vaughan, 2010). Indeed, an increasing duration of surface meltwater on ice shelves on the Antarctic Peninsula has been observed over the past fifty years (Abram et al., 2013; Barrand et al., 2013; Vaughan, 2006). This is particularly the case in the eastern Antarctic Peninsula (Pritchard & Vaughan, 2007; Scambos et al., 2004; van den Broeke, 2005) in response to atmospheric warming (Scambos et al., 2000) and a result most vulnerable to meltwater-induced hydrofracture.

Active surface hydrology systems in East Antarctica ice shelves were previously considered to be rare, as highlighted by Kingslake et al. (2017). However, an inventory from the peak of the 2017 melt season reveals extensive and active surface lake formation in East Antarctica. Over 80% of the area of these lakes was located on ice shelves, making the ice shelves vulnerable to meltwater induced fracturing (Stokes et al., 2019). East Antarctic ice shelves also show evidence of surface hydrology processes (Langley et al., 2016, 2011; Phillips, 1998), which may be driven by different processes (e.g., a positive feedback on surface melting by wind-albedo interaction; Lenaerts et al., 2017) but can affect ice shelf disintegration through similar hydrofracturing mechanisms to those observed on the Antarctic Peninsula.

Surface meltwater can trigger ice shelf collapse through meltwater induced fracture propagation, a process referred to as hydrofracturing. Ice shelf breakup can result from a combination of both flexure stresses, due to changes in stress load from filling and draining of surface lakes and hydrofracture (i.e., increasing crevasse depths) (Banwell et al., 2013; Banwell & MacAyeal, 2015; MacAyeal & Sergienko, 2013; MacAyeal et al., 2015). Direct observations of ice shelf flexure on time scales of weeks from the McMurdo Ice Shelf, a small portion of the Ross Ice Shelf, due to changes in the surface meltwater load (Banwell et al., 2019) provide much needed constraints for implementing this process in ice sheet models. Developments in model parameterization of hydrofracturing by Robel and Banwell et al. (2019) suggest that the time scales

(weeks to years) of ice shelf collapse by hydrofracturing are limited by the rate of surface melting, with an intrinsic limit defined by the flexual length scale of the ice shelf.

The impact of meltwater on the basal conditions of grounded ice is not well known for Antarctica compared with the Greenland Ice Sheet. Rapid transfer of meltwater to the ice sheet base, via meltwater-induced fracturing of crevasses, provides a mechanism for changing conditions at the ice-bed interface (van der Veen, 2007). However, Bell et al. (2017) suggest that efficient export of surface meltwater off the ice shelf, through an extensive drainage network, can act to stabilize the ice shelf. Limitations on the depth of meltwater ponds likely play an important role in preventing ice shelf collapse (Robel & Banwell, 2019). However, the first evidence for meltwater-induced speed up of glacier velocity on the Antarctic Peninsula suggests that a direct coupling and positive feedback between atmospheric forcing and ice flow dynamics can occur (Tuckett et al., 2019).

To address the difference between simulations of ice sheet retreat and paleoevidence for, and sea level requirements of, major WAIS collapse, as well as retreat in portions of marine-based sectors of the EAIS, Pollard et al. (2015) proposed the MICI. This mechanism describes the vulnerability of ice shelves to both atmospheric and oceanic warming. MICI includes the physical processes of cliff failure and hydrofracturing, which can cause ice sheet instability with climatic warming: (DeConto & Pollard, 2016; Pattyn, 2018; Pollard et al., 2015). Under MICI scenarios, atmospheric warming generates meltwater ponding at the ice shelf surface, leading to extensive crevassing. Crevassed and damaged ice undergoes mechanical failure at lower cliff heights than noncrevassed ice. Reduction in buttressing from this mechanical failure, in combination with ocean-driven ice shelf thinning from below, can excite grounding line retreat (Figure 8) and rapid ice sheet collapse if sustained. By including the hydrofracture and cliff failure mechanisms, MICI has been used to reconcile ice sheet simulations of past climate conditions within the geological record, especially for warmer-than-present and Pliocene climates (Cook et al., 2013; Patterson et al., 2014; Williams et al., 2010; Young et al., 2011) (section 5.2.3).

Under conditions representative of a warm Pliocene period, Pollard et al. (2015) simulated a MICI-driven grounding line retreat of large regions of the EAIS into the major subglacial basins. DeConto and Pollard (2016) developed the representation of MICI further, coupling the ice sheet model to a regional climate model. To explore uncertainty in their parameterization of MICI, they perform a large ensemble analysis, fitting their model to LIG and Pliocene sea level targets of 3.6–7.4 and 10–20 m, respectively. Under an LIG climate, and without the MICI mechanism, subsurface ocean warming greater than 4°C is required to simulate WAIS retreat. However, by accounting for the additional ice-ocean-atmosphere feedback mechanism described by MICI, the model predicted WAIS collapse with ocean forcing of 3°C.

Under Pliocene conditions, the model with the MICI mechanism simulated an Antarctic contribution of <12 m to GMSL. This estimate is consistent with a Pliocene-maximum contribution of no more than 13 m from the AIS during the mid-Pliocene inferred from Pliocene ice sheet simulations constrained by the oxygen isotope composition of benthic foraminifera (Gasson et al., 2016). DeConto and Pollard (2016) used the tuned MICI parameterization in simulations of future AIS sea level contributions under the IPCC RCP8.5 scenario, finding a GMSL contribution of 15.65 ± 2.00 m by 2500. The rates of sea level rise corresponding to the DeConto and Pollard (2016) assessment are at the higher end of estimates based on natural climate forcing of sea level rise from paleoclimate data, which reveal an average of 1–2 m per century across past deglaciations, and 4–5 m per century during rapid pulses of sea level rise (Deschamps et al., 2012b; Grant et al., 2014; Rohling et al., 2013, 2019).

Observational evidence to support MICI is scarce and is currently limited to one study of the maximum water depths and shapes of iceberg-keel plow marks eroded during the post-Last Glacial Maximum (LGM) deglaciation on the West Antarctic continental shelf (Wise et al., 2017) and another based on glaciological evidence of rapid ice cliff calving in Greenland (Parizek et al., 2019). Wise et al. (2017) found iceberg-keel plow marks on the floor of the Pine Island Trough in West Antarctica that may indicate rapid deglacial ice sheet retreat into Pine Island Bay. Radiocarbon dating of foraminifera used to constrain the timing of the formation of grounding zone wedges present in this paleo ice stream trough indicates that the retreat commenced around 12.3 ka and terminated before 11.2 ka (Kirshner et al., 2012; Larter et al., 2014). The keel plow marks in the study of Wise et al. (2017) indicate smaller icebergs with pinnacle-shaped keels calved from an ice cliff front, rather than large tabular icebergs calved from the regions of the current ice

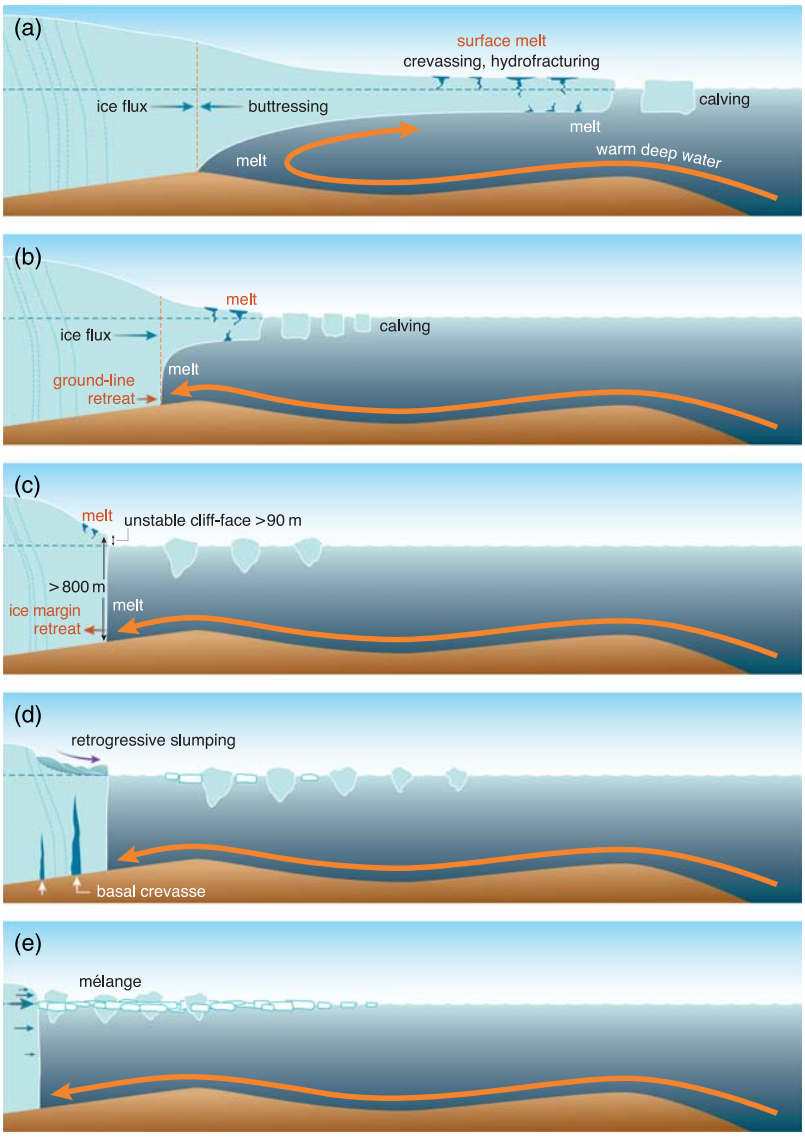


Figure 8. Schematic of marine ice cliff instability. (a) Warm ocean water access drives basal melting, while surface melting causes hydrofracturing and surface crevasse formation. (b) Loss of buttressing due to enhanced basal melting or calving results in grounding line retreat, which on a retrograde sloping bed leads to a feedback loop of increased melt, calving and increased in ice flow across the grounding line resulting in rapid further retreat (i.e., MISI). Basal crevasses, possibly enhanced by basal melting, connect with surface crevasses, leading to enhanced iceberg calving. (c) Melting and calving has advanced to the stage that an ice shelf no longer exists. An unstable ice cliff face of >90 m leads to loss of structural integrity due to stress buildup exceeding yield strength. (d) The unstable cliff-face can fail by retrogressive slumping, leading to buoyancy-driven, full-thickness calving (i.e., MICI). (e) An ice melange forms in front of the newly calved, marine-terminating glacier, possibly providing some cliff stabilizing buttressing. Figure redrawn from Parizek et al. (2019) and Pollard et al. (2016).

shelf configuration. The inferred calving-margin thicknesses of the bergs during this period of retreat are consistent with the threshold predicted to trigger ice shelf collapse as a result of MICI. Observed calving of ice cliffs ~100 m above sea level in Helheim Glacier, East Greenland (Parizek et al., 2019), provides evidence for rapid ice loss by a rotational slumping mechanism that was suggested in a modeling study by Bassis and Walker (2012). The observations of Parizek et al. (2019) show how surface melting at the glacier front, driven by atmospheric forcing, results in basal crevassing that promotes rapid calving and ice loss (Figure 8). This slumping mechanism is relevant to smaller cliffs of 100 m in height above sea level, as opposed to the 200 m high ice cliffs collapsing under brittle failure in the model of

Pollard et al. (2016), and provides a mechanism to support rapid ice loss and sea level rise observed from a paleo sea level and perspectives for future ice sheet stability (e.g., Rohling et al., 2013). However, this MICI mechanism has not (yet) been observed in Antarctic glaciers.

MICI was proposed in an attempt to reconcile historical estimates of sea level with ice sheet model simulations. The study by Edwards et al. (2019) revisited the analysis of DeConto and Pollard (2016). Edwards et al. (2019) attempted to take into account model errors and the uncertainties in reconstructions of past changes in sea level. They were able to reconcile the model with proxy-based estimates of the Antarctic contribution to global sea level during the Pliocene Epoch and the LIG, even when using a version of the modeling framework that did not include MICI. However, the large and undefined nature of the uncertainties in the reconstructions mean that past changes in sea level have limited utility for constraining the physics of ice sheet models. It therefore remains a parameterized mechanism that requires further testing and validation involving field studies, model development, and the comparison of ice sheet models with paleoenvironmental and paleoclimate records with improved uncertainty constraints.

3.2. Ice Sheet Processes Influencing Ice Flow

Understanding the processes governing the flow of ice and its spatial and temporal variability is crucial for determining ice discharge from the AIS. Different processes influence ice flow in different regions of the ice sheet and at different spatial and temporal scales: viscous ice deformation (creep) operates throughout the ice sheet, dominating in regions where the ice is frozen to the bedrock below and on ice shelves, while basal processes (including basal sliding over a wet bed and bed deformation) dominate in fast-flowing areas, such as ice streams. The relative contributions of basal sliding and bed deformation to ice flow can vary both spatially (Bueler & Brown, 2009) and temporally (Stearns et al., 2008). The following section primarily focuses on recent developments in ice deformation relations and basal sliding laws. The development of these numerical descriptions relies on synthesis between observations, laboratory experiments, and numerical model simulations.

3.2.1. Ice Deformation

Ice deformation is a key process contributing to the large-scale flow of the AIS. Ice is a polycrystalline material that deforms in response to an applied stress. Deformation is dependent on the microstructural properties of ice crystals and the type of stresses applied (Budd & Jacka, 1989). Under prolonged exposure to the same type of stress, patterns of preferred crystal orientations (fabric) develop that are related to the nature of the stress configuration. The ice strain rates and fabric are both a function of the stress configuration, that is, the relative proportions of simple shear and normal stresses (Figure 6). Other factors, such as temperature and impurities, also influence flow rates. Laboratory experiments show that the type of stress applied to the ice mass is important to the overall ice flow regime, with the ice flow response to simple shear stresses greater than that under compression stresses (Treverrow et al., 2012). Developing and validating flow relations that incorporate these features of ice deformation and are appropriate for investigating large-scale AIS evolution requires a combined observational and modeling approach.

Studies of ice deformation have been widely used to investigate the relationship between applied stresses and corresponding strain rates. The pioneering laboratory work of Glen (Glen, 1952, 1953, 1955, 1958) and Nye (1953) on isotropic ice samples led to the development of an empirical power law flow relation for isotropic ice—the Glen flow relation—which is arguably the most widely used flow relation in numerical ice sheet models. Subsequent laboratory work (Steinemann, 1954, 1958) highlighted the importance of anisotropy (i.e., ice having a preferred crystal orientation) and microstructural properties of ice, following which numerous flow relations describing the steady-state creep of polar, anisotropic ice have been proposed. Broadly speaking, there are two general categories of flow relations for anisotropic ice: (1) those that directly account for the anisotropy through parameterization of specific properties of individual ice crystals driving deformation (e.g., Azuma & Goto-Azuma, 1996; Gagliardini et al., 2009; Gillet-Chaulet et al., 2005; Pettit et al., 2007; Placidi et al., 2010; Thorsteinsson, 2002) and (2) those that use empirical methods, describing the deformation of anisotropic ice as being consistent with the broad-scale stress configuration (Breuer et al., 2006; Budd & Jacka, 1989; Budd et al., 2013; Graham et al., 2018; Li et al., 1996; Treverrow et al., 2012; W. Wang et al., 2012). Flow relations in the former category rely on knowledge of the ice fabric at the crystal scale, often with an explicit evolution equation for the ice crystal fabric. However, flow relations of this type may be too computationally costly to be feasible for

continental-scale modeling applications over long time scales. As an alternative, most continental-scale ice sheet models use the Glen flow relation for isotropic ice, adding an ad hoc enhancement factor to account for the tertiary creep mode of deformation prevalent in polar ice sheets relative to the empirical relationships based on secondary creep laboratory data (Greve & Blatter, 2009). A recent idealized modeling study (Graham et al., 2018) showed that the Glen flow relation can distort ice shelf geometry and overestimate shelf flow compared with a flow relation for anisotropic ice developed from empirical studies (Budd et al., 2013; Graham et al., 2018), which has implications for its reliability in modeling AIS evolution and its contribution to sea level change.

Geophysical studies using polarimetric radar (Fujita et al., 2006; Matsuoka et al., 2003, 2012; B. Wang et al., 2018) and seismic (Diez & Eisen, 2015; Diez et al., 2014, 2015) systems have demonstrated that ice crystal fabric and microstructural properties that influence deformation play an important role in ice sheet and glacier evolution. For example, Matsuoka et al. (2012) used radar-derived estimates of ice crystal fabric and anisotropy to infer the migration history of the WAIS Divide between the Ross and Amundsen Seas, arguing that the strain history, and hence evolution, in this region has been consistent for the past five to eight thousand years. More recently, B. Wang et al. (2018) used ice crystal fabric and age information at Dome A, East Antarctica, to infer characteristics about the dynamics that controlled deformation in the past. Their results suggest that accounting for processes governing ice deformation is important in accurately dating englacial ice layers in the AIS and that ice deformation processes can provide alternative explanations for the formation and evolution of internal structures in the ice, with implications for estimates of past accumulation rates. Other studies have used seismic methods to demonstrate the importance of the ice fabric in influencing the dynamics of fast-flowing ice streams (Harland et al., 2013; Picotti et al., 2015; Smith, Baird, et al., 2017) and highlight the importance of accounting for the deformation of anisotropic ice in numerical simulations to accurately predict ice mass loss into the future.

3.2.2. Basal Motion

Basal motion arises from the processes of till deformation and from ice sliding over a wet bed. While these processes may occur simultaneously, they are mechanistically distinct, although both are influenced by conditions at the ice base: temperature, bed elevation and roughness, and meltwater pressure, volume, and evolution (section 4.2.3). Following Cuffey and Paterson (2010), we refer to the processes of basal sliding and till deformation collectively as "basal slip" and the relation used to describe these processes, that is, relating basal shear stress to basal velocity, water pressure, and basal conditions, as a "friction law."

A variety of friction laws has been developed to capture the relationship between basal shear stresses and sliding over a rigid bed. One of the most commonly used formulae (Weertman, 1957) is a power law relationship between basal shear stress and sliding velocities that includes a basal friction coefficient to represent bed properties. However, there are a number of limitations of the power law. First, laboratory studies show that the basal shear stresses are also dependent on the effective pressure at the base (Budd et al., 1979), which the Weertman-type friction law neglects. Second, basal shear stress magnitudes in power law relations are often unconstrained, despite observational evidence to indicate an upper limit. Other friction laws address these issues by explicitly including effective pressure to represent flow over a rigid bed with water filled cavities or an upper bound on basal shear stresses (Gagliardini et al., 2007; Lliboutry, 1968; Schoof, 2005). For example, Schoof (2005) proposed a regularized Coulomb friction law with cavitation, that is, the effect of pockets of liquid water between the ice and basal substrate, with an effective limit on the magnitude of the basal shear stresses, even for increasing basal sliding.

The friction laws described above account for basal slip over a rigid bed and do not include basal motion as a result of till deformation—this process generally being described in separate friction laws (e.g., Boulton & Hindmarsh, 1987; Bueler & Brown, 2009; Hindmarsh, 1997). Recently, Zoet and Iverson (2020) used laboratory experiments of ice motion over both hard and soft beds to develop a unifying friction law that accounts for basal motion as a result of sliding over a rigid bed and from till deformation. This friction law describes the dependence of basal shear stress on water pressure, basal sliding, and a transition velocity—an experimentally determined parameter that captures the ice speed at which till deformation begins. That is, below the transition velocity, basal motion occurs by sliding; at or above the transition velocity, basal motion occurs by sliding and bed deformation. There is evidence to suggest that this new friction law agrees well with observations of glacier surface velocities in Iceland and Greenland (Zoet & Iverson, 2020).

Being one of the most fundamental components of an ice sheet model, the friction relation can significantly impact the ability of the model to reproduce observed glacier behavior. Joughin et al. (2019) compared numerical simulations of Pine Island Glacier from 2002–2017 using a variety of friction laws and showed that a regularized Coulomb friction law (e.g., Schoof, 2005) produced the best match to observed patterns in grounding line retreat and glacier acceleration, due to cavitation effects. That is, the effect of cavitation reduces the sensitivity of the basal friction to speed, redistributing the stresses over a wider area. This result has implications for the choice of friction laws used in studies assessing future mass balance and sea level calculations.

Due to difficulties in directly observing the subglacial environment, there remain uncertainties in how to accurately parameterize friction laws in ice sheet models. This may be addressed using a technique called the adjoint (or control) method (MacAyeal, 1992b). For example, the adjoint method has been used to generate spatially and dynamically consistent values of the basal friction coefficients in friction laws through matching observed and modeled fields—usually the present ice surface flow field—for a given snapshot in time. The use of the adjoint method in this context has improved numerical model accuracy in matching observed fields, providing insight into the AIS dynamics and its evolution (Favier et al., 2014; Gillet-Chaulet et al., 2016; Morlighem et al., 2010, 2013). Nevertheless, errors and uncertainties may be introduced into the basal friction coefficient as a result of incomplete model physics and parameterizations, inaccuracies in fields used to initialize the model, and by way of its stationarity in time.

Technological advances may also provide the capacity to address uncertainties in friction law parameters. For example, tomographic radar systems (Jezek et al., 2013) that provides off-nadir swath coverage (i.e., data coverage beyond the single or series of lines from ice penetrating radar tracks) have been increasingly used to improve constraints on the cross track variation in bed properties that are useful for calculating basal roughness and water distribution (e.g., Rippin et al., 2011; Siegert et al., 2005). New methods have also been developed that allow for direct observations of the ice sheet base and subglacial hydrology drainage systems, through the use of chemical (Chandler et al., 2013) and electronic (Bagshaw et al., 2012) tracers, and the deployment of untethered sensors beneath the ice sheet utilizing wireless communications (Lishman et al., 2013).

4. Solid-Earth Interaction and Ice Sheet Bed Conditions

The solid Earth interacts with the AIS over time scales of hours to millions of years, and from local (i.e., kilometer) to global spatial scales (Figure 9). The long response time scales of solid Earth processes mean that these processes are currently out of equilibrium, and continue to adjust in the background, on top of the current climate forcing. It has long been understood that ice-solid Earth interactions are two-way: the solid Earth influences the ice sheet dynamics and properties through changing large-scale ocean and atmospheric circulation, basal geometry, and heat input; and the ice sheet affects the evolution of the solid Earth through erosion and sedimentation, GIA, and hydrogeology. However, recent research has revealed new spatial complexity of the interactions (e.g., Burton-Johnson et al., 2017; Martos et al., 2017) and relevance to Antarctica of mechanisms previously demonstrated elsewhere (e.g., Loose et al., 2018) and, in more than one case, more rapid interactions than previously thought (e.g., Barletta et al., 2018; Larour et al., 2019). The need to understand these interactions is pressing, especially with regard to the need to produce accurate projections of future sea levels. The following sections review the various interactions that have improved our understanding of AIS dynamics.

4.1. Template-Setting Interactions

The characteristics of the ice sheet bed are required to understand past and future AIS dynamics. These characteristics can be thought of as "template setting" interactions. A template-setting process is one that generates boundary conditions that are stable over the desired time scale, for example, glacial-interglacial time scales. For example, topographic controls include the elevation and morphology of the ice sheet bed (Fretwell et al., 2013), the geothermal heat flux across the ice-rock interface (Martos et al., 2017), and how these change through time due to erosion, sedimentation, and tectonic processes (Paxman et al., 2019). Accurate models of past ice sheet states demand a good understanding of these processes despite the fact that they evolve more slowly than other boundary conditions. Several recent studies focused on the

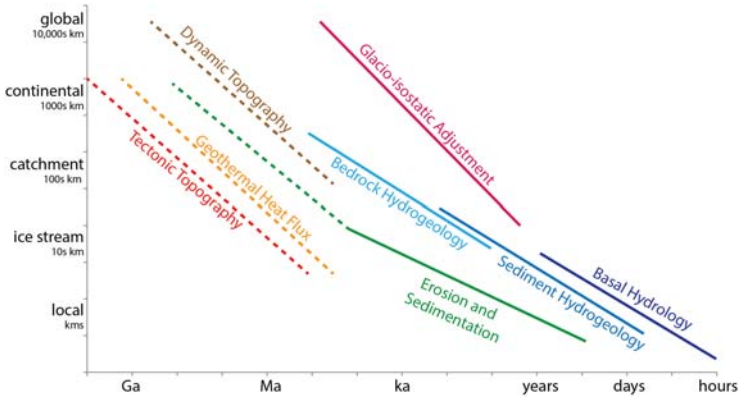


Figure 9. Earth processes and time scales. Illustrative plot showing typical length and time scale for ice sheet interactive processes at the base of the ice sheet. Template-setting (see text) interactions (dashed lines) occur over time scales of millions of years and direct interactions (solid lines) are short-term processes that result in a dynamic relationship between the ice sheet and surface processes of the solid Earth. Under typical conditions, these processes operate on length and time scales below and left of the line. Note the different scaling of the solid Earth processes relative to the surface processes. Threshold responses are not represented.

reconstruction of past periods of change, such as the last interglacial or the Pliocene as indicators for potential future ice sheet states (Cook et al., 2013; de Boer et al., 2015; Golledge, Levy, et al., 2017; Patterson et al., 2014). Knowledge of the nature of the ice sheet bed at these times has been inadequate to constrain such studies within acceptable bounds for them to be used in a predictive capacity. The following section reviews recent progress in understanding the long-term evolution of the basal boundary conditions to the AIS, including tectonically generated topography, geothermal heat flux, and dynamic topography.

4.1.1. Topography Resulting From Tectonic Processes

Tectonic processes, such as rifting, subduction, and mountain building, are the primary drivers of topography within the Antarctic continent and have determined the long-term evolution of the AIS (Figure 9). Most fundamentally, significant differences in the structure of the thick cratonic lithosphere and high viscosity mantle of East Antarctica and the thin lithosphere and low viscosity mantle of West Antarctica have caused substantial differences in topography (An et al., 2015a; O'Donnell et al., 2017) as well as in the response of the AIS to external climate forcing. These tectonic differences play a significant role in determining the rates and importance of feedback processes that affect ice sheet dynamics on medium to long time scales (Pollard et al., 2017).

Despite the substantial growth in knowledge of present day AIS topography, uncertainties in bedrock elevation (on the order of 100–1,000 m) can result in large differences in the retreat patterns of glaciers in key regions, such as the areas drained by the Recovery and Support Force Glaciers in East Antarctica (Gasson et al., 2015) and Pine Island Glacier in West Antarctica (Sun et al., 2014). Compounding these uncertainties, past ice sheet reconstructions may be affected by lack of knowledge of past tectonic movements.

Widespread rifting in West Antarctica has been linked to dynamic thinning of the WAIS (Bingham et al., 2012; Pritchard et al., 2009). The resulting subglacial topographic setting of the WAIS controls the ice sheet's susceptibility to MISI (Schoof, 2007; section 3.1) and has caused the WAIS, particularly in the Amundsen Sea sector, to be vulnerable to external climate forcing (Vaughan et al., 2011) (sections 2.1 and 5.2). These regions of tectonic activity have been preferentially eroded first by river systems and later during continental glaciation into deep troughs through erosion by ice streams across the continental shelf (Gohl, 2012). The Ross and Weddell embayments formed due to rift processes associated with Gondwana breakup. The Weddell Embayment ceased rifting in the Jurassic (Jordan et al., 2017) and has exerted only passive topographic control on AIS evolution. In contrast, the Ross Embayment experienced episodic rifting due to the West Antarctic Rift System (WARS) since the late Cretaceous and continues to show active rifting today in the Terror Rift, which has been active since the Miocene (Fielding, 2018; Fielding et al., 2008; Huerta & Harry, 2007). Neogene rifting is also suggested for the Amundsen Sea (Bingham et al., 2012; Jordan et al., 2010; Kalberg & Gohl, 2014).

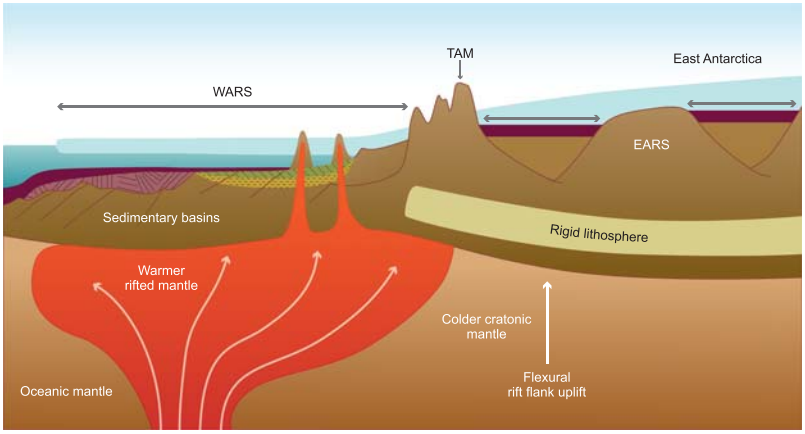


Figure 10. The role of tectonic processes on Antarctic topography. Schematic figure showing the effects of rifting, subduction, and mountain building on the current topographic relief of Antarctica. (WARS: West Antarctic Rift System; TAM: Transantarctic Mountains; EARS: East Antarctic Rift System).

Present accelerating AIS mass changes are focused in regions of active rifting that are characterized by continental shelves cross cut by deep troughs (e.g., overdeepened glacial troughs in the Amundsen Sea Embayment; Morlighem et al., 2020), which can be narrow or broad, with easily eroded sedimentary deposits, and elevated geothermal heat flux (Bingham et al., 2012; Buck, 1991). Narrow-rift processes create deep valleys, which are modified by fluvial conditions (Sugden & Jamieson, 2018) and are also are repeatedly exploited by ice streams over multiple glacial cycles. Well-defined troughs are created that today can route warm open ocean waters across the continental shelf to the interior of the WAIS (Joughin et al., 2014). Flanking high ground is also generated, which can further strengthen the topographic focusing (Egholm et al., 2017). Examples of this include some rapidly changing glacier systems that are currently shown to be most sensitive to ocean-atmospheric forcing (e.g., Pine Island Glacier and Ferrigno Glacier; Bingham et al., 2012; Jordan et al., 2010). In other cases, broader depressions do not show the same degree of topographic focusing but have high geothermal heat flux and well-lubricated sedimentary beds (e.g., Siple Coast and Thwaites Glacier) (Damiani et al., 2014).

Active rifting is also associated with upwelling of warm buoyant mantle and thermal support of the lithosphere, which varies over time. The warm rifted mantle of the WARS provides buoyant support to the Ross Embayment and may also partially support the Transantarctic Mountains (TAM) (Brenn et al., 2017; Graw et al., 2016) (Figure 10). Recent seismic studies in the Ross Sea suggest a complex seismic velocity structure in the lithospheric mantle (Accardo et al., 2014; Hansen et al., 2014; O'Donnell et al., 2017), indicating strong thermal heterogeneity. This implies a highly variable topography with different amounts of thermal uplift and subsidence throughout West Antarctica (see section 4.1.3). In addition, motion will occur at different rates associated with a variable viscosity in the mantle. Early paleotopography models accounted for thermal subsidence (Wilson et al., 2012) but did not capture these heterogeneities. Two recent studies have reconstructed paleotopography since circa 34 Ma, one from an iterative topographic reconstruction method (Paxman et al., 2019) and another based on subglacial sedimentary processes in an ice sheet model (Pollard & DeConto, 2019). Although more sophisticated than their predecessors, incorporating new process and including variable flexural rigidity, these models do not possess variable mantle properties. Incorporation of thermal support of topography and variable viscosity in the mantle is important to constrain past and future changes in subglacial topography associated with changing conditions of the AIS, and resolving the associated feedbacks into AIS dynamics, and thus future projections of ice sheet evolution and sea level change (Colleoni et al., 2018; Whitehouse et al., 2019).

East Antarctica is tectonically more stable than West Antarctica but has very substantial topographic variations (O'Donnell et al., 2017). New geophysical data sets have helped to resolve tectonic influences on topography extending back to the Archean in the form of compositionally buoyant Archean lithosphere that underlies much of East Antarctica (An et al., 2015b; Shapiro & Ritzwoller, 2004). Superimposed on this is a variety of morphologies associated with younger deformations. These include orogenic belts (e.g., the

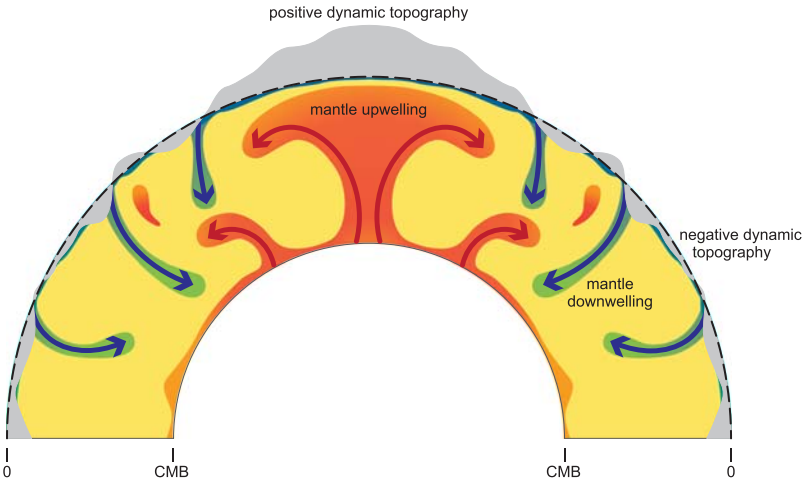


Figure 11. Dynamic topography. Schematic figure (not to scale) showing how heterogeneous deep mantle circulation alters the elevation of the solid Earth surface (gray); regions of hot mantle upwelling cause high dynamic topography and cold-mantle downwelling causes a low dynamic topography. CMB; core-mantle boundary. Figure drawn based on Kiefer and Kellogg (1998).

Gamburtsev Subglacial Mountains (Ferraccioli et al., 2011; Paxman et al., 2016) and various forms of rift basin, including narrow rift (e.g., the Lambert Trough; Phillips & Läufer, 2009), wide rifts (e.g., Wilkes Subglacial Basin; Jordan et al., 2013), and sag basins (e.g., Sabrina Subglacial Basin; Aitken et al., 2016). Thermochronology studies suggest that most of these features date back to at least the Mesozoic (e.g., Lisker et al., 2007), with focused Cenozoic erosion (S. N. Thomson et al., 2013), and therefore have had a passive influence on AIS development.

4.1.2. Dynamic Topography

Dynamic topography is the uplift or subsidence of the Earth's surface due to heterogeneities in mantle circulation (Figure 11), which cause long-wavelength topographic changes over million year time scales (Conrad, 2013; Flament et al., 2013) with typical magnitudes of hundreds of meters. The long time scales of dynamic topography, and the dependence on global mantle circulation patterns, means that it has a template-setting influence on ice sheet dynamics. Although dynamic topography does not possess direct feedbacks with ice sheet evolution (in contrast with GIA, section 4.2.2), a knowledge of past dynamic topography is nevertheless important for accurate reconstruction of the past AIS in two main ways.

The first is the global effect of dynamic topography on estimates of eustatic sea level (Dutton, Carlson, et al., 2015; Rowley et al., 2013). In this case, corrections to eustatic sea level beyond the last interglacial are significantly affected by dynamic topography (Dutton, Carlson, et al., 2015). The geoid (and hence regional sea level) is affected by dynamic topography on the order of tens of meters. Positive (negative) dynamic topography is associated with geoid highs (lows), although the underlying low-density mantle responsible may generate the opposite relation (Hager et al., 1985). With current levels of model uncertainty, a reliable correction cannot be made for past dynamic topography. Models can, however, provide indications of which areas may be most and least affected (Rowley et al., 2013) and so aid in avoiding misinterpretations. Comparison with ice-volume reconstructions (e.g., based on deep-sea benthic oxygen isotope ratios, which have their own uncertainties but are not affected by dynamic topography) may help with removing dynamic-topography influences from sea level benchmark data that are affected by crustal movements.

The second relates to dynamic topography in Antarctica itself. Raising or lowering relative topography impacts directly on the susceptibility of the AIS to marine instabilities (Austermann et al., 2015) and also to climatic influences. Global models suggest that the current topography of Antarctica may support as much as ±1 km of dynamic topography. Features in common for the present day include neutral to positive dynamic topography of the Indo-African sector of East Antarctica, neutral to negative dynamic topography in Wilkes Land, central East Antarctica, and the Weddell Sea, and high dynamic topography along the Pacific Margin (Conrad & Husson, 2009; Flament et al., 2013; Spasojevic & Gurnis, 2012;

Steinberger, 2007). These variations suggest that some of the topographic-induced sensitivities of the AIS, including MISI affecting the Wilkes Subglacial Basin, and the current high elevation of Dronning Maud Land, may have changed through time due to dynamic topography. However, dynamic topography within Antarctica has been explicitly addressed by only a few studies in the Scotia Sea and Ross Sea region (Nerlich et al., 2013; Spasojevic et al., 2010) and several studies on mantle-plume derived support of the Marie Byrd Dome (LeMasurier & Landis, 1996; Spasojevic et al., 2010; Wobbe et al., 2014).

The potential influence of dynamic topography on the AIS has been examined for the warm mid-Pliocene period (Austermann et al., 2015). The dynamic topography model used in this study predicted that topography was 100 to 200 m lower at 3 Ma, and the modeling results suggest that this lowering causes a destabilizing effect on the AIS. In the ice sheet model, an additional 200 to 560 km of grounding line retreat into the Wilkes Basin was found, relative to present-day topography.

The influence of past dynamic topography on the AIS depends on the direction and magnitude of dynamic topography change and also on the susceptibility of the ice sheet to relatively small changes in bed elevation (Austermann et al., 2015). Subglacial regions with deep narrow troughs may be little affected by dynamic topography, whereas regions with broader shallow depressions may be more affected. In the latter, slight overdeepening may allow greater ocean access to the ice sheet, as seen in the Wilkes Subglacial Basin modeling study (Austermann et al., 2015). Conversely, a similar magnitude change in the opposite direction may mean that once-vulnerable catchments are then better protected from MISI than before.

Dynamic topography is now widely recognized as a substantial driver of topographic change, with substantial impact on AIS sensitivity, and in our ability to understand past ocean and ice sheet changes. Despite this, a better understanding of how Antarctic topography has evolved under the influence of dynamic topography remains a significant challenge. Model uncertainties remain high, and the data needed to help reduce these uncertainties are sparse, especially within Antarctica. In the future, sensitivity studies will be important for constraining the timing and spatial scale of dynamic topography. In particular, quantitative models have substantial diversity at regional scales, which means that catchment-scale understanding remains very limited. An important goal is to define the potential sensitivity of the AIS to dynamic topography.

4.1.3. Geothermal Heat Flux

The range and spatial distribution of geothermal heat flux at the base of the AIS influences ice dynamics through changes in ice deformation from changing ice temperature, and via the production of subglacial meltwater, both of which affect the ice base, and thus flow of grounded ice (section 3.2.1). Except in rare circumstances, such as subglacial volcanism (Behrendt, 2013; Blankenship et al., 1993; van Wyk de Vries et al., 2017), geothermal heat flux is a stable feature of the geology on glacial to interglacial cycles, and changes little over millions of years. It is, however, affected by erosion or sedimentation and the topography, so paleoreconstructions may need to consider those influences. Despite being a stable condition over glacial to interglacial cycles, its interactions with the ice sheet may change rapidly as the thermodynamic setting of the interface changes (Loose et al., 2018). Under certain conditions, the thermodynamics of ice are very sensitive to heat flux, and a change in the overall thermodynamic system may lead to a changing association with the heat flux, despite the heat flux itself has remained stable. Therefore, a more accurate and precise knowledge of geothermal heat flux is required for greater confidence in understanding past and present basal conditions and the pattern of AIS flow.

There are no direct measurements of subglacial heat flux in East Antarctica and only a few from West Antarctica (Begeman et al., 2017; Fisher et al., 2015; Siple Coast). Measurements of thermal gradients within the ice support studies of the AIS, particularly in search for basal conditions that enable preservation of the oldest ice for climatic records modeled for ice core drill sites (Price et al., 2002, South Pole; Salamatin et al., 1998, Vostok). Temperature gradients within the ice have been used to suggest the contribution of heat from beneath but can only be trusted if the thermal conditions at the base are well known. In the case of offshore temperature gradients, these can be collected in a simpler and quicker manner than over the continent. These values can be useful to understand tectonic settings and lithospheric response of the continent if the measurements are acquired in close proximity to the coastal regions (e.g., measurements in the Amundsen Sea Embayment; Dziadek et al., 2017, 2019).

New drilling programs to access the base of the ice sheet (Goodge & Severinghaus, 2016) will increase the coverage of these data. However, point measurements of geothermal heat flux remain highly localized,

with high spatial variability due to the underlying geology and may not be representative of regional conditions.

Regional geothermal heat flux studies provide insight in the local thermal properties at the base of the AIS. Lateral variability of crustal heat production is used to refine models that assume constant values (Antarctic Peninsula; Burton-Johnson et al., 2017). Studies of Antarctic heat production include those from central East Antarctica (Goodge, 2018) and around Prydz Bay (Carson et al., 2014). Heat production data have been compiled in a recent study by Gard et al. (2019). Estimates of geothermal heat flux have also been derived from ice mass balance calculations in ice streams, heat flux derived by ice structure from radar data in Dome C (Parrenin et al., 2017), and analyses of hydrological conditions beneath Thwaites Glacier (Schroeder et al., 2014). These regional maps provide insight into key areas of change, but upscaling of these methods is difficult due to the highly localized nature of the information and limited access to continental bedrock.

Previous work has sought to improve continental-scale estimates of geothermal heat flux. Antarctic heat flow maps derived from temperature gradients based on seismic wave speed (An et al., 2015b; Shapiro & Ritzwoller, 2004), magnetic equivalent dipole models (Maule et al., 2005), and ice sheet models (Pollard & Deconto, 2012) showed continent-wide and/or regional discrepancies. Recently, however, Martos et al. (2017) derived a geothermal heat flux model from spectral analysis of airborne magnetic data to determine the depth to the Curie temperature isotherm. In particular, spectral methods were used to determine the magnetic structure of the lithosphere (in particular, depth of the Curie isotherm), from which the geothermal heat flux was estimated. This geothermal heat flux map (Figure 12) provides higher spatial variability compared with previous estimates based on other techniques (e.g., seismic, An et al., 2015a) and characterizes uncertainty in geothermal heat flux estimates. Higher heat flux is found in West Antarctica, where the majority of the volcanoes lie, while East Antarctica is mostly characterized by low heat flux values, in agreement with the cratonic nature of this part of the continent.

The large difference in geothermal heat flux estimates between East and West Antarctica are related to the tectonic evolution of these sectors. Subglacial volcanism can lead to rapid changes in the local geothermal heat flux, and the corresponding feedbacks with the ice sheet may lead to a more direct interaction (Behrendt, 2013; Blankenship et al., 1993; Loose et al., 2018; van Wyk de Vries et al., 2017). However, anomalously high geothermal heat flux has recently been reported for the South Pole region, where high heat producing Precambrian basement rocks and hydrothermal circulation along a major fault system have been reported (Jordan, Martin, et al., 2018). Alongside geophysical modeling, efforts have been made to estimate basal temperatures and basal melt rates by using ice sheet velocity models (Pattyn, 2010; Van Liefferinge & Pattyn, 2013), which suggest that the interior of East Antarctica represents a frozen bed while coastal East Antarctica and regions in West Antarctica are characterized by basal melting reaching up to 30 mm yr^{-1}, generally coinciding with higher geothermal heat flux locations (Figure 12).

Despite this recent progress in proxy-based methods and their application, resolving the geothermal heat flux still remains challenging. These methods complement each other, as each represents a different physical phenomenon, and the methods have different sensitivities in depth-sensitivity and spatial resolution. Each method also depends on a set of assumptions, and the impact of these on the modeled outputs is difficult to assess using the resulting geothermal heat flux maps. Not all studies and local estimates have provided uncertainties, which limits their usefulness. Notwithstanding potential errors, the differences in results may reflect different but complimentary facets of the complex system required understand Antarctica's heat flux. Higher-quality and more consistent geothermal heat flux models are needed to enable a more systematic knowledge of the geothermal heat flux on the generation of subglacial meltwater, the dynamics of subglacial hydrological systems, and their role in AIS dynamics. In addition, advanced sensitivity studies of geothermal heat flux with respect to basal temperatures and melt rates are needed to understand the influence of geothermal heat flux on ice sheet behavior, which depends strongly on the thermodynamic setting.

4.2. Direct Interactions

4.2.1. Erosion and Sedimentation

The erosion of rocks and the subsequent redistribution of sediments at the base of the AIS influences the sensitivity of the ice sheet to marine forcing, through changes in ice dynamics and sedimentary processes beneath ice shelves at the coastal margin, and on the continental shelf, over tens of millions of years down to subdecadal time scales (e.g., Bart et al., 2016). Broadly, we may separate erosion and sedimentation into

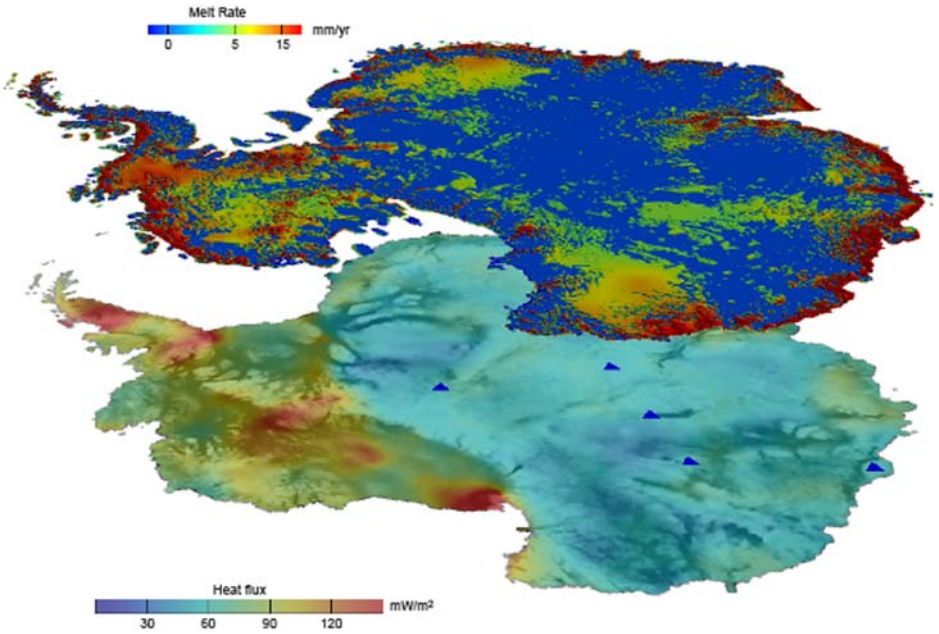


Figure 12. The upper map shows a model of the basal melt rate (Pattyn, 2010) with boundary conditions set by averaging three geothermal heat flux data sets from Fox Maule et al. (2005) and Shapiro and Ritzwoller (2004). The lower map shows the geothermal heat flux distribution of Antarctica modified from Martos et al. (2017). Blue triangles show the location of ice cores where rare vertical temperature profiles of the ice sheet exist.

longer-term systems that reconfigure the landscape over millions of years, setting the template for individual glacial cycles, and shorter-term systems that interact more directly with glacial and oceanic processes.

In general, local sedimentation shallows the bathymetry, while erosion deepens the bathymetry. Both processes may generate landforms that act to modify ocean circulation, and both may impinge on the ice shelf. The regional response to mass loading changes is dictated by flexural-isostatic processes, and it is common that focused erosion or deposition will generate a regional uplift or subsidence, respectively. In certain circumstances, the changing morphology of the seafloor is important in dictating access of CDW to ice shelf cavities, thus promoting or inhibiting MISI (Bart et al., 2016; Millan et al., 2017; Nitsche et al., 2017). Similarly, ridges and troughs formed through these processes dictate the likelihood of ice shelf grounding, and have a particular influence on calving (Arndt et al., 2018).

Relict eroded landscapes are evident in maps of subglacial topography throughout Antarctica (Fretwell et al., 2013; Morlighem et al., 2020). The degree to which this erosion is associated with fluvial or glacial action remains unclear (Paxman et al., 2019; Pollard & DeConto, 2019; Sugden & Jamieson, 2018). Geomorphological features on both the continental margin and buried under the ice can potentially be used to constrain past ice sheet models (Jamieson et al., 2014). Recent studies both onshore and offshore have tackled the mapping of these eroded landscapes, and, in some cases, their relationships with offshore depositional systems (Aitken et al., 2016; Gohl et al., 2013; Lindeque et al., 2013; Paxman et al., 2016; Young et al., 2011). In general, the landscapes that exist have the potential to be long-lived or more transient; however, limited exposures of these features (Sugden & Denton, 2004) prevent precise dating to establish when they were formed. Over the long term, sediment flux to the ocean has modified the topography of the continental shelf and shelf break. In particular, the continental shelf has been extended by up to 220 km over the past 34 Ma, with an overall increase in area of 7% (Hochmuth & Gohl, 2019). In the rest of this section we will focus on the more short-lived processes that interact most closely with the AIS.

Sedimentation during phases of grounding line retreat can form stabilizing grounding-zone wedges, which are subaqueous moraines at the terminus of ice streams (Alley et al., 1989; Batchelor & Dowdeswell, 2015). These form at the grounding line and can lead to a temporary pause in retreat (e.g., Alley et al., 2007; Jamieson et al., 2012; Ó Cofaigh et al., 2008) and may provide stable pinning points (Christianson

et al., 2016; Klages et al., 2017). Deposition of grounding zone wedges influence ice stream systems over time scales from a few hundred to a few thousand years (e.g., Bart et al., 2017; Graham et al., 2010; Jakobsson et al., 2012) and locally significant sediment erosion and redeposition can occur on time scales as short as years (Smith et al., 2007) to decades (Smith et al., 2012).

Early on, landward extent of bathymetric cross-shelf troughs was unknown (Hughes, 1977), but further research since then has shown that cross-shelf troughs, which can exceed 1,000 m water depth but are generally between 200 and 500 m deep (Patton et al., 2016), are indeed paleo-ice stream troughs extending beneath the modern AIS. These cross-shelf bathymetric troughs have been eroded repeatedly by the advance and retreat of paleo-ice streams and are found on the West Antarctic shelves in the Ross, Amundsen, Bellingshausen, and Weddell Seas (e.g., Belgica Trough, Ó Cofaigh et al., 2005; Ferrigno Trough, Bingham et al., 2012; Filchner Trough, Larter et al., 2012; Rosier et al., 2018; Thiel Trough, Fretwell et al., 2013; Pine Island-Thwaites paleo-ice stream Trough, Graham et al., 2010; Larter et al., 2014; Lowe & Anderson, 2002; and Thwaites, Holt et al., 2006, subglacial troughs). Overdeepened troughs that we know about from East Antarctica are less well defined and include along the Totten (Nitsche et al., 2017; Rintoul et al., 2016) as well as the Academy and Foundation ice streams from East Antarctica (Fretwell et al., 2013).

Cross-shelf troughs may increase the vulnerability of the ice sheet to melting at the grounding line by allowing CDW to penetrate directly to the WAIS margin (Bingham et al., 2012; Heywood et al., 2016; Jenkins et al., 2016; Nitsche et al., 2007; Turner et al., 2017). Historic erosion rates within these troughs may be as much as 1 m yr^{-1} where the bed is weak (Smith et al., 2012). Repeated selective erosion over glacial to interglacial cycles within these troughs may total kilometers in magnitude since the Eocene (Wilson et al., 2012). An important factor is the width of the basin in which erosion is focused.

Narrow basins exert strong topographic focusing on ice flow, which efficiently focuses erosion within the trough (Egholm et al., 2017; Jamieson et al., 2005; Maritati et al., 2016; S. N. Thomson et al., 2013). Over time, selective erosion is associated with an isostatic-flexural uplift that will be accommodated over a broader region. This character leads to increasingly focused ice sheet flow through time as the elevated flanks become cold based, but the lows become more susceptible to either MISI, if marine terminating (Golledge, Levy, et al., 2017; S. N. Thomson et al., 2013), or to the development of connected subglacial hydrological systems (section 4.2.4).

In contrast, relatively broad basins, in particular the Wilkes Basin and Ross Embayment, may allow retreat to occur along broad fronts, with more poorly focused ice streams, resulting in erosion across broad regions, and relatively subdued trough development (Aitken et al., 2016; Cook et al., 2013) and/or the development of regional unconformities (Bart, 2003; Bart et al., 2000; Bart & de Santis, 2012; Brancolini et al., 1995, 1997; De Santis et al., 1999). In such cases, erosion over time may act to enhance future vulnerability to change as the eroded region forms a broad subsided region increasingly susceptible to MISI processes. Concurrently, the deposition of sediments in a prograding shelf edge will extend the shelf and increase the distance to the source of CDW and may contribute to the shallowing of the shelf break, inhibiting CDW incursion. With respect to AIS stability, these regional negative feedbacks may counteract the increased ocean access provided by the deeper bathymetry. With a degree of selective erosion, and the associated topographic feedbacks, a broad erosional system may evolve into a more selective system, with uplifted regions developing adjacent to troughs (Egholm et al., 2017; Kessler et al., 2008).

4.2.2. GIA

GIA is the solid Earth response to past ice-ocean surface loading changes that resulted in deformation of the solid Earth and geoid and in changes to the location of Earth's rotation pole and spin rate (Mitrovica et al., 2009). Due to the viscous properties of the mantle, changes in surface loading at a given point in time continue to produce effects for thousands of years (Figure 13). For example, the Earth is continuing to respond to the rearrangement of surface mass loading following the LGM (27–19 ka); this response is measurable and important to consider when interpreting data that give insight into past and present geophysical processes (Peltier, 2004). Past and present-day observations of change in geophysical parameters can also help to inform our understanding of Earth's rheology and ice-ocean load history (Argus, 1996; Barletta et al., 2018; Chen et al., 2013; Milne et al., 2001; Mitrovica et al., 2006).

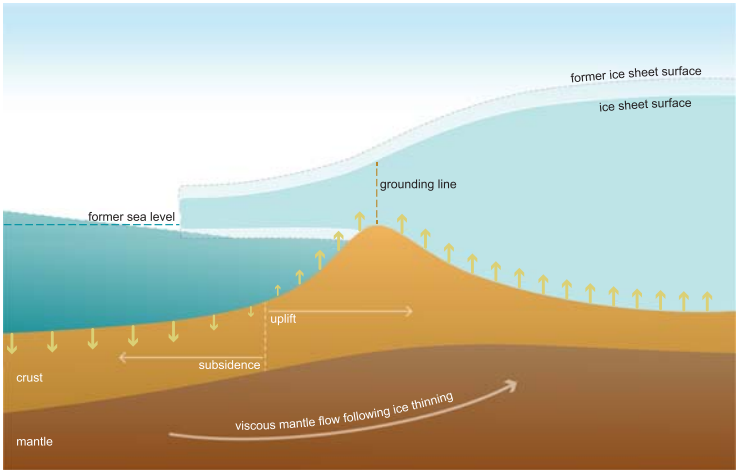


Figure 13. Local glacial isostatic adjustment (GIA) schematic. Following ice loss, the loss of gravitational attraction immediately draws down the local sea surface, and over slower response time scales the solid Earth uplifts elastically in the vicinity of the region of ice loss, leading to a sea level fall near the ice sheet grounding line. On longer time scales, the Earth viscously deforms toward isostatic equilibrium, leading to further uplift and sea level fall under the region of ice loss (upward pointing yellow arrows) and a subsidence of peripheral bulges in surrounding regions (downward pointing yellow arrows). If the grounding line were to retreat beyond the bedrock high it currently rests on, it would be in an unstable configuration due to MISI processes. The grounding line may then be subject to irreversible retreat. The aforementioned sea level fall acts against the MISI, acting to slow or stop grounding line retreat. The importance of this sea level feedback depends on the shape and depth of the bed beneath the ice, the nature of the climate (oceanic and atmospheric) forcing on the ice sheet, and the Earth viscosity structure. The viscosity structure determines the timing and spatial pattern of deformation in response to ice loss and varies by several orders of magnitude in three dimensions across the Antarctic continent.

Accurate sea level projections and measurements of present-day sea level change cannot be obtained without knowledge of GIA. However, Antarctic GIA is poorly constrained by data. Limitations in GIA models for Antarctica stem from large uncertainties in AIS evolution during past glacial to interglacial cycles (section 5.2) and the response of the solid Earth determined by the structure of the lithosphere and mantle (section 4.1). Advances have been made in understanding the interaction between the solid Earth response that results in grounding line migration and near-field sea level change; improved seismic data coverage and more Global Positioning System (GPS) and Global Navigation Satellite System (GNSS)-derived surface deformation measurements; and the inclusion of three-dimensional (3-D) Antarctic rheology, which determines the deformation of the bedrock topography beneath the ice sheet and varies according to the viscoelastic properties of the Earth (Gomez et al., 2018), into GIA models.

Study of Antarctic GIA has intensified over the past two decades as a result of the launch of the Gravity Recovery and Climate Experiment (GRACE) and GRACE Follow-on (GRACE-FO) satellite missions that have a primary aim of measuring ice sheet contributions to sea level change (Tapley et al., 2004). However, the accuracy of GRACE-derived estimates of AIS mass change rely on the accuracy of background models of other mass-change processes, with GIA the dominant "contaminating" signal, which is of a similar magnitude to the estimated ice mass change (King et al., 2012; Velicogna & Wahr, 2006). More recently, the potential for GIA processes to alter ice sheet dynamics has been suggested, leading to the development of a new class of models that couple ice sheet and GIA processes (Adhikari et al., 2014; De Boer et al., 2014; Gomez, Mitrovia, Huybers, et al., 2010, Gomez et al., 2012, 2013, 2015, 2018; Konrad et al., 2015, 2016).

Incorporating GIA processes into ice sheet and sea level models drives a significant advance in the understanding of AIS dynamics. GIA feedbacks on ice sheet evolution were first investigated by Gomez, Mitrovia, Huybers, et al. (2010), who coupled a canonical MISI model to a model of the sea level equation (Farrell & Clark, 1976) that considers both the solid Earth response to ice mass change and the consequent changes to the geoid and hence regional sea level. Ice mass loss associated with ice sheet retreat leads to regional bedrock uplift and a drop in the sea surface gravitational equipotential, producing a combined effect of sea level lowering at the ice sheet grounding line that impacts ice flow (Figure 13). Gomez, Mitrovia,

Huybers, et al. (2010) and Gomez et al. (2012) adopted a simplified ice sheet stability model and in turn a flowline model of ice dynamics to show that this sea level feedback could slow or even stabilize ice sheet grounding line retreat on retrograde bed slopes, a configuration regarded as fundamentally unstable (e.g., Schoof, 2007; Weertman, 1972; section 3.1.2). Building on this, realistic 3-D ice sheet models have been coupled with GIA models that consider 1-D Earth rheologies to explore the potential effect on ice retreat (De Boer et al., 2014; Gomez et al., 2015, 2013; Konrad et al., 2014). These coupled models demonstrate that GIA effects are important in modeling past and future ice sheet changes, notably acting to slow or limit future and Pliocene ice sheet contribution to sea level, with strong sensitivity to the Earth model adopted in the GIA models (Gomez et al., 2015; Pollard et al., 2017).

Coupling between ice sheet models and solid Earth models with a gravitationally consistent description of sea level is an active area of research. Challenges lie in correctly translating between the different model grid types. For example, ice sheet models use regional Cartesian grids, and solid Earth models operate on global Gauss-Legendre grids. Many solid Earth models operate in the Laplace domain (see glossary). However, some now use explicit time stepping to evolve the solid Earth dynamics and are therefore less computationally expensive (e.g., Konrad et al., 2014). GIA changes have been incorporated into ice sheet models to resolve grounding line dynamics so that the ice sheet and sea level varies consistently in space and time (De Boer et al., 2014; Gomez et al., 2018, 2015, 2013; Konrad et al., 2015). These studies highlight the negative feedback associated with a more realistic viscoelastic deformation of the solid Earth and stabilization of MISI in West Antarctica with a coupled ice sheet-sea-level model. de Boer et al. (2017) provide an overview of the recent developments in coupled ice sheet-sea-level modeling and emphasize how synthesis between two distinct disciplines—GIA and ice sheet dynamics—can greatly enhance our understanding of the interactions between sea level change and ice sheet dynamics.

Modeling GIA processes requires knowledge of the temporal evolution of past ice-ocean load changes and Earth's rheological properties. For Antarctica, both are sparsely observed and are highly uncertain; as a consequence, models of Antarctic GIA are also highly uncertain with large intermodel differences. In particular, the post-LGM ice loading history for Antarctica is sparsely observed in space and time (Bentley et al., 2014; Whitehouse, Bentley, & Le Brocq, 2012), as demonstrated by the wide range (~5–23 m) of recent estimates of Antarctica's contribution to post-LGM sea levels (Argus et al., 2014; Lambeck et al., 2014; Pollard et al., 2016) (see section 5.2). Nonetheless, substantial advances have been made in modeling GIA processes in recent years, and these have contributed to improved understanding of ice sheet mass balance (Shepherd et al., 2012; 2019).

A range of observations is useful in improving and/or validating GIA models, including proxy observations of past ice extent and ice retreat history, proxy, and tide gauge measurements of local and far-field post-LGM relative sea level (RSL), ancient and geodetic observations of Earth's rotation pole, and geodetic observations of solid Earth deformation and gravity changes (Mitrovica et al., 2009; Tamisiea et al., 2014). These may be separated into local and global-scale observations: relevant to Antarctica are paleo RSL data from less than 20 sites across Antarctica (Whitehouse, Bentley, Milne, et al., 2012), spanning the last 12–15 ka, and GPS-derived surface deformation measurements at approximately 80 sites with varying time series quality and length (Martín-Español, Zammit-Mangion, et al., 2016). Sediment records of RSL for the period before 15 ka to the LGM are lacking but can be preserved within isolated basins, where lake sediment cores record the transition from marine outlets or basins during the glaciation to freshwater lakes following deglaciation, as isostatic rebound outpaced eustatic sea level rise (Hodgson et al., 2016; Roberts et al., 2011).

GPS and GNSS deployments on bedrock outcrops in Antarctica provide estimates of bedrock uplift rates that are used to validate GIA models and understand missing processes through identification of differences in the magnitudes of the predicted uplifts and their spatial patterns (Bevis et al., 2009; Groh et al., 2012; Thomas et al., 2011). Ice sheet reconstructions have been improved by new evidence from ice sheet history proxy data that the LGM volume of the WAIS was smaller than previous estimates (Whitehouse, Bentley, & Le Brocq, 2012). Results from dynamic ice sheet modeling driven by climatic changes also support a smaller LGM AIS volume (e.g., Pollard et al., 2016). These new AIS history proxy data are not uniformly accepted as reliable constraints on past ice history. Consideration of AIS volume required to explain LGM sea levels that account for global ice sheet contributions indirectly suggests a larger (23–30 m) contribution from Antarctica, based on a global sea level budget approach (Lambeck et al., 2014). Nonetheless, based on these

ice proximal data, a new generation of GIA models has been developed (Ivins et al., 2013; Whitehouse, Bentley, Milne, et al., 2012) that predict present-day GIA uplift velocities substantially closer to observed GPS/GNSS velocities than the previous generation. In combination with GRACE measurements, these models yield a systematically smaller estimate of AIS mass loss during the last deglaciation (Argus et al., 2014; Ivins et al., 2013; King et al., 2012) compared to Lambeck et al. (2014). However, these 1-D GIA models are unrealistic based on seismic tomographic constraints on Earth rheological structure, which show substantial rheological variation, notably between East and West Antarctica but also within the regions (Kaufmann et al., 2005).

Seismology is unable to determine the absolute mantle viscosity. Since 2014, geodetic studies of surface displacement in Antarctica have provided constraints on this missing information. Thomas et al. (2011) demonstrated nonlinear deformation of the northern Antarctic Peninsula associated with ice mass loss that was initiated by the breakup of the Larsen B Ice Shelf. This nonlinearity could be explained by a model of viscoelastic deformation, with local upper mantle viscosities of $<3 \times 10^{18}$Pa s (Nield et al., 2014). This is around 2 orders of magnitude lower than conventionally adopted viscosities in global GIA models. Meanwhile, 500 km further south, upper mantle viscosities were estimated to be at least 1–2 orders of magnitude higher (Zhao et al., 2017). Higher viscosities have also been suggested in the southwest Weddell Sea region (Wolstencroft et al., 2015) and the Siple Coast (Nield et al., 2016). Considering the spatial pattern of change and high bedrock uplift rates measured by GPS/GNSS, the Amundsen Sea Coast region has also been suggested to be underlain by low-viscosity mantle (Groh et al., 2012), and this has been confirmed using a more dense network of 3-D displacement measurements (Barletta et al. 2018). In contrast to West Antarctica, no geodetic constraints are available for East Antarctica although there is a consensus supported by seismic studies and geological history of the region, which suggests that, aside from some localized regions where the viscosity could be as low as 10^{18} Pa s, East Antarctica is underlain by high viscosity mantle and is responding slowly to LGM-time scale changes in ice loading.

Global and regional seismic studies indicate substantial 3-D variations in Antarctic rheology, both between and within East and West Antarctica. Regional seismic tomography studies have improved our knowledge of upper mantle structure and spatial variation (An et al., 2015b; Chaput et al., 2014; Heeszel et al., 2016; O'Donnell et al., 2017). These seismic data indicate that effective upper mantle viscosity may vary by 3–4 orders of magnitude across Antarctica, with values as low as 10^{18} Pa s in parts of West Antarctica (O'Donnell et al., 2017). Such low viscosities, if realistic, suggest relaxation times in the upper mantle on the order of decades compared to the conventional understanding of thousands of years, as well as more smaller spatial scale patterns of deformation. However, LGM-scale ice loading changes will have perturbed the lower mantle, producing deformation patterns on millennial time scales and large spatial scales in addition to the deformation occurring in the upper mantle over smaller spatial scales and shorter time scales.

Including lateral variation in GIA models produces distinctly different spatiotemporal patterns of deformation and associated gravity field change (Kaufmann et al., 2005; King, Whitehouse, & van der Wal, 2016; van der Wal et al., 2015). For example, regions of lower than average upper mantle viscosity and a thinner lithosphere such as the in the Amundsen Sea Embayment (Barletta et al., 2018) result in faster viscous deformation toward isostatic equilibrium that is more localized to the region of ice loading changes. Various approaches have been used to convert seismic tomography models into mantle viscosity, but uncertainties in these approaches result in a wide range of model predictions (e.g., van der Wal et al., 2015), and independent data are required to validate models. One characteristic of 3-D models is that the spatial gradients of deformation are larger, and peak uplift and subsidence are more smoothed than in 1-D models (Nield et al., 2018).

The presence of low upper-mantle viscosity in parts of West Antarctica, including the Antarctic Peninsula, implies a strong dependence of present-day GIA on late Holocene or centennial-scale ice loading changes; this is particularly problematic for modeling studies because almost no Antarctic paleoproxy data exist for this period. Certain regions may have experienced substantial changes in ice cover during the Holocene with retreat beyond modern grounding lines followed by readvance (Bradley et al., 2015; Kingslake et al., 2018; Siegert et al., 2013). For example, field data and modeling have been combined to suggest that ice streams in the Siple Coast region and in the Weddell Sea Embayment have readvanced in the last few thousand years and that this readvance may have been due to a GIA feedback (Kingslake et al., 2018; Siegert et al., 2019).

However, these simulations used an upper mantle viscosity of 5×10^{20} Pa s, which is unrealistically high for West Antarctica—by perhaps as much as two orders of magnitude. Kingslake et al. (2018) find that even reducing the viscosity to 1×10^{20} Pa s prevents this response because, "the bed responds too quickly to ice unloading." The most widely adopted global and regional GIA models assume no ice loading change over the last 2 to 4 ka; therefore, predictions of present-day deformation and GIA in West Antarctica, including the Antarctic Peninsula, remain highly uncertain. This has been highlighted by inverse solutions for GIA based on satellite altimetry, and GRACE and spatially continuous GPS/GNSS measurements (Gunter et al., 2014; Martín-Español, Zammit-Mangion, et al., 2016; Riva et al., 2009; Sasgen et al., 2017). These models show many of the features of the forward models, although without a clear convergence between the inverse solutions or with a particular forward model (Martín-Español, Zammit-Mangion, et al., 2016). However, inverse models consistently demonstrate rapid uplift, for instance, in the Amundsen Sea region that is compatible with the GPS estimates, and have been demonstrated through modeling to originate purely from unloading due to ice mass loss since 1900 CE (Barletta et al., 2018).

The negative feedback between ice dynamics and bedrock uplift has the potential to stabilize dynamic retreat of vulnerable WAIS glaciers such as the Thwaites and Pine Island Glaciers over a multicentennial time scales (Gomez et al., 2015; Larour et al., 2019). A high spatial resolution (1 km) modeling approach for the ice sheet grounding line migration in response to rapid elastic uplift demonstrated a significant increase in elastic uplift rates (10 cm $year^{-1}$) beyond 2300 CE (Larour et al., 2019).

The implications of 3-D variations in Earth structure on ice dynamics are just beginning to be explored. Given the substantial lateral structural variability beneath the Antarctic, 1-D Earth models are unable to accurately capture the response of the Earth to, and feedbacks on, changes in ice loading across the whole continent. In regions of lower viscosity and thinned lithosphere, uplift in response to ice unloading will take place faster and be more localized to the ice sheet grounding line, where it can more effectively slow ice sheet retreat. Building on earlier work, Gomez et al. (2018) developed a coupled model incorporating 3-D variations in Earth structure and applied it to the last deglaciation, showing substantial local differences in predicted ice cover, sea level, and Earth deformation between simulations adopting a 3-D Earth model and those using average 1-D Earth models. They also found that it will be important to consider the impact of 3-D Earth viscosity structure in future ice sheet projections, particularly given the low viscosities in regions of expected future ice sheet retreat. Hay et al. (2017) adopted a sea level model with 3-D Earth structure to show that viscous Earth deformation, which is typically neglected in sea level projections on century time scales, will increase sea level fall in regions of ice loss by up to 50% in 100 years, thereby contributing to the negative feedbacks acting on grounding line dynamics.

4.2.3. Basal Hydrology and Fluid-Interchange Processes

The presence or absence of liquid water at the ice sheet bed, as well as its distribution, influences ice sheet flow and discharge and thus affects mass balance (e.g., Ashmore & Bingham, 2014; Bell, 2008, and references therein; Siegert et al., 2017). Understanding the nature of the ice sheet bed is essential to understanding AIS dynamics and in particular to accurately model flow over a variably rough and partially lubricated substrate (section 3.2). Factors influencing the subglacial hydrology include the ice overburden pressure, subglacial topography, and production and removal of meltwater. New research shows that hydrological systems consisting of active lakes and channel networks are a near-ubiquitous feature of Antarctica, and a significant driver of AIS dynamics (Ashmore & Bingham, 2014; Bell, 2008; Fricker et al., 2016; Kirkham et al., 2019; Siegert et al., 2016; Smith, Gourmelen, et al., 2017; Stearns et al., 2008).

Subglacial fluid transport networks can form continuous or semicontinuous flow paths from the interior of the ice sheet to the grounding line (Ashmore & Bingham, 2014). These can provide a direct connection between the inland ice sheet and sub-ice shelf cavities (Figure 14). The discharge of freshwater to ice shelf cavities can affect ice shelf dynamics by increasing basal sub-ice shelf melting rates (e.g., Le Brocq et al., 2013) and changing the buoyancy-driven ocean circulation (section 2.2.2). Recent work to map, interpret, and model subglacial hydrological systems has resulted in new insights into (1) the role of basal accretion processes in modifying ice sheet thickness, (2) flow network topologies and their influence on ice flow, (3) the role of active lake systems in providing time-variable fluid flux, (4) the nature of the interaction of freshwater melts with ice shelves and their cavities, and (5) the development and validation of new subglacial hydrology modeling approaches.

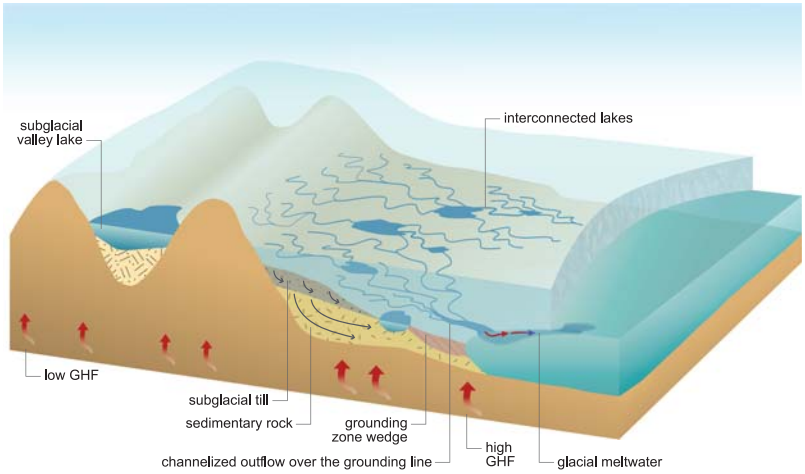


Figure 14. Basal hydrology and fluid-interchange processes. Schematic showing channelized subglacial drainage network (after Ashmore & Bingham, 2014) beneath a major ice stream. The cross section shows subglacial lakes and channels, and active subglacial hydrogeology in sedimentary sequences. A basal channel in the ice shelf cavity reflects a localized input of fresh meltwater to the cavity that will impact on the sub-ice-shelf melt rates, particularly at the grounding line, which will in turn affect the ice stream behavior (e.g., Le Brocq et al., 2013). Red arrows represent variable geothermal heat flux (GHF) interacting with the base of the ice sheet to produce meltwater.

A wide range of subglacial flow topologies has been observed beneath the AIS, which may have a role in stabilization and destabilization of glaciers. These flow network topologies include distributed flow, where water is transported diffusely across a broad region of the bed; and channelized flow, where the flow is concentrated into discrete channels incised either into the ice (Röthlisberger, 1972) or into the substrate below, forming channels (Nye, 1976) or tunnel valleys (Kehew et al., 2012) (Figure 14). The flow network topology beneath the ice sheet is affected by variations in subglacial environment, including the geothermal heat flux, subglacial topography and substrate composition, and presence of meltwater. The downstream switch from distributed to concentrated channels, for example, observed in the upstream and downstream sections of the Thwaites Glacier (Schroeder et al., 2013), results from characteristics of the substrate and changes in surface slope, meltwater flux, and basal shear stress. It is not clear the extent to which the distinct anisotropy imaged at Thwaites Glacier is a general rule; however, the tendency for channelized flow increases from the ice sheet interior to the margin, as meltwater flux increases (Ashmore & Bingham, 2014). A more distributed flow network topology is associated with more variable behavior in ice stream dynamics, as seen in the Siple Coast (Bougamont et al., 2015). Subglacial hydrology models have been shown to be able to capture the transition from distributed to channelized flow, agreeing well with specular reflection estimates derived from radar echo sounding used to detect the transition in hydrological flow (Dow et al., 2020).

Basal accretion of ice by refreezing of subglacial water influences the thickness and flow characteristics of the EAIS. A key example of these basal accretion mechanisms is found in the Gamburtsev Subglacial Mountains, where alpine-like valleys are well preserved by current ice sheet processes (Bo et al., 2009; Creyts et al., 2014; Rose et al., 2013). In this system subglacial meltwater is formed in the deeper valley bottoms and is driven through pressure gradients up the ancestral drainage paths toward the valley heads, where it encounters thin ice and freezing conditions (Creyts et al., 2014). The accretion of ice occurs through two main processes. Conduction-dominated freezing is driven by the increasingly cold conditions toward the ice sheet surface, which cause ponded water to freeze; glaciohydraulic supercooling is driven by the reduction in pressure associated with flow up a steep gradient (Alley et al., 1998; Creyts et al., 2013). The role of basal accretion in the overall evolution of the ice sheet remains poorly defined. However, observations suggest that basal accretion is an important process in ice dynamics in some areas, and that it has operated over long time scales (Bell et al., 2011).

Active subglacial lake systems beneath the AIS can modify the flow of ice streams and outlet glaciers depending on the mechanism of lake drainage. Drainage events from active lake systems have been observed to influence ice sheet dynamics at several locations including Byrd Glacier (Victoria Land) (Stearns

et al., 2008), Whillans Ice Plain (Siple Coast) (Siegfried et al., 2014), Crane Glacier (Antarctic Peninsula) (Scambos et al., 2004), and Cook Glacier (McMillan et al., 2013; Miles et al., 2018). The incorporation of lake drainage processes in subglacial hydrology models is still under development. Understanding of lake drainage processes in Antarctica is based largely on theories for the drainage of lakes in alpine environments (e.g., G. K. C. Clarke, 2003; Nye, 1976; Werder et al., 2013), with knowledge that the spatial and temporal scales over which the subglacial network evolves are greater in Antarctica (Fricker et al., 2007). However, the validation of lake drainage mechanisms in Antarctica is difficult in the absence of comprehensive observations of the subglacial environment. A new model by Carter et al. (2017) for the AIS suggests a lake filling phase is followed by distributed flow once the lake level reaches a maximum, after which channelized flow develops during peak outflow conditions. The filling phase is likely associated with slowed ice sheet flow downstream, through the withdrawal of basal water from the hydrological system, and an associated increase in basal shear stress (B. E. Smith et al., 2009). Conversely, the drainage phase is associated with accelerated flow downstream, with reduced basal shear stress (Fricker et al., 2016). Although these concepts have been defined and modeled, much uncertainty remains regarding their spatial and temporal frequency, and the intensity of active lake drainage events on large-scale AIS dynamics. The same applies to Antarctic subglacial lake environments and processes in general, which are still mainly inferred from theoretical considerations, combined with findings from ice accreted at the roof of subglacial Lake Vostok (Karl et al., 1999; Shtarkman et al., 2013; Siegert et al., 2001), ice penetrating geophysical data (e.g., Smith et al., 2018), and or the paleorecord (Kuhn et al., 2017). However, recent drilling projects, such as drilling of the Subglacial Lake Whillans as part of the WISSARD project (Christner et al., 2014; Hodson et al., 2016; Michaud et al., 2016), and Subglacial Lake Mercer on behalf of the SALSA project (https://salsa-antarctica.org/), may soon have the potential to answer many open questions.

The transport of freshwater to the ice shelf cavity can have profound impacts on ice shelf basal melt rates (Jenkins, 2011; Le Brocq et al., 2013), ice streaming (Stearns et al., 2008), ocean stratification and mixing, and nutrient fluxes (Corbett et al., 2017). For example, Le Brocq et al. (2013) used satellite and airborne remote sensing to identify large channels under the Filchner-Ronne Ice Shelf. These channels likely formed due to the discharge of cool, fresh subglacial hydrological meltwater entering the sub-ice shelf cavity at the grounding line. Being fresh relative to the ocean water, this fresh subglacial meltwater rises to the ice shelf boundary layer, entraining warm ocean water that enhances ice shelf melt rates. However, another assessment by Alley et al. (2016), which mapped the basal channels in the ice shelves surrounding Antarctica, found that the majority of channels in regions undergoing rapid change and ice mass loss, for example, the Amundsen Sea sector, are more likely generated by ocean-driven mechanisms alone rather than by subglacial hydrology processes.

Concerted efforts over recent years have led to the development of numerical models that simulate the spatial and temporal variability in Antarctic subglacial hydrological networks (Carter & Fricker, 2012; Dow et al., 2016; Le Brocq et al., 2009). Nevertheless, due to a paucity of observations, validation of these models is difficult, in particular with respect to the dynamics governing their development, evolution, and feedbacks to ice sheet dynamics. Efforts to improve model physics and represent the processes governing drainage systems are ongoing, through initiatives such as the Subglacial Hydrology Model Intercomparison Project (SHMIP; De Fleurian et al., 2018). Furthermore, the application of coupled subglacial hydrology/ice sheet models will enable sensitivity studies on relatively poorly known hydrological parameters and boundary conditions (Werder et al., 2013). Combining numerical modeling efforts with field measurements into the future is an essential step toward a systematic understanding of subglacial hydrology and ice sheet dynamics in Antarctica.

4.2.4. Hydrogeology Within the Subglacial Bed

Fluid exchanges across the ice sheet bed, and interactions with the groundwater beneath, are likely to be common in Antarctica and may have a substantial impact on regional ice sheet dynamics (Gooch et al., 2016; Person et al., 2012). Currently, this aspect of ice sheet behavior is not captured in large-scale ice sheet models. Subglacial water at the base of the ice sheet is subject to several forms of exchange with the subglacially eroded, transported, and deposited sediments (till) and permeable bedrock that underlies the till and the ice sheet. Fluid exchange occurs across the bed on a variety of depth and time scales. Here we make a distinction between hydrogeology of the till that is characterized by a thin layer of very high permeability and low-rigidity sediments operating on short time scales and bedrock-aquifer exchange that is characterized

by deeper storage, lower permeability, and higher rigidity strata, operating on longer time scales. The presence of relatively weak sedimentary strata is an important precondition for the development of a till-rich bed (Anandakrishnan et al., 1998; Bell et al., 1998), so that these hydrogeological systems are likely connected over longer time scales.

The existence of water-saturated and easily deformed till at the base of the AIS was identified in key studies of the Siple Coast region (Alley et al., 1986; Blankenship et al., 1987; MacAyeal, 1989). Recent studies there have continued to define the hydrogeology of till beds, with particular developments in the understanding of hydrogeological processes in the stagnation and reactivation of ice streams, including interactions between the ice sheet, water, and till. Important factors include the mechanical behavior of till, which can absorb and release water under ice sheet loading and influence basal friction (Christoffersen et al., 2014). Till loading time scales include weeks to months as a result of tidal loading, causing till compaction with the accumulation of tidal effects (Christianson et al., 2013; Leeman et al., 2016). The response of till to tidal loading is suggested as a key factor in stabilizing the grounding zone as the till becomes dewatered and stiffer under repeated loading (Christianson et al., 2013). Till loading can also be impacted on decadal time scales as a result of the distribution and routing of water, which can influence ice sheet flow due to changes in the distribution of highly consolidated and unconsolidated till units associated with hydrological changes. This flow reorganization will be most substantial where ice streams are defined by the dynamics of flow rather than by topography, and water is more easily transferred from one ice stream to another. Overall, AIS dynamics are highly sensitive to the hydrogeology and mechanics of till layers, with processes that operate rapidly but are associated with substantial reorganizations of ice flow at a regional scale.

Evidence for the role of deformable till layers in ice dynamics has also been observed for other West Antarctic glaciers, such as Thwaites Glacier (Parizek et al., 2013), Pine Island Glacier (Brisbourne et al., 2017) and Rutford ice Stream (King et al., 2009; King, Pritchard, & Smith, 2016; Smith & Murray, 2009). East Antarctica is likely to possess similar characteristic in places where fast-flowing ice streams flow over sedimentary-substrate and generate a till layer on top. However, systematic studies are yet to be conducted in many places. Further investigation of the existence and characteristics of till layers beneath the AIS, and a fuller understanding of how these systems evolve over longer time scales is required to integrate these behaviors more fully into models of AIS evolution.

In comparison with the highly active hydrogeology of till layers, aquifers in sedimentary strata and crystalline bedrock beneath the AIS have received relatively little attention over recent decades (Siegert et al., 2016). It is very likely, however, that these systems are linked (Anandakrishnan et al., 1998; Bell et al., 1998, 2007) and so longer-term cycling of water through bedrock aquifers may be significant in releasing or storing subglacial water at centennial to multimillennial time scales and transporting heat from within the crust to the base of the AIS.

Ice sheets of the Northern Hemisphere, including the Laurentide and Fennoscandian paleo ice sheets, are known to have generated substantial changes in bedrock hydrogeology (Person et al., 2012, 2007). Key processes include recharge of aquifers from glacial meltwater, with up to 40% of meltwater infiltrating into the bedrock (Lemieux et al., 2008), and the establishment of excess hydraulic head by glacial loading and water transport over hundreds of meters to kilometers vertically, and tens to hundreds of kilometers laterally (McIntosh et al., 2011). Deglaciation is associated with opposite tendencies, that is, discharge and a reduction in head. These processes generate a positive feedback that may enhance the supply of water to the ice sheet bed during deglaciation and increase the potential for dynamic ice mass loss. Advance and retreat effects are not equal because sediment compressibility is partially irreversible (Fowler & Yang, 2002). Because of this, "fossil" hydraulic head can be preserved from one glacial cycle to the next (Person et al., 2012). This means that a knowledge of loading history during previous cycles is needed to understand present conditions, which may lead to longer-term feedbacks that are not accounted for in short model runs.

]?twb.]Few studies exist of deep-penetrating groundwater within Antarctica. However, recent evidence suggests that processes operating under the AIS are similar to those understood for the Northern Hemisphere ice sheets. Gooch et al. (2016) studied the potential for a hydrogeological and hydrothermal system in the Wilkes Land region. This region is characterized by widespread sedimentary basins (Aitken et al., 2014, 2016; Frederick et al., 2016; Jordan et al., 2013), with the likelihood of active subglacial hydrology, including many lakes (Wright et al., 2012), and suggestions of moderate to high geothermal heat flux (Carson

et al., 2014), which are key factors associated with hydrogeological feedbacks. Gooch et al. (2016) model a single cycle of glacial loading and unloading and find that subsurface pressure effects in the subglacial aquifer are of the order of 10–30 MPa and extend to depths of a kilometer. Following unloading, overpressures of up to 10 MPa remain in the aquifer. Under the conditions modeled, discharge of water is associated with increased heat flux, with an additional ~40 mW m^{-2} for a flux of 1 mm yr^{-1} (Gooch et al., 2016). While relatively simple, this study demonstrates that glacial activity is linked to groundwater processes which are very poorly characterized, but to which the AIS may be highly sensitive.

5. Evidence for Ice Sheet Change

Direct observations of AIS mass balance changes, with sufficiently low uncertainty to reveal meaningful changes over time, have revealed accelerating mass loss over the past twenty years, and spatially highly variable AIS change. However, large internal variability of the AIS, predominantly driven by changes in atmospheric and ocean dynamics (section 2), means that attributing the drivers of ice sheet evolution to natural or human-induced causes is difficult. One approach to understanding the AIS response to natural climate forcing is to look at its past history, when the ice sheet went through phases of disequilibrium with the ambient climate. Ice and sediment core records reveal the natural long-term ice sheet evolution over time scales of decades to multiple millennia. The following section reviews the advances in observations and understanding of AIS dynamics over the past 5 years based on modern measurements and paleoreconstructions, based mostly on marine sediment cores.

5.1. Modern Observations

All approaches to estimating the overall AIS mass balance suffer from systematic and random errors that affect estimates in different ways. Three methods are commonly used: (1) The mass budget method where surface mass balance (snowfall minus surface ablation) is calculated using a regional atmospheric model, while perimeter loss (flow across the grounding line) is calculated using satellite radar interferometry (Gardner et al., 2018; Rignot et al., 2008, 2019); (2) satellite laser or radar altimetry (e.g., ICESAT-1/2 and Cryosat-2) where surface elevation changes are repeatedly mapped over distinct tracks and then averaged to provide estimates of volumetric change (McMillan et al., 2014; Paolo et al., 2015; Pritchard et al., 2009, 2012; The IMBIE Team et al., 2018) that are converted to mass change; and (3) gravimetry (e.g., GRACE and GRACE-Follow On) where changes in the strength of the gravitational field over the Earth are used to estimate changing ice sheet mass (e.g., King et al., 2012; Velicogna et al., 2014). Each method has uncertainties and limitations, and we gain confidence in estimates of mass balance when results from different methods converge (e.g., Shepherd et al., 2012; The IMBIE Team et al., 2018). Overall, the remote sensing data reveal that Antarctica is losing mass and contributing to sea level rise (Table 1 and Figure 15).

Assessment of the AIS mass over the past four decades reveals an accelerating rate of ice mass loss, from 40 ± 9 Gt yr^{-1} in 1979–1990 to 50 ± 14 Gt yr^{-1} in 1989–2000, 166 ± 18 Gt yr^{-1} in 1999–2009, and 252 ± 26 Gt yr^{-1} in 2009–2017 (Rignot et al., 2019). The accelerating decline in AIS mass has been driven by the dramatic increase in ice loss of the WAIS during the period 2009–2017 (163 Gt yr^{-1}), compared to 1999–2009 (73 Gt yr^{-1}) (Rignot et al., 2019). Major outlet glaciers of Pine Island and Thwaites draining the WAIS into the Amundsen Sea exhibit the most striking changes (Shepherd et al., 2019), including surface lowering, ice flow acceleration, ice shelf thinning, and grounding line retreat (Christie et al., 2016; Konrad et al., 2018; Mouginot et al., 2014; Rignot et al., 2014). Significant ice volume reduction is also recorded in the Antarctic Peninsula, where approximately 30 Gt yr^{-1} of ice has been lost to the oceans over the last 10–15 years (Table 1). One of the most significant and concerning findings since publication of the IPCC AR5 in 2013 is that MISI (see section 3.1.2) may have initiated at Thwaites and Pine Island glaciers in the Amundsen Sea sector of the WAIS (Favier et al., 2014; Joughin et al., 2014). Although a recent study suggests that grounding line retreat at Pine Island Glacier may have stabilized (Konrad et al., 2018) several ice sheet models show that projected retreat of glaciers in the Amundsen Sea embayment due to MISI can potentially cause hundreds of kilometers of grounding line retreat and high rates of ice loss on centennial time scales (Cornford et al., 2015; Ritz et al., 2015). In some projections (RCP 4.5 and above) this leads to deglaciation of much of the WAIS (DeConto & Pollard, 2016; Golledge et al., 2015), and multimeter sea level rise on centennial to millennial time scales (see section 6.1).

Reviews of Geophysics

10.1029/2019RG000663

Table 1

Recent Antarctic Mass Balance Estimates in Gigatons per Year (Gt yr^{-1}) for Different Sectors and the Continent as a Whole (Total)

Method	East Antarctica	West Antarctica	Antarctic Peninsula	Total
Mass Budget (Gardner et al., 2018)	+61 ± 73 Gt yr^{-1} (2008.0–2016.0)	−214 ± 51 Gt yr^{-1} (2008.0–2016.0)	−31 ± 29 Gt yr^{-1} (2008.0–2016.0)	−183 ± 94 Gt yr^{-1} (2008.0–2016.0)
Cryosat2 (McMillan et al., 2014)	−3 ± 36 Gt yr^{-1} (2010.8–2013.8)	−134 ± 27 Gt yr^{-1} (2010.8–2013.8)	−23 ± 18 Gt yr^{-1} (2010.8–2013.8)	−159 ± 48 Gt yr^{-1} (2010.8–2013.8)
GRACE (Harig & Simons, 2015)	+56 ± 5 Gt yr^{-1} (2003.0–2014.5)	−121 ± 8 Gt yr^{-1} (2003.0–2014.5)	−27 ± 2 Gt yr^{-1} (2003.0–2014.5)	−92 ± 10 Gt yr^{-1} (2010.8–2013.8)
GRACE (Forsberg et al., 2017)				−92 ± 50 Gt yr^{-1} (2002.3–2016.0)
GRACE+SLR (Talpe et al., 2017)				−56 ± 28 Gt yr^{-1} (1993.0–2000.0)
Combined method[a] (Martín-Español, King, et al., 2016)	+56 ± 18 Gt yr^{-1} (2003.0–2014.0)	−112 ± 10 Gt yr^{-1} (2003.0–2014.0)	−28 ± 7 Gt yr^{-1} (2003.0–2014.0)	−84 ± 22 Gt yr^{-1} (2003.0–2014.0)
IMBIE 2 Reconciled mass balance[b] (The IMBIE Team et al., 2018)	+5 ± 46 Gt yr^{-1} (1992–2017)	−94 ± 27 Gt yr^{-1} (1992–2017)	−20 ± 15 Gt yr^{-1} (1992–2017)	−109 ± 56 Gt yr^{-1} (1992–2017)
Rignot et al. (2019)[c]	−31 Gt yr^{-1} (1979–2017)	−68 Gt yr^{-1} (1979–2017)	−23 Gt yr^{-1} (1979–2017)	−123 Gt yr^{-1} (1979–2017)

Note. Mass balance estimates are from the three remote sensing approaches mentioned in the text, one combined method and the IMBIE reconciled estimate. Observational periods are listed in brackets. Uncertainties represent 1σ values. Note that ~363 Gt yr^{-1} of mass loss will cause ~1 mm yr^{-1} of sea level rise.

[a]A Bayesian method combining altimetry and gravimetry data, incorporating glacio-isostatic adjustment information (Martín-Español, King, et al., 2016). [b]Reconciled estimate includes all three methods of assessing mass balance over a common time scale, updated to IMBIE 2 (The IMBIE Team et al., 2018). [c]Values from Table 1, Cumulative Balance (Gt) between 1979 and 2017.

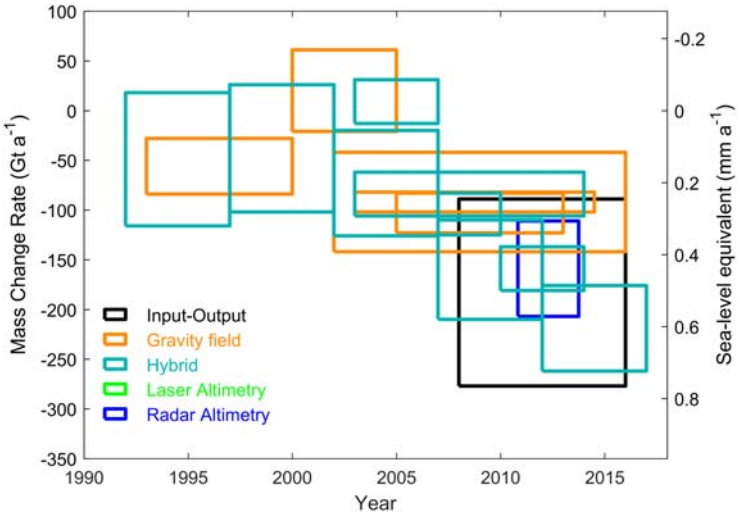


Figure 15. A selection of recent estimates of Antarctic ice mass change (left axis) and its sea level equivalent (right axis) as given in Table 1. Estimates based on the combination of multiple data sets are labeled "Hybrid." Updated from Allison et al. (2018).

Prior to the assessment of Rignot et al. (2019), which estimated an EAIS mass loss of -57.0 ± 2 Gt yr^{-1} since 1979, multiple and independent satellite observations indicated that the EAIS was in near balance, with estimates ranging from -3 to $+36$ to $+61 \pm 73$ Gt yr^{-1} (Table 1). One set of estimates from radar and laser altimetry suggests substantially greater growth, but these estimates have been controversial (Richter et al., 2016; Scambos & Shuman, 2016; Zwally et al., 2015). EAIS mass balance is regionally heterogeneous, and there are two notable regions that show anomalies. The Wilkes Land margin exhibits a large amount of interannual variability in mass balance. In the period from 2010–2013, the Wilkes Land sector of the EAIS lost up to 30 Gt yr^{-1} (Martín-Español, King, et al., 2016), with ice shelf thinning and inland ice flow acceleration, which is believed to be a result of increased CDW incursion (Flament & Rémy, 2012; Li et al., 2016; Rignot et al., 2019). In East Antarctica, this mass loss was balanced or exceeded by mass gain in the Dronning Maud Land sector, where increased snowfall between 2009 and 2011 resulted in a mass gain of ~350 Gt, equivalent to an ~1 mm sea level drop (Boening et al., 2012). This sector of the ice sheet has also experienced recent grounding line advance (Konrad et al., 2018), likely indicating rapid coupling between surface accumulation and ice sheet dynamics at a regional scale.

Attributing sea level rise to changes in AIS mass balance requires closure of the sea level budget, where the observed changes in sea level equal the sum of changes in ocean properties (temperature and salinity) and exchange between various water reservoirs (groundwater, glaciers, and major ice sheets) (Leuliette & Willis, 2011). Corrections based on geophysical responses to changes in sea level and the response of the ocean and solid Earth to past ice loading history remain significant sources of uncertainty. The contribution of Antarctica to sea level change calculated from GRACE data, available since 2003, shows an accumulated sea level rise of 5 mm (Forsberg et al., 2017) and a clear acceleration in Antarctic ice melt between 2002 and 2016. Systematic effects are introduced into estimates of the rate of Antarctic ice mass change derived from GRACE, due to mismodeled mantle mass change associated with GIA (King et al., 2012). Models of GIA do not fully represent lateral variations in Earth properties and are poorly constrained by a lack of understanding of post-LGM ice mass changes, which has resulted in large intermodel differences (section 4.2.2) (Martín-Español, King, et al., 2016). The acceleration in ice mass loss is not debated, but differences arise in temporal and regional estimates depending on the method (Table 1). Despite the uncertainties, attempts have been made to improve the attribution of the observed sea level rise into its constituent parts (Chen et al., 2017; Dieng et al., 2017). These attempts have been aided (Clark et al., 2015) by GRACE observations of ocean mass and Argo float measurements of thermal expansion in the upper 2,000 m of the ocean (Durack et al., 2014; Roemmich et al., 2015), at least since the early to middle 2000s. Improved constraints on the history of the AIS (e.g., LGM to late Holocene) and on heterogeneities in the solid Earth response will improve

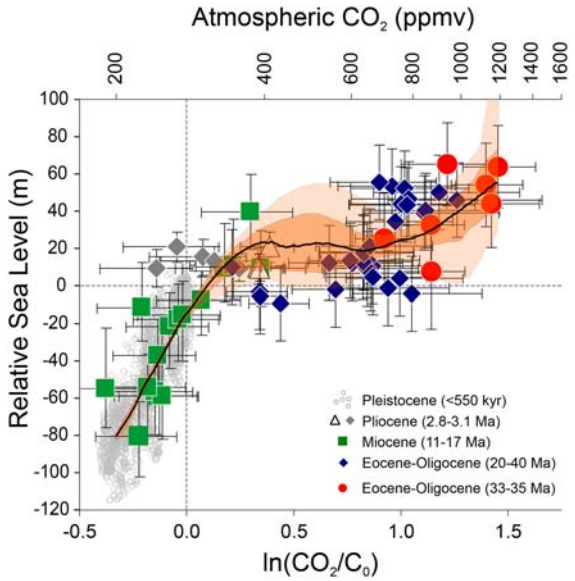


Figure 16. Sea level versus CO_2 concentrations (and the logarithmic radiative forcing influence of CO_2 changes expressed by ln (CO_2/C_0), where C_0 represents the preindustrial CO_2 level of 278 ppmv) (after Foster & Rohling, 2013). Symbols represent reconstructions with uncertainties for different intervals of the past 40 million years. The black line and orange envelopes represent a probabilistic assessment that takes into account full propagation of all uncertainties (black line is the probability maximum; dark orange is the 68% probability interval; light orange is the 95% probability interval).

estimates of global sea level change. As mentioned above (section 5.1), Antarctica has been, overall, losing mass into the oceans since the 1990s and is estimated to have contributed ~0.4 mm yr^{-1} to GMSL over 2005–2015 (WCRP Global Sea Level Budget Group, 2018, and references therein), and has been shown to be accelerating, to an Antarctic contribution over 2012–2016 of ~0.55 mm yr^{-1} (Oppenheimer et al., 2019).

5.2. Paleoenvironmental Observations

The long-term relationship between sea level and atmospheric carbon dioxide concentrations in Earth's geological past can provide insight into future sea level responses and reveal the vulnerability of the polar ice sheets to relatively small changes in temperature. Foster and Rohling (2013) demonstrated a sigmoidal relationship between atmospheric CO_2 levels and global sea level throughout the past 40 million years, which holds despite significant changes in boundary conditions related to plate tectonic changes (Figure 16). Their assessment indicates that climate warming of 2°C relative to preindustrial (CO_2 between 400 and 450 ppm) results in sea level rise of more than 9 m above present (68% confidence) in the long term (see also Rohling et al., 2013). This evaluation is within the range of estimated sea level rise of 6–9 m for the LIG (Dutton & Lambeck, 2012; Dutton, Carlson, et al., 2015; Hay et al., 2014; Kopp et al., 2009; Rohling et al., 2008) when global temperatures were ≤1°C warmer (i.e., similar to today; Hansen et al., 2017; Hoffman et al., 2017; Otto-Bliesner et al., 2013; Turney & Jones, 2010). However, reconsideration of the ice mass distributions of the preceding glaciation (Marine Isotope Stage 6), and thus of the glacio-isostatic changes through the previous deglaciation (Termination II), suggests that existing LIG highstand estimates may need revising upward by roughly 2 m (Rohling et al., 2017).

Four periods in Earth history are especially important for gaining a better understanding of the sensitivity of the AIS to changes in the climate system: The Holocene (11 ka [thousand years ago] to present), the last deglaciation (19–11 ka) when temperatures rose by 4–5°C and GMSL rose by 120–140 m; the LIG period (130–115 ka) when global temperatures were similar to modern values but GMSL stood potentially up to 10 m higher; and the Pliocene (5.33–2.58 million years ago) when global temperatures were 2–3°C higher and GMSL was 10–30 m above the present. Constraining the spatial and temporal behavior of the AIS and the corresponding sea level change during these time intervals requires not only AIS-specific information (e.g., its geographical extent and inferred mass) but also the rheological properties of the solid Earth and their interaction through time. These complexities are highlighted in the following sections, in addition to the chronological dating issues that arise when working close to Antarctica (e.g., see Livingstone et al., 2012; Siegert et al., 2019) and the complex and regionally variable patterns of deglaciation (The RAISED Consortium et al., 2014).

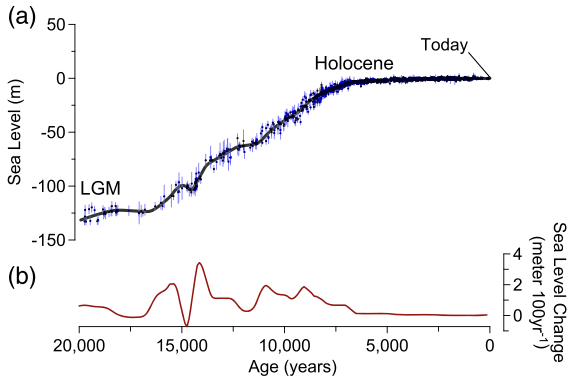


Figure 17. (a) The global sea level curve (thick black line) based on paleo sea level records (black dots with depth uncertainties shown in vertical blue lines) (Lambeck et al., 2014) and (b) rate of sea level change in meters per century for the past 20 ka, modified from Clark et al. (2016).

5.2.1. Holocene Ice Dynamics

The Holocene is defined as the period from about 11.6 ka to the onset of industrial-era warming (about 1850 CE; see Abram et al., 2016) and follows the transition out of the last glacial period. Sea level rise continued from the last glacial termination into the Holocene, but most of the 60 m of global sea level rise in the Holocene occurred over a broad multimillennial interval between 11 and 7 ka (Lambeck et al., 2014; Stanford et al., 2011) (Figure 17). The AIS contribution to Holocene sea level rise remains poorly constrained. Geological studies on and off the continent (e.g., Anderson et al., 2014; Hillenbrand et al., 2014; Leventer et al., 2006; Mackintosh

et al., 2014; Ó Cofaigh et al., 2014) and GIA modeling (Argus et al., 2014) are complex and show regional heterogeneity in the timing and rates of ice sheet retreat since the LGM. Determining the nature of this heterogeneity is important in the context of constraining AIS contribution to global sea level rise during the Holocene. The aforementioned studies do clearly suggest a limited contribution from either the WAIS or the EAIS, relative to Northern Hemisphere sources, but data and modeling comparison studies indicate that rapid and millennial-scale variability of the AIS was a feature of Holocene AIS dynamics (Bakker et al., 2016; Johnson et al., 2019; Spector et al., 2017). In particular, many studies on AIS deglaciation, based on ice thinning histories, point to rapid deflation events near the present-day ice sheet margin in the Weddell and Ross Sea sectors during the middle to late Holocene, as the main phase of ice sheet retreat (Hein et al., 2016; Johnson et al., 2019; Jones et al., 2015; Spector et al., 2017, and references therein). Conversely, finite radiocarbon ages obtained from sediments sampled from beneath the grounded WAIS suggest retreat upstream of its present location, and then readvance back to its modern position during the Holocene (Kingslake et al., 2018). This readvance scenario is proposed to have resulted from continuing isostatic rebound of the seafloor, and although the radiocarbon ages cannot pinpoint the timing of retreat, model experiments conducted to test the feasibility of this scenario suggest that the readvance likely happened after the grounding line had reached its minimum extent by the early Holocene (>9.6 ka) (Kingslake et al., 2018).

Along the margins of West Antarctica, internal processes relating to the overdeepened continental shelf (Patton et al., 2016) and MISI are thought to have led to ongoing retreat into the Holocene (Anderson et al., 2014; Hillenbrand et al., 2014; Larter et al., 2014; McKay, Golledge, et al., 2016; Ó Cofaigh et al., 2014; Smith et al., 2014). Whether this retreat was relatively gradual and sustained through to the present day, or was more rapid with periods of greatly accelerated retreat, remains open to debate and may have varied between sectors (Bart et al., 2017; Hillenbrand et al., 2013). However, the pattern and exact timing of retreat are ambiguous and vary from region to region, in part due to issues defining the chronology and differences relating to geometry of the ice sheet, as well as dynamic feedback processes, such as basal topography (e.g., Kingslake et al., 2018) and sediment deposition (e.g., Bart et al., 2018) that control ice sheet retreat. Despite uncertainties in the Holocene WAIS configuration, mismatches between grounding lines and isostatic rebound have revealed a more complex Late Holocene retreat pattern than previously accepted and are heavily influenced by geological processes (Bradley et al., 2015; Kingslake et al., 2018; Lowry et al., 2020; Siegert et al., 2013), while it is also increasingly apparent that GIA variations throughout the Holocene need to be considered in the context of AIS dynamics (Simms et al., 2018) and the impact of GIA corrections and previous ice history models on ice sheet thinning histories determined by cosmogenic exposure dating (Jones et al., 2019).

Evidence exists for abrupt mid-Holocene ice sheet loss events (e.g., Fogwill et al., 2014; Johnson et al., 2019), which have been linked in some cases to atmosphere-ocean forcing and ice shelf collapse (Hillenbrand et al., 2017). Rapid ice sheet thinning in the central Ross embayment during the early to mid-Holocene has been shown by comparisons of foraminifera-based radiocarbon dates from a marine sediment core near Ross Island and cosmogenic (^{10}Be) exposure ages from Transantarctic Mountain outlet glaciers. Accordingly, to the south of the modern Ross Ice Shelf calving line, model comparisons with geological data indicate that most of this embayment retreated between 9 and 8 ka (Lowry et al., 2019; McKay, Golledge, et al., 2016; Spector et al., 2017). However, to the north of the Ross Ice Shelf at Mackay Glacier, rapid thinning occurred at around 7 ka, due to MISI as this EAIS outlet glacier retreated into an overdeepened marine basin. The rate of AIS outlet glacier deflation events during the early to mid-Holocene in the Ross and Amundsen Sea sectors of WAIS was similar to that observed in other rapidly changing parts of Antarctica today (Johnson et al., 2014; Jones et al., 2015). The contradiction in timing between the cosmogenic data to the north and south of Ross Island could potentially be resolved by high-resolution multibeam studies which indicate that residual EAIS outlet glaciers readvanced into the Western Ross Sea, following widespread grounding line retreat in the wider Ross Sea embayment (Greenwood et al., 2018; Lee et al., 2017).

Abrupt mid-Holocene changes have also been observed in the WAIS section that drains into the Weddell Sea. Cosmogenic data in the Ellsworth Mountains suggest that the catchment feeding into the Weddell Sea remained at close to maximum ice thickness at 10 ka, but a rapid thinning event occurred in the eastern Weddell Sea embayment between 8 and 6 ka (Johnson et al., 2019), while thinning near the modern grounding line occurred rapidly between 6.5 and 3.5 ka (Hein et al., 2016). However, determining the significance of

these ice sheet thinning events to the offshore extent of grounded ice is more ambiguous in this region, than in the Ross Sea, due to a sparse offshore data set and large disagreements in the interpretation relating to terrestrial- and marine-based data sets in this region (Hillenbrand et al., 2014). Model comparisons with terrestrial geological data from cosmogenic studies in mountain ranges at the margins of the Filchner-Ronne Ice Shelves suggest that an ice sheet was grounded on bathymetric highs toward the continental shelf edge, with floating ice shelves over the deep bathymetric troughs. One model-based interpretation, constrained by cosmogenic deflation data, proposes that the grounding lines had retreated near to their present-day locations by 10 ka (Whitehouse, Bentley, Milne, et al., 2012). Conversely, interpretations of reworked foraminifera from marine sediment cores and multibeam analysis imply an ice sheet that was grounded near the continental shelf break until at least 20 kyr BP and that most grounding line retreat was more gradual and postdates 10 ka (Arndt et al., 2017; Hillenbrand et al., 2014; Hodgson et al., 2018). Review of these two different scenarios by Siegert et al. (2019) highlights that geophysical and cosmogenic data remain consistent with either scenario but clearly indicate that there was a major redirection of ice flow in the Weddell Sea embayment during the mid-Holocene. It was proposed isostatically driven processes could be invoked to explain either scenario: either through a redirection of subglacial hydrology leading to a change in dynamic ice flow in the mid-Holocene or through rebound of the seafloor following early Holocene retreat, resulting a the regrounding of the ice shelf and subsequent a readvance of the grounding line in the mid-Holocene (Siegert et al., 2019, and references therein).

The role of CDW in driving the deglaciation in the Amundsen Sea region and west of the Antarctic Peninsula, similar to modern observations of wind-driven incursions of relatively warm CDW onto continental shelf regions of drivers of deglaciation (Christianson, Jacobel, et al., 2016; Jacobs et al., 2011, 2012; Jenkins et al., 2018; Klinck et al., 2004; Nakayama et al., 2013; Smith et al., 1999; Wåhlin et al., 2016) have been investigated using geochemical data and ecological constraints from foraminifera and diatoms. These paleoenvironmental studies suggest the presence of CDW during the deglaciation, which ceased by ~7.5 ka (Hillenbrand et al., 2017; Minzoni et al., 2017; Peck et al., 2015). The decrease in CDW inflow onto the Antarctic continental shelves during the mid-Holocene is proposed to be due to reduced upwelling at the Antarctic margin as the westerly winds migrated northward during the early to mid-Holocene (Anderson et al., 2009; McGlone et al., 2010; Toggweiler et al., 2006).

Whether the final Holocene retreat, which happened after the main deglaciation, was relatively gradual and sustained through to present day, or was more rapid with periods of accelerated retreat, is still open to debate (Bakker et al., 2016; The RAISED Consortium et al., 2014). Furthermore, finite radiocarbon ages obtained from sediment cores collected beneath the WAIS have revealed that the grounding line in the Siple Coast region retreated to the south of its modern position and subsequently readvanced as a consequence of isostatic rebound although the exact timing of this retreat is unconstrained (Kingslake et al., 2018). Despite these uncertainties, it is clear that each catchment area in West Antarctica responded in different ways during the deglaciation, due to differences in regional oceanographic forcings, bathymetry, GIA, and internal ice dynamics.

5.2.2. The Last Deglaciation

The most recent interval in Earth history when global ice sheets reached their maximum integrated volume was the LGM. This period is traditionally defined by a sea level lowstand and lasted from ~27–19 ka (Clark et al., 2009; Rohling et al., 2009). The transition out of the LGM into the present day, referred to as the last deglaciation (~19–11 ka), saw 5 ± 2°C global mean temperature rise that resulted in loss of large ice sheets in the Northern Hemisphere. There is a range of estimates for the resulting deglacial sea level rise from ~120 to 130 m (Austermann et al., 2013; Clark et al., 2009; Denton et al., 2010; Masson-Delmotte et al., 2013; Peltier & Fairbanks, 2006) to as much as ~134 to 140 m (Lambeck et al., 2014) (Figure 17).

Quantitative assessments of the AIS contribution to the deglacial sea level rise vary substantially depending on the applied methodology, from 5–8 m based on regional assessments (Briggs et al., 2014; Gomez et al., 2013; Pollard et al., 2016; Whitehouse, Bentley, & Le Brocq, 2012), to 14–23 m based on GIA models (Argus et al., 2014; Lambeck et al., 2014). The geological evidence used for these reconstructions and model assessments derives from marine and ice core records, cosmogenic dating of glacial erratics and nearby sea level and geodetic data. The lower estimate of 5 m is based on a large ensemble of model runs (Pollard et al., 2016) and only considers a deglacial sea level contribution from the WAIS. Other studies have

Table 2

The Values Show the Contribution in Meters of Equivalent Global Mean Sea Level Rise From Melting of the AIS for Past Climate Periods (See Section 5.2) and Estimates for Future Time Intervals

Study	Pliocene	Last interglacial	Last deglaciation	To 2100	To 2300[a] or 2500[b]
IPCC: Church *et al*., (2013)				RCP2.6 and RCP4.5: 0.05 (-0.03 to 0.14) RCP8.5: 0.04 (-0.06 to 0.12)	
Whitehouse, Bentley, Le Brocq (2012) Gomez *et al*. (2013); Ivins *et al*. (2013)			<8		
Lambeck *et al*. (2014); Argus *et al*. (2014)			14 to 23		
de Boer *et al*. (2015)	6				
Golledge *et al*. (2015)				RCP2.6: 0.01 to 0.10 RCP8.5: 0.10 to 0.39	RCP2.6: 0.14 to 0.23[a] RCP8.5: 1.60 to 2.69[a]
DeConto and Pollard (2016)	11.26	6.09[c] to 7.54[d]		RCP2.6: 0.11 (±0.11) RCP8.5: 1.05 (±0.30)	RCP2.6: 0.25[b] (±0.23) RCP8.5: 15.65[b] (±2.00)
Gasson *et al*. (2016)	8 to 12				
Pollard *et al*. (2017)	9 to 16		3 to 8		RCP8.5: 11.51[b]
Yan *et al*. (2016)	6.2 to 13				
Golledge, Thomas, et al. (2017)	8.6 ±2.8				
Golledge *et al*. (2019)				RCP4.5: 0.02[e] to 0.05[f] RCP8.5: 0.08[e] to 0.14[f]	
Edwards *et al*. (2019)				RCP2.6: -0.06[h] to 0.15[i] RCP4.5: 0[h] to 0.24[i] RCP8.5: 0.15[h] to 0.45[i]	
Bamber *et al*. (2019)				Low: 0.02 to 0.23 (W) -0.03 to 0.04 (E) High: 0.03 to 0.46 (W) -0.04 to 0.11 (E)	Low: 0.06 to 1.31 (W)[a] -0.08 to 0.24 (E)[a] High: 0.07 to 2.28 (W)[a] -0.14 to 0.51 (E)[a]

Note. Projections from IPCC AR5 (Church et al., 2013) show the medi\an and likely ranges and do not include ice dynamic feedbacks. Church et al. (2013) reported an estimate of 0.07 (−0.01 to 0.16) for "Antarctic ice-sheet rapid dynamics." Note that DeConto and Pollard (2016) estimates are lower when tuned to Pliocene sea level targets (e.g., 0.64 ± 0.49 to 13.11 ± 3.04 for RCP8.5). Their range for LIG estimates is based on modern initial conditions (c) and glacial initial conditions (d), which reflects the difference and uncertainty in the ice sheet size. Global sea level projections by Golledge et al. (2019) show modeled contributions with (e) no melt feedback and (f) with melt feedback, where fresh meltwater drives a positive feedback due to stratification of the water column that drives basal melting (see section 6.2). Edwards et al. (2019) estimated sea level contributions with (h) no MICI and (i) with MICI. The expert judgment estimates of Bamber et al. (2019) are based on a low (+2°C above preindustrial) and high (+5°C above preindustrial) temperature change scenarios for contributions from the WAIS (W) and EAIS (E).

estimated an AIS contribution of 6.7 m when only cosmogenic surface exposure ages are used as constraints on ice sheet thickness (Golledge et al., 2012) to 14.5 m, when isotope measurements from Antarctic ice cores are instead used to guide modeled ice sheet thickness (Golledge et al., 2014) (Table 2). GIA model-based estimates depend on the viscosity of the upper mantle, which depending on the ice volume can result in the same observed rates of rebound, but very different deglacial histories (cf. Argus et al., 2014). These large discrepancies in the deglacial AIS contribution to post-LGM sea level rise result from uncertainties associated with quantifying the exact extent, thickness and therefore volume of the AIS during the LGM (Golledge et al., 2014; Golledge et al., 2013; Whitehouse, Bentley, Milne, et al., 2012). This is due to not only the poor data coverage and general inaccessibility but also the range of different approaches, each with their own limitations and uncertainties that have contributed to this problem.

The maximum thickness and thinning history of the AIS has been reconstructed by terrestrial cosmogenic exposure dating of glacially transported erratics, or previously ice-covered bedrock and by geomorphological bedforms mapped on land (e.g., Hein et al., 2016; Johnson et al., 2014; Mackintosh et al., 2011; Small et al., 2019; Spector et al., 2017; Stone et al., 2003; Todd et al., 2010), as well as radiocarbon ages from glacial drift deposits, lake sediments, or raised beaches (e.g., Hall et al., 2015). Maximum ice sheet extent has been reconstructed from subglacial and proglacial bedforms preserved on the continental shelf and dated using radiocarbon ages from carbonate material in marine sediment cores (Bart et al., 2018; Mackintosh et al., 2014; Ó Cofaigh et al., 2016; Smith et al., 2019). High-resolution mapping of glacial bedforms on the Antarctic continental shelves provides unequivocal evidence for the expansion of grounded ice sheets, although improved chronological constraints are required to understand the spatial variability of the timing at which the maximum extent was reached in each sector (Arndt et al., 2017; Dowdeswell et al., 2016; Fernandez et al., 2018; Halberstadt et al., 2016; Hodgson et al., 2018; Klages et al., 2014; Larter et al., 2019; Lee et al., 2017; Lynch et al., 2014; Simkins et al., 2017; The RAISED Consortium et al., 2014; Wise et al., 2017). Quantifying the LGM extent, and the timing of subsequent retreat, is required to test hypotheses regarding the climate or oceanographic mechanisms for initiating widespread Antarctic marine ice sheet retreat. In this context, it is essential to constrain the role that internal ice sheet dynamics, solid Earth processes (e.g., feedbacks from the historical ice load), and oceanic/sea ice feedbacks had in either accelerating or slowing retreat during both the last glacial termination and the Holocene.

A full synthesis of reconstructing Antarctic deglaciation since the LGM based on nearshore and onshore archives was presented by Livingstone et al. (2012), Wright et al. (2008) and more recently The RAISED Consortium (Anderson et al., 2014; Hillenbrand et al., 2014; Larter et al., 2014; Mackintosh et al., 2014; Ó Cofaigh et al., 2014; The RAISED Consortium et al., 2014). A number of previous reconstructions favored a minor AIS retreat that occurred late (after 14 ka) and continued well into the late Holocene (Bentley, 2010; Mackintosh et al., 2011, 2014; Peltier, 2004). The majority of Antarctic ice mass loss may have occurred on the overdeepened continental shelves of West Antarctica. These topographic depressions (e.g., 300–1,500 m deep) can result in increased sensitivity to ocean forcing (see section 2.2.2) and MISI. Topographic lows can be tectonically controlled, through extension and subsidence associated with the West Antarctic Rift, (see section 4.1.1) in the Weddell and Ross Seas, and also formed by prior glacial erosion, such as those observed on the inner shelves in the Amundsen and Bellingshausen Seas, and west of the Antarctic Peninsula (e.g., Livingstone et al., 2012).

The RAISED Consortium concluded that Antarctica may have only contributed a few meters to global meltwater pulses during the deglaciation; although no quantitative estimate was provided. The GIA-based I6G model supports ~13.6 m AIS contribution to global sea level rise since the LGM, with the most rapid period of ice loss occurring between 12 and 5 ka (Argus et al., 2014). However, such estimates are highly dependent on the values used for mantle viscosity in those models, and other estimates are approximately half of this value (Whitehouse, Bentley, & Le Brocq, 2012). Large uncertainties remain regarding the EAIS contributions to post-LGM sea level rise. GIA-based models constrained by RSL records along the East Antarctic coastline, and by elevation constraints from ice cores, suggest that there was thinning of several hundred meters in coastal regions, however inland of the continental shelf edge ice thickness changes were minimal (Argus et al., 2014). This assessment is consistent with the Mackintosh et al. (2014) data-model synthesis of a modest (1 m) EAIS contribution deglacial sea level rise.

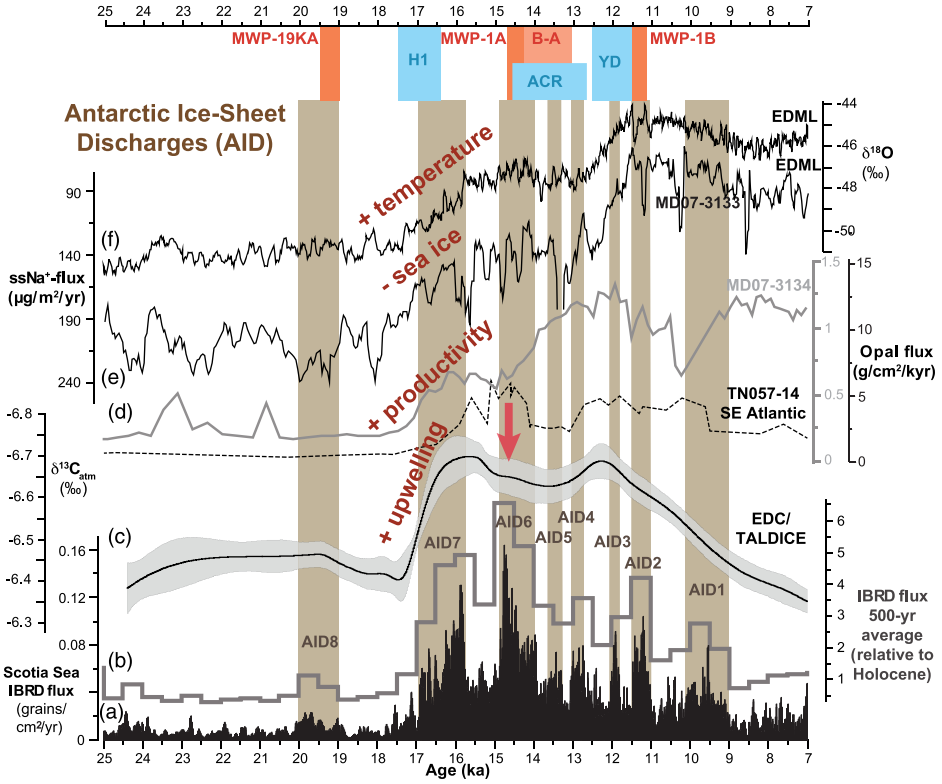


Figure 18. Iceberg-rafted debris (IBRD) flux in Iceberg Alley of the Scotia Sea and other climate proxies during the last deglaciation. (a) Stacked IBRD flux record. (b) The 500 year averages of stacked IBRD flux relative to Holocene average (Weber et al., 2014). (c) Antarctic deglacial $\delta^{13}C_{atm}$ stack (Schmitt et al., 2012). (d) Biogenic opal flux records from SE Atlantic Site TN057-14 (dashed) (Anderson et al., 2009) and Scotia Sea Site MD07-3134 (gray) (Sprenk et al., 2013). (e) EDML ice core record of sea salt (ss) Na^+-flux. f) $\delta^{18}O$ record from EDML ice core (EPICA Community Members et al., 2006). Note that Meltwater Pulse 1A (MWP-1a, red vertical arrow) is coeval with Antarctic Ice-Sheet Discharge Event 6 (AID6), within the dating uncertainties. Note further that major changes in Southern Hemisphere commenced ~17 ka when the Northern Hemsiphere was cold during Heinrich Event 1 (H1). ACR: Antarctic Cold Reversal, B-A: Bœlling-Allerœd, YD: Younger Dryas. Figure modified from Weber et al. (2014).

An early hypothesis was that post-LGM ice sheet retreat in the Antarctic was primarily triggered by global sea level rise, where orbitally driven melting of the Northern Hemisphere ice sheets drove sea level rise around Antarctica and caused the destabilization of the grounded portion of the ice (Denton & Hughes, 1983; Thomas & Bentley, 1978). However, recent modeling studies suggest that Southern Ocean heat advection was a more significant driver for initiating glacial retreat during the LGM (Golledge et al., 2012; Pollard & DeConto, 2009). Ocean thermal forcing and sea level control have also been used to argue that, contrary to earlier assessments, the advance to (at 29–28 ka) and retreat from the maximum extent of parts of the AIS during the LGM was nearly synchronous with Northern Hemisphere ice sheets (Weber et al., 2011), with deglaciation commencing between 19 and 20 ka—although the timing does vary regionally (e.g., Livingstone et al., 2012). A new understanding of deglacial AIS dynamics, as a series of multiple rapid ice discharge events that lasted from centuries to a millennium, has been informed by iceberg rafted debris records in the so-called "Iceberg Alley" of the Scotia Sea (Figure 18) (Weber et al., 2014). The records provide an integrated signal of iceberg discharge from the Indian and South Atlantic sectors of the AIS and show that Antarctic deglaciation accelerated between 17 and 9 ka, with multiple ice discharge events that lasted from centuries to a millennium and that closely coincided with times of global meltwater pulses (Figure 17). Although these records do not quantify the volume of AIS loss or rule out that the AIS was destabilized by rapid sea level rise originating elsewhere, they do present evidence of centennial to millennial response time scales of the AIS during the deglaciation, with abrupt discharge events that have comparable time scales to ice discharge events in the Northern Hemisphere ice sheets (Weber et al., 2014).

An Antarctic contribution to rapid sea level rise over multicentennial periods, such as Meltwater Pulse 1a (MWP-1a; 14.6 ka) when GMSL rose by ~20 m in 400 years (Deschamps et al., 2012a; Grant et al., 2014; Lambeck et al., 2014; Stanford et al., 2011), is supported by the timing of largest iceberg rafted debris flux in the Scotia Sea record (Figure 17). Other millennial-scale sea level rise events during the last glacial (Siddall et al., 2003) have also been inferred to reflect considerable AIS meltwater contribution in addition to melting of the Greenland Ice Sheet (Rohling et al., 2004). These studies challenge scenarios in which the AIS made only a relatively small contribution to sea level rise since the LGM lowstand (e.g., Whitehouse, Bentley, & Le Brocq, 2012). Iceberg-rafted debris records from Weber et al. (2014) are supported by an ice sheet model that predicts an AIS contribution of 6 mm yr^{-1} during the largest peak in deglacial Antarctic ice loss centered on the MWP-1a interval, compared to a deglacial average of 1 mm yr^{-1} (Golledge et al., 2014). Overall this equates to a 2–3 m sea level equivalent (SLE) AIS contribution to the MWP-1a event, with the remainder coming from the Northern Hemisphere ice sheets (Golledge et al., 2014).

However, further evidence for an Antarctic contribution to MWP-1a from data on land and the continental margin in other regions such as the Weddell Sea (Arndt et al., 2017; Nichols et al., 2019) is absent, and this issue remains a conundrum (Goehring et al., 2019; Hall et al., 2015; Prothro et al., 2020). The large uncertainties in the underpinning sea level constraints (Hibbert et al., 2016, 2018; Stanford et al., 2011) and dating of geological material on land and in the ocean (e.g., see discussion of cosmogenic dating in Siegert et al., 2019, and radiocarbon dating in Anderson et al., 2014), and the uncertainty around the AIS size, seaward extent, thickness and volume above flotation at the LGM, mean that currently it remains difficult to quantify the exact contribution of AIS melting to the sea level rise recorded during MWP-1a.

Ocean forcing was inferred as the key driver of deglacial AIS dynamics, modulated by global atmospheric teleconnections, that decoupled ice sheet elevation and air temperatures in a high-resolution ice core near the Weddell Sea and resulted in rapid thinning of the AIS during the period coinciding with MWP1-a (Fogwill et al., 2017). The coincidence between changes in AIS elevation (Fogwill et al., 2017), enhanced iceberg flux (Weber et al., 2014), and atmospheric temperature trends (Pedro et al., 2016) through the deglaciation suggests a tight coupling between the ice-ocean-atmosphere system. A positive feedback mechanism was proposed where reinvigoration of the Atlantic Meridional Overturning Circulation (AMOC) following Heinrich Event 1 increased Southern Ocean subsurface heat content and triggered initial melting of AIS margins. Consequent freshening of surface waters led to a weakening of Southern Ocean overturning, resulting in reduced AABW formation, surface ocean stratification, and sea ice expansion (Fogwill et al., 2017; Golledge et al., 2014; Weber et al., 2014). Sea ice expansion would result in ice-albedo feedbacks that drive atmospheric cooling (negative feedback), but the strong insulating effect of sea ice would also trap subsurface heat, which in addition to ocean stratification from AIS meltwater would trap ocean heat close to the grounding line of the AIS and enhance thermal erosion to maintain a positive ice-ocean feedback. Defining the details of this dynamic feedback during periods of past climate change is critical to understanding the implications of the high-latitude Southern Hemisphere environmental changes today. This includes the need for ocean temperature and circulation records close to the Antarctic margin to improve our understanding of the role of ocean forcing in driving ice sheet change, which mostly relies on model results and ice core data.

Simulations of ocean oxygen isotopes ($\delta^{18}O$) suggest that potentially significant disruption of global overturning circulation may have coincided with AIS melt between 75 and 20 ka BP (Rohling et al., 2004). During this period of highly variable climate (Bereiter et al., 2012; Dansgaard et al., 1993; EPICA, 2006; North Greenland Ice Core Project members, 2004) and sea level (Cutler et al., 2003; Siddall et al., 2003) millennial-scale Antarctic warming of 2–3°C events (known as Antarctic Isotope Maxima) were associated with global seal level rise events of 30 m, at rates of about 2 m per century (Grant et al., 2014). The glacial ocean simulations of Rohling et al. (2004) highlight major changes in Atlantic overturning circulation, with severely reduced or near-collapsed North Atlantic Deep Water (NADW) export, associated with a 50:50 ± 20% contribution of meltwater from both Northern and Southern Hemisphere ice sheets that match global sea level, marine $\delta^{18}O$, and ice sheet temperature records. Turney et al. (2017) modeled the impact of WAIS meltwater from the Weddell and Ross Seas on the Southern Ocean during times when changes in Atlantic overturning circulation where insufficient to explain smaller amplitude antiphased temperature relationships between the Northern and Southern Hemispheres during the last glacial. The simulations of Turney et al. (2017) showed how atmospheric teleconnections were driven by AIS discharge between 30

and 28 ka (inferred from ice-rafted detritus [IRD] layer in the South Atlantic south of the Polar Front; Kanfoush et al., 2000) and the rapid ocean-atmosphere feedbacks that followed may have contributed high-latitude temperature trends in the Northern Hemisphere.

5.2.3. Last Interglacial and Pleistocene Evidence for a Retreated Ice Margin

During the Last Interglacial period (LIG; 130–115 ka, the geological interval also referred to the Eemian), globally distributed records of local sea levels indicate that GMSL likely stood 6–9 m higher and mean global temperatures were 0.7° ± 0.6°C warmer than in preindustrial times, although atmospheric CO_2 concentrations were similar to preindustrial values (Dutton & Lambeck, 2012; Dutton, Webster, et al., 2015; Hoffman et al., 2017; ;Kopp et al., 2009; McKay et al., 2011; Petit et al., 1999). Data from the North Greenland Eemian (NEEM) ice core record revealed that the Greenland Ice Sheet's sea level contribution to the LIG highstand was <2 m (NEEM Community Members, 2013). If this estimate is correct, then combined with a possible contribution of <1 m from thermal expansion of the ocean and melting of glaciers (McKay et al., 2011), this requires a contribution from the AIS. Even the lower bound (6 m) of these sea level estimates implies ice mass loss equivalent to the marine-based sectors of the WAIS (4.9 m SLE), while the upper bounds (9 m) require some loss of the marine margins of the EAIS (21.1 m; SLE estimate based on Bedmap2 data; Fretwell et al., 2013), such as the Aurora, Wilkes, and Recovery subglacial basins.

In spite of the above circumstantial evidence pointing to a substantial contribution to the LIG sea level highstand from the marine-based portions of West and East Antarctica, geological archives close to the Antarctic margin have only provided limited and contradicting direct evidence for AIS retreat during the LIG. This is due to both logistical expense and difficulty in working in Antarctica, and factors relating to sedimentation rates, erosion and preservation, and accurate dating of sediments proximal to the margin. For example, glaciomarine environments are commonly sediment starved on the Antarctic continental shelves (with sediment mass accumulation rates <10 cm kyr^{-1}; Larter et al., 2012). Indirect yet notable, marine sediment archives off the continental slope of the Adelie Land margin have been used in provenance studies, where the mineralogical and geochemical characteristics of glacially eroded sediment transported to the Antarctic margin provide information about past changes in AIS dynamics, as well as information about the hidden geology beneath the ice (Figure 18) (Cook et al., 2017; Licht & Hemming, 2017). The Pleistocene provenance record of these sediments suggests substantial retreat in the Wilkes Subglacial Basin during the LIG, which could have contributed up to a few meters of global sea level rise (Wilson et al., 2018).

The LIG sea level commitment is further complicated by recent, higher estimates for the Greenland contribution: Yau et al. (2016) suggest a Greenland Ice Sheet contribution of 5.1 m (4.1–6.2 m, 95% probability interval) toward the end of the Eemian, although the authors acknowledge several unexplained discrepancies between their study and the NEEM ice core-based reconstructions. Note also that a recent reevaluation of GIA corrections suggests that LIG GMSL estimates (including the lower bound) may need upward adjustment by ~2 m (Rohling et al., 2017). This is based on revised ice volume constraints for the preceding glacial maximum that consider GIA corrections of a considerably different ice volume distribution (larger Eurasian and smaller North America ice sheets) during the glacial period preceding the LIG, relative to the LGM. If Yau et al. (2016) are right and the Greenland contribution to GMSL was ~5 m, then the ~2 m upward adjustment of LIG GMSL estimates of Rohling et al. (2017) to 8–11 m above the present-day level would require Antarctic ice loss during the LIG of ~5 m, even after accounting for an ~1 m contribution from thermal ocean expansion (Turney et al., 2020). Note that this argument does not include asynchroneity in the contributions from Northern and Southern Hemisphere ice sheets, which suggest that the estimated ~5 m Antarctic contribution is a low-end estimate (Rohling et al., 2019).

Centennial-scale rates of sea level rise during the LIG were quantified through statistical analysis of Red Sea based sea level records and comparison with global coral/reef, and speleothem data (Rohling et al., 2019), as discussed in section 5.2.5. That study also deconvolved the relative contributions from Greenland and Antarctica by subtraction of the Greenland contributions based on two independent reconstructions from the global signal. This assessment revealed an early AIS-derived highstand between 129.5 to 125 ka of 5–10 m, the timing of which had previously been inferred qualitatively (Dutton, Webster, et al., 2015; Marino et al., 2015; Yau et al., 2016). This may have occurred in response to a warm early-LIG temperature "overshoot" during the main Termination 2 deglaciation phase (Marino et al., 2015).

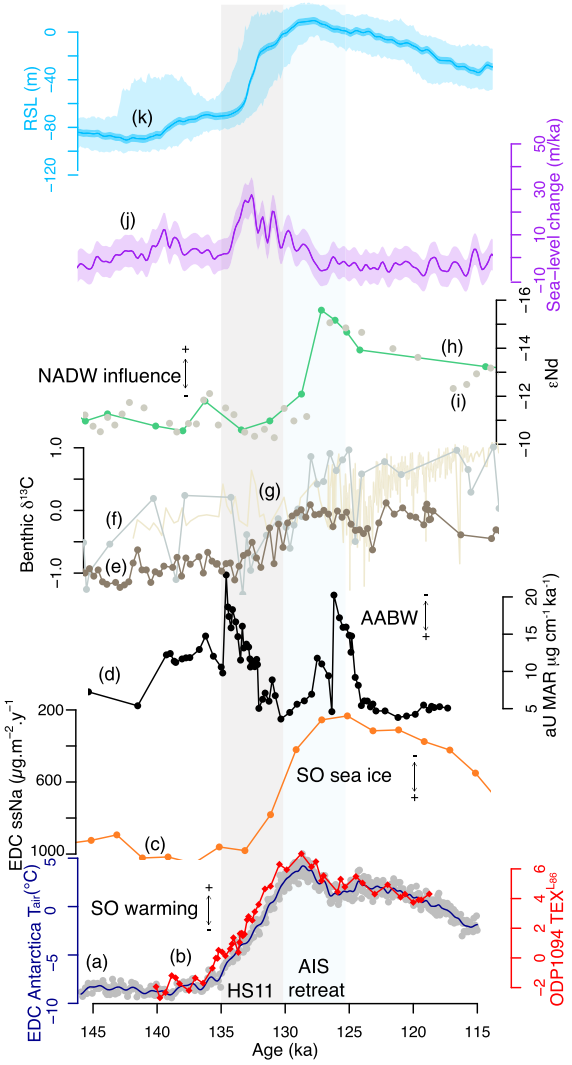


Figure 19. Paleoceanographic data consistent with reorganization of the Southern Ocean climate system during the Last Interglacial period from proxies records: (a) EDC Antarctic air temperature difference (gray dots and blue line) (Jouzel et al., 2007), (b) sea surface temperature proxy TEX_{86}^{L} (Hayes et al., 2014), (c) Antarctic sea ice extent inferred from sea-salt sodium flux (ssNa) (orange) (Wolff et al., 2006), (d) AABW formation inferred from authigenic uranium concentrations which reflect bottom water oxygenation (black) (Hayes et al., 2014), (e–g) benthic $\delta^{13}C$ (*Cibicidoides wuellerstorfi)* records from Site 1089 (brown) (Hodell et al., 2003), (f) Site 1063 (gray) (Deaney et al., 2017), and (g) MD03-2664 (beige) (Galaasen et al., 2014), (h and i) water mass tracer Nd isotopes measured in (h) fossil fish teeth (Deaney et al., 2017), and (i) sediment leachate (Böhm et al., 2015), (j) the rate of the LIG sea level change and 95% confidence limits (Marino et al., 2015), and (k) the relative sea level curve with 95% confidence limits (Grant et al., 2014). Figure modified based on (Rohling et al., 2019). HS11: Heinrich Stadial 11.

Global mean temperature might not be the critical parameter or driving process when considering Antarctica's contribution to sea level rise (Marino et al., 2015). These authors indicated that the LIG highstand likely occurred from millennial-scale warming of Antarctica on the order of 4°C, due to a bipolar see-saw temperature event initiated by a massive meltwater injection to the North Atlantic as the Northern Hemisphere ice sheets retreated. This interval, known as Heinrich Stadial 11 (HS11:135–130 ka) was in fact the main deglaciation event of Termination II when sea level rose by 70 m in 5,000 years at a rate of 28 m ± 8 m kyr^{-1} (Grant et al., 2012, 2014) (Figure 19). The HS11 freshwater flux into the North Atlantic coincided with Northern Hemisphere cooling and a typical see-saw response of strong Antarctic warming of 9° C (Jouzel et al., 2007), of which only 5°C can be apportioned to radiative forcing (Masson-Delmotte et al., 2010). The remaining warming is likely to have resulted from the buildup of ocean heat, located in the global interior ocean north of the ACC rather than in the Southern Ocean itself (Pedro et al., 2018), and eddy-driven heat flux across the ACC to Antarctica. Proxy evidence supports a reduction in sea ice extent (Chadwick et al., 2020; Crosta et al., 2004; Esper & Gersonde, 2014) and AABW formation coincident with warmer surface waters, as well as inferred surface stratification (Ninnemann et al., 1999) and freshwater input that was associated with the rise in sea level between 135 and 143 ka (Figure 19). This HS11 climate event was unlike the last glacial termination (Termination 1) when the highest rate of sea level rise, MWP-1a, occurred after, not during, the abrupt North Atlantic cooling and associated reduction in AMOC of Heinrich Stadial 1 (HS1: 16–17 ka; Lambeck et al., 2014).

Ice and environmental data from the Patriot Hills blue ice region landward of the Weddell Sea Embayment provide evidence for significant ice mass loss during the LIG (Turney et al., 2020). This study is the first direct of substantial WAIS loss during the LIG, which is supported by regional ice sheet modeling results that reinforce the notion of a centennial-scale (200 year) response time scale to 2°C of ocean warming relative to today.

Further afield in the Southern Ocean, there are additional indicators of oceanographic change (Figure 19) associated with ocean stratification and a reduction of AABW formation when the LIG sea level high suggested an AIS meltwater contribution (see Rohling et al., 2019). Warming in Southern Ocean sea surface temperature (SST) reconstructions (Hayes et al., 2014; Ninnemann et al., 1999) corresponds to a peak in reconstructed air temperature over Antarctica (Petit et al., 1999) at the time of early LIG sea level rise, when the Northern Hemisphere was much cooler (Marino et al., 2015). The SST rise based on TEX_{86}^{L} shows a maximum of +7°C during MIS 5e (Hayes et al., 2014), although diatom-derived surface temperature reconstructions suggest that this value may have been closer to +5°C (Bianchi & Gersonde, 2002; Chadwick et al., 2020; Etourneau et al., 2013; Schneider Mor et al., 2012). Local atmospheric warming would tend to result in a contraction of sea ice, as has been suggested by a reconstruction of sea ice extent during MIS 5e (Wolff et al., 2006). Ice-ocean simulations (e.g., Hellmer et al., 2012) have indicated how reductions in sea ice can redirects warm CDW toward the coast and drives basal melting of ice shelves. Taken together, these observations may be related to AIS change through meltwater release that results in water column stratification and disrupts the formation of dense AABW, and sets up a positive feedback that traps ocean heat in the subsurface, and drives further basal melting of the AIS and ice shelf breakup (e.g., Phipps et al., 2016). Paleoceanographic data to support this mechanism of AIS loss include surface ocean

stratification changes (differences between surface to deep foraminifera $\delta^{18}O$; Ninnemann et al., 1999); reduced bottom water oxygenation in the deep Southern Ocean following the peak in Antarctic warming due to reduced AABW formation (Hayes et al., 2014); $\delta^{13}C$ records from benthic foraminifera, which document the transition from low-$\delta^{13}C$ deep waters indicative of AABW, to high-$\delta^{13}C$ in bottom waters from increased NADW north (Galaasen et al., 2014; Hodell et al., 2003); and neodymium isotopes in sediment leachates and fossil fish teeth (Böhm et al., 2015; Deaney et al., 2017), that suggest an expansion of NADW at the end of Heinrich 11 into the South Atlantic.

More paleoenvironmental studies close to the Antarctic margin are required to adequately constrain the magnitude and pattern of AIS retreat during the LIG. The relatively indirect and far-field inferences for LIG AIS retreat (Figure 19) have yet to be supported by proximal records of stronger CDW upwelling and advection onto the continental shelf. All of the marine sediment proxy data presented in Figure 19 derive from north of the Southern Boundary of the ACC or ACC/Weddell Gyre Boundary, which forms an important oceanographic front that helps to restrict CDW access to the Antarctic margin (e.g., see Vernet et al., 2019). Furthermore, the southward expansion of NADW does not necessarily correspond to warmer CDW reaching the Antarctic margin, and a reduction in AABW formation could instead result from a northward shift and/or weakening of Southern Hemisphere westerly winds (Glasscock et al., 2020). Stratification and freshening due to meltwater inputs south of the ACC might be explained sea ice changes, particularly in the Atlantic relative to the Pacific sector of the Southern Ocean (Holloway et al., 2017). Reduced LIG sea ice is consistent with the hypothesis of a weakened AMOC resulting in heat accumulation in the Southern Hemisphere and subsequent sea ice reduction but without a major collapse of the WAIS (Holloway et al., 2016). Targeted data collection close to the Antarctic margin is needed to resolve this issue.

There is a broader base of evidence for large-scale retreat of the WAIS in other periods. For example, Quaternary diatoms and elevated ^{10}Be concentrations in subglacial till samples recovered from beneath the grounded WAIS indicate that they have been exposed to open marine conditions at least once during the past 1.3 Ma, implying at least one significant grounding line retreat along the Siple Coast (Kerr, 1998; Scherer et al., 1998). However, the advection of diatoms and adhering ^{10}Be beneath an ice shelf to the sites studied by Scherer et al. (1998) may have occurred without complete collapse of the WAIS, due to the stabilizing influence of isostatic rebound following the initial grounding line retreat (see Kingslake et al., 2018).

In the ANDRILL McMurdo Ice Shelf Project drill-core AND-1B, recovered beneath the northwestern margin of the Ross Ice Shelf recovered as part of the ANDRILL project, deposition of diatomaceous sediments bearing Pleistocene calcareous nanofossils was assigned to Marine Isotope Stage 31 (~1 Ma)—a well-documented warm period in circum-Antarctic and the Southern Ocean (Villa et al., 2012). This provides evidence of the last known time with a smaller-than-present ice shelf in the Ross Sea (McKay, Naish, Powell, et al., 2012; Naish et al., 2009; Scherer et al., 2008; Villa et al., 2012). Deep-sea cores from the Amundsen Sea are inconclusive regarding WAIS retreat during the past 1 Ma (Hillenbrand et al., 2002), but a depositional anomaly hints at a reduced WAIS in this sector between 621 and 478 ka (Hillenbrand et al., 2009). Further data from AND-1B indicated that in the Ross Sea sector, the WAIS has oscillated in the Ross Sea sector between an ice sheet and ice shelf state at least seven times since 0.8 Ma, and at least once in the past 250 ka, with a Ross Ice Shelf that was similar to or less extensive than today during past warm periods of Marine isotope Stages (MIS) 5 and 7 (McKay, Naish, Powell, et al., 2012). Reworked, marine sediments recovered in ice cores on Ross Island also indicate that ice shelves formed during the LIG in the southern Ross Sea, but evidence that the grounded ice retreated further south of Ross Island than today remains equivocal.

Marine Isotope Stage 11 is one of the longest interglacial periods of the Pleistocene (374–424 ka) (Lisiecki & Raymo, 2005), with warmer global temperatures (by 1–2°C) and similar CO_2 concentrations relative to the Holocene (Lüthi et al., 2008). Sea level estimates for MIS 11 have been debated, with a suggested highstand of ~20 m higher than today (Hearty et al., 1999; McMurtry et al., 2007; Olson & Hearty, 2009; van Hengstum et al., 2009), which would require collapse of the Greenland and WAIS, in addition to significant contributions from the EAIS. This initial estimate was revised downward between 6–13 m after taking into account the influence of GIA (Raymo & Mitrovica, 2012), and refined further to 8–11.5 m (Chen et al., 2014). Raymo and Mitrovica (2012) argued that these revised estimates would require meltwater contributions most of Greenland and West Antarctica but without significant contribution from the EAIS. However, retreat of the EAIS, specifically the Wilkes Subglacial Basin, is suggested for MIS 11 based on detrital sediment

provenance in an offshore sediment core (Wilson et al., 2018) and further supported by the very low initial $\delta^{234}U$ measured in subglacial precipitates of calcite and opal (Blackburn et al., 2020). The low $\delta^{234}U$ values suggest that subglacial fluids recorded by the precipitates were not isolated for millions of years, as would be expected based on EAIS stability (e.g., Sugden et al., 1993). Instead, these data reveal that the ^{234}U-rich subglacial fluids were renewed around 400 ka, by flooding in the low-lying Wilkes Subglacial Basin, and groundling line retreat (Blackburn et al., 2020). Paleoceanographic evidence to support this hypothesis is currently limited. However, (Hodell et al., 2000) observed a strong export of NADW into the South Atlantic Southern Ocean and upwelling of CDW with a greater proportion of NADW, while Glasscock et al. (2020) observed an authigenic U peak (similar to that observed during MIS 5e) that could be interpreted as a reduction in AABW formation during MIS 11 associated with meltwater forcing. Ocean warming and basal melting of the marine-based EAIS have been speculated as driving the EAIS retreat, without significant climate (atmospheric) warming (Blackburn et al., 2020), but further proximal evidence is needed to fully understand the processes driving MIS 11 AIS change.

5.2.4. Pliocene Evidence for a Retreated Ice Margin

Research on the Pliocene AIS is relevant due to the similarity between the current climate and conditions of the early-to-middle Pliocene, 5.3–2.6 Ma, when atmospheric CO_2 concentrations were between 350 and 400 parts per million (ppm), global surface temperatures were 2–3°C higher and the Southern Ocean was 4–6°C warmer than present (Pagani et al., 2010; Seki et al., 2010; Martínez-Botí et al., 2015; McKay, Naish, Carter, et al., 2012). A range of globally distributed sea level records, alongside considerations of the benthic oxygen isotope record, suggests that GMSL stood 10–30 m above present, which requires a marked decline of the Greenland Ice Sheet and WAIS, as well as contributions from marine-based regions of the EAIS (Foster & Rohling, 2013; Gasson et al., 2016; Miller et al., 2012; Winnick & Caves, 2015) (Figure 16). However, determining the exact extent and location of ice sheet loss, and thus eustatic sea level change, from far-field sea level records has significant caveats. Critically, this requires a robust understanding of tectonic and mantle processes, and GIA that may result in a departure from eustasy in a sea level record at any given location (Raymo et al., 2011). Therefore, Pliocene sea level records must be considered in the context of model results that incorporate these processes, alongside more direct evidence of AIS retreat from the Antarctic margin.

Pliocene sea level and geological evidence for elevated Pliocene shorelines are limited by a dynamic topography overprint on the order of 10 m of vertical motion, which makes GIA corrections highly uncertain (see section 4.1.2 on dynamic topography) (Austermann et al., 2015; Raymo et al., 2011; Rovere et al., 2014; Rowley et al., 2013). This, superimposed on true sea level variability within the Pliocene, may explain why global sea level reconstructions for this period span range from 6 to 20 m or even 30 m (Dumitru et al., 2019; Foster & Rohling, 2013; Grant et al., 2019). A study that attempted to deconvolve the different processes used phreatic overgrowth in Mallorcan cave deposits and concluded that sea level during the early-middle Pliocene reached between 6 and 27 m above present, at 68% confidence (mean values of 16 and 24 m; Dumitru et al., 2019).

There are currently insufficient geological constraints on the size and extent of the Pliocene AIS, resulting in many synthesis studies on geological data and climate modeling (de Boer et al., 2015; Haywood et al., 2016, 2016). Susceptibility of the marine-based WAIS to retreat, for example, during warm intervals of the Pliocene, was suggested by modeling (Pollard & DeConto, 2009) and supported by the deposition of diatomaceous oozes under surface water temperatures a few degrees warmer than today at the ANDRILL AND-1B site in the Ross Sea during Pliocene interglacial periods (McKay, Naish, Carter, et al., 2012; Naish et al., 2009). Pliocene deglaciation and retreat of marine-based EAIS portions during Pliocene warm periods had previously been debated (e.g., see Barrett, 2013), based on observations of deglaciation-indicating diatoms in sediments of the Sirius Group (now Sirius Formation) in the TAM (Webb et al., 1984). This contrasted with field evidence from the Dry Valleys (e.g., Sugden et al., 1995; Sugden et al., 2017) that indicated no thinning and the presence of >8 Ma old ice, suggesting that the climate did not warm enough for large-scale EAIS deglaciation. However, Bertram et al. (2018) and Cook et al. (2013) provided additional evidence for the (at least partial) collapse of marine-based EAIS portions during Pliocene warm periods (next paragraph). Subsequent ice sheet modeling work used alternative ice sheet model physics (Pollard et al., 2015) and suggested significant EAIS retreat and wind-blown emplacement of Pliocene marine diatoms in the TAMs (Scherer et al., 2016).

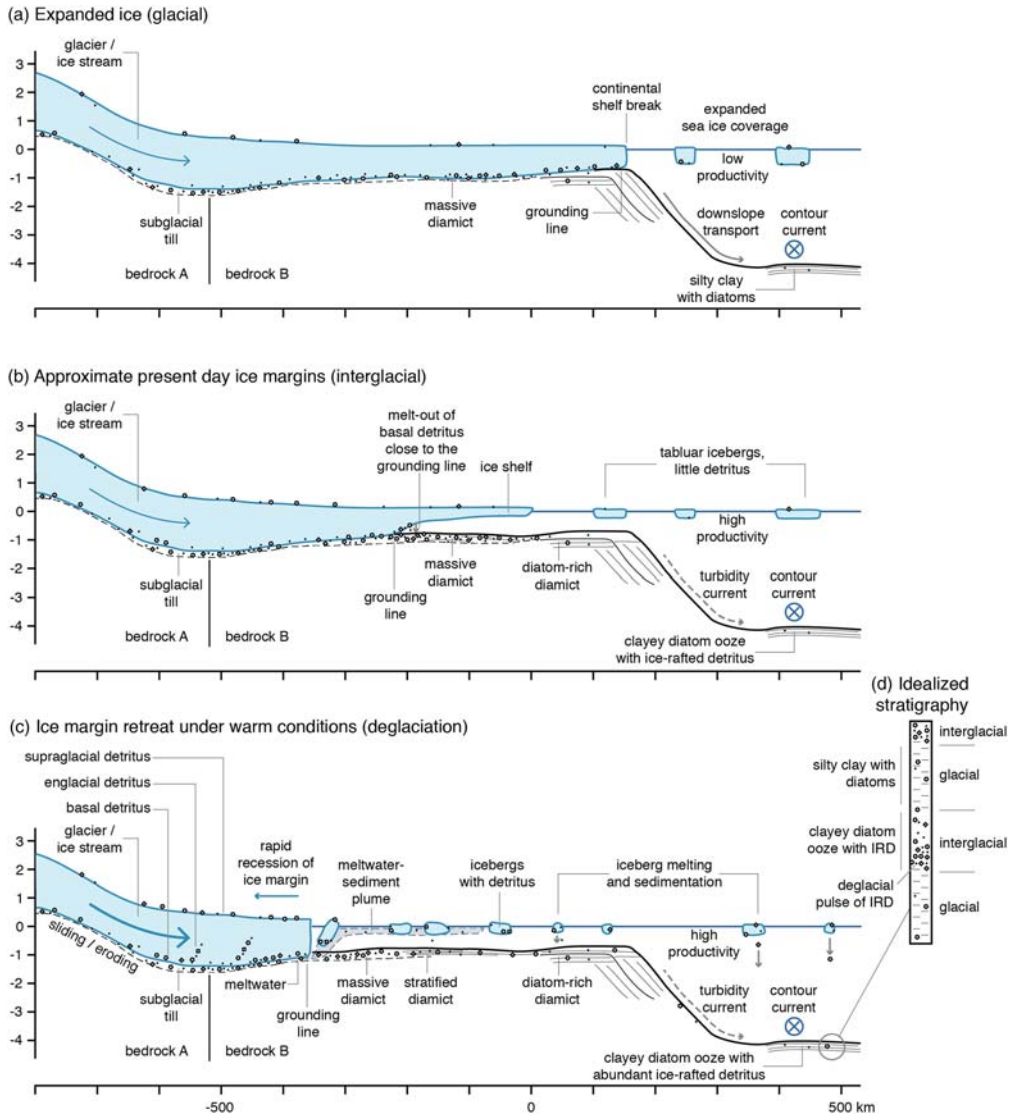


Figure 20. Reconstructing past AIS dynamics based on sediment archives. The conceptual model shows an Antarctic glacier (a) advanced to the shelf edge over two different bedrock lithologies, (b) with an ice shelf, similar to the present day, and (c) retreating under warm conditions, for example, the Pliocene. The provenance of ice-rafted detritus (IRD) found at a deep-water site (d) changes with the location of the grounding line for example, in panel (c), proportionately more IRD is sourced from inland bedrock (a) due to increased basal erosion and entrainment of sediment, which is transported into the Southern Ocean via ice bergs (figure based on Ehrmann & Grobe, 1991; Hambrey & McKelvey, 2000).

Observational evidence for retreat into the marine-based portions of the EAIS includes geochemical proxy data in marine sediment records offshore Adelie Land that suggest significant ice retreat inland of the Wilkes Subglacial Basin, one of the largest subglacial basins of the EAIS, which may have contributed 3–4 m to Pliocene sea levels (Bertram et al., 2018; Cook et al., 2013; Patterson et al., 2014; Valletta et al., 2018) (Figure 20). Quantification of the subglacial sediment thickness of the northern Wilkes Subglacial Basin by airborne gravity and geophysical data reveals thin sediment deposits influenced by glacial erosion (Frederick et al., 2016; Paxman et al., 2018) that may suggest more frequent Pliocene to Pleistocene ice sheet retreat and advance. Uplifted glacimarine sediments from four separate formations of the Pagodroma Group on the flanks of the Prince Charles Mountains adjacent to Amery Ice Shelf suggest a reduced glacial extent of the AIS margin in the Prydz Bay region at some time between the early Miocene (or older) and the Pliocene or early Pleistocene (Hambrey & McKelvey, 2000; Whitehead et al., 2004).

The Pliocene retreat patterns reconstructed from geochemical sediment provenance (e.g., Cook et al., 2013) were not reproduced by the concurrent generation of ice sheet models around that time. Since then, new

models have been developed, both including MISI and MICI (DeConto & Pollard, 2016; Pollard et al., 2015) and excluding MICI (Golledge, Thomas, et al., 2017), which simulate ice sheet retreat in better agreement with observed Pliocene highstand sea levels.

Pollard et al. (2017) show the effect of different Earth viscoelastic properties on the varying Antarctic contribution to Pliocene sea level estimates. Following on from the sea level feedback model of Gomez et al. (2015), Gomez et al. (2018) and Pollard et al. (2017) show that estimates of the AIS contribution to the sea level highstand during the Pliocene are sensitive to lateral changes in the viscosity and lithospheric thickness of the Earth beneath the ice sheet. Pliocene ice retreat from Antarctica is limited to 9 m of equivalent sea level rise using an Earth profile of a weak upper mantle and thin lithosphere; this compares to 15 m in Earth profiles with slower viscous bedrock rebound (Pollard et al., 2017). The properties of the solid Earth beneath the ice sheet have been shown to be more important in the Pliocene compared to the solid Earth response to ice volume changes during the last deglaciation (Gomez et al., 2018) (also see section 4.2.1). These results highlight the need for more detailed resolution of the Earth's structure in regions of the ice sheet that are currently experiencing change and/or are susceptible to future change.

Despite the large uncertainty in Pliocene sea level reconstructions and ice volume, Pliocene records have been used to tune ice sheet models projecting future sea level contributions from Antarctica (see section 4.1). Results from the Pliocene Ice Sheet Modeling Intercomparison project revealed the high dependency of Pliocene AIS configuration and sea level contribution based on variable climatology and ice sheet models (Dolan et al., 2018) (Table 2). Recent Pliocene ice sheet simulations suggest an Antarctic contribution of 3 to 12 m (Gasson et al., 2016); 7.8 to 11.4 m (Golledge, Thomas, et al., 2017), and 11.3 m (DeConto & Pollard, 2016); all these values imply that the AIS has significant sensitivity under warmer than present climates.

Ice sheet models that incorporate hydrofracturing of ice shelves and ice cliff collapse processes (see section 3.1.3) can simulate significant retreat in the East Antarctic Aurora Basin during the Pliocene (DeConto & Pollard, 2016). In contrast, seismic data suggest minimal retreat of the Totten Glacier by no more than 150 km into the Sabrina subglacial basin, although these data are equivocal with regards to absolute timing of the last retreat of the margin deep into this basin (Aitken et al., 2016; Gulick et al., 2017). More robust data of past retreat or stability of this margin are required in order to determine the climate thresholds or physical processes that govern retreat in this region. Currently, the geological evidence for WAIS and EAIS retreat during past warm periods of the Pliocene can only provide a qualitative estimate of AIS contribution to higher sea levels during warm periods in the geological past. Direct evidence of glacial retreat combined with geophysical modeling of Antarctica could help to confirm the extent of deglaciation beneath now-grounded portions of the AIS, to fully quantify the AIS contribution to sea level rise during warm climate intervals (McKay, Barrett, et al., 2016).

5.2.5. Paleoperspective on Current Rates of Sea Level Change

For Late Pliocene interglacials, mean rates of sea level rise were reconstructed at typical values of 0.3–0.5 m per century, with four interglacials that exceeded 0.5 m per century (Grant et al., 2019). Including hydrofracture and cliff-collapse mechanisms, Pollard et al. (2015) simulated rates of Antarctic mass loss under a warm Pliocene-like climate of approximately 1 m per century SLE. Alternative simulations that did not include these particular processes yielded rates of 0.45–0.65 m per century (Golledge, Thomas, et al., 2017).

Last interglacial sea level records provide a basis for understanding the main ocean-climate drivers behind sea level changes within a more recent warm period, including their rates of change. Likewise, sea level records through deglaciations may help in identifying the main driving processes behind very fast rates of sea level change and their relationship to changes in the radiative forcing of climate and interhemispheric heat redistribution within the ocean-climate system. Although past changes arose from different (preanthropogenic) rates of climate forcing than those observed today, the identification of critical processes in the past may still be relevant to the future. For example, the current incursion of warm CDW onto the Antarctic shelves (section 5.2.2) bears similarity to the consequences of bipolar temperature see-saw events of the past, when the ice sheet-climate perturbation response time was ~500–700 years (Grant et al., 2012, 2014). This similarity emphasizes the urgency of including encroachment of warmer water onto the Antarctic shelves and detailed processes of under-ice melting, in models for simulating the Antarctic response to future climate change.

Sea level fluctuations during the LIG and the timing and magnitude of ice sheet retreat have been widely debated (Bruggemann et al., 2004; Dutton, Webster, et al., 2015; Kopp et al., 2009; O'Leary et al., 2013; Orszag-Sperber et al., 2001; Rohling et al., 2008, 2009; W. G. Thompson et al., 2011). The lack of consensus on the timing, magnitude of the peak, and variability of sea level (stable, two prominent peaks, several oscillations) relates to difficulties in establishing consistent chronologies and correcting for the effects of tectonically driven vertical movements and GIA (see section 4.2.2) on paleoshorelines or sill depths. However, the fossil coral and coralline algae based sea level record from the Seychelles (Dutton, Webster, et al., 2015) seem to have little sensitivity to different GIA reconstructions that vary according to Earth models and ice sheet configurations used in the GIA models (see, e.g., the results over a wide range of Earth models and MIS6-MIS5e ice histories in Rohling et al., 2017). But a lack of (near)continuity in the Seychelles record means that inferred rates of sea level change are low-end estimates.

Other work has used the highly resolved Red Sea sea level records, where relative chronology is tightly constrained by stratigraphy, in comparison with coral and speleothem based records (Grant et al., 2012, 2014; Rohling et al., 2019). A focused study for the LIG suggests that mean rates of sea level rise may have reached 2.3–2.8 m per century (0.9–3.7 m per century at 2σ) (Rohling et al., 2019). However, 122 sea level rise events in the Red Sea records observed throughout the past 500,000 years, including other interglacial times when total global ice volume was similar to the present, revealed rates of sea level rise that were more commonly characterized by rates of up to 1.4 m per century (2σ) (Grant et al., 2012, 2014). These rates were driven by relatively slow natural climate forcing and feedback processes, and they likely form low-end estimates of the rates that may be expected due to the current fast anthropogenic climate forcing. Fitting of theoretical growth functions for rates of sea level rise, using broad probability distributions for ice volume (sea level) response times and rates of change obtained from the Red Sea results, suggests potential sea level rise by 2100 to about +1.8 m above the Year 2000 level (upper 95% probability bound) (Rohling et al., 2013). Again, this considers only naturally precedented rates of change, and addition of historically unprecedented (new) ice-dynamical processes may cause exceedance of that value. One exception is the initial fast sea level rise of the LIG, which may be a case where the ice response was trying to "catch up" with abrupt (regional) temperature forcing, and hence may provide an example where an ice sheet was responding to a disequilibrium with climate, not unlike today. This event might therefore portray a potential Antarctic melt scenario for the future, but it is predicated on large-scale and long-lasting invasion of warm waters onto the continent's shelf areas. Meltwater Pulse 1A may (partially) represent another such event, albeit much smaller in amplitude, which hinders signal-to-noise distinction.

6. Potential Consequences of AIS Melt

Global sea level change is a well-known consequence of climate change, due to the thermal expansion of ocean water, and glacier and ice sheet melt. The evidence suggests that most of the AIS loss will come from the WAIS in the coming century (Shepherd et al., 2019), although the rate and concentration of future greenhouse gas emissions will dictate the exact rate of sea level rise and also the wider AIS contributions. Aside from uncertainty around future emissions, an increasing number of studies has shown a spread in estimates of the Antarctic sea level contribution to the Year 2100 (Table 2), based on differences in how ice dynamics are modeled. Another complexity associated with sea level predictions is that the spatial pattern of regional sea level change is heterogeneous due to the impacts of Earth's gravitation, rotation, and deformation as a consequence of changes in ice mass. Improvements have been made in assessing the regional sea level impact or fingerprint of AIS melt, which have been aided by more accurate considerations of Earth's rheology beneath the AIS. While most of this paper deals with how climate and solid Earth processes affect the AIS, the following section also details how AIS sensitivity will in turn affect the climate system. In particular, this concerns the consequences of increased fresh water supplied to the Southern Ocean in response to increased ice melt, although we do not consider the impact on ecosystems.

6.1. Future Global Sea Level Change

6.1.1. Projected Sea Level Change

GMSL is projected in IPCC AR5 to rise through the 21st century by 0.26 (RCP2.6) to 0.98 m (RCP8.5), primarily in response to expansion of the warming oceans, and contributions from melting glaciers and ice sheets of Antarctica and Greenland (Church et al., 2013). The largest uncertainty in these estimates comes from

quantifying the Antarctic contribution to future sea level rise due to historically unprecedentedly rapid dynamic ice sheet mass loss (see section 2.1; Oppenheimer et al., 2019). AR5 concluded that collapse of marine-based sectors of the AIS is unlikely (<33% probability), but if initiated could add "up to several tenths of a meter" to the range predicted for 2100. Recent work suggests the possibility of an even larger AIS contribution to global sea level rise of ~1 m by 2100 (DeConto & Pollard, 2016; Pattyn et al., 2017). Goodwin et al. (2017) considered a very large ensemble of model projections of sea level change from an analytical model that show a high degree of congruence with CMIP5-based IPCC AR5 simulations, with a subset chosen based on additional consistency with time series of historical observation. They found a higher ice-melt sensitivity than previously recognized, with the consequence that ensemble mean sea level rise would be 13–16 cm higher than projected in IPCC AR5, even without additional consideration of ice dynamics.

Alternative methodologies to those used in AR5 have since been developed to provide an assessment of events beyond 2100. Slangen et al. (2017) highlighted the shift in sea level projection methodology toward a probabilistic approach using skewed uncertainty distributions to provide better assessments of low probability but high risk events in the future. Kopp et al. (2014) presented the first probability distribution for local sea level change, which can differ significantly from GMSL rise due to nonlinear changes in ocean dynamics, variations in Earth's gravitational field and crustal height, GIA and local effects of tectonics, and groundwater/hydrocarbon withdrawal and sedimentation. Sensitivity analyses showed that the nature of ice sheet mass changes had the largest effect on global and local sea level predictions. Kopp et al. (2014) highlighted the need for improved ice sheet models that do not depend on expert elicitation, which requires better constraints on the magnitude of positive and negative feedbacks on ice loss. Since this work, advances have been made in understanding static-equilibrium sea level and grounding line retreat processes, and the sea level feedback (Gomez et al., 2015), as well as the inclusion of new processes in ice sheet models.

Several studies have highlighted the major scientific challenges (e.g., Kennicutt et al., 2019, 2014, 2015, 2016) of accurately predicting the AIS response, and the consequent global sea level rise, to current and future ocean atmosphere-ocean warming (DeConto & Pollard, 2016; Edwards et al., 2019; Golledge et al., 2019, 2015; Ritz et al., 2015). Of these, all except the DeConto and Pollard (2016) study suggest a modest AIS contribution by 2100 within the range of the AR5 suggestion for high temperature forcing—less than 0.30 m (with 95% confidence; Ritz et al., 2015) or 0.39 m (upper bound; Golledge et al., 2015), with the latter predicting as little as 0.01 m by 2100 in low or moderate emission scenarios. In contrast, the results of DeConto and Pollard (2016) predicted an Antarctic contribution to GMSL rise of up to 1.05 cm ($1\sigma = 0.30$ m) by 2100 using RCP8.5 (see Table 2). The key difference between that study and the other studies is the inclusion of two MICI processes not previously considered at the continental ice sheet scale: hydrofracturing of ice due to surface melt ponding, and ice cliff failure (cf. section 3.1.3). When ice sheet models include these processes, the sea level contribution from AIS melt to 2100 may be closer to 0.45 m under an RCP 8.5 scenario (Golledge et al., 2019) versus 0.15 m using traditional ice sheet modeling approaches without MICI (similar to the AR5 predictions; Golledge et al., 2019). Pliocene sea level estimates are not sufficiently well quantified to be of use in constraining model projections of the AIS contribution to sea level rise; hence, the most recent sea level projections are calibrated using the satellite data (The IMBIE Team et al., 2018). The incorporation of ice-ocean-atmosphere feedbacks into simulations of the future AIS response suggests that the process of hydrofracturing by surface melting may not be important for sea level predictions to 2100 (Golledge, 2020; Golledge et al., 2019). However, the latest expert judgment assessment of Bamber et al. (2019) highlighted the increased uncertainty in sea level projections in response to uncertainty in ice processes and feedbacks and high scenario estimates that are significantly higher than AR5 with a combined contribution of 0.57 m from WAIS and EAIS (see Table 2). Importantly, all studies show that post-2100 Antarctica will continue to lose mass, even in the absence of continued forcing, resulting in many meters of eventual sea level contribution.

Incorporation of hydrofracturing and ice cliff failure processes into a probabilistic framework for sea level projections by Kopp et al. (2017) resulted in GMSL rise of 80–150 cm by 2100 for RCP 8.5. Using this approach, there was little correlation between the current rate of ice mass loss and the contribution to GMSL by 2100, highlighting the need to better understand the processes driving ice sheet melting. Three key, but highly uncertain model parameters that are limited by modern analogues and observations include (1) the rate of sub-ice shelf melt in response to ocean warming, (2) the sensitivity of crevasse penetration to meltwater input, and (3) the rate of ice cliff collapse. DeConto and Pollard (2016) and Kopp et al. (2017),

applied a temperature correction of 3°C to ocean temperatures to 400 m depth, in order to match the observed sub-ice shelf melt rates (Mouginot et al., 2014; Rignot et al., 2013). Improvements are required in these ice sheet models to achieve melt rates that are driven by more realistic ocean forcing, so that regional melting better matches the current observations. These can be used to understand the downstream feedbacks associated with freshwater input to the oceans (e.g., Silvano et al., 2018). It is also crucial to develop deep-water temperature reconstructions on the AIS margin during past times of sea level highstands (LIG and Pliocene), in order to test and improve models and their results.

By limiting sea level projections to 2100, the commitment to sea level rise into the future as a consequence of ocean and atmospheric heating and ice sheet instabilities initiated during the 21st century, is not fully realized (Bamber et al., 2019; Church et al., 2013; Golledge et al., 2015; Oppenheimer et al., 2019). Projections beyond 2100 using IPCC RCP-based warming scenarios highlight both the long-term lag in ice sheet/ice shelf responses to current perturbations in the climate and the importance of ocean-forced warming (e.g., Cornford et al., 2015; Golledge et al., 2015; Winkelmann et al., 2015). Anthropogenic warming exceeding 1.5–2°C above present was sufficient in these models to produce a collapse of the major Antarctic ice shelves within 100–300 years, with a subsequent long-term commitment to sea level rise due to the centennial to millennial scale response of the AIS.

6.1.2. Patterns of Sea Level Fingerprints From Antarctica

The sea level changes associated with variations in grounded ice cover are spatially heterogeneous due to effects associated with gravity, Earth rotation, and viscoelastic deformation of the solid Earth (Clark & Lingle, 1977; Farrell & Clark, 1976; Mitrovica et al., 2001). The spatial pattern of sea level change is dependent on the source of the ice melt, and hence, these patterns are therefore called "sea level fingerprints." In the vicinity of ice loss, sea level falls due to (1) a drawdown of the sea surface associated with changes to the gravitational field and (2) an uplift of the solid Earth beneath the missing mass (see Figure 13). Conversely, in the far field away from the ice margin, sea level rises more than the GMSL change associated with the ice loss, due to first-order gravitational effects. The sea level fall in the near field can be an order of magnitude, or more, greater than the sea level rise in the far field (Mitrovica et al., 2001). Earth deformation associated with adding water to the oceans and a shift of the Earth's rotation axis toward the missing ice mass impart second order effects to increase spatial and temporal variability of the pattern globally. The modeling and physics of sea level fingerprints is relatively well understood and reviewed in detail in for example Mitrovica et al. (2011) and Vermeersen and Schotman (2009).

Several recent studies have considered the sea level fingerprint that would follow collapse of sectors of the AIS in a warming climate (e.g., Bamber et al., 2009; Gomez, Mitrovia, Tamisiea, et al., 2010; Hay et al., 2017; Mitrovica et al., 2009; Mitrovica et al., 2011). Most of these studies have focused on the sea level change following a rapid retreat of the WAIS over time scales of hundreds of years or less, for which the solid Earth deformation has (until recently, see below) been considered purely elastic. Far-field peaks in the sea level fingerprint of 1.3 times the global average sea level change are predicted along the U.S. East Coast and in the Indian Ocean, and a sea level fall is predicted in the near field of WAIS reaching up to 15 times that of the global average sea level change (Gomez, Mitrovia, Tamisiea, et al., 2010; Mitrovica et al., 2009). Peaks from melting of the marine-based sectors of the EAIS are shifted relative to the fingerprint for the WAIS due in large part to Earth rotational effects and occur in the North Pacific and South Atlantic oceans (Gomez, Mitrovia, Tamisiea, et al., 2010). Bamber et al. (2009) found lower-amplitude peaks and minima in the WAIS fingerprint pattern than Mitrovica et al. (2009), but Mitrovica et al. (2011) later showed that these differences arose from the adoption of an elastically incompressible Earth model used in Bamber et al. (2009). In contrast, Mitrovica et al. (2011) and other studies (Golledge et al., 2019; Gomez, Mitrovia, Tamisiea, et al, 2010; Hay et al., 2017) employed a more realistic, elastically compressible Earth model and treatment of the inundation of water into marine sections of the WAIS as they were freed of ice.

Sea level fingerprints for melting from different AIS sectors may be combined to estimate the total contribution from ice loss to sea level change globally. However, until recently, modern sea level records (tide gauges and satellite records) have been too short or spatially sparse to distinguish the signal from individual ice sheets over and above the natural variability of the oceans (Hay et al., 2015). The first fully global data assessment of sea level fingerprint contributions to sea level change for 2002–2014 was published by Hsu and Velicogna (2017), based on GRACE data and ocean pressure measurements from Argo floats. This study used an updated time series of mass loss in Antarctica, which included mass loss from the WAIS and the

Antarctic Peninsula Ice Sheet as well as the Aurora basin sector of the EAIS, and mass gain in Queen Maud Land (Velicogna et al., 2014). The assessment for the period 2002–2014 showed, for example, an Antarctic sea level fingerprint along the North American coastline that is larger than those presented in previous studies that considered collapse of the WAIS (e.g., Mitrovica et al., 2009). Examining tide gauges from the Antarctic Peninsula and West Antarctica, Galassi and Spada (2017) suggested that they could observe the first evidence of detectable sea level fingerprints from the current melting of Antarctica. Along with these recent data-analysis advances, new sea level modeling tools have been developed that apply inverse modeling to determine the sensitivity of site-specific sea level changes to evolving ice mass loss geometries (Larour et al., 2017; Mitrovica et al., 2017). These new tools along with improvements in sea level and ice sheet mass change data sets hold a strong potential for future work using sea level fingerprinting to constrain the sea level hazards associated with regional ice mass changes around Antarctica in the future.

Fingerprint studies have generally assumed that viscous Earth deformation is negligible on time scales of a few centuries and so have adopted a purely elastic Earth model in their calculations. However, seismic tomography studies and geological evidence suggest that upper mantle viscosities across the Antarctic are highly laterally variable and may be several orders of magnitude lower than the average (see section 4.2.1). Hay et al. (2017) have adopted a realistic, 3-D Earth viscosity model that includes variability in lithospheric thickness and mantle viscosity and a more realistic ice loss geometry to reassess the fingerprint of WAIS collapse and its contribution to GNSS/GPS and gravity data. This and other studies (e.g., Barletta, et al., 2018; Powell et al., 2019) suggest that viscous effects may in fact be nonnegligible on decadal to centennial time scales in West Antarctica. For example, Hay et al. (2017) assessed a 100 year collapse event, including lateral variability in Earth structure. They found that this leads to a slightly reduced peak sea level rise predicted in the far field and a sea level fall in the vicinity of the WAIS that is up to 50% larger than the aforementioned estimates from simple 1-D elastic Earth models. The sea level fall continued to increase for ice sheet retreat scenarios over longer time scales. The difference between 1-D and more realistic 3-D Earth viscosity models on the AIS contribution to global sea levels (i.e., the pattern of global sea level change) highlights the need for further work to define the viscosity profile beneath West Antarctica (e.g., in the Amundsen Sea Embayment, Barletta et al., 2018).

6.2. Ocean State and Circulation

Increased melting of the AIS will have implications for the Southern Ocean and in turn for the wider global climate through changes in the MOC. Observations around Antarctica are beginning to show that increased basal melt can significantly change the local stratification, with potential implications for both the local circulation and water mass formation. Freshwater input from melting ice shelves (Jacobs et al., 2011; Kim et al., 2016; Loose et al., 2009; Nakayama et al., 2013; Naveira Garabato et al., 2017; Silvano et al., 2017) can partly reduce or completely inhibit sea ice-driven convection (Petty et al., 2013; Williams et al., 2016; Silvano et al., 2018). This prevents the formation of dense (cold and/or salty) shelf water (DSW) masses, which form the precursors for AABW, and thus an important component of the MOC.

The processes governing AABW formation are complex and include the formation and export of sea ice linked to wind strength and pattern (Santoso & England, 2008), glacial meltwater input from the AIS and sea level (Paillard & Parrenin, 2004), and the creation of polynyas close to the coast by winds (Tamura et al., 2016). Modeling studies show that the role of AABW in controlling heat transport across the shelf varies between models, depending on which of the aforementioned processes are present and how they interact.

For example, coarse-resolution models suggest that meltwater addition in the near the surface close to the Antarctic coast reduces surface density and thus the potential for AABW formation (Fogwill et al., 2015; Menviel et al., 2010; Phipps et al., 2016). As a result, the rate of AABW formation can be reduced by as much as ~50% (Fogwill et al., 2015). Weakened AABW formation decreases the oceanic meridional heat transport to high southern latitudes and leads to lower SSTs over the Southern Ocean and a larger sea ice extent (Menviel et al., 2015). Moreover, the increased surface stratification and reduced convection were found to lead to a subsurface warming. This warming occurs below the mixed layer south of 60°S and reaches an amplitude of 0.5°C to 1°C (Fogwill et al., 2015; Menviel et al., 2010; Phipps et al., 2016; Swingedouw et al., 2009). The strongest warming can occur adjacent to sectors of the WAIS (e.g., along the Antarctic Peninsula, Amundsen Sea, Marie Byrd Land, and Ross Sea) that are particularly vulnerable to grounding

line retreat and MISI (Fogwill et al., 2015). A high-resolution modeling study suggests that the magnitude of the subsurface warming could exceed 3.5°C and 2.5°C along the coast in the Ross and Weddell Seas, respectively (Bronselaer et al., 2018). If this warming extends to other areas of Antarctic continental shelf, then it could lead to thermal erosion of the WAIS and sectors the EAIS (e.g., Recovery, Aurora, Wilkes Basins, and Marie Byrd Land; Fogwill et al., 2015; Golledge, Levy, et al., 2017) and induce a positive feedback, accelerating disintegration of sectors of the ice sheet that are highly sensitive to ocean temperature changes (Golledge et al., 2014; Menviel et al., 2010). Moreover, given that coastal currents around the Antarctic continent can carry fresher surface waters westward (Phipps et al., 2016; Rignot & Jacobs, 2002), initial melting of a single sector of the AIS could impact upon the wider ice sheet. Under this scenario, meltwater-induced changes in the Southern Ocean could act as a strong positive feedback mechanism, amplifying the response to climate forcings. However, this theory has not yet been confirmed by observations.

The process of DSW suppression by meltwater is well understood (e.g., Lago & England, 2019; Snow, Sloyan, et al., 2016). However, it remains poorly represented in coarse resolution models, in which dense waters are primarily formed through open ocean convection outside the shelves. The effect of meltwater is likely to be amplified in coastal polynyas, relative to open ocean convection sites, as polynyas in close proximity to the meltwater sources are particularly sensitive to freshwater input (Silvano et al., 2018; Williams et al., 2016).

Models suggest that the strength of the deep MOC cell, which involves AABW, decreases under warming scenarios. This is due to both a reduction in sea ice formation associated with the change in heat flux (Cougnon et al., 2013; Kusahara & Hasumi, 2013; Morrison et al., 2015; St-Laurent et al., 2015) and the increased stratification associated with enhanced glacial meltwater (Pauling et al., 2016). Models without an ice shelf component underestimate the response of the deep MOC cell in a warming climate (Kusahara & Hasumi, 2013). Oceanographic data collected along the Sabrina Coast and in the Amundsen Sea, combined with a mixed-layer ocean model, also demonstrate that freshwater input from the basal melt of ice shelves can inhibit the formation of DSW and allow CDW to reach ice shelf cavities (Silvano et al., 2018). At a regional scale, an increase in freshwater flux due to basal melting is likely to enhance heat exchange across different sectors of Antarctic shelves due to a more vigorous buoyancy-driven coastal current (Nakayama et al., 2014).

AIS meltwater input to the surface of the Southern Ocean has been shown in models to result in cooling of the stratified surface ocean, sea ice expansion, and warming of the subsurface water (500–1,500 m) (Menviel et al., 2010; Richardson et al., 2005; Stouffer et al., 2007), which reduces the formation of AABW in the areas where it forms today. This feedback mechanism was demonstrated to encourage further melting at the base of the ice shelves (Golledge et al., 2014) and has since been supported by other modeling studies (e.g., Bronselaer et al., 2018; Fogwill et al., 2015; Phipps et al., 2016). Note, however, that this is different from the mechanism proposed for the inferred AIS sea level contribution to the LIG highstand, where proxy records show a decrease (rather than increase) in sea ice and AABW formation following Southern Hemisphere warming during HS11 (see section 5.2.3). We tentatively suggest that a possible explanation for the difference between LIG proxy data and modeling results may be the unprecedented scale and duration of the LIG changes, which related to an extremely pronounced bipolar temperature see-saw effect that lasted some 5,000 years. Initial AIS retreat may have driven sea ice expansion as models suggest, but maintained Southern Ocean warming over 5,000 years may have overwhelmed the initial response, resulting in an overall sea ice retreat as suggested by the proxy data. This hypothesis will require testing with runs of high-resolution models over >5,000 years. The LIG response to climate warming may be more similar to the future anthropogenic climate change scenarios, where reduced sea ice would be the result of warming of the climate system. Under such scenarios, future freshwater input into the Southern Ocean due to melting of the AIS would be expected to result in stratification of the ocean, a reduction in AABW formation and warming of the ocean at depth (Phipps et al., 2016).

Models also suggest that AABW reduction could also have significant far-field effects, such as a reduction in the formation of NADW within half a century of a meltwater pulse (Swingedouw et al., 2009). Further work has suggested that meltwater input into the Southern Ocean can have global-scale impacts upon the climate system, including an increase in Southern Hemisphere sea ice area, which increases global albedo; cooling of

the atmosphere throughout the Southern Hemisphere and much of the Northern Hemisphere; and a northward shift in the position of the Intertropical Convergence Zone (Bronselaer et al., 2018).

It has also been suggested that freshwater may not enter the ocean as a simple meltwater pulse but instead as an armada of melting icebergs in the Southern Ocean. Such an iceberg scenario may enhance the formation of sea ice and models suggest a minor increase in open ocean deep water formation (Jongma et al., 2009). Modern observations suggest that the most likely future scenario consists of a combination of both large iceberg calving, as seen with the Larsen ice shelves (Hogg & Gudmundsson, 2017; Rack & Rott, 2004; Rott et al., 1996) and significant meltwater input in areas like the Amundsen and Bellingshausen Sea where currently no AABW is formed (Rignot et al., 2013). Thus, it is likely that the formation of AABW may decrease in some locations but may be less affected in other regions around the Antarctic margin. An underestimated and/or unknown component relating to freshwater loss from the AIS concerns subglacial-fluvial transport from deep inland under Antarctica (e.g., from Recovery Lakes, Vostok, and Prince Elizabeth Land) (Le Brocq et al., 2013).

Increased melting of the AIS may furthermore have biogeochemical implications relating to oceanic carbon storage and cycling. A 2010–2013 satellite survey of giant icebergs in the Southern Ocean observed increased chlorophyll concentrations in their wake, which was inferred to result in an increased carbon export, as a result of iron fertilization (Duprat et al., 2016). Increased iron supply from melting of the AIS (Death et al., 2014; Gerringa et al., 2012) may act to fertilize the Southern Ocean and increase productivity due to the supply of iron-rich glacial meltwater. In the biogeochemical model of Death et al. (2014), Southern Ocean productivity was increased by 40% in runs that included iron release from the AIS, relative to those without such an iron source.

Experiments using the intermediate complexity LOVECLIM model suggest that increased AIS meltwater input leads to an expansion of sea ice, an intensification of the Southern Hemisphere westerly winds, and a reduction of biological productivity in the Southern Ocean south of 40^{o}S (Menviel et al., 2010). Yet this model also simulates an increased subduction of Subantarctic Mode Water, leading to greater export of nutrients to the equator. This drives an increase in tropical productivity, thus resulting in no overall change in the global biological export. Note that the results of this simulation depend on the strength and position of the Southern Hemisphere westerly winds and that changes in iron fertilization were not taken into account. While an expansion of sea ice may act to reduce Southern Ocean productivity by decreasing light availability, enhanced productivity in the high-latitude Southern Ocean has been suggested to play a significant role in lowering atmospheric CO_2 through sea ice feedbacks (Fogwill et al., 2020), during a period of cooling known as the Antarctic Cold Reversal (14.6–12.7 ka), which interrupted the climate warming of the last deglaciation (Pedro et al., 2016). High seasonal variability in sea ice extent during this period are suggested to enhance productivity by increasing nutrient availability through deepening of the mixed layer, and iron supply during sea ice melt, and through the absorption of CO_2 within the melting sea ice (Delille et al., 2014)

Together, the examples from paleoclimate records and mechanistic insights from coupled climate models highlight the existence of strong links between changes in the AIS and global ocean circulation, and hint at important implications of a dynamic AIS. They also highlight the uncertainty around the climate feedbacks resulting from anthropogenically induced melting of the AIS. Ocean freshening associated with glacial meltwater input in model simulations shows positive feedbacks regarding both the expansion of sea ice and subsurface warming (e.g., Fogwill et al., 2015; Phipps et al., 2016; Menviel et al., 2010) and reduction of sea ice and subsurface warming (Bronselaer et al., 2018), as well as a number of negative feedbacks associated increased Southern Ocean carbon storage through sea ice feedbacks (Fogwill et al., 2020), the reduction of MISI due to sea level lowering in the region of AIS mass loss, and the stabilizing effect of rapid bedrock uplift in regions of West Antarctica (see section 4.2.2). This demonstrates a compelling need to conduct further research into ice-ocean and solid Earth feedbacks and incorporate such feedbacks into future climate projections through the development of coupled climate-ice sheet models. In doing so, due care is needed in distinguishing impacts over different time scales and for different amplitudes of ice melt and warming. While sea ice responses, for example, might lean initially toward expansion, they might reverse toward reduction during long-term sustained, large-amplitude warming.

Table 3
The Key Scientific Questions Discussed in This Review From Three of Seven Clusters Developed by the Antarctic and Southern Ocean Science Horizon Scan (Kennicutt et al., 2015)

Southern Ocean and sea ice in a warming world	Antarctic ice sheet and sea level	The dynamic Earth: probing beneath Antarctic ice
12. Will changes in the Southern Ocean result in feedbacks that accelerate or slow the pace of climate change?	24. How does small-scale morphology in subglacial and continental shelf bathymetry affect Antarctic ice sheet response to changing environmental conditions? (Crosscuts "Dynamic Earth")	37. What is the crust and mantle structure of Antarctica and the Southern Ocean, and how do they affect surface motions due to glacial isostatic adjustment?
13. Why are the properties and volume of Antarctic Bottom Water changing, and what are the consequences for global ocean circulation and climate?	25. What are the processes and properties that control the form and flow of the Antarctic ice sheet?	38. How does volcanism affect the evolution of the Antarctic lithosphere, ice sheet dynamics, and global climate? (Crosscuts "Antarctic ice sheet")
14. How does Southern Ocean circulation, including exchange with lower latitudes, respond to climate forcing?	26. How does subglacial hydrology affect ice sheet dynamics, and how important is it? (Crosscuts "Dynamic Earth")	40. How do tectonics, dynamic topography, ice loading, and isostatic adjustment affect thespatial pattern of sea level change on all timescales? (Crosscuts "Antarctic ice sheet")
15. What processes and feedbacks drive changes in the mass, properties, and distribution of Antarctic sea ice?	27. How do the characteristics of the ice sheet bed, such as geothermal heat flux and sedimentdistribution, affect ice flow and ice sheet stability? ("Crosscuts Dynamic Earth")	
20. How do extreme events affect the Antarctic cryosphere and Southern Ocean? (Crosscuts "Antarctic ice sheet")	28. What are the thresholds that lead to irreversible loss of all or part of the Antarctic ice sheet?	
21. How did the Antarctic cryosphere and the Southern Ocean contribute to glacial/interglacial cycles? (Crosscuts "Antarctic ice sheet")	29. How will changes in surface melt over the ice shelves and ice sheet evolve, and what will be the impact of these changes?	
23. How will changes in freshwater inputs affect ocean circulation and ecosystem processes? (Crosscuts "Antarctic life")	30. How do oceanic processes beneath ice shelves vary in space and time, how are they modified by sea ice, and do they affect ice loss and ice sheet mass balance? (Crosscuts "Southern Ocean")	
	32. How fast has the Antarctic ice sheet changed in the past and what does that tell us about the future?	
	33. How did marine-based Antarctic ice sheets change during previous interglacial periods?	
	34. How will the sedimentary record beneaththe ice sheet inform our knowledge of the presence or absence of continental ice? (Crosscuts ("Dynamic Earth")	

Note. The numbering has been maintained as originally published and does not indicate the relative importance of the questions.

7. Summary and Future Research Priorities

The societal impact of sea level rise calls for an understanding of how the AIS will evolve in a warming world, in terms of which portions of the marine-based sectors will retreat, including the time scales and rates of change. This review has focused on research that covers many different processes and feedbacks governing AIS dynamics with an emphasis on the period since IPCC AR5 and on evidence concerning the potential for rapid AIS evolution. Understanding the processes, feedbacks, and tipping points that govern the AIS is key to our ability to accurately predict its future behavior. We have highlighted the developments across multiple disciplines of Earth Science that underpin such insights. The pace of research to address uncertainties in the AIS response to anthropogenic warming and global sea level rise has been, and continues to be, rapid across all the disciplines. Exciting new interdisciplinary efforts have been facilitated by the community-based identification of the major science priorities (Antarctic Science Horizon Scan ("the Scan"); Kennicutt et al., 2014, 2015, 2019) and the essential technology and infrastructure requirements (The Antarctic Roadmap Challenges; Kennicutt et al., 2016). The Scan identified the 80 most important scientific questions clustered into seven groups. This review has touched on 19 of the questions across three of the groups, including all but one of the 12 questions in the group "Antarctic ice sheet and sea level" (Table 3). In this section, we highlight some of the unknowns across the different research areas that will help in improve our understanding of future AIS change and summarize some of the key points from this multidisciplinary review.

7.1. AIS Interactions With the Southern Ocean

Observations extending back to 1979 show that the AIS has been losing mass. Later oceanographic observations linked high glacier melt rates to the presence of warm CDW on the Antarctic shelves of West Antarctica (Jacobs et al., 1996). The rate of ice mass loss has accelerated since 2000s and resulted in an increasing contribution of AIS melt to GMSL rise, mainly from thinning and retreat of the WAIS. The mass balance of the EAIS is currently still unclear and associated with larges uncertainty in estimates, which requires improved observations of precipitation and constraints on GIA. The rate of global ocean warming has continued to increase in response to anthropogenic emissions, with the majority of the heat being absorbed by the Southern Ocean and transported north away from the Antarctic margin (Swart et al., 2018). More observations are required to attribute and quantify the observed slowdown in AMOC to anthropogenic forcing (Frajka-Williams et al., 2019). However, the link between AMOC collapse and buildup of heat in the Southern Ocean resulting in subsequent AIS mass loss is supported by paleoenvironmental studies, particularly for the Last Interglacial (Marino et al., 2015; Rohling et al., 2019). The temporal resolution of proximal sediment records around the Antarctic margin currently limits the assessment of abrupt (centennial-scale) climatic events in the paleorecord, but modeling work (e.g., Pedro et al., 2018) reveals a physical mechanism for the centennial-scale response to AMOC collapse, with the accumulation of heat in the Southern Ocean, and eddy-driven heat flux across the ACC resulting in surface warming and sea ice retreat.

The observed increase in Southern Ocean stratification and increased surface buoyancy of the Southern Ocean in response to accelerated ice mass loss and retreat in Antarctica will have impacts on both sea ice and overturning circulation. Improvements are required in the representation of DSW and AABW in ice sheet-climate models. Since a large part of the AIS mass loss is driven by incursions of warm CDW onto the shelf including a more accurate quantification of sub-ice shelf melt rates, well-resolved measurements and model representations of subsurface temperature changes on the Antarctic shelf are required for accurate future projections of AIS change. Long-term ice and ocean monitoring programs are all needed to improve understanding of the feedbacks and interactions leading to warm water incursions on the Antarctic shelf, and how these respond to a changing climate.

7.2. Ice Sheet Dynamics, the Solid Earth, and Sea Level

The paleoclimate record can provide insight into the behavior of the natural system over longer time scales and can be used to assess the validity of coupled Earth system models that are widely used to predict future changes. These longer millennial-scale records also reveal the importance of understanding the solid Earth feedbacks on AIS dynamics. Temperature increases of 1° to 3° warming could result in a fourfold difference of 6 to 27 cm in sea level rise to 2070 (Rintoul et al., 2018). Predicting the long-term equilibrated AIS response and subsequent sea level rise requires insight from past warm interglacial periods of the Pliocene (400 ppm; 2–4°C warmer) and Pleistocene warm times (~280 ppm; 1–2°C). Geological records from close to Antarctica and ice sheet modeling experiments indicate that the AIS, including the EAIS, was highly sensitive to past changes in atmospheric CO_2 concentrations. Indeed, a strong correlation exists between GMSL and atmospheric CO_2 concentrations (indicator for global temperature) for these geological times, which cannot be explained considering the Northern Hemisphere ice sheets alone (Foster & Rohling, 2013).

Ice sheet models incorporating dynamic ice processes forced by ocean-driven melting indicate up to 0.45 (no MICI; Edwards et al., 2019; Golledge et al., 2019) to 1 m (MICI; DeConto & Pollard, 2016) of GMSL rise from the AIS alone by 2100, and up to ~11 m (RPC8.5; Pollard et al., 2017) by the Year 2500. However, the inclusion of hydrofracturing and ice cliff instability processes in ice sheet models compared to traditional ice flow physics remains uncertain. There is a definite role for improved constraints on past sea level estimates from the geological record, for robust calibration of ice sheet models where the suitability of dynamic ice mechanisms is currently unknown.

Improved projections of sea level rise from the AIS based on ice sheet modeling requires reduced uncertainty in reconstructions of past global sea level and its rates of change, for the interglacial periods of the Pleistocene (e.g., LIG; Marine Isotope Stage 11), and the warm Pliocene (e.g., Mid Pliocene Warm Period or early Pliocene). Paleo sea level estimates for the AIS contributions to global sea level change are hampered by our limited knowledge of past ice sheet configuration and volumes for key glacial periods, such as the penultimate glacial maximum (MIS 6) and those preceding the warm interglacials of interest. Such reconstructions require increased spatial sampling of marine sediment deposits around Antarctica with improved

dating techniques and novel proxies to constrain AIS retreat and meltwater input. These data can be used to inform models of GIA, grounding line migration and ice flow, and help reduce uncertainties in future global sea level predictions. Related to this, more studies of dynamic topography are needed to improve the accuracy of sea level estimates in the geological past. Ice core evidence from the subglacial basins of the WAIS and Wilkes Subglacial Basin (East Antarctica) could be drilled to establish the presence or absence of ice dating back to the Last Interglacial Period. In addition, ice cores from the AIS periphery could be used to establish the prevalence of surface melt layers, as indicators of conditions where hydrofracturing may have occurred at the coast, during past warm climates.

New paleoenvironmental archives have been drilled from different sectors of Antarctica by the International Ocean Drilling Program (e.g., Ross Sea, IODP 374; McKay et al., 2019); Amundsen Sea, IODP 379; Gohl et al., 2019); Scotia Sea, IODP 382;Weber et al., 2019) and will facilitate reconstructions of both AIS dynamics and Southern Ocean feedbacks. Observations are needed over a range of spatial scales (catchment to subcatchment), and with well-defined uncertainty bounds, for parameters such as ocean temperature changes around the Antarctic margin. In addition, proxies that capture ice mass loss as well as interaction between the Southern Ocean and the AIS (e.g., changes in stratification and sea ice cover) would be valuable for calibration of coupled ice-climate modeling studies.

Quantifying the extent and timing of deglacial retreat in multiple sectors of Antarctica is required to test hypotheses regarding the climatic mechanisms for initiating widespread marine AIS retreat. In this context, it is essential to constrain the roles that internal ice sheet dynamics, solid Earth processes and atmosphere-oceanic feedbacks had in either accelerating or slowing retreat during the last glacial termination and the Holocene. Isostatic feedbacks are also critical to consider when comparing model and data-based reconstructions, with mantle viscosity being a fundamental control on the glacio-isostatic adjustment rate and therefore ice mass loss. The sensitivity of this feedback between the solid Earth rebound and ice mass change is important for regions of low Earth viscosity, such as beneath the WAIS, in order to accurately predict the future AIS contribution to, and rate of, sea level rise. In a similar way, the interaction of glacial retreat and advance events with other basal conditions (e.g., till mechanics, hydrology, and hydrogeology) is likely significant, although the overall role of these in AIS dynamics remains a key knowledge gap.

Understanding the ice flow processes that could lead to rapid AIS grounding line retreat is essential in improving model projections of sea level rise. Key areas for improvement include basal friction laws and their impact on grounding line dynamics and migration; ice flow relations and the role of deformation in ice shelves, the slow-flowing interior of the AIS, and at transitions between deformation-dominated and sliding-dominated flow; and regional investigations of interactions between ice dynamic processes, pinning points, ocean circulation, and ice shelf response. Improving ice sheet model representation of flow processes will be facilitated by increased accuracy in boundary conditions, including bed topography and ice shelf melt rates, and synthesis of observations, for example, in time-dependent adjoint modeling frameworks.

Collaborative initiatives incorporating both observational and modeling efforts to ascertain the current state and evolution of entire glacial basins, such as currently being undertaken for the Thwaites Basin as part of the International Thwaites Glacier Collaboration, will be instrumental in improving our understanding of grounding line controls and in predicting future mass flux changes to the AIS. Similar programs are required to understand the time scales of risk in the key marine-grounded basins of East Antarctica (i.e., in the Aurora and Wilkes Subglacial Basins).

For progress across disciplines, high-resolution bed topography and bathymetry data sets are paramount in development of accurate numerical model simulations of the AIS and Southern Ocean interactions, as well as solid Earth and paleoenvironmental reconstructions. High-resolution information of the Earth structure beneath the ice sheet is needed for incorporation of these 3-D Earth properties in ice sheet models to advance predictions of the AIS response to future climate change. The solid Earth has a long memory for past ice loading changes, so accurate knowledge of Earth's rheology is vital for understanding the interactions and feedbacks relating to changes between the solid Earth and ice mass, as well as accurate GIA corrections for past sea level reconstructions.

It is clear that our best chance of making major progress in understanding how the AIS will evolve in the future will come from a cross-disciplinary approach. Advances will require integrated modeling and observational studies across the atmosphere, ocean, ice (ice sheet, ice shelves, and sea ice), and solid Earth

including subglacial hydrology and high-resolution bathymetry, across a wide range of temporal and spatial scales. This review demonstrates the value of integrating knowledge from paleoenvironmental observations and modeling with modern observations of change in the AIS and climate system, for developing a sufficiently detailed understanding of the processes required to accurately predict the future AIS evolution.

Data Availability Statement

No new data were used in the review article, which is based on existing data from previously published sources. The sources of the public or published data used in the figures are detailed in the legend.

Acronyms and Glossary

ACR	Antarctic Cold Reversal
AIS	Antarctic Ice Sheet
ASF	Antarctic Slope Front
CDW	Circumpolar Deep Water
DSW	Dense shelf water
EAIS	East Antarctic Ice Sheet
ENSO	El Niño–Southern Oscillation
GIA	Glacial isostatic adjustment
GMSL	Global mean sea level
GRACE	Gravity Recovery and Climate Experiment
LGM	Last Glacial Maximum
LIG	Last Interglacial Period
MIS	Marine Isotope Stage
MICI	Marine ice cliff instability
MISI	Marine ice sheet instability
MWP-1a	Meltwater Pulse 1a
MOC	Meridional Ocean Circulation
NEEM	North Greenland Eemian
RCPs	Representative Concentration Pathways
SAM	Southern Annual Mode
WAIS	West Antarctic Ice Sheet
Anisotropic ice fabric	patterns of preferred ice crystal orientations that is consistent with the underlying stress regime
Buttressing	tendency of an ice shelf to slow or halt the flow of upstream grounded ice through interaction with topography, for example, basal or lateral pinning points
Cartesian grid	a regular grid composed of unit square or cube elements with vertices defined on the integer lattice.
Diamict	poorly sorted terrigenous material (e.g., cobbles, sand, silt, and clay) a wide range of particle sizes associated with ice transport and deposition.
Geothermal heat flux	the amount of heat through unit area and unit time coming from the Earth's interior. This contains the primordial heat trapped in the interior of the planet and the heat produced by radiogenic elements within the crust. The main sources of geothermal heat flux variation are heat flux from the mantle, linked to tectonic events such as rifting and collision; heat production within the crust, derived from high concentrations of radiogenic isotopes, for example, uranium, thorium, and potassium; and more local effects of volcanic and shallow intrusive magmatism.

Glacial erratics	rocks carried by glaciers over large distances away from the source of origin, ranging in size from pebbles to car-sized boulders
Grounding line/zone	transition line/zone between grounded ice sheet and floating ice shelf
Holocene	the last ~11,600 years of climate history
Ice shelf draft	elevation of the base of the ice shelf
Laplace domain in solid Earth modeling	mathematical tool used to work in a spatial-frequency domain when dealing with complex signals.
Last deglaciation	the period where the climate transitioned from cold to warm conditions (~19,000–11,600 years ago)
Last Glacial Maximum	the most recent glacial period approximately 27,000–19,000 years ago
Last Interglacial Period	the penultimate warm period in Earth's climate history around 130,000–115,000 years ago
Pleistocene	Geological epoch spanning the last 2.5 million years of Earth history until the beginning of the Holocene.
Overdeepened continental shelves	topographically confined depressions formed by glacier erosion across the continental shelves, which can be 200–500 m and up to 1,000 m below sea level.
Rheology	The response of a material to deformation when stress or strain is applied. Relevant to both the solid Earth, which can deform elastically, viscously, and plastically; and the ice sheet.
Termination II	the transition from glacial climate to interglacial climate following the end of Marine Isotope Stage 6 (the penultimate glaciation).
Shallow ice approximation	approximation to the full Stokes equations; assumes that ice flows as a result of gravitational driving stresses, balanced by basal shear stresses.
Stokes equations	equations of motion for ice flow

Acknowledgments

This review paper is the result of a workshop sponsored by the Australian Academy of Sciences Frederick and Elizabeth White Award, the Australian Research Council's Special Research Initiative for Antarctic Gateway Partnership (Project ID SR140300001), and the University of Tasmania. This work contributes to The Australian Centre for Excellence in Antarctic Science funded by Australian Research Council Project ID SR200100008. T. L. N. was supported by the Science Industry Endowment Fund John Stocker Postdoctoral Fellowship. The authors are grateful to C.-D. Hillenbrand and S. S. R. Jamieson for extensive and thorough reviews and for sharing their knowledge of all things Antarctic. Thanks to A. Durand for initial reference support, S. Cook and T. Staal for editing text, and L. Bell for graphic design.

References

Abram, N. J., McGregor, H. V., Tierney, J. E., Evans, M. N., McKay, N. P., Kaufman, D. S., et al. (2016). Early onset of industrial-era warming across the oceans and continents. *Nature*, *536*(7617), 411–418. https://doi.org/10.1038/nature19082

Abram, N. J., Mulvaney, R., Vimeux, F., Phipps, S. J., Turner, J., & England, M. H. (2014). Evolution of the Southern Annular Mode during the past millennium. *Nature Climate Change.*, *4*(7), 564–569. https://doi.org/10.1038/nclimate2235

Abram, N. J., Mulvaney, R., Wolff, E. W., Triest, J., Kipfstuhl, S., Trusel, L. D., et al. (2013). Acceleration of snow melt in an Antarctic Peninsula ice core during the twentieth century. *Nature Geoscience*, *6*(5), 404–411. https://doi.org/10.1038/ngeo1787

Accardo, N. J., Wiens, D. A., Hernandez, S., Aster, R. C., Nyblade, A., Huerta, A., et al. (2014). Upper mantle seismic anisotropy beneath the West Antarctic Rift System and surrounding region from shear wave splitting analysis. *Geophysical Journal International*, *198*(1), 414–429. https://doi.org/10.1093/gji/ggu117

Adhikari, S., Ivins, E. R., Larour, E., Seroussi, H., Morlighem, M., & Nowicki, S. (2014). Future Antarctic bed topography and its implications for ice sheet dynamics. *Solid Earth*, *5*(1), 569–584. https://doi.org/10.5194/se-5-569-2014

Aitken, A. R. A., Roberts, J. L., Ommen, T. D., Young, D. A., Golledge, N. R., Greenbaum, J. S., et al. (2016). Repeated large-scale retreat and advance of Totten Glacier indicated by inland bed erosion. *Nature*, *533*(7603), 385–389. https://doi.org/10.1038/nature17447

Aitken, A. R. A., Young, D. A., Ferraccioli, F., Betts, P. G., Greenbaum, J. S., Richter, T. G., et al. (2014). The subglacial geology of Wilkes Land, East Antarctica. *Geophysical Research Letters*, *41*, 2390–2400. https://doi.org/10.1002/2014GL059405

Albrecht, T., & Levermann, A. (2014). Spontaneous ice-front retreat caused by disintegration of adjacent ice shelf in Antarctica. *Earth and Planetary Science Letters*. https://doi.org/10.1016/j.epsl.2014.02.034

Alley, K. E., Scambos, T. A., Siegfried, M. R., & Fricker, H. A. (2016). Impacts of warm water on Antarctic ice shelf stability through basal channel formation. *Nature Geoscience*, *9*(4), 290–293. https://doi.org/10.1038/ngeo2675

Alley, R. B., Anandakrishnan, S., Dupont, T. K., Parizek, B. R., & Pollard, D. (2007). Effect of sedimentation on ice-sheet grounding-line stability. *Science*, *315*(5820), 1838–1841. https://doi.org/10.1126/science.1138396

Alley, R. B., Blankenship, D. D., Bentley, C. R., & Rooney, S. T. (1986). Deformation of till beneath ice stream B, West Antarctica. *Nature*, *322*(6074), 57–59. https://doi.org/10.1038/322057a0

Alley, R. B., Blankenship, D. D., Rooney, S. T., & Bentley, C. R. (1989). Sedimentation beneath ice shelves—The view from ice stream B. *Marine Geology*, *85*(2–4), 101–120. https://doi.org/10.1016/0025-3227(89)90150-3

Alley, R. B., Lawson, D. E., Evenson, E. B., Strasser, J. C., & Larson, G. J. (1998). Glaciohydraulic supercooling: A freeze-on mechanism to create stratified, debris-rich basal ice: II. Theory. *Journal of Glaciology*, *44*(148), 563–569. https://doi.org/10.1017/S0022143000002070

Allison, I., Hock, R., King, M. A., & Mackintosh, A. N. (2018). Future Earth and the cryosphere. In J. Li, K. Alverson, T. Beer (Eds.), *Global change and future Earth: The geoscience perspective* (pp. 91–113). Cambridge: Cambridge University Press. https://doi.org/10.1017/9781316761489.011

An, M., Wiens, D. A., Zhao, Y., Feng, M., Nyblade, A. A., Kanao, M., et al. (2015a). S-velocity model and inferred Moho topography beneath the Antarctic Plate from Rayleigh waves. *Journal of Geophysical Research: Solid Earth*, *120*, 359–383. https://doi.org/10.1002/2014JB011332

An, M., Wiens, D. A., Zhao, Y., Feng, M., Nyblade, A., Kanao, M., et al. (2015b). Temperature, lithosphere-asthenosphere boundary, and heat flux beneath the Antarctic Plate inferred from seismic velocities. *Journal of Geophysical Research: Solid Earth*, *120*, 8720–8742. https://doi.org/10.1002/2015JB011917

Anandakrishnan, S., Blankenship, D. D., Alley, R. B., & Stoffa, P. L. (1998). Influence of subglacial geology on the position of a West antarctic ice stream from seismic observations. *Nature*, *394*(6688), 62–65. Cited By (since 1996) 108Export Date 13 March 2013. https://doi.org/10.1038/27889

Anderson, J. B., Conway, H., Bart, P. J., Witus, A. E., Greenwood, S. L., McKay, R. M., et al. (2014). Ross Sea paleo-ice sheet drainage and deglacial history during and since the LGM. *Quaternary Science Reviews*, *100*(September), 31–54. https://doi.org/10.1016/j.quascirev.2013.08.020

Anderson, R. F., Ali, S., Bradtmiller, L. I., Nielsen, S. H. H., Fleisher, M. Q., Anderson, B. E., & Burckle, L. H. (2009). Wind-driven upwelling in the Southern Ocean and the deglacial rise in atmospheric CO_2. *Science*, *323*(5920), 1443–1448. https://doi.org/10.1126/science.1167441

Arblaster, J. M., Gillett, N. P., Calvo, N., Forster, P. M., Polvani, L. M., Son, W. S., et al. (2014). Stratospheric ozone changes and climate. World Meteorological Organization. Retrieved from https://research.monash.edu/en/publications/stratospheric-ozone-changes-and-climate

Argus, D. F. (1996). Postglacial rebound from VLBI geodesy: On establishing vertical reference. *Geophysical Research Letters*, *23*(9), 973–976. https://doi.org/10.1029/96GL00735

Argus, D. F., Peltier, W. R., Drummond, R., & Moore, A. W. (2014). The Antarctica component of postglacial rebound model ICE-6G_C (VM5a) based on GPS positioning, exposure age dating of ice thicknesses, and relative sea level histories. *Geophysical Journal International*, *198*(1), 537–563. https://doi.org/10.1093/gji/ggu140

Arndt, J. E., Hillenbrand, C. D., Grobe, H., Kuhn, G., & Wacker, L. (2017). Evidence for a dynamic grounding line in outer Filchner Trough, Antarctica, until the early Holocene. *Geology*, *45*(11), 1035–1038. https://doi.org/10.1130/G39398.1

Arndt, J. E., Larter, R. D., Friedl, P., Gohl, K., & Höppner, K. (2018). Bathymetric controls on calving processes at Pine Island Glacier. *The Cryosphere*, *12*(6), 2039–2050. https://doi.org/10.5194/tc-12-2039-2018

Arndt, J. E., Schenke, H. W., Jakobsson, M., Nitsche, F. O., Buys, G., Goleby, B., et al. (2013). The international bathymetric chart of the Southern Ocean (IBCSO) version 1.0—A new bathymetric compilation covering circum-Antarctic waters. *Geophysical Research Letters*, *40*, 3111–3117. https://doi.org/10.1002/grl.50413

Asay-Davis, X. S., Cornford, S. L., Durand, G., Galton-Fenzi, B. K., Gladstone, R. M., Gudmundsson, G. H., et al. (2016). Experimental design for three interrelated marine ice sheet and ocean model intercomparison projects: MISMIP v. 3 (MISMIP +), ISOMIP v. 2 (ISOMIP +) and MISOMIP v. 1 (MISOMIP1). *Geoscientific Model Development*, *9*(7), 2471–2497. https://doi.org/10.5194/gmd-9-2471-2016

Ashmore, D. W., & Bingham, R. G. (2014). Antarctic subglacial hydrology: Current knowledge and future challenges. *Antarctic Science*, *26*(6), 758–773. https://doi.org/10.1017/S0954102014000546

Austermann, J., Mitrovica, J. X., Latychev, K., & Milne, G. A. (2013). Barbados-based estimate of ice volume at Last Glacial Maximum affected by subducted plate. *Nature Geoscience*, *6*(7), 553–557. https://doi.org/10.1038/ngeo1859

Austermann, J., Pollard, D., Mitrovica, J. X., Moucha, R., Forte, A. M., DeConto, R. M., et al. (2015). The impact of dynamic topography change on antarctic ice sheet stability during the mid-pliocene warm period. *Geology*, *43*(10), 927–930. https://doi.org/10.1130/g36988.1

Azuma, N., & Goto-Azuma, K. (1996). An anisotropic flow law for ice sheet ice and its implications. *Annals of Glaciology*, *23*, 202–208.

Bagshaw, E. A., Burrow, S., Wadham, J. L., Bowden, J., Lishman, B., Salter, M., et al. (2012). E-tracers: Development of a low cost wireless technique for exploring sub-surface hydrological systems. *Hydrological Processes*, *26*(20), 3157–3160. https://doi.org/10.1002/hyp.9451

Bakker, P., Clark, P. U., Golledge, N. R., Schmittner, A., & Weber, M. E. (2016). Centennial-scale Holocene climate variations amplified by Antarctic Ice Sheet discharge. *Nature*, *541*(7635), 72–76. https://doi.org/10.1038/nature20582

Bamber, J. L., Oppenheimer, M., Kopp, R. E., Aspinall, W. P., & Cooke, R. M. (2019). Ice sheet contributions to future sea-level rise from structured expert judgment. *Proceedings of the National Academy of Sciences*, *116*(23), 11,195–11,200. https://doi.org/10.1073/PNAS.1817205116

Bamber, J. L., Riva, R. E. M., Vermeersen, B. L. A., & Lebrocq, A. M. (2009). Reassessment of the potential sea-level rise from a collapse of the west antarctic ice sheet. *Science*, *324*(5929), 901–903. https://doi.org/10.1126/science.1169335

Banwell, A. F., & MacAyeal, D. R. (2015). Ice-shelf fracture due to viscoelastic flexure stress induced by fill/drain cycles of supraglacial lakes. *Antarctic Science*, *27*(6), 587–597. https://doi.org/10.1017/S0954102015000292

Banwell, A. F., MacAyeal, D. R., & Sergienko, O. V. (2013). Breakup of the Larsen B Ice Shelf triggered by chain reaction drainage of supraglacial lakes. *Geophysical Research Letters*, *40*, 5872–5876. https://doi.org/10.1002/2013GL057694

Banwell, A. F., Willis, I. C., Macdonald, G. J., Goodsell, B., & MacAyeal, D. R. (2019). Direct measurements of ice-shelf flexure caused by surface meltwater ponding and drainage. *Nature Communications*, *10*(1), 730. https://doi.org/10.1038/s41467-019-08522-5

Barletta, V. R., Bevis, M., Smith, B. E., Wilson, T., Brown, A., Bordoni, A., et al. (2013). Trends in Antarctic Peninsula surface melting conditions from observations and regional climate modeling. *Journal of Geophysical Research: Earth Surface*, *118*, 315–330. https://doi.org/10.1029/2012JF002559

Barrett, P. J. (2013). Resolving views on Antarctic Neogene glacial history—The Sirius debate. *Earth and Environmental Science Transactions of the Royal Society of Edinburgh*, *104*, 31–53. https://doi.org/10.1017/S175569101300008X

Bart, P. J. (2003). Were West Antarctic Ice Sheet grounding events in the Ross Sea a consequence of East Antarctic Ice Sheet expansion during the middle Miocene? *Earth and Planetary Science Letters*, *216*(1–2), 93–107. https://doi.org/10.1016/s0012-821x(03)00509-0

Bart, P. J., Anderson, J. B., Trincardi, F., & Shipp, S. S. (2000). Seismic data from the Northern basin, Ross Sea, record extreme expansions of the East Antarctic Ice Sheet during the late Neogene. *Marine Geology*, *166*(1–4), 31–50. https://doi.org/10.1016/s0025-3227(00)00006-2

Bart, P. J., & de Santis, L. (2012). Glacial intensification during the Neogene a review of seismic Stratigraphic evidence from the Ross sea, Antarctica, continental shelf. *Oceanography*, *25*(3), 166–183. https://doi.org/10.5670/oceanog.2012.92

Bart, P. J., DeCesare, M., Rosenheim, B. E., Majewski, W., & McGlannan, A. (2018). A centuries-long delay between a paleo-ice-shelf collapse and grounding-line retreat in the Whales Deep Basin, eastern Ross Sea, Antarctica. *Scientific Reports*, *8*(1), 12392. https://doi.org/10.1038/s41598-018-29911-8

Bart, P. J., Krogmeier, B. J., Bart, M. P., & Tulaczyk, S. (2017). The paradox of a long grounding during West Antarctic Ice Sheet retreat in Ross Sea. *Scientific Reports*, *7*(1), 1262. https://doi.org/10.1038/s41598-017-01329-8

Bart, P. J., Mullally, D., & Golledge, N. R. (2016). The influence of continental shelf bathymetry on Antarctic Ice Sheet response to climate forcing. *Global and Planetary Change*, *142*, 87–95. https://doi.org/10.1016/j.gloplacha.2016.04.009

Bassis, J. N., & Walker, C. C. (2012). Upper and lower limits on the stability of calving glaciers from the yield strength envelope of ice. *Proceedings of the Royal Society A: Mathematical, Physical and Engineering Sciences*, *468*(2140), 913–931. https://doi.org/10.1098/rspa.2011.0422

Batchelor, C. L., & Dowdeswell, J. A. (2015). Ice-sheet grounding-zone wedges (GZWs) on high-latitude continental margins. *Marine Geology*, *363*, 65–92. https://doi.org/10.1016/j.margeo.2015.02.001

Begeman, C. B., Tulaczyk, S. M., & Fisher, A. T. (2017). Spatially variable geothermal heat flux in West Antarctica: Evidence and implications. *Geophysical Research Letters*, *44*, 9823–9832. https://doi.org/10.1002/2017GL075579

Behrendt, J. C. (2013). The aeromagnetic method as a tool to identify Cenozoic magmatism in the West Antarctic Rift System beneath the West Antarctic Ice Sheet—A review; Thiel subglacial volcano as possible source of the ash layer in the WAISCORE. *Tectonophysics*, *585*, 124–136. https://doi.org/10.1016/j.tecto.2012.06.035

Bell, R. E. (2008). The role of subglacial water in ice-sheet mass balance. *Nature Geoscience*. Nature Publishing Group, *1*(5), 297–304. https://doi.org/10.1038/ngeo186

Bell, R. E., Banwell, A. F., Trusel, L. D., & Kingslake, J. (2018). Antarctic surface hydrology and impacts on ice-sheet mass balance. *Nature Climate Change*, *8*(12), 1044–1052. https://doi.org/10.1038/s41558-018-0326-3

Bell, R. E., Blankenship, D. D., Finn, C. A., Morse, D. L., Scambos, T. A., Brozena, J. M., & Hodge, S. M. (1998). Influence of subglacial geology on the onset of a West antarctic ice stream from aerogeophysical observations. *Nature*, *394*(6688), 58–62. Cited By (since 1996) 104Export Date 13 March 2013. https://doi.org/10.1038/27883

Bell, R. E., Chu, W., Kingslake, J., Das, I., Tedesco, M., Tinto, K. J., et al. (2017). Antarctic ice shelf potentially stabilized by export of meltwater in surface river. *Nature*, *544*(7650), 344–348. https://doi.org/10.1038/nature22048

Bell, R. E., Ferraccioli, F., Creyts, T. T., Braaten, D., Corr, H., Das, I., et al. (2011). Widespread persistent thickening of the east antarctic ice sheet by freezing from the base. *Science*, *331*(6024), 1592–1595. https://doi.org/10.1126/science.1200109

Bell, R. E., Studinger, M., Shuman, C. A., Fahnestock, M. A., & Joughin, I. (2007). Large subglacial lakes in East Antarctica at the onset of fast-flowing ice streams. *Nature*, *445*(7130), 904–907. Cited By (since 1996) 68Export Date 13 March 2013. https://doi.org/10.1038/nature05554

Benn, D. I., Åström, J., Zwinger, T., Todd, J., Nick, F. M., Cook, S., et al. (2017). Melt-under-cutting and buoyancy-driven calving from tidewater glaciers: New insights from discrete element and continuum model simulations. *Journal of Glaciology*, *63*, 1–12. https://doi.org/10.1017/jog.2017.41

Bentley, M. J. (2010). The Antarctic palaeo record and its role in improving predictions of future Antarctic ice sheet change. *Journal of Quaternary Science*, *25*(1), 5–18. https://doi.org/10.1002/jqs.1287

Bereiter, B., Lüthi, D., Siegrist, M., Schüpbach, S., Stocker, T. F., & Fischer, H. (2012). Mode change of millennial CO_2 variability during the last glacial cycle associated with a bipolar marine carbon seesaw. *Proceedings of the National Academy of Sciences of the United States of America*, *109*(25), 9755–9760. https://doi.org/10.1073/pnas.1204069109

Berger, S., Favier, L., Drews, R., Derwael, J. J., & Pattyn, F. (2016). The control of an uncharted pinning point on the flow of an Antarctic ice shelf. *Journal of Glaciology*, *62*(231), 37–45. https://doi.org/10.1017/jog.2016.7

Bernales, J., Rogozhina, I., & Thomas, M. (2017). Melting and freezing under Antarctic ice shelves from a combination of ice-sheet modelling and observations. *Journal of Glaciology*, *63*(240), 731–744. https://doi.org/10.1017/jog.2017.42

Bertram, R. A., Wilson, D. J., van de Flierdt, T., McKay, R. M., Patterson, M. O., Jimenez-Espejo, F. J., et al. (2018). Pliocene deglacial event timelines and the biogeochemical response offshore Wilkes Subglacial Basin, East Antarctica. *Earth and Planetary Science Letters*, *494*, 109–116. https://doi.org/10.1016/j.epsl.2018.04.054

Bevis, M., Kendrick, E., Smalley, R. Jr., Dalziel, I., Caccamise, D., Sasgen, I., et al. (2009). Geodetic measurements of vertical crustal velocity in West Antarctica and the implications for ice mass balance. *Geochemistry, Geophysics, Geosystems*, *10*, Q10005. https://doi.org/10.1029/2009GC002642

Bianchi, C., & Gersonde, R. (2002). The Southern Ocean surface between Marine Isotope Stages 6 and 5d: Shape and timing of climate changes. *Palaeogeography, Palaeoclimatology, Palaeoecology*, *187*(1–2), 151–177. https://doi.org/10.1016/S0031-0182(02)00516-3

Bindschadler, R., Vaughan, D. G., & Vornberger, P. (2011). Variability of basal melt beneath the Pine Island Glacier ice shelf, West Antarctica. *Journal of Glaciology*, *57*(204), 581–595. https://doi.org/10.3189/002214311797409802

Bingham, R. G., Ferraccioli, F., King, E. C., Larter, R. D., Pritchard, H. D., Smith, A. M., & Vaughan, D. G. (2012). Inland thinning of West Antarctic Ice Sheet steered along subglacial rifts. *Nature*, *487*(7408), 468–471. https://doi.org/10.1038/nature11292

Blackburn, T., Edwards, G., Tulaczyk, S., Scudder, M., Piccione, G., Hallet, B., et al. (2020). Ice retreat in Wilkes Basin of East Antarctica during a warm interglacial. *Nature*, *583*(7817), 554–559. https://doi.org/10.1038/s41586-020-2484-5

Blankenship, D. D., Bell, R. E., Hodge, S. M., Brozena, J. M., Behrendt, J. C., & Finn, C. A. (1993). Active volcanism beneath the West Antarctic ice sheet and implications for ice-sheet stability. *Nature*, *361*(6412), 526–529. https://doi.org/10.1038/361526a0

Blankenship, D. D., Bentley, C. R., Rooney, S. T., & Alley, R. B. (1987). Till beneath ice stream B. 1. Properties derived from seismic travel times. *Journal of Geophysical Research*, *92*(B9), 8903–8911.

Bo, S., Siegert, M. J., Mudd, S. M., Sugden, D., Fujita, S., Xiangbin, C., et al. (2009). The Gamburtsev mountains and the origin and early evolution of the Antarctic Ice Sheet. *Nature*, *459*(7247), 690–693. https://doi.org/10.1038/nature08024

Boening, C., Lebsock, M., Landerer, F., & Stephens, G. (2012). Snowfall-driven mass change on the East Antarctic ice sheet. *Geophysical Research Letters*, *39*, L21501. https://doi.org/10.1029/2012GL053316

Böhm, E., Lippold, J., Gutjahr, M., Frank, M., Blaser, P., Antz, B., et al. (2015). Strong and deep Atlantic meridional overturning circulation during the last glacial cycle. *Nature*, *517*(7532), 73–76. https://doi.org/10.1038/nature14059

Bougamont, M., Christoffersen, P., Price, S. F., Fricker, H. A., Tulaczyk, S., & Carter, S. P. (2015). Reactivation of Kamb Ice Stream tributaries triggers century-scale reorganization of Siple Coast ice flow in West Antarctica. *Geophysical Research Letters*, *42*, 8471–8480. https://doi.org/10.1002/2015GL065782

Boulton, G. S., & Hindmarsh, R. C. A. (1987). Sediment deformation beneath glaciers: Rheology and geological consequences. *Journal of Geophysical Research*, *92*(B9), 9059. https://doi.org/10.1029/JB092iB09p09059

Bradley, S. L., Hindmarsh, R. C. A., Whitehouse, P. L., Bentley, M. J., & King, M. A. (2015). Low post-glacial rebound rates in the Weddell Sea due to Late Holocene ice-sheet readvance. *Earth and Planetary Science Letters*, *413*, 79–89. https://doi.org/10.1016/j.epsl.2014.12.039

Brancolini, G., Busetti, M., Marchetti, A., De Santis, L., De Cillia, C., Zanolla, C., et al. (1995). The seismic stratigraphic atlas of the Ross Sea, Antarctica. In A. K. Cooper, P. F. Barker, & G. Brancolini (Eds.), *Geology and seismic stratigraphy of the Antarctic margin* (pp. 271–286). Washington: AGU.

Brancolini, G., De Santis, L., Lovo, M., & Prato, S. (1997). Cenozoic glacial history in the Ross Sea (Antarctica); Constraints from seismic reflection data. *Terra Antarctica*, *4*(1), 57–60.

Brearley, J. A., Meredith, M. P., Naveira Garabato, A. C., Venables, H. J., & Inall, M. E. (2017). Controls on turbulent mixing on the West Antarctic Peninsula shelf. *Deep-Sea Research Part II: Topical Studies in Oceanography*, *139*, 18–30. https://doi.org/10.1016/j.dsr2.2017.02.011

Brenn, G. R., Hansen, S. E., & Park, Y. (2017). Variable thermal loading and flexural uplift along the Transantarctic Mountains, Antarctica. *Geology*, *45*(5), 463–466. https://doi.org/10.1130/g38784.1

Breuer, B., Lange, M. A., & Blindow, N. (2006). Sensitivity studies on model modifications to assess the dynamics of a temperate ice cap, such as that on King George Island, Antarctica. *Journal of Glaciology*, *52*(177), 235–247. https://doi.org/10.3189/172756506781828683

Briggs, R. D., Pollard, D., & Tarasov, L. (2014). A data-constrained large ensemble analysis of Antarctic evolution since the Eemian. *Quaternary Science Reviews*, *103*, 91–115. https://doi.org/10.1016/j.quascirev.2014.09.003

Brisbourne, A. M., Smith, A. M., Vaughan, D. G., King, E. C., Davies, D., Bingham, R. G., et al. (2017). Bed conditions of Pine Island Glacier, West Antarctica. *Journal of Geophysical Research: Earth Surface*, *122*, 419–433. https://doi.org/10.1002/2016JF004033

Brondex, J., Gagliardini, O., & Gillet-chaulet, F. (2017). Sensitivity of grounding line dynamics to the friction law formulation. *Journal of Glaciology*, *63*(241), 854–866. https://doi.org/10.1017/jog.2017.51

Bronselaer, B., Winton, M., Griffies, S. M., Hurlin, W. J., Rodgers, K. B., Sergienko, O. V., et al. (2018). Change in future climate due to Antarctic meltwater. *Nature*, *564*(7734), 53–58. https://doi.org/10.1038/s41586-018-0712-z

Bruggemann, J. H., Buffler, R. T., Guillaume, M. M. M., Walter, R. C., Von Cosel, R., Ghebretensae, B. N., & Berhe, S. M. (2004). Stratigraphy, palaeoenvironments and model for the deposition of the Abdur Reef Limestone: Context for an important archaeological site from the last interglacial on the Red Sea coast of Eritrea. *Palaeogeography, Palaeoclimatology, Palaeoecology*, *203*(3–4), 179–206. https://doi.org/10.1016/S0031-0182(03)00659-X

Buck, W. R. (1991). Modes of continental lithospheric extension. *Journal of Geophysical Research*, *96*(B12), 20,161–20,178.

Budd, W. F., & Carter, D. B. (1971). An analysis of the relation between the surface and bedrock profiles of ice caps. *Journal of Glaciology*, *10*(59), 197–209. https://doi.org/10.3189/S0022143000013174

Budd, W. F., & Jacka, T. H. (1989). A review of ice rheology for ice sheet modelling. *Cold Regions Science and Technology*, *16*(2), 107–144. https://doi.org/10.1016/0165-232X(89)90014-1

Budd, W. F., Keage, P. L., & Blundy, N. A. (1979). Empirical studies of ice sliding. *Journal of Glaciology*, *23*(89), 157–170. https://doi.org/10.1017/S0022143000029804

Budd, W. F., Warner, R. C., Jacka, T. H., Li, J., & Treverrow, A. (2013). Ice flow relations for stress and strain-rate components from combined shear and compression laboratory experiments. *Journal of Glaciology*, *59*(214), 374–392. https://doi.org/10.3189/2013JoG12J106

Bueler, E., & Brown, J. (2009). Shallow shelf approximation as a "sliding law" in a thermomechanically coupled ice sheet model. *Journal of Geophysical Research*, *114*, F03008. https://doi.org/10.1029/2008JF001179

Burton-Johnson, A., Halpin, J. A., Whittaker, J. M., Graham, F. S., & Watson, S. J. (2017). A new heat flux model for the Antarctic Peninsula incorporating spatially variable upper crustal radiogenic heat production. *Geophysical Research Letters*, *44*, 5436–5446. https://doi.org/10.1002/2017GL073596

Cai, W., Santoso, A., Wang, G., Yeh, S.-W., An, S.-I., Cobb, K. M., et al. (2015). ENSO and greenhouse warming. *Nature Climate Change*, *5*(9), 849–859. https://doi.org/10.1038/nclimate2743

Carson, C. J., McLaren, S., Roberts, J. L., Boger, S. D., & Blankenship, D. D. (2014). Hot rocks in a cold place: High sub-glacial heat flow in East Antarctica. *Journal of the Geological Society*, *171*(1), 9–12. https://doi.org/10.1144/jgs2013-030

Carter, S. P., & Fricker, H. A. (2012). The supply of subglacial meltwater to the grounding line of the siple coast, west antarctica. *Annals of Glaciology*, *53*(60), 267–280. https://doi.org/10.3189/2012AoG60A119

Carter, S. P., Fricker, H. A., & Siegfried, M. R. (2017). Antarctic subglacial lakes drain through sediment-floored canals: Theory and model testing on real and idealized domains. *The Cryosphere*, *11*(1), 381–405. https://doi.org/10.5194/tc-11-381-2017

Cenedese, C., & Gatto, V. M. (2016). Impact of two plumes' interaction on submarine melting of tidewater glaciers: A laboratory study. *Journal of Physical Oceanography*, *46*(1), 361–367. https://doi.org/10.1175/JPO-D-15-0171.1

Chadwick, M., Allen, C. S., Sime, L. C., & Hillenbrand, C. D. (2020). Analysing the timing of peak warming and minimum winter sea-ice extent in the Southern Ocean during MIS 5e. *Quaternary Science Reviews*, *229*, 106134. https://doi.org/10.1016/j.quascirev.2019.106134

Chandler, D. M., Wadham, J. L., Lis, G. P., Cowton, T., Sole, A., Bartholomew, I., et al. (2013). Evolution of the subglacial drainage system beneath the Greenland Ice Sheet revealed by tracers. *Nature Geoscience*, *6*(3), 195–198. https://doi.org/10.1038/ngeo1737

Chaput, J., Aster, R. C., Huerta, A., Sun, X., Lloyd, A., Wiens, D., et al. (2014). The crustal thickness of West Antarctica. *Journal of Geophysical Research: Solid Earth*, *119*, 378–395. https://doi.org/10.1002/2013JB010642

Chen, F., Friedman, S., Gertler, C. G., Looney, J., O'Connell, N., Sierks, K., & Mitrovica, J. X. (2014). Refining estimates of polar ice volumes during the MIS11 interglacial using sea level records from South Africa. *Journal of Climate*, *27*(23), 8740–8746. https://doi.org/10.1175/JCLI-D-14-00282.1

Chen, J. L., Wilson, C. R., Ries, J. C., & Tapley, B. D. (2013). Rapid ice melting drives Earth's pole to the east. *Geophysical Research Letters*, *40*, 2625–2630. https://doi.org/10.1002/grl.50552

Chen, X., Zhang, X., Church, J. A., Watson, C. S., King, M. A., Monselesan, D., et al. (2017). The increasing rate of global mean sea-level rise during 1993–2014. *Nature Climate Change*, *7*(7), 492–495. https://doi.org/10.1038/nclimate3325

Christianson, K., Bushuk, M., Dutrieux, P., Parizek, B. R., Joughin, I. R., Alley, R. B., et al. (2016). Sensitivity of Pine Island Glacier to observed ocean forcing. *Geophysical Research Letters*, *43*, 10,817–10,825. https://doi.org/10.1002/2016GL070500

Christianson, K., Jacobel, R. W., Horgan, H. J., Alley, R. B., Anandakrishnan, S., Holland, D. M., & DallaSanta, K. J. (2016). Basal conditions at the grounding zone of Whillans Ice Stream, West Antarctica, from ice-penetrating radar. *Journal of Geophysical Research: Earth Surface*, *121*, 1954–1983. https://doi.org/10.1002/2015JF003806

Christianson, K., Parizek, B. R., Alley, R. B., Horgan, H. J., Jacobel, R. W., Anandakrishnan, S., et al. (2013). Ice sheet grounding zone stabilization due to till compaction. *Geophysical Research Letters*, *40*, 5406–5411. https://doi.org/10.1002/2013GL057447

Christie, F. D. W., Bingham, R. G., Gourmelen, N., Tett, S. F. B., & Muto, A. (2016). Four-decade record of pervasive grounding line retreat along the Bellingshausen margin of West Antarctica. *Geophysical Research Letters*, *43*, 5741–5749. https://doi.org/10.1002/2016GL068972

Christner, B. C., Priscu, J. C., Achberger, A. M., Barbante, C., Carter, S. P., Christianson, K., et al. (2014). A microbial ecosystem beneath the West Antarctic ice sheet. *Nature*, *512*(7514), 310–313. https://doi.org/10.1038/nature13667

Christoffersen, P., Bougamont, M., Carter, S. P., Fricker, H. A., & Tulaczyk, S. (2014). Significant groundwater contribution to Antarctic ice streams hydrologic budget. *Geophysical Research Letters*, *41*, 2003–2010. https://doi.org/10.1002/2014GL059250

Church, J. A., Clark, P. U., Cazenave, A., Gregory, J. M., Jevrejeva, S., Levermann, A., et al. (2013). *Sea level change. Climate Change 2013: The Physical Science Basis. Contribution of Working Group I to the Fifth Assessment Report of the Intergovernmental Panel on Climate Change*, 1137–1216. https://doi.org/10.1017/CB09781107415315.026

Clark, J. A., & Lingle, C. S. (1977). Future sea-level changes due to West Antarctic ice sheet fluctuations. *Nature*, *269*(5625), 206–209. https://doi.org/10.1038/269206a0

Clark, P. U., Church, J. A., Gregory, J. M., & Payne, A. J. (2015). Recent progress in understanding and projecting regional and global mean sea level change. *Current Climate Change Reports*, *1*(4), 224–246. https://doi.org/10.1007/s40641-015-0024-4

Clark, P. U., Dyke, A. S., Shakun, J. D., Carlson, A. E., Clark, J., Wohlfarth, B., et al. (2009). The Last Glacial Maximum. *Science (Washington)*, *325*(5941), 710–714. https://doi.org/10.1126/science.1172873

Clark, P. U., Shakun, J. D., Marcott, S. A., Mix, A. C., Eby, M., Kulp, S., et al. (2016). Consequences of twenty-first-century policy for multi-millennial climate and sea-level change. *Nature Climate Change*, *6*(4), 360–369. https://doi.org/10.1038/nclimate2923

Clarke, G. K. C. (2003). Hydraulics of subglacial outburst floods: New insights from the Spring-Hutter formulation. *Journal of Glaciology*, *49*(165), 299–313. https://doi.org/10.3189/172756503781830728

Colleoni, F., De Santis, L., Montoli, E., Olivo, E., Sorlien, C. C., Bart, P. J., et al. (2018). Past continental shelf evolution increased Antarctic ice sheet sensitivity to climatic conditions. *Scientific Reports*, *8*(1), 11323. https://doi.org/10.1038/s41598-018-29718-7

Conrad, C. P. (2013). The solid Earth's influence on sea level. *Bulletin of the Geological Society of America*, *125*(7–8), 1027–1052. https://doi.org/10.1130/b30764.1

Conrad, C. P., & Husson, L. (2009). Influence of dynamic topography on sea level and its rate of change. *Lithosphere*, *1*(2), 110–120. https://doi.org/10.1130/L32.1

Cook, A. J., Holland, P. R., Meredith, M. P., Murray, T., Luckman, A., & Vaughan, D. G. (2016). Ocean forcing of glacier retreat in the western Antarctic Peninsula. *Science*, *353*(6296), 283–286. https://doi.org/10.1126/science.aae0017

Cook, A. J., & Vaughan, D. G. (2010). Overview of areal changes of the ice shelves on the Antarctic Peninsula over the past 50 years. *The Cryosphere*, *4*(1), 77–98. https://doi.org/10.5194/tc-4-77-2010

Cook, C. P., Hemming, S. R., van de Flierdt, T., Pierce Davis, E. L., Williams, T., Galindo, A. L., et al. (2017). Glacial erosion of East Antarctica in the Pliocene: A comparative study of multiple marine sediment provenance tracers. *Chemical Geology*, *466*, 199–218. https://doi.org/10.1016/j.chemgeo.2017.06.011

Cook, C. P., van de Flierdt, T., Williams, T., Hemming, S. R., Iwai, M., Kobayashi, M., et al. (2013). Dynamic behaviour of the East Antarctic ice sheet during Pliocene warmth. *Nature Geoscience*, *6*(9), 765–769. https://doi.org/10.1038/ngeo1889

Corbett, D. R., Crenshaw, J., Null, K., Peterson, R. N., Peterson, L. E., & Lyons, W. B. (2017). Nearshore mixing and nutrient delivery along the western Antarctic Peninsula. *Antarctic Science*, *29*(5), 397–409. https://doi.org/10.1017/s095410201700013x

Cornford, S. L., Martin, D. F., Payne, A. J., Ng, E. G., le Brocq, A. M., Gladstone, R. M., et al. (2015). Century-scale simulations of the response of the West Antarctic Ice Sheet to a warming climate. *The Cryosphere*, *9*(4), 1579–1600. https://doi.org/10.5194/tc-9-1579-2015

Cougnon, E. A., Galton-Fenzi, B. K., Meijers, A. J. S., & Legrésy, B. (2013). Modeling interannual dense shelf water export in the region of the Mertz Glacier Tongue (1992–2007). *Journal of Geophysical Research: Oceans*, *118*, 5858–5872. https://doi.org/10.1002/2013JC008790

Cougnon, E. A., Galton-Fenzi, B. K., Rintoul, S. R., Legrésy, B., Williams, G. D., Fraser, A. D., & Hunter, J. R. (2017). Regional changes in icescape impact shelf circulation and basal melting. *Geophysical Research Letters*, *44*, 11,519–11,527. https://doi.org/10.1002/2017GL074943

Couto, N., Martinson, D. G., Kohut, J., & Schofield, O. (2017). Distribution of Upper Circumpolar Deep Water on the warming continental shelf of the West Antarctic Peninsula. *Journal of Geophysical Research: Oceans*, *122*, 5306–5315. https://doi.org/10.1002/2017JC012840

Creyts, T. T., Clarke, G. K. C., & Church, M. (2013). Evolution of subglacial overdeepenings in response to sediment redistribution and glaciohydraulic supercooling. *Journal of Geophysical Research: Earth Surface*, *118*, 423–446. https://doi.org/10.1002/jgrf.20033

Creyts, T. T., Ferraccioli, F., Bell, R. E., Wolovick, M., Corr, H., Rose, K. C., et al. (2014). Freezing of ridges and water networks preserves the Gamburtsev Subglacial Mountains for millions of years. *Geophysical Research Letters*, *41*, 8114–8122. https://doi.org/10.1002/2014GL061491

Crosta, X., Sturm, A., Armand, L., & Pichon, J. J. (2004). Late Quaternary sea ice history in the Indian sector of the Southern Ocean as recorded by diatom assemblages. *Marine Micropaleontology*, *50*(3–4), 209–223. https://doi.org/10.1016/S0377-8398(03)00072-0

Cuffey, K. M., & Paterson, W. S. B. (2010). *The physics of glaciers* (4th ed., pp. 236–297). Academic Press. ISBN: 9780080919126.

Cutler, K., Edwards, R. L., Taylor, F. W., Cheng, H., Adkins, J., Gallup, C. D., et al. (2003). Rapid sea-level fall and deep-ocean temperature change since the last interglacial period. *Earth and Planetary Science Letters*, *206*(3–4), 253–271. https://doi.org/10.1016/S0012-821X(02)01107-X

Damiani, T. M., Jordan, T. A., Ferraccioli, F., Young, D. A., & Blankenship, D. D. (2014). Variable crustal thickness beneath Thwaites Glacier revealed from airborne gravimetry, possible implications for geothermal heat flux in West Antarctica. *Earth and Planetary Science Letters*, *407*, 109–122. https://doi.org/10.1016/j.epsl.2014.09.023

Dansgaard, W., Johnsen, S. J., Clausen, H. B., Dahl-Jensen, D., Gundestrup, N. S., Hammer, C. U., et al. (1993). Evidence for general instability of past climate from a 250-kyr ice-core record. *Nature*, *364*(6434), 218–220. https://doi.org/10.1038/364218a0

Dätwyler, C., Neukom, R., Abram, N. J., Gallant, A. J. E., Grosjean, M., Jacques-Coper, M., et al. (2018). Teleconnection stationarity, variability and trends of the Southern Annular Mode (SAM) during the last millennium. *Climate Dynamics*, *51*(5–6), 2321–2339. https://doi.org/10.1007/s00382-017-4015-0

Davis, P. E. D., Jenkins, A., Nicholls, K. W., Brennan, P. V., Abrahamsen, E. P., Heywood, K. J., et al. (2018). Variability in basal melting beneath Pine Island Ice Shelf on weekly to monthly timescales. *Journal of Geophysical Research: Oceans*, *123*, 8655–8669. https://doi.org/10.1029/2018JC014464

De Angelis, H., & Skvarca, P. (2003). Glacier surge after ice shelf collapse. *Science*, *299*(5612), 1560–1562. https://doi.org/10.1126/science.1077987

de Boer, B., Dolan, A. M., Bernales, J., Gasson, E., Goelzer, H., Golledge, N. R., et al. (2015). Simulating the Antarctic ice sheet in the late-Pliocene warm period: PLISMIP-ANT, an ice-sheet model intercomparison project. *The Cryosphere*, *9*(3), 881–903. https://doi.org/10.5194/tc-9-881-2015

De Boer, B., Stocchi, P., & Van De Wal, R. S. W. (2014). A fully coupled 3-D ice-sheet-sea-level model: Algorithm and applications. *Geoscientific Model Development*, *7*(5), 2141–2156. https://doi.org/10.5194/gmd-7-2141-2014

de Boer, B., Stocchi, P., Whitehouse, P. L., & van de Wal, R. S. W. (2017). Current state and future perspectives on coupled ice-sheet—Sea-level modelling. *Quaternary Science Reviews*, *169*, 13–28. https://doi.org/10.1016/j.quascirev.2017.05.013

De Fleurian, B., Werder, M. A., Beyer, S., Brinkerhoff, D. J., Delaney, I. A. N., Dow, C. F., et al. (2018). SHMIP the subglacial hydrology model intercomparison Project. *Journal of Glaciology*, *64*(248), 897–916. https://doi.org/10.1017/jog.2018.78

De Rydt, J., & Gudmundsson, G. H. (2016). Coupled ice shelf-ocean modeling and complex grounding line retreat from a seabed ridge. *Journal of Geophysical Research: Earth Surface*, *121*, 865–880. https://doi.org/10.1002/2015JF003791

De Rydt, J., Holland, P. R., Dutrieux, P., & Jenkins, A. (2014). Geometric and oceanographic controls on melting beneath Pine Island Glacier. *Journal of Geophysical Research: Oceans*, *119*, 2420–2438. https://doi.org/10.1002/2013JC009513

De Santis, L., Prato, S., Brancolini, G., Lovo, M., & Torelli, L. (1999). The Eastern Ross Sea continental shelf during the Cenozoic: Implications for the West Antarctic ice sheet development. *Global and Planetary Change*, *23*(1–4), 173–196. https://doi.org/10.1016/s0921-8181(99)00056-9

Deaney, E. L., Barker, S., & Van De Flierdt, T. (2017). Timing and nature of AMOC recovery across Termination 2 and magnitude of deglacial CO_2 change. *Nature Communications*, *8*, 14595. https://doi.org/10.1038/ncomms14595

Death, R., Wadham, J. L., Monteiro, F., le Brocq, A. M., Tranter, M., Ridgwell, A., et al. (2014). Antarctic ice sheet fertilises the Southern Ocean. *Biogeosciences*, *11*(10), 2635–2643. https://doi.org/10.5194/bg-11-2635-2014

DeConto, R. M., & Pollard, D. (2016). Contribution of Antarctica to past and future sea-level rise. *Nature*, *531*(7596), 591–597. https://doi.org/10.1038/nature17145

Delille, B., Vancoppenolle, M., Geilfus, N.-X., Tilbrook, B., Lannuzel, D., Schoemann, V., et al. (2014). Southern Ocean CO_2 sink: The contribution of the sea ice. *Journal of Geophysical Research: Oceans*, *119*, 6340–6355. https://doi.org/10.1002/2014JC009941

Denton, G. H., Anderson, R. F., Toggweiler, J. R., Edwards, R. L., Schaefer, J. M., & Putnam, A. E. (2010). The Last Glacial Termination. *Science*, *328*(5986), 1652–1656. https://doi.org/10.1126/science.1184119

Denton, G. H., & Hughes, T. J. (1983). Milankovitch theory of ice ages: Hypothesis of ice-sheet linkage between regional insolation and global climate. *Quaternary Research*, *20*(2), 125–144. https://doi.org/10.1016/0033-5894(83)90073-X

Depoorter, M. A., Bamber, J. L., Griggs, J. A., Lenaerts, J. T. M., Ligtenberg, S. R. M., van den Broeke, M. R., & Moholdt, G. (2013). Calving fluxes and basal melt rates of Antarctic ice shelves. *Nature*, *502*(7469), 89–92. https://doi.org/10.1038/nature12567

Deschamps, P., Durand, N., Bard, E., Hamelin, B., Camoin, G., Thomas, A. L., et al. (2012a). Ice-sheet collapse and sea-level rise at the Bolling warming 14,600 years ago. *Nature*, *483*(7391), 559–564. https://doi.org/10.1038/nature10902

Deschamps, P., Durand, N., Bard, E., Hamelin, B., Camoin, G., Thomas, A. L., et al. (2012b). Ice-sheet collapse and sea-level rise at the Bølling warming 14,600 years ago. *Nature*, *483*(7391), 559–564. https://doi.org/10.1038/nature10902

Dieng, H. B., Cazenave, A., Meyssignac, B., & Ablain, M. (2017). New estimate of the current rate of sea level rise from a sea level budget approach. *Geophysical Research Letters*, *44*, 3744–3751. https://doi.org/10.1002/2017GL073308

Diez, A., & Eisen, O. (2015). Seismic wave propagation in anisotropic ice—Part 1: Elasticity tensor and derived quantities from ice-core properties. *The Cryosphere*, *9*(1), 367–384. https://doi.org/10.5194/tc-9-367-2015

Diez, A., Eisen, O., Hofstede, C., Lambrecht, A., Mayer, C., Miller, H., et al. (2015). Seismic wave propagation in anisotropic ice—Part 2: Effects of crystal anisotropy in geophysical data. *The Cryosphere*, *9*(1), 385–398. https://doi.org/10.5194/tc-9-385-2015

Diez, A., Eisen, O., Weikusat, I., Eichler, J., Hofstede, C., Bohleber, P., et al. (2014). Influence of ice crystal anisotropy on seismic velocity analysis. *Annals of Glaciology*, *55*(67), 97–106. https://doi.org/10.3189/2014AoG67A002

Dinniman, M. S., & Klinck, J. M. (2004). A model study of circulation and cross-shelf exchange on the west Antarctic Peninsula continental shelf. *Deep-Sea Research Part II: Topical Studies in Oceanography*, *51*(17–19), 2003–2022. https://doi.org/10.1016/j.dsr2.2004.07.030

Dinniman, M. S., Klinck, J. M., Bai, L. S., Bromwich, D. H., Hines, K. M., & Holland, D. M. (2015). The effect of atmospheric forcing resolution on delivery of ocean heat to the antarctic floating ice shelves. *Journal of Climate*, *28*(15), 6067–6085. https://doi.org/10.1175/JCLI-D-14-00374.1

Dinniman, M. S., Klinck, J. M., & Hofmann, E. E. (2012). Sensitivity of circumpolar deep water transport and ice shelf basal melt along the west antarctic peninsula to changes in the winds. *Journal of Climate*, *25*(14), 4799–4816. https://doi.org/10.1175/JCLI-D-11-00307.1

Doake, C. S. M., Corr, H. F. J., Rott, H., Skvarca, P., & Young, N. W. (1998). Breakup and conditions for stability of the northern Larsen Ice Shelf, Antarctica. *Nature*, *391*, 778–780. EP-. Retrieved from https://doi.org/10.1038/35832

Dolan, A. M., De Boer, B., Bernales, J., Hill, D. J., & Haywood, A. M. (2018). High climate model dependency of Pliocene Antarctic ice-sheet predictions. *Nature Communications*, *9*(1), 2799. https://doi.org/10.1038/s41467-018-05179-4

Dow, C. F., McCormack, F. S., Young, D. A., Greenbaum, J. S., Roberts, J. L., & Blankenship, D. D. (2020). Totten Glacier subglacial hydrology determined from geophysics and modeling. *Earth and Planetary Science Letters*, *531*. https://doi.org/10.1016/j.epsl.2019.115961

Dow, C. F., Werder, M. A., Nowicki, S., & Walker, R. T. (2016). Modeling Antarctic subglacial lake filling and drainage cycles. *The Cryosphere*, *10*(4), 1381–1393. https://doi.org/10.5194/tc-10-1381-2016

Dowdeswell, J. A., Canals, M., Jakobsson, M., Todd, B. J., Dowdeswell, E. K., & Hogan, K. A. (2016). Introduction: An atlas of submarine glacial landforms, 3–14.

Drouet, A. S., Docquier, D., Durand, G., Hindmarsh, R., Pattyn, F., Gagliardini, O., & Zwinger, T. (2013). Grounding line transient response in marine ice sheet models. *The Cryosphere*, *7*(2), 395–406. https://doi.org/10.5194/tc-7-395-2013

Dumitru, O. A., Austermann, J., Polyak, V. J., Fornós, J. J., Asmerom, Y., Ginés, J., et al. (2019). Constraints on global mean sea level during Pliocene warmth. *Nature*, *574*(7777), 233–236. https://doi.org/10.1038/s41586-019-1543-2

Dupont, T. K., & Alley, R. B. (2005a). Assessment of the importance of ice-shelf buttressing to ice-sheet flow. *Geophysical Research Letters*, *32*, L04503. https://doi.org/10.1029/2004GL022024

Dupont, T. K., & Alley, R. B. (2005b). Conditions for the reversal of ice/air surface slope on ice streams and shelves: A model study. *Annals of Glaciology*, *40*, 139–144. https://doi.org/10.3189/172756405781813780

Duprat, L. P. A. M., Bigg, G. R., & Wilton, D. J. (2016). Enhanced Southern Ocean marine productivity due to fertilization by giant icebergs. *Nature Geoscience*, *9*(3), 219–221. https://doi.org/10.1038/ngeo2633

Durack, P. J., Wijffels, S. E., & Gleckler, P. J. (2014). Long-term sea-level change revisited: The role of salinity. *Environmental Research Letters*, *9*(11), 114017. https://doi.org/10.1088/1748-9326/9/11/114017
Durand, G., Gagliardini, O., Zwinger, T., Le Meur, E., & Hindmarsh, R. C. A. (2009). Full Stokes modeling of marine ice sheets: Influence of the grid size. *Annals of Glaciology*, *50*(52), 109–114. https://doi.org/10.3189/172756409789624283
Dutrieux, P., de Rydt, J., Jenkins, A., Holland, P. R., Ha, H. K., Lee, S. H., et al. (2014). Strong sensitivity of pine Island ice-shelf melting to climatic variability. *Science*, *343*(6167), 174–178. https://doi.org/10.1126/science.1244341
Dutton, A., Carlson, A. E., Long, A. J., Milne, G. A., Clark, P. U., DeConto, R., et al. (2015). Sea-level rise due to polar ice-sheet mass loss during past warm periods. *Science. American Association for the Advancement of Science*, *349*(6244), aaa4019-1. https://doi.org/10.1126/science.aaa4019
Dutton, A., & Lambeck, K. (2012). Ice volume and sea level during the last interglacial. *Science*, *337*(6091), 216–219. https://doi.org/10.1126/science.1205749
Dutton, A., Webster, J. M., Zwartz, D., Lambeck, K., & Wohlfarth, B. (2015). Tropical tales of polar ice: Evidence of Last Interglacial polar ice sheet retreat recorded by fossil reefs of the granitic Seychelles islands. *Quaternary Science Reviews*, *107*, 182–196. https://doi.org/10.1016/j.quascirev.2014.10.025
Dziadek, R., Gohl, K., Diehl, A., & Kaul, N. (2017). Geothermal heat flux in the Amundsen Sea sector of West Antarctica: New insights from temperature measurements, depth to the bottom of the magnetic source estimation, and thermal modeling. *Geochemistry, Geophysics, Geosystems*, *18*, 2657–2672. https://doi.org/10.1002/2016GC006755
Dziadek, R., Gohl, K., & Kaul, N. (2019). Elevated geothermal surface heat flow in the Amundsen Sea Embayment, West Antarctica. *Earth and Planetary Science Letters*, *506*, 530–539. https://doi.org/10.1016/j.epsl.2018.11.003
Edwards, T. L., Brandon, M. A., Durand, G., Edwards, N. R., Golledge, N. R., Holden, P. B., et al. (2019). Revisiting Antarctic ice loss due to marine ice-cliff instability. *Nature*, *566*(7742), 58–64. https://doi.org/10.1038/s41586-019-0901-4
Egholm, D. L., Jansen, J. D., Braedstrup, C. F., Pedersen, V. K., Andersen, J. L., Ugelvig, S. V., et al. (2017). Formation of plateau landscapes on glaciated continental margins. *Nature Geoscience*, *10*. https://doi.org/10.1038/NGEO2980
Ehrmann, W. U., & Grobe, H. (1991). Cyclic sedimentation at Sites 745 and 746, Leg 119. In *Proceedings of the Ocean Drilling Program, 119 Scientific Results*. Ocean Drilling Program. https://doi.org/10.2973/odp.proc.sr.119.123.1991
EPICA Community Members, Barbante, C., Barnola, J. M., Becagli, S., Beer, J., Bigler, M., et al. (2006). One-to-one coupling of glacial climate variability in Greenland and Antarctica. *Nature*, *444*(7116), 195–198. https://doi.org/10.1038/nature05301
Esper, O., & Gersonde, R. (2014). New tools for the reconstruction of Pleistocene Antarctic sea ice. *Palaeogeography, Palaeoclimatology, Palaeoecology*, *399*, 260–283. https://doi.org/10.1016/j.palaeo.2014.01.019
Etourneau, J., Collins, L. G., Willmott, V., Kim, J. H., Barbara, L., Leventer, A., et al. (2013). Holocene climate variations in the western Antarctic Peninsula: Evidence for sea ice extent predominantly controlled by changes in insolation and ENSO variability. *Climate of the Past*, *9*(4), 1431–1446. https://doi.org/10.5194/cp-9-1431-2013
Farrell, W. E., & Clark, J. A. (1976). On postglacial sea level. *Geophysical Journal of the Royal Astronomical Society*, *46*(3), 647–667. https://doi.org/10.1111/j.1365-246X.1976.tb01252.x
Favier, L., Durand, G., Cornford, S. L., Gudmundsson, G. H., Gagliardini, O., Gillet-Chaulet, F., et al. (2014). Retreat of Pine Island Glacier controlled by marine ice-sheet instability. *Nature Climate Change*, *4*(2), 117–121. https://doi.org/10.1038/nclimate2094
Favier, L., Gagliardini, O., Durand, G., & Zwinger, T. (2012). A three-dimensional full Stokes model of the grounding line dynamics: Effect of a pinning point beneath the ice shelf. *The Cryosphere*, *6*(1), 101–112. https://doi.org/10.5194/tc-6-101-2012
Favier, L., Pattyn, F., Berger, S., & Drews, R. (2016). Dynamic influence of pinning points on marine ice-sheet stability: A numerical study in Dronning Maud Land, East Antarctica. *Cryosphere*, *10*(6), 2623–2635. https://doi.org/10.5194/tc-10-2623-2016
Feldmann, J., Albrecht, T., Khroulev, C., Pattyn, F., & Levermann, A. (2014). Resolution-dependent performance of grounding line motion in a shallow model compared with a full-Stokes model according to the MISMIP3d intercomparison. *Journal of Glaciology*, *60*(220), 353–360. https://doi.org/10.3189/2014JoG13J093
Fernandez, R., Gulick, S., Domack, E., Montelli, A., Leventer, A., Shevenell, A., & Frederick, B. (2018). Past ice stream and ice sheet changes on the continental shelf off the Sabrina Coast, East Antarctica. *Geomorphology*, *317*, 10–22. https://doi.org/10.1016/j.geomorph.2018.05.020
Ferraccioli, F., Finn, C. A., Jordan, T. A., Bell, R. E., Anderson, L. M., & Damaske, D. (2011). East Antarctic rifting triggers uplift of the Gamburtsev Mountains. *Nature*, *479*(7373), 388–392. https://doi.org/10.1038/nature10566
Fielding, C. R. (2018). Stratigraphic architecture of the Cenozoic succession in the McMurdo Sound region, Antarctica: An archive of polar palaeoenvironmental change in a failed rift setting. *Sedimentology*, *65*(1), 1–61. https://doi.org/10.1111/sed.12413
Fielding, C. R., Whittaker, J., Henrys, S. A., Wilson, T. J., & Naish, T. R. (2008). Seismic facies and stratigraphy of the Cenozoic succession in McMurdo Sound, Antarctica: Implications for tectonic, climatic and glacial history. *Palaeogeography, Palaeoclimatology, Palaeoecology*, *260*(1–2), 8–29. https://doi.org/10.1016/J.PALAEO.2007.08.016
Fisher, A. T., Mankoff, K. D., Tulaczyk, S. M., Tyler, S. W., & Foley, N. (2015). High geothermal heat flux measured below the West Antarctic Ice Sheet. *Science Advances*, *1*(6), e1500093. https://doi.org/10.1126/sciadv.1500093
Flament, N., Gurnis, M., & Dietmar Müller, R. (2013). A review of observations and models of dynamic topography. *Lithosphere*, *5*(2), 189–210. https://doi.org/10.1130/L245.1
Flament, T., & Rémy, F. (2012). Dynamic thinning of Antarctic glaciers from along-track repeat radar altimetry. *Journal of Glaciology*, *58*(211), 830–840. https://doi.org/10.3189/2012JoG11J118
Fogwill, C. J., Phipps, S. J., Turney, C. S. M., & Golledge, N. R. (2015). Sensitivity of the Southern Ocean to enhanced regional Antarctic ice sheet meltwater input. *Earth's Future*, *3*, 317–329. https://doi.org/10.1002/2015EF000306
Fogwill, C. J., Turney, C. S. M., Golledge, N. R., Etheridge, D. M., Rubino, M., Thornton, D. P., et al. (2017). Antarctic ice sheet discharge driven by atmosphere-ocean feedbacks at the Last Glacial Termination. *Scientific Reports*, *7*(November 2016), 39979. https://doi.org/10.1038/srep39979
Fogwill, C. J., Turney, C. S. M., Golledge, N. R., Rood, D. H., Hippe, K., Wacker, L., et al. (2014). Drivers of abrupt Holocene shifts in West Antarctic ice stream direction determined from combined ice sheet modelling and geologic signatures. *Antarctic Science*, *26*(6), 674–686. https://doi.org/10.1017/S0954102014000613
Fogwill, C. J., Turney, C. S. M., Menviel, L., Baker, A., Weber, M. E., Ellis, B., et al. (2020). Southern Ocean carbon sink enhanced by sea-ice feedbacks at the Antarctic Cold Reversal. *Nature Geoscience*, *13*(7), 489–497. https://doi.org/10.1038/s41561-020-0587-0
Forsberg, R., Sørensen, L., & Simonsen, S. (2017). Greenland and Antarctica Ice Sheet mass changes and effects on global sea level. *Surveys in Geophysics*, *38*(1), 89–104. https://doi.org/10.1007/s10712-016-9398-7

Foster, G. L., & Rohling, E. J. (2013). Relationship between sea level and climate forcing by CO_2 on geological timescales. *Proceedings of the National Academy of Sciences*, *110*(4), 1209–1214. https://doi.org/10.1073/pnas.1216073110

Fowler, A. C., & Yang, X.-S. (2002). Loading and unloading of sedimentary basins: The effect of rheological hysteresis. *Journal of Geophysical Research*, *107*(B4), ETG 1-1–1-ETG 1-8. https://doi.org/10.1029/2001JB000389

Fox Maule, C., Purucker, M. E., Olsen, N., & Mosegaard, K. (2005). Geophysics: Heat flux anomalies in Antarctica revealed by satellite magnetic data. *Science*, *309*(5733), 464–467. https://doi.org/10.1126/science.1106888

Frajka-Williams, E., Ansorge, I. J., Baehr, J., Bryden, H. L., Chidichimo, M. P., Cunningham, S. A., et al. (2019). Atlantic meridional overturning circulation: Observed transport and variability. *Frontiers in Marine Science*, *6*(JUN), 1–18. https://doi.org/10.3389/fmars.2019.00260

Frederick, B. C., Young, D. A., Blankenship, D. D., Richter, T. G., Kempf, S. D., Ferraccioli, F., & Siegert, M. J. (2016). Distribution of subglacial sediments across the Wilkes Subglacial Basin, East Antarctica. *Journal of Geophysical Research: Earth Surface*, *121*, 790–813. https://doi.org/10.1002/2015JF003760

Fretwell, P., Pritchard, H. D., Vaughan, D. G., Bamber, J. L., Barrand, N. E., Bell, R., et al. (2013). Bedmap2: Improved ice bed, surface and thickness datasets for Antarctica. *The Cryosphere*, *7*(1), 375–393. https://doi.org/10.5194/tc-7-375-2013

Fricker, H. A., Scambos, T., Bindschadler, R., & Padman, L. (2007). An active subglacial water system in West Antarctica mapped from space. *Science*, *315*(5818), 1544–1548. https://doi.org/10.1126/science.1136897

Fricker, H. A., Siegfried, M. R., Carter, S. P., & Scambos, T. A. (2016). A decade of progress in observing and modelling Antarctic subglacial water systems. *Philosophical Transactions of the Royal Society A: Mathematical, Physical and Engineering Sciences*, *374*(2059), 20140294. https://doi.org/10.1098/rsta.2014.0294

Frölicher, T. L., Sarmiento, J. L., Paynter, D. J., Dunne, J. P., Krasting, J. P., & Winton, M. (2015). Dominance of the Southern Ocean in anthropogenic carbon and heat uptake in CMIP5 models. *Journal of Climate*, *28*(2), 862–886. https://doi.org/10.1175/JCLI-D-14-00117.1

Fujita, S., Maeno, H., & Matsuoka, K. (2006). Radio-wave depolarization and scattering within ice sheets: A matrix-based model to link radar and ice-core measurements and its application. *Journal of Glaciology*, *52*(178), 407–424. https://doi.org/10.3189/172756506781828548

Fürst, J. J., Durand, G., Gillet-Chaulet, F., Tavard, L., Rankl, M., Braun, M., & Gagliardini, O. (2016). The safety band of Antarctic ice shelves. *Nature Climate Change*, *6*(5), 479–482. https://doi.org/10.1038/nclimate2912

Gagliardini, O., Cohen, D., Råback, P., & Zwinger, T. (2007). Finite-element modeling of subglacial cavities and related friction law. *Journal of Geophysical Research*, *112*, F02027. https://doi.org/10.1029/2006JF000576

Gagliardini, O., Gillet-Chaulet, F., & Montagnat, M. (2009). A review of anisotropic polar ice models: From crystal to ice-sheet flow models. Low Temperature Science (Vol. 68). Retrieved from http://citeseerx.ist.psu.edu/viewdoc/download?doi=10.1.1.496.2886&rep=rep1&type=pdf

Galaasen, E. V., Ninnemann, U. S., Irvalı, N., Kleiven, H. K. F., Rosenthal, Y., Kissel, C., & Hodell, D. A. (2014). Rapid reductions in North Atlantic Deep Water during the peak of the last interglacial period. *Science (New York, N.Y.)*, *343*(6175), 1129–1132. https://doi.org/10.1126/science.1248667

Galassi, G., & Spada, G. (2017). Tide gauge observations in Antarctica (1958–2014) and recent ice loss. *Antarctic Science*, *29*(4), 369–381. https://doi.org/10.1017/S0954102016000729

Galton-Fenzi, B., Asay-Davis, X., Holland, P., Timmermann, R., Jenkins, A., & Dinniman, M. (2016). Modeling ice shelf/ocean interaction in Antarctica: A review. *Oceanography*, *29*(4), 144–153. https://doi.org/10.5670/oceanog.2016.106

Galton-Fenzi, B. K., Hunter, J. R., Coleman, R., Marsland, S. J., & Warner, R. C. (2012). Modeling the basal melting and marine ice accretion of the Amery Ice Shelf. *Journal of Geophysical Research*, *117*, C09031. https://doi.org/10.1029/2012JC008214

Gard, M., Hasterok, D., & Halpin, J. A. (2019). Global whole-rock geochemical database compilation. *Earth System Science Data*, *11*(4), 1553–1566. https://doi.org/10.5194/essd-11-1553-2019

Gardner, A. S., Moholdt, G., Scambos, T., Fahnstock, M., Ligtenberg, S., Van Den Broeke, M., & Nilsson, J. (2018). Increased West Antarctic and unchanged East Antarctic ice discharge over the last 7 years. *The Cryosphere*, *12*, 521–547. https://doi.org/10.5194/tc-12-521-2018

Gasson, E., DeConto, R., & Pollard, D. (2015). Antarctic bedrock topography uncertainty and ice sheet stability. *Geophysical Research Letters*, *42*, 5372–5377. https://doi.org/10.1002/2015GL064322

Gasson, E., DeConto, R. M., & Pollard, D. (2016). Modeling the oxygen isotope composition of the Antarctic ice sheet and its significance to Pliocene sea level. *Geology*, *44*(10), 827–830. https://doi.org/10.1130/G38104.1

Gayen, B., Griffiths, R. W., & Kerr, R. C. (2015). Melting Driven Convection at the Ice-seawater Interface. *Procedia IUTAM*, *15*, 78–85. https://doi.org/10.1016/J.PIUTAM.2015.04.012

Gayen, B., Griffiths, R. W., & Kerr, R. C. (2016). Simulation of convection at a vertical ice face dissolving into saline water. *Journal of Fluid Mechanics*, *798*, 284–298. https://doi.org/10.1017/jfm.2016.315

Gerringa, L. J. A., Alderkamp, A. C., Laan, P., Thuróczy, C. E., De Baar, H. J. W., Mills, M. M., et al. (2012). Iron from melting glaciers fuels the phytoplankton blooms in Amundsen Sea (Southern Ocean): Iron biogeochemistry. *Deep-Sea Research Part II: Topical Studies in Oceanography*, *71–76*, 16–31. https://doi.org/10.1016/j.dsr2.2012.03.007

Giles, A. B. (2017). The Mertz Glacier Tongue, East Antarctica. Changes in the past 100 years and its cyclic nature—Past, present and future. *Remote Sensing of Environment*, *191*, 30–37. https://doi.org/10.1016/j.rse.2017.01.003

Gillet-Chaulet, F., Gagliardini, O., Meyssonnier, J., Montagnat, M., & Castelnau, O. (2005). A user-friendly anisotropic flow law for ice-sheet modelling. *Journal of Glaciology*, *51*(172), 3–14. https://doi.org/10.3189/172756505781829584

Gillet-Chaulet, F., G., D., Gagliardini, O., Mosbeux, C., Mouginot, J., Remy, F., & Ritz, C. (2016). Assimilation of surface velocities acquired between 1996 and 2010 to constrain the form of the basal friction law under Pine Island Glacier. *Geophysical Research Letters*, *43*, 10,311–10,321. https://doi.org/10.1002/2016GL069937

Gladstone, R. M., Lee, V., Rougier, J., Payne, A. J., Hellmer, H., Le Brocq, A., et al. (2012). Calibrated prediction of Pine Island Glacier retreat during the 21st and 22nd centuries with a coupled flowline model. *Earth and Planetary Science Letters*, *333–334*, 191–199. https://doi.org/10.1016/j.epsl.2012.04.022

Gladstone, R. M., Lee, V., Vieli, A., & Payne, A. J. (2010). Grounding line migration in an adaptive mesh ice sheet model. *Journal of Geophysical Research*, *115*, F04014. https://doi.org/10.1029/2009JF001615

Gladstone, R. M., Payne, a. J., & Cornford, S. L. (2010). Parameterising the grounding line in flow-line ice sheet models. *The Cryosphere*, *4*(4), 605–619. https://doi.org/10.5194/tc-4-605-2010

Gladstone, R. M., Warner, R. C., Galton-Fenzi, B. K., Gagliardini, O., Zwinger, T., Greve, R., & Gladstone, R. (2017). Marine ice sheet model performance depends on basal sliding physics and sub-shelf melting. *The Cryosphere*, *11*, 319–329. https://doi.org/10.5194/tc-11-319-2017

Glasscock, S. K., Hayes, C. T., Redmond, N., & Rohde, E. (2020). Changes in Antarctic Bottom Water formation during interglacial periods. *Paleoceanography and Paleoclimatology*, *35*, e2020PA003867. https://doi.org/10.1029/2020PA003867
Glen, J. W. (1952). Experiments on the deformation of ice. *Journal of Glaciology*, *2*(12), 111–114. https://doi.org/10.1017/S0022143000034067
Glen, J. W. (1953). Rate of flow of polycrystalline ice. *Nature*, *172*(4381), 721–722. https://doi.org/10.1038/172721a0
Glen, J. W. (1955). The creep of polycrystalline ice. *Proceedings of the Royal Society of London. Series A. Mathematical and Physical Sciences*, *228*(1175), 519–538.
Glen, J. W. (1958). The flow law of ice: A discussion of the assumptions made in glacier theory, their experimental foundations and consequences. *IASH Publ*, *47*, 171–183.
Goehring, B. M., Balco, G., Todd, C., Moening-Swanson, I., & Nichols, K. (2019). Late-glacial grounding line retreat in the northern Ross Sea, Antarctica. *Geology*, *47*(4), 291–294. https://doi.org/10.1130/G45413.1
Gohl, K. (2012). Basement control on past ice sheet dynamics in the Amundsen Sea Embayment, West Antarctica. *Palaeogeography, Palaeoclimatology, Palaeoecology*, *335–336*, 35–41. https://doi.org/10.1016/j.palaeo.2011.02.022
Gohl, K., Uenzelmann-Neben, G., Larter, R. D., Hillenbrand, C. D., Hochmuth, K., Kalberg, T., et al. (2013). Seismic stratigraphic record of the Amundsen Sea Embayment shelf from pre-glacial to recent times: Evidence for a dynamic West Antarctic ice sheet. *Marine Geology*, *344*, 115–131. https://doi.org/10.1016/j.margeo.2013.06.011
Gohl, K., Wellner, J., & Klaus, A. (2019). IODP Expedition 379 Preliminary Report: Amundsen Sea West Antarctic Ice Sheet History. *IODP Proceedings*, (March). https://doi.org/10.14379/iodp.pr.379.2019
Goldberg, D., Holland, D. M., & Schoof, C. (2009). Grounding line movement and ice shelf buttressing in marine ice sheets. *Journal of Geophysical Research*, *114*, F04026. https://doi.org/10.1029/2008JF001227
Goldberg, D. N., Little, C. M., Sergienko, O. V., Gnanadesikan, A., Hallberg, R., & Oppenheimer, M. (2012). Investigation of land ice-ocean interaction with a fully coupled ice-ocean model: 1. Model description and behavior. *Journal of Geophysical Research*, *117*, F02037. https://doi.org/10.1029/2011JF002246
Golledge, N. R. (2014). Selective erosion beneath the Antarctic Peninsula Ice Sheet during LGM retreat. *Antarctic Science*, *26*(6), 698–707. https://doi.org/10.1017/S0954102014000340
Golledge, N. R. (2020). Long-term projections of sea-level rise from ice sheets. *Wiley Interdisciplinary Reviews: Climate Change*, (December 2019), *11*(2), 1–21. https://doi.org/10.1002/wcc.634
Golledge, N. R., Fogwill, C. J., Mackintosh, A. N., & Buckley, K. M. (2012). Dynamics of the last glacial maximum Antarctic ice-sheet and its response to ocean forcing. *Proceedings of the National Academy of Sciences*, *109*(40), 16,052–16,056. https://doi.org/10.1073/pnas.1205385109
Golledge, N. R., Keller, E. D., Gomez, N., Naughten, K. A., Bernales, J., Trusel, L. D., & Edwards, T. L. (2019). Global environmental consequences of twenty-first-century ice-sheet melt. *Nature*, *566*(7742), 65–72. https://doi.org/10.1038/s41586-019-0889-9
Golledge, N. R., Kowalewski, D. E., Naish, T. R., Levy, R. H., Fogwill, C. J., & Gasson, E. G. W. (2015). The multi-millennial Antarctic commitment to future sea-level rise. *Nature*, *526*(7573), 421–425. https://doi.org/10.1038/nature15706
Golledge, N. R., Levy, R. H., McKay, R. M., Fogwill, C. J., White, D. A., Graham, A. G. C., et al. (2013). Glaciology and geological signature of the Last Glacial Maximum Antarctic ice sheet. *Quaternary Science Reviews*, *78*, 225–247. https://doi.org/10.1016/j.quascirev.2013.08.011
Golledge, N. R., Levy, R. H., McKay, R. M., & Naish, T. R. (2017). East Antarctic ice sheet most vulnerable to Weddell Sea warming. *Geophysical Research Letters*, *44*, 2343–2351. https://doi.org/10.1002/2016GL072422
Golledge, N. R., Menviel, L., Carter, L., Fogwill, C. J., England, M. H., Cortese, G., & Levy, R. H. (2014). Antarctic contribution to meltwater pulse 1A from reduced Southern Ocean overturning. *Nature Communications*, *5*, 1–10. https://doi.org/10.1038/ncomms6107
Golledge, N. R., Thomas, Z. A., Levy, R. H., Gasson, E. G. W., Naish, T. R., McKay, R. M., et al. (2017). Antarctic climate and ice-sheet configuration during the early Pliocene interglacial at 4.23 Ma. *Climate of the Past*, *13*(7), 959–975. https://doi.org/10.5194/cp-13-959-2017
Gomez, N., Latychev, K., & Pollard, D. (2018). A coupled ice sheet-sea level model incorporating 3D Earth structure: Variations in Antarctica during the last deglacial retreat. *Journal of Climate*, *31*, 4041–4054. https://doi.org/10.1175/JCLI-D-17-0352.1
Gomez, N., Mitrovica, J. X., Huybers, P., & Clark, P. U. (2010). Sea level as a stabilizing factor for marine-ice-sheet grounding lines. *Nature Geoscience*, *3*(12), 850–853. https://doi.org/10.1038/Ngeo1012
Gomez, N., Mitrovica, J. X., Tamisiea, M. E., & Clark, P. U. (2010). A new projection of sea level change in response to collapse of marine sectors of the Antarctic Ice Sheet. *Geophysical Journal International*, *180*(2), 623–634. https://doi.org/10.1111/j.1365-246X.2009.04419.x
Gomez, N., Pollard, D., & Holland, D. (2015). Sea-level feedback lowers projections of future Antarctic Ice-Sheet mass loss. *Nature Communications*, *6*, 8798. https://doi.org/10.1038/ncomms9798
Gomez, N., Pollard, D., & Mitrovica, J. X. (2013). A 3-D coupled ice sheet—Sea level model applied to Antarctica through the last 40 ky. *Earth and Planetary Science Letters*, *384*, 88–99. https://doi.org/10.1016/j.epsl.2013.09.042
Gomez, N., Pollard, D., Mitrovica, J. X., Huybers, P., & Clark, P. U. (2012). Evolution of a coupled marine ice sheet-sea level model. *Journal of Geophysical Research*, *117*, F01013. https://doi.org/10.1029/2011JF002128
Gooch, B. T., Young, D. A., & Blankenship, D. D. (2016). Potential groundwater and heterogeneous heat source contributions to ice sheet dynamics in critical submarine basins of East Antarctica. *Geochemistry, Geophysics, Geosystems*, *17*, 395–409. https://doi.org/10.1002/2015GC006117
Goodge, J. W. (2018). Crustal heat production and estimate of terrestrial heat flow in central East Antarctica, with implications for thermal input to the East Antarctic ice sheet. *The Cryosphere*, *12*(2), 491–504. https://doi.org/10.5194/tc-12-491-2018
Goodge, J. W., & Severinghaus, J. P. (2016). Rapid Access Ice Drill: A new tool for exploration of the deep Antarctic ice sheets and subglacial geology. *Journal of Glaciology*, *62*(236), 1049–1064. https://doi.org/10.1017/jog.2016.97
Goodwin, B. P., Mosley-Thompson, E., Wilson, A. B., Porter, S. E., & Sierra-Hernandez, M. R. (2016). Accumulation variability in the Antarctic Peninsula: The role of large-scale atmospheric oscillations and their interactions*. *Journal of Climate*, *29*(7), 2579–2596. https://doi.org/10.1175/JCLI-D-15-0354.1
Goodwin, P., Haigh, I. D., Rohling, E. J., & Slangen, A. (2017). A new approach to projecting 21st century sea-level changes and extremes. *Earth's Future*, *5*(2), 240–253. https://doi.org/10.1002/2016EF000508
Gorodetskaya, I. V., Tsukernik, M., Claes, K., Ralph, M. F., Neff, W. D., & Van Lipzig, N. P. M. (2014). The role of atmospheric rivers in anomalous snow accumulation in East Antarctica. *Geophysical Research Letters*, *41*, 6199–6206. https://doi.org/10.1002/2014GL060881
Graham, A. G. C., Larter, R. D., Gohl, K., Dowdeswell, J. A., Hillenbrand, C.-D., Smith, J. A., et al. (2010). Flow and retreat of the Late Quaternary Pine Island-Thwaites palaeo-ice stream, West Antarctica. *Journal of Geophysical Research*, *115*, F03025. https://doi.org/10.1029/2009JF001482

Graham, F. S., Morlighem, M., Warner, R. C., & Treverrow, A. (2018). Implementing an empirical scalar constitutive relation for ice with flow-induced polycrystalline anisotropy in large-scale ice sheet models. *The Cryosphere*, *12*(3), 1047–1067. https://doi.org/10.5194/tc-12-1047-2018

Grant, G. R., Naish, T. R., Dunbar, G. B., Stocchi, P., Kominz, M. A., Kamp, P. J. J., et al. (2019). The amplitude and origin of sea-level variability during the Pliocene epoch. *Nature*, *574*(7777), 237–241. https://doi.org/10.1038/s41586-019-1619-z

Grant, K. M., Rohling, E. J., Bar-Matthews, M., Ayalon, A., Medina-Elizalde, M., Ramsey, C. B., et al. (2012). Rapid coupling between ice volume and polar temperature over the past 50,000 years. *Nature*, *491*(7426), 744–747. https://doi.org/10.1038/nature11593

Grant, K. M., Rohling, E. J., Bronk Ramsey, C., Cheng, H., Edwards, R. L., Florindo, F., et al. (2014). Sea-level variability over five glacial cycles. *Nature Communications*, *5*, 5076. https://doi.org/10.1038/ncomms6076

Graw, J. H., Adams, A. N., Hansen, S. E., Wiens, D. A., Hackworth, L., & Park, Y. (2016). Upper mantle shear wave velocity structure beneath northern Victoria Land, Antarctica: Volcanism and uplift in the northern Transantarctic Mountains. *Earth and Planetary Science Letters*, *449*, 48–60. https://doi.org/10.1016/j.epsl.2016.05.026

Greene, C. A., Young, D. A., Gwyther, D. E., Galton-Fenzi, B. K., & Blankenship, D. D. (2018). Seasonal dynamics of Totten Ice Shelf controlled by sea ice buttressing. *The Cryosphere*, *12*(9), 2869–2882. https://doi.org/10.5194/tc-12-2869-2018

Greenwood, S. L., Simkins, L. M., Halberstadt, A. R. W., Prothro, L. O., & Anderson, J. B. (2018). Holocene reconfiguration and readvance of the East Antarctic Ice Sheet. *Nature Communications*, *9*(1), 3176. https://doi.org/10.1038/s41467-018-05625-3

Greve, R., & Blatter, H. (2009). *Dynamics of ice sheets and glaciers*. Berlin, Germany etc.: Springer. https://doi.org/10.1007/978-3-642-03415-2

Groh, A., Ewert, H., Scheinert, M., Fritsche, M., Rülke, A., Richter, A., et al. (2012). An investigation of Glacial Isostatic Adjustment over the Amundsen Sea sector, West Antarctica. *Global and Planetary Change*, *98–99*(December 2012), 45–53. https://doi.org/10.1016/j.gloplacha.2012.08.001

Groh, A., Horwath, M., Horvath, A., Meister, R., Sørensen, L. S., Barletta, V. R., et al. (2019). Evaluating GRACE mass change time series for the antarctic and Greenland ice sheet-methods and results. *Geosciences*, *9*(10), 415. https://doi.org/10.3390/geosciences9100415

Gudmundsson, G. H. (2013). Ice-shelf buttressing and the stability of marine ice sheets. *The Cryosphere*, *7*(2), 647–655. https://doi.org/10.5194/tc-7-647-2013

Gulick, S. P. S., Shevenell, A. E., Montelli, A., Fernandez, R., Smith, C., Warny, S., et al. (2017). Initiation and long-term instability of the East Antarctic Ice Sheet. *Nature*, *552*(7684), 225–229. https://doi.org/10.1038/nature25026

Gunter, B. C., Didova, O., Riva, R. E. M., Ligtenberg, S. R. M., Lenaerts, J. T. M., King, M. A., et al. (2014). Empirical estimation of present-day Antarctic glacial isostatic adjustment and ice mass change. *The Cryosphere*, *8*(2), 743–760. https://doi.org/10.5194/tc-8-743-2014

Gwyther, D. E., Cougnon, E. A., Galton-Fenzi, B. K., Roberts, J. L., Hunter, J. R., & Dinniman, M. S. (2016). Modelling the response of ice shelf basal melting to different ocean cavity environmental regimes. *Annals of Glaciology*, *57*(73), 131–141. https://doi.org/10.1017/aog.2016.31

Gwyther, D. E., Galton-Fenzi, B. K., Dinniman, M. S., Roberts, J. L., & Hunter, J. R. (2015). The effect of basal friction on melting and freezing in ice shelf-ocean models. *Ocean Modelling*, *95*, 38–52. https://doi.org/10.1016/j.ocemod.2015.09.004

Gwyther, D. E., Galton-Fenzi, B. K., Hunter, J. R., & Roberts, J. L. (2014). Simulated melt rates for the Totten and Dalton ice shelves. *Ocean Science*, *10*(3), 267–279. https://doi.org/10.5194/os-10-267-2014

Gwyther, D. E., O'Kane, T. J., Galton-Fenzi, B. K., Monselesan, D. P., & Greenbaum, J. S. (2018). Intrinsic processes drive variability in basal melting of the Totten Glacier Ice Shelf. *Nature Communications*, *9*(1), 3141. https://doi.org/10.1038/s41467-018-05618-2

Hager, B. H., Clayton, R. W., Richards, M. A., Comer, R. P., & Dziewonski, A. M. (1985). Lower mantle heterogeneity, dynamic topography and the geoid. *Nature*, *313*(6003), 541–545. https://doi.org/10.1038/313541a0

Halberstadt, A. R., Simkins, L. M., Greenwood, S. L., & Anderson, J. B. (2016). Past ice-sheet behaviour: Retreat scenarios and changing controls in the Ross Sea, Antarctica. *The Cryosphere Discussions*, 1–36. https://doi.org/10.5194/tc-2016-33

Hall, B. L., Denton, G. H., Heath, S. L., Jackson, M. S., & Koffman, T. N. B. (2015). Accumulation and marine forcing of ice dynamics in the western Ross Sea during the last deglaciation. *Nature Geoscience*, *8*(8), 625–628. https://doi.org/10.1038/ngeo2478

Hambrey, M. J., & McKelvey, B. (2000). Major Neogene fluctuations of the East Antarctic ice sheet: Stratigraphic evidence from the Lambert Glacier region. *Geology*, *28*(10), 887–890. https://doi.org/10.1130/0091-7613(2000)28<887:MNFOTE>2.0.CO;2

Hansen, J., Sato, M., Kharecha, P., von Schuckmann, K., Beerling, D. J., Cao, J., et al. (2017). Young people's burden: Requirement of negative CO_2 emissions. *Earth System Dynamics*, *8*(3), 577–616. https://doi.org/10.5194/esd-8-577-2017

Hansen, S. E., Graw, J. H., Kenyon, L. M., Nyblade, A. A., Wiens, D. A., Aster, R. C., et al. (2014). Imaging the Antarctic mantle using adaptively parameterized *P*-wave tomography: Evidence for heterogeneous structure beneath West Antarctica. *Earth and Planetary Science Letters*, *408*, 66–78. https://doi.org/10.1016/j.epsl.2014.09.043

Harig, C., & Simons, F. J. (2015). Accelerated West Antarctic ice mass loss continues to outpace East Antarctic gains. *Earth and Planetary Science Letters*, *415*, 134–141. https://doi.org/10.1016/j.epsl.2015.01.029

Harland, S. R., Kendall, J. M., Stuart, G. W., Lloyd, G. E., Baird, A. F., Smith, A. M., et al. (2013). Deformation in Rutford Ice Stream, West Antarctica: Measuring shear-wave anisotropy from icequakes. *Annals of Glaciology*, *54*(64), 105–114. https://doi.org/10.3189/2013AoG64A033

Hay, C., Mitrovica, J. X., Gomez, N., Creveling, J. R., Austermann, J., & Kopp, R. R. (2014). The sea-level fingerprints of ice-sheet collapse during interglacial periods. *Quaternary Science Reviews*, *87*, 60–69. https://doi.org/10.1016/j.quascirev.2013.12.022

Hay, C. C., Lau, H. C. P., Gomez, N., Austermann, J., Powell, E., Mitrovica, J. X., et al. (2017). Sea level fingerprints in a region of complex Earth structure: The case of WAIS. *Journal of Climate*, *30*(6), 1881–1892. https://doi.org/10.1175/JCLI-D-16-0388.1

Hay, C. C., Morrow, E., Kopp, R. E., & Mitrovica, J. X. (2015). Probabilistic reanalysis of twentieth-century sea-level rise. *Nature*, *517*(7535), 481–484. https://doi.org/10.1038/nature14093

Hayes, C. T., Martínez-García, A., Hasenfratz, A. P., Jaccard, S. L., Hodell, D. A., Sigman, D. M., et al. (2014). A stagnation event in the deep South Atlantic during the last interglacial period. *Science (New York, N.Y.)*, *346*(6216), 1514–1517. https://doi.org/10.1126/science.1256620

Haywood, A. M., Dowsett, H. J., & Dolan, A. M. (2016). Integrating geological archives and climate models for the mid-Pliocene warm period. *Nature Communications*, *7*(1), 10646. https://doi.org/10.1038/ncomms10646

Haywood, A. M., Dowsett, H. J., Dolan, A. M., Rowley, D., Abe-Ouchi, A., Otto-Bliesner, B., et al. (2016). The Pliocene Model Intercomparison Project (PlioMIP) Phase 2: Scientific objectives and experimental design. *Climate of the Past*, *12*(3), 663–675. https://doi.org/10.5194/cp-12-663-2016

Hearty, P. J., Kindler, P., Cheng, H., & Edwards, R. L. (1999). A +20 m middle Pleistocene sea-level highstand (Bermuda and the Bahamas) due to partial collapse of Antarctic ice. *Geology*, *27*(4), 375–378. https://doi.org/10.1130/0091-7613(1999)027<0375:AMMPSL>2.3.CO;2

Heeszel, D. S., Wiens, D. A., Anandakrishnan, S., Aster, R. C., Dalziel, I. W. D., Huerta, A. D., et al. (2016). Upper mantle structure of central and West Antarctica from array analysis of Rayleigh wave phase velocities. *Journal of Geophysical Research: Solid Earth*, *121*, 1758–1775. https://doi.org/10.1002/2015JB012616

Hein, A. S., Marrero, S. M., Woodward, J., Dunning, S. A., Winter, K., Westoby, M. J., et al. (2016). Mid-Holocene pulse of thinning in the Weddell Sea sector of the West Antarctic ice sheet. *Nature Communications*, *7*(1), 12511. https://doi.org/10.1038/ncomms12511

Hellmer, H. H. (2004). Impact of Antarctic ice shelf basal melting on sea ice and deep ocean properties. *Geophysical Research Letters*, *31*, L10307. https://doi.org/10.1029/2004GL019506

Hellmer, H. H., Kauker, F., Timmermann, R., Determann, J., & Rae, J. (2012). Twenty-first-century warming of a large Antarctic ice-shelf cavity by a redirected coastal current. *Nature*, *485*(7397), 225–228. https://doi.org/10.1038/nature11064

van Hengstum, P. J., Scott, D. B., & Javaux, E. J. (2009). Foraminifera in elevated Bermudian caves provide further evidence for +21 m eustatic sea level during Marine Isotope Stage 11. *Quaternary Science Reviews*, *28*(19–20), 1850–1860. https://doi.org/10.1016/j.quascirev.2009.05.017

Herraiz-Borreguero, L., Church, J. A., Allison, I., Peña-Molino, B., Coleman, R., Tomczak, M., & Craven, M. (2016). Basal melt, seasonal water mass transformation, ocean current variability, and deep convection processes along the Amery Ice Shelf calving front, East Antarctica. *Journal of Geophysical Research: Oceans*, *121*, 4946–4965. https://doi.org/10.1002/2016JC011858

Heywood, K., Biddle, L., Boehme, L., Dutrieux, P., Fedak, M., Jenkins, A., et al. (2016). Between the devil and the deep blue sea: The role of the Amundsen Sea continental shelf in exchanges between ocean and ice shelves. *Oceanography*, *29*(4), 118–129. https://doi.org/10.5670/oceanog.2016.104

Hibbert, F. D., Rohling, E. J., Dutton, A., Williams, F. H., Chutcharavan, P. M., Zhao, C., & Tamisiea, M. E. (2016). Coral indicators of past sea-level change: A global repository of U-series dated benchmarks. *Quaternary Science Reviews*, *145*, 1–56. https://doi.org/10.1016/j.quascirev.2016.04.019

Hibbert, F. D., Williams, F. H., Fallon, S. J., & Rohling, E. J. (2018). A database of biological and geomorphological sea-level markers from the Last Glacial Maximum to present. *Scientific Data*, *5*(1), 180088. https://doi.org/10.1038/sdata.2018.88

Hillenbrand, C.-D., Bentley, M. J., Stolldorf, T. D., Hein, A. S., Kuhn, G., Graham, A. G. C., et al. (2014). Reconstruction of changes in the Weddell Sea sector of the Antarctic Ice Sheet since the Last Glacial Maximum q. *Quaternary Science Reviews*, *100*, 111–136. https://doi.org/10.1016/j.quascirev.2013.07.020

Hillenbrand, C.-D., Fütterer, D. K., Grobe, H., & Frederichs, T. (2002). No evidence for a Pleistocene collapse of the West Antarctic Ice Sheet from continental margin sediments recovered in the Amundsen Sea. *Geo-Marine Letters*, *22*(2), 51–59. https://doi.org/10.1007/s00367-002-0097-7

Hillenbrand, C. D., Kuhn, G., & Frederichs, T. (2009). Record of a Mid-Pleistocene depositional anomaly in West Antarctic continental margin sediments: An indicator for ice-sheet collapse? *Quaternary Science Reviews*, *28*(13–14), 1147–1159. https://doi.org/10.1016/j.quascirev.2008.12.010

Hillenbrand, C. D., Kuhn, G., Smith, J. A., Gohl, K., Graham, A. G. C., Larter, R. D., et al. (2013). Grounding-line retreat of the West Antarctic Ice Sheet from inner Pine Island Bay. *Geology*, *41*(1), 35–38. https://doi.org/10.1130/G33469.1

Hillenbrand, C. D., Smith, J. A., Hodell, D. A., Greaves, M., Poole, C. R., Kender, S., et al. (2017). West Antarctic Ice Sheet retreat driven by Holocene warm water incursions. *Nature*, *547*(7661), 43–48. https://doi.org/10.1038/nature22995

Hindmarsh, R. (1997). Deforming beds: Viscous and plastic scales of deformation. *Quaternary Science Reviews*, *16*(9), 1039–1056. https://doi.org/10.1016/S0277-3791(97)00035-8

Hobbs, W. R., Massom, R., Stammerjohn, S., Reid, P., Williams, G., & Meier, W. (2016). A review of recent changes in Southern Ocean sea ice, their drivers and forcings. *Global and Planetary Change*, *143*, 228–250. https://doi.org/10.1016/j.gloplacha.2016.06.008

Hochmuth, K., & Gohl, K. (2019). Seaward growth of Antarctic continental shelves since establishment of a continent-wide ice sheet: Patterns and mechanisms. *Palaeogeography, Palaeoclimatology, Palaeoecology*, *520*, 44–54. https://doi.org/10.1016/j.palaeo.2019.01.025

Hodell, D. A., Charles, C. D., & Ninnemann, U. S. (2000). Comparison of interglacial stages in the South Atlantic sector of the southern ocean for the past 450 kyr: Implifications for Marine Isotope Stage (MIS) 11. *Global and Planetary Change*, *24*(1), 7–26. https://doi.org/10.1016/S0921-8181(99)00069-7

Hodell, D. A., Venz, K. A., Charles, C. D., & Ninnemann, U. S. (2003). Pleistocene vertical carbon isotope and carbonate gradients in the South Atlantic sector of the Southern Ocean. *Geochemistry, Geophysics, Geosystems*, *4*(1), 1004. https://doi.org/10.1029/2002GC000367

Hodgson, D. A., Hogan, K., Smith, J. M., Smith, J. A., Hillenbrand, C. D., Graham, A. G. C., et al. (2018). Deglaciation and future stability of the Coats Land ice margin, Antarctica. *The Cryosphere*, *12*(7), 2383–2399. https://doi.org/10.5194/tc-12-2383-2018

Hodgson, D. A., Whitehouse, P. L., de Cort, G., Berg, S., Verleyen, E., Tavernier, I., et al. (2016). Rapid early Holocene sea-level rise in Prydz Bay, East Antarctica. *Global and Planetary Change*, *139*, 128–140. https://doi.org/10.1016/j.gloplacha.2015.12.020

Hodson, T. O., Powell, R. D., Brachfeld, S. A., Tulaczyk, S., & Scherer, R. P. (2016). Physical processes in Subglacial Lake Whillans, West Antarctica: Inferences from sediment cores. *Earth and Planetary Science Letters*, *444*, 56–63. https://doi.org/10.1016/j.epsl.2016.03.036

Hoffman, J. S., Clark, P. U., Parnell, A. C., & He, F. (2017). Regional and global sea-surface temperatures during the last interglaciation. *Science*, *355*(6322). https://doi.org/10.1126/science.aai8464

Hogg, A. E., & Gudmundsson, G. H. (2017). Commentary: Impacts of the Larsen-C Ice Shelf calving event. *Nature Climate Change*, *7*(8), 540–542. https://doi.org/10.1038/nclimate3359

Holland, D. M., Galton-Fenzi, B., Parizek, B., Holland, P., Menemenlis, D., Larour, E., et al. (2015). Projecting Sea-Level Rise from West Antarctica. *Eos*. under review

Holland, P. R. (2017). The transient response of ice shelf melting to ocean change. *Journal of Physical Oceanography*, *47*(8), 2101–2114. https://doi.org/10.1175/JPO-D-17-0071.1

Holland, P. R., Bracegirdle, T. J., Dutrieux, P., Jenkins, A., & Steig, E. J. (2019). West Antarctic ice loss influenced by internal climate variability and anthropogenic forcing. *Nature Geoscience*, *12*(9), 718–724. https://doi.org/10.1038/s41561-019-0420-9

Holland, P. R., Jenkins, A., & Holland, D. M. (2008). The response of ice shelf basal melting to variations in ocean temperature. *Journal of Climate*, *21*(11), 2558–2572. https://doi.org/10.1175/2007JCLI1909.1

Holland, P. R., Jenkins, A., & Holland, D. M. (2010). Ice and ocean processes in the Bellingshausen sea, Antarctica. *Journal of Geophysical Research*, *115*, C05020. https://doi.org/10.1029/2008JC005219

Holloway, M. D., Sime, L. C., Allen, C. S., Hillenbrand, C. D., Bunch, P., Wolff, E., & Valdes, P. J. (2017). The spatial structure of the 128 ka Antarctic sea ice minimum. *Geophysical Research Letters*, *44*, 11,129–11,139. https://doi.org/10.1002/2017GL074594

Holloway, M. D., Sime, L. C., Singarayer, J. S., Tindall, J. C., Bunch, P., & Valdes, P. J. (2016). Antarctic last interglacial isotope peak in response to sea ice retreat not ice-sheet collapse. *Nature Communications*, *7*, 1–9. https://doi.org/10.1038/ncomms12293

Holt, J. W., Blankenship, D. D., Morse, D. L., Young, D. A., Peters, M. E., Kempf, S. D., et al. (2006). New boundary conditions for the West Antarctic Ice Sheet: Subglacial topography of the Thwaites and Smith glacier catchments. *Geophysical Research Letters*, *33*, L09502. https://doi.org/10.1029/2005GL025561

Howat, I., Morin, P., Porter, C., & Noh, M.-J. (2018). The reference elevation model of Antarctica, V1. Harvard Dataverse. https://doi.org/10.7910/DVN/SAIK8B

Hsu, C. W., & Velicogna, I. (2017). Detection of sea level fingerprints derived from GRACE gravity data. *Geophysical Research Letters*, *44*, 8953–8961. https://doi.org/10.1002/2017GL074070

Huerta, A. D., & Harry, D. L. (2007). The transition from diffuse to focused extension: Modeled evolution of the West Antarctic Rift system. *Earth and Planetary Science Letters*, *255*(1–2), 133–147. https://doi.org/10.1016/j.epsl.2006.12.011

Hughes, T. (1977). West Antarctic ice streams. *Reviews of Geophysics*, *15*(1), 1–46. https://doi.org/10.1029/RG015i001p00001

Hughes, T., Zhao, Z., Hintz, R., & Fastook, J. (2017). Instability of the Antarctic Ross Sea Embayment as climate warms. *Reviews of Geophysics*, *55*, 434–469. https://doi.org/10.1002/2016RG000545

Humbert, A., & Steinhage, D. (2011). The evolution of the western rift area of the Fimbul Ice Shelf, Antarctica. *Cryosphere*, *5*(4), 931–944. https://doi.org/10.5194/tc-5-931-2011

Huneke, W. G. C., Klocker, A., & Galton-Fenzi, B. K. (2019). Deep bottom mixed layer drives intrinsic variability of the Antarctic Slope Front. *Journal of Physical Oceanography*, *49*(12), 3163–3177. https://doi.org/10.1175/JPO-D-19-0044.1

Huppert, H. E., Josberger, E. G., Huppert, H. E., & Josberger, E. G. (1980). The melting of ice in cold stratified water. *Journal of Physical Oceanography*, *10*(6), 953–960. https://doi.org/10.1175/1520-0485(1980)010<0953:TMOIIC>2.0.CO;2

Huppert, H. E., & Turner, J. S. (1978). On melting icebergs. *Nature*, *271*(5640), 46–48. https://doi.org/10.1038/271046a0

Huppert, H. E., & Turner, J. S. (1980). Ice blocks melting into a salinity gradient. *Journal of Fluid Mechanics*, *100*(02), 367–384. https://doi.org/10.1017/S0022112080001206

Hutter, K. (1982). Dynamics of glaciers and large ice masses. *Annual Review of Fluid Mechanics*, *14*(1), 87–130. https://doi.org/10.1146/annurev.fl.14.010182.000511

Ivins, E. R., James, T. S., Wahr, J., Schrama, E. J. O., Landerer, F., & Simon, K. (2013). Antarctic contribution to sea-level rise observed by GRACE with improved GIA correction. *Journal of Geophysical Research: Solid Earth*, *118*, 3126–3141. https://doi.org/10.1002/jgrb.50208

Jacobs, S., Giulivi, C., Dutrieux, P., Rignot, E., Nitsche, F., & Mouginot, J. (2013). Getz Ice Shelf melting response to changes in ocean forcing. *Journal of Geophysical Research: Oceans*, *118*, 4152–4168. https://doi.org/10.1002/jgrc.20298

Jacobs, S. S., Hellmer, H. H., & Jenkins, A. (1996). Antarctic Ice Sheet melting in the southeast Pacific. *Geophysical Research Letters*, *23*(9), 957–960. https://doi.org/10.1029/96GL00723

Jacobs, S. S., Helmer, H. H., Doake, C. S. M., Jenkins, A., & Frolich, R. M. (1992). Melting of ice shelves and the mass balance of Antarctica. *Journal of Glaciology*, *38*(130), 375–387. https://doi.org/10.3189/S0022143000002252

Jacobs, S. S., Jenkins, A., Giulivi, C. F., & Dutrieux, P. (2011). Stronger ocean circulation and increased melting under Pine Island Glacier ice shelf. *Nature Geoscience*, *4*, 519–523. https://doi.org/10.1038/ngeo1188

Jacobs, S. S., Jenkins, A., Hellmer, H. H., Giulivi, C. F., Nitsche, F., Huber, B., & Guerrero, R. (2012). The Amundsen Sea and the Antarctic Ice Sheet. *Ocenaography*, *25*(3), 154–163. https://doi.org/10.5670/oceanog.2012.90

Jakobsson, M., Anderson, J. B., Nitsche, F. O., Gyllencreutz, R., Kirshner, A. E., Kirchner, N., et al. (2012). Ice sheet retreat dynamics inferred from glacial morphology of the central Pine Island Bay Trough, West Antarctica. *Quaternary Science Reviews*, *38*, 1–10. https://doi.org/10.1016/j.quascirev.2011.12.017

Jamieson, S. S. R., Hulton, N. R. J., Sugden, D. E., Payne, A. J., & Taylor, J. (2005). Cenozoic landscape evolution of the Lambert basin, East Antarctica: The relative role of rivers and ice sheets. *Global and Planetary Change*, *45*(1–3), 35–49. https://doi.org/10.1016/j.gloplacha.2004.09.015

Jamieson, S. S. R., Stokes, C. R., Ross, N., Rippin, D. M., Bingham, R. G., Wilson, D. S., et al. (2014). The glacial geomorphology of the Antarctic ice sheet bed. *Antarctic Science*, *26*(6), 724–741. https://doi.org/10.1017/S0954102014000212

Jamieson, S. S. R., Vieli, A., Livingstone, S. J., Ó Cofaigh, C., Stokes, C., Hillenbrand, C. D., & Dowdeswell, J. A. (2012). Ice-stream stability on a reverse bed slope. *Nature Geoscience*, *5*(11), 799–802. https://doi.org/10.1038/ngeo1600

Jenkins, A. (2011). Convection-driven melting near the grounding lines of ice shelves and tidewater glaciers. *Journal of Physical Oceanography*, *41*(12), 2279–2294. https://doi.org/10.1175/JPO-D-11-03.1

Jenkins, A. (2016). A simple model of the ice shelf-ocean boundary layer and current. *Journal of Physical Oceanography*, *46*(6), 1785–1803. https://doi.org/10.1175/JPO-D-15-0194.1

Jenkins, A., Dutrieux, P., Jacobs, S., McPhail, S., Perrett, J., Webb, A., & White, D. (2010). Observations beneath Pine Island Glacier in West Antarctica and implications for its retreat. *Nature Geoscience*, *3*, 468–472. https://doi.org/10.1038/ngeo890

Jenkins, A., Dutrieux, P., Jacobs, S., Steig, E., Gudmundsson, H., Smith, J., & Heywood, K. (2016). Decadal ocean forcing and Antarctic ice sheet response: Lessons from the Amundsen Sea. *Oceanography*, *29*(4), 106–117. https://doi.org/10.5670/oceanog.2016.103

Jenkins, A., Shoosmith, D., Dutrieux, P., Jacobs, S., Kim, T. W., Lee, S. H., et al. (2018). West Antarctic Ice Sheet retreat in the Amundsen Sea driven by decadal oceanic variability. *Nature Geoscience*, *11*(10), 733–738. https://doi.org/10.1038/s41561-018-0207-4

Jezek, K., Wu, X., Paden, J., & Leuschen, C. (2013). Radar mapping of Isunnguata Sermia, Greenland. *Journal of Glaciology*, *59*(218), 1135–1146. https://doi.org/10.3189/2013JoG12J248

Johnson, J. S., Bentley, M. J., Smith, J. A., Finkel, R. C., Rood, D. H., Gohl, K., et al. (2014). Rapid Thinning of Pine Island Glacier in the Early Holocene. *Science*, *343*(6174), 999–1001. https://doi.org/10.1126/science.1247385

Johnson, J. S., Nichols, K. A., Goehring, B. M., Balco, G., & Schaefer, J. M. (2019). Abrupt mid-Holocene ice loss in the western Weddell Sea Embayment of Antarctica. *Earth and Planetary Science Letters*, *518*, 127–135. https://doi.org/10.1016/J.EPSL.2019.05.002

Jones, R. S., Mackintosh, A. N., Norton, K. P., Golledge, N. R., Fogwill, C. J., Kubik, P. W., et al. (2015). Rapid Holocene thinning of an East Antarctic outlet glacier driven by marine ice sheet instability. *Nature Communications*, *6*, 8910. https://doi.org/10.1038/ncomms9910

Jones, R. S., Whitehouse, P. L., Bentley, M. J., Small, D., & Dalton, A. S. (2019). Impact of glacial isostatic adjustment on cosmogenic surface-exposure dating. *Quaternary Science Reviews*, *212*, 206–212. https://doi.org/10.1016/j.quascirev.2019.03.012

Jong, L. M., Gladstone, R. M., Galton-Fenzi, B. K., & King, M. A. (2018). Simulated dynamic regrounding during marine ice sheet retreat. *The Cryosphere*, *12*(7), 2425–2436. https://doi.org/10.5194/tc-12-2425-2018

Jongma, J. I., Driesschaert, E., Fichefet, T., Goosse, H., & Renssen, H. (2009). The effect of dynamic-thermodynamic icebergs on the Southern Ocean climate in a three-dimensional model. *Ocean Modelling*, *26*(1–2), 104–113. https://doi.org/10.1016/j.ocemod.2008.09.007

Jordan, J. R., Holland, P. R., Goldberg, D., Snow, K., Arthern, R., Campin, J. M., et al. (2018). Ocean-forced ice-shelf thinning in a synchronously coupled ice-ocean model. *Journal of Geophysical Research: Oceans*, *123*, 864–882. https://doi.org/10.1002/2017JC013251

Jordan, T. A., Ferraccioli, F., & Leat, P. T. (2017). New geophysical compilations link crustal block motion to Jurassic extension and strike-slip faulting in the Weddell Sea Rift System of West Antarctica. *Gondwana Research*, *42*, 29–48. https://doi.org/10.1016/j.gr.2016.09.009

Jordan, T. A., Ferraccioli, F., Ross, N., Corr, H. F. J., Leat, P. T., Bingham, R. G., et al. (2013). Inland extent of the Weddell Sea Rift imaged by new aerogeophysical data. *Tectonophysics*, *585*, 137–160. https://doi.org/10.1016/j.tecto.2012.09.010

Jordan, T. A., Ferraccioli, F., Vaughan, D. G., Holt, J. W., Corr, H., Blankenship, D. D., & Diehl, T. M. (2010). Aerogravity evidence for major crustal thinning under the Pine Island Glacier region (West Antarctica). *Bulletin of the Geological Society of America*, *122*(5–6), 714–726. https://doi.org/10.1130/b26417.1

Jordan, T. A., Martin, C., Ferraccioli, F., Matsuoka, K., Corr, H., Forsberg, R., et al. (2018). Anomalously high geothermal flux near the South Pole. *Scientific Reports*, *8*(1), 16785. https://doi.org/10.1038/s41598-018-35182-0

Josberger, E. G. (1983). Sea ice melting in the marginal ice zone. *Journal of Geophysical Research*, *88*(C5), 2841–2844. https://doi.org/10.1029/JC088iC05p02841

Joughin, I., & Alley, R. B. (2011). Stability of the West Antarctic ice sheet in a warming world. *Nature Geoscience*, *4*(8), 506–513. https://doi.org/10.1038/ngeo1194

Joughin, I., Smith, B. E., & Medley, B. (2014). Marine ice sheet collapse potentially under way for the thwaites glacier basin, West Antarctica. *Science*, *344*(6185), 735–738. https://doi.org/10.1126/science.1249055

Joughin, I., Smith, B. E., & Schoof, C. G. (2019). Regularized Coulomb friction laws for ice sheet sliding: Application to Pine Island Glacier, Antarctica. *Geophysical Research Letters*, *46*, 4764–4771. https://doi.org/10.1029/2019GL082526

Jouzel, J., Masson-Delmotte, V., Cattani, O., Dreyfus, G., Falourd, S., Hoffmann, G., et al. (2007). Orbital and millennial antarctic climate variability over the past 800,000 years. *Science*, *317*(5839), 793–796. https://doi.org/10.1126/science.1141038

Kalberg, T., & Gohl, K. (2014). The crustal structure and tectonic development of the continental margin of the Amundsen sea embayment, West Antarctica: Implications from geophysical data. *Geophysical Journal International*, *198*(1), 327–341. https://doi.org/10.1093/gji/ggu118

Kanfoush, S. L., Hodell, D. A., Charles, C. D., Guilderson, T. P., Graham Mortyn, P., & Ninnemann, U. S. (2000). Millennial-scale instability of the Antarctic Ice Sheet during the last glaciation. *Science*, *288*(5472), 1815–1819. https://doi.org/10.1126/science.288.5472.1815

Karl, D. M., Bird, D. F., Björkman, K., Houlihan, T., Shackelford, R., & Tupas, L. (1999). Microorganisms in the accreted ice of Lake Vostok. *Antarctic Science*, *286*(5447), 2144–2147. https://doi.org/10.1126/science.286.5447.2144

Kaufmann, G., Wu, P., & Ivins, E. R. (2005). Lateral viscosity variations beneath Antarctica and their implications on regional rebound motions and seismotectonics. *Journal of Geodynamics*, *39*(2), 165–181. https://doi.org/10.1016/j.jog.2004.08.009

Kehew, A. E., Piotrowski, J. A., & Jørgensen, F. (2012). Tunnel valleys: Concepts and controversies—A review. *Earth-Science Reviews*, *113*(1–2), 33–58. https://doi.org/10.1016/j.earscirev.2012.02.002

Keitzl, T., Mellado, J. P., & Notz, D. (2016). Reconciling estimates of the ratio of heat and salt fluxes at the ice-ocean interface. *Journal of Geophysical Research: Oceans*, *121*, 8419–8433. https://doi.org/10.1002/2016JC012018

Kennicutt, M. C., Bromwich, D., Liggett, D., Njåstad, B., Peck, L., Rintoul, S. R., et al. (2019). Sustained Antarctic research: A 21st century imperative. *One Earth*, *1*(1), 95–113. https://doi.org/10.1016/j.oneear.2019.08.014

Kennicutt, M. C., Chown, S. L., Cassano, J. J., Liggett, D., Massom, R., Peck, L. S., et al. (2014). Polar research: Six priorities for Antarctic science. *Nature*, *512*(7512), 23–25. https://doi.org/10.1038/512023a

Kennicutt, M. C., Chown, S. L., Cassano, J. J., Liggett, D., Peck, L. S., Massom, R., et al. (2015). A roadmap for Antarctic and Southern Ocean science for the next two decades and beyond. *Antarctic Science*, *27*(1), 3–18. https://doi.org/10.1017/S0954102014000674

Kennicutt, M. C., Kim, Y. D., Rogan-Finnemore, M., Anandakrishnan, S., Chown, S. L., Colwell, S., et al. (2016). Delivering 21st century Antarctic and Southern Ocean science. *Antarctic Science*, *28*(6), 407–423. https://doi.org/10.1017/S0954102016000481

Kerr, R. A. (1998). Signs of past collapse beneath Antarctic ice. *Science*, *281*(5373), 17. https://doi.org/10.1126/science.281.5373.17

Kerr, R. C., & McConnochie, C. D. (2015). Dissolution of a vertical solid surface by turbulent compositional convection. *Journal of Fluid Mechanics*, *765*, 211–228. https://doi.org/10.1017/jfm.2014.722

Kessler, M. A., Anderson, R. S., & Briner, J. P. (2008). Fjord insertion into continental margins driven by topographic steering of ice. *Nature Geoscience*, *1*(6), 365–369. https://doi.org/10.1038/ngeo201

Khazendar, A., Schodlok, M. P., Fenty, I., Ligtenberg, S. R. M., Rignot, E., & van den Broeke, M. R. (2013). Observed thinning of Totten Glacier is linked to coastal polynya variability. *Nature Communications*, *4*, 2857. https://doi.org/10.1038/ncomms3857

Khazendar, A., Borstad, C. P., Scheuchl, B., Rignot, E., & Seroussi, H. (2015). The evolving instability of the remnant Larsen B Ice Shelf and its tributary glaciers. *Earth and Planetary Science Letters*, *419*, 199–210. https://doi.org/10.1016/j.epsl.2015.03.014

Kiefer, W. S., & Kellogg, L. H. (1998). Geoid anomalies and dynamic topography from time-dependent, spherical axisymmetric mantle convection. *Physics of the Earth and Planetary Interiors*, *106*(3–4), 237–256. https://doi.org/10.1016/S0031-9201(98)00078-8

Kim, I., Hahm, D., Rhee, T. S., Kim, T. W., Kim, C. S., & Lee, S. H. (2016). The distribution of glacial meltwater in the Amundsen Sea, Antarctica, revealed by dissolved helium and neon. *Journal of Geophysical Research: Oceans*, *121*, 1654–1666. https://doi.org/10.1002/2015JC011211

King, E. C., Hindmarsh, R. C. A., & Stokes, C. R. (2009). Formation of mega-scale glacial lineations observed beneath a West Antarctic ice stream. *Nature Geoscience*, *2*(8), 585–588. https://doi.org/10.1038/ngeo581

King, E. C., Pritchard, H. D., & Smith, A. M. (2016). Subglacial landforms beneath Rutford Ice Stream, Antarctica: Detailed bed topography from ice-penetrating radar. *Earth System Science Data*, *8*(1), 151–158. https://doi.org/10.5194/essd-8-151-2016

King, M. A., Bingham, R. J., Moore, P., Whitehouse, P. L., Bentley, M. J., & Milne, G. A. (2012). Lower satellite-gravimetry estimates of Antarctic sea-level contribution. *Nature*, *491*(7425), 586–589. https://doi.org/10.1038/nature11621

King, M. A., Whitehouse, P. L., & van der Wal, W. (2016). Incomplete separability of Antarctic plate rotation from glacial isostatic adjustment deformation within geodetic observations. *Geophysical Journal International*, *204*(1), 324–330. https://doi.org/10.1093/gji/ggv461

Kingslake, J., Ely, J. C., Das, I., & Bell, R. E. (2017). Widespread movement of meltwater onto and across Antarctic ice shelves. *Nature*, *544*(7650), 349–352. https://doi.org/10.1038/nature22049

Kingslake, J., Scherer, R. P., Albrecht, T., Coenen, J., Powell, R. D., Reese, R., et al. (2018). Extensive retreat and re-advance of the West Antarctic Ice Sheet during the Holocene. *Nature*, *558*(7710), 430–434. https://doi.org/10.1038/s41586-018-0208-x

Kirkham, J. D., Hogan, K. A., Larter, R. D., Arnold, N. S., Nitsche, F. O., Golledge, N. R., & Dowdeswell, J. A. (2019). Past water flow beneath Pine Island and Thwaites glaciers, West Antarctica. *Cryosphere*, *13*(7), 1959–1981. https://doi.org/10.5194/tc-13-1959-2019

Kirshner, A. E., Anderson, J. B., Jakobsson, M., O'regan, M., Majewski, W., & Nitsche, F. O. (2012). Post-LGM deglaciation in Pine Island Bay, West Antarctica. *Quaternary Science Reviews*, *38*, 11–26. https://doi.org/10.1016/j.quascirev.2012.01.017

Klages, J. P., Kuhn, G., Hillenbrand, C. D., Graham, A. G. C., Smith, J. A., Larter, R. D., et al. (2014). Retreat of the West Antarctic Ice Sheet from the western Amundsen Sea shelf at a pre- or early LGM stage. *Quaternary Science Reviews*, *91*, 1–15. https://doi.org/10.1016/j.quascirev.2014.02.017

Klages, J. P., Kuhn, G., Hillenbrand, C.-D., Smith, J. A., Graham, A. G. C., Nitsche, F. O., et al. (2017). Limited grounding-line advance onto the West Antarctic continental shelf in the easternmost Amundsen Sea Embayment during the last glacial period. *PLoS ONE*, *12*(7), e0181593. https://doi.org/10.1371/journal.pone.0181593

Klinck, J. M., & Dinniman, M. S. (2010). Exchange across the shelf break at high southern latitudes. *Ocean Science*, *6*(2), 513–524. https://doi.org/10.5194/os-6-513-2010

Klinck, J. M., Hofmann, E. E., Beardsley, R. C., Salihoglu, B., & Howard, S. (2004). Water-mass properties and circulation on the west Antarctic Peninsula Continental Shelf in Austral Fall and Winter 2001. *Deep-Sea Research Part II: Topical Studies in Oceanography*, *51*(17–19), 1925–1946. https://doi.org/10.1016/j.dsr2.2004.08.001

Konrad, H., Gilbert, L., Cornford, S. L., Payne, A., Hogg, A., Muir, A., & Shepherd, A. (2017). Uneven onset and pace of ice-dynamical imbalance in the Amundsen Sea Embayment, West Antarctica. *Geophysical Research Letters*, *44*, 910–918. https://doi.org/10.1002/2016GL070733

Konrad, H., Sasgen, I., Klemann, V., Thoma, M., Grosfeld, K., & Martinec, Z. (2016). Sensitivity of grounding-line dynamics to viscoelastic deformation of the solid-earth in an idealized scenario. *Polarforschung*, *85*(2), 89–99. https://doi.org/10.2312/polarforschung.85.2.89

Konrad, H., Sasgen, I., Pollard, D., & Klemann, V. (2015). Potential of the solid-Earth response for limiting long-term West Antarctic Ice Sheet retreat in a warming climate. *Earth and Planetary Science Letters*, *432*, 254–264. https://doi.org/10.1016/j.epsl.2015.10.008

Konrad, H., Shepherd, A., Gilbert, L., Hogg, A. E., McMillan, M., Muir, A., & Slater, T. (2018). Net retreat of Antarctic glacier grounding lines. *Nature Geoscience*, *11*(4), 258–262. https://doi.org/10.1038/s41561-018-0082-z

Konrad, H., Thoma, M., Sasgen, I., Klemann, V., Grosfeld, K., Barbi, D., & Martinec, Z. (2014). The deformational response of a viscoelastic solid Earth model coupled to a thermomechanical ice sheet model. *Surveys in Geophysics*, *35*(6), 1441–1458. https://doi.org/10.1007/s10712-013-9257-8

Kopp, R. E., DeConto, R. M., Bader, D. A., Hay, C. C., Horton, R. M., Kulp, S., et al. (2017). Evolving understanding of Antarctic ice-sheet physics and ambiguity in probabilistic sea-level projections. *Earth's Future*, *5*, 1217–1233. https://doi.org/10.1002/2017EF000663

Kopp, R. E., Horton, R. M., Little, C. M., Mitrovica, J. X., Oppenheimer, M., Rasmussen, D. J., et al. (2014). Probabilistic 21st and 22nd century sea-level projections at a global network of tide-gauge sites. *Earth's Future*, *2*, 383–406. https://doi.org/10.1002/2014EF000239

Kopp, R. E., Simons, F. J., Mitrovica, J. X., Maloof, A. C., & Oppenheimer, M. (2009). Probabilistic assessment of sea level during the last interglacial stage. *Nature*, *462*(7275), 863–867. https://doi.org/10.1038/nature08686

Kuhn, G., Hillenbrand, C. D., Kasten, S., Smith, J. A., Nitsche, F. O., Frederichs, T., et al. (2017). Evidence for a palaeo-subglacial lake on the Antarctic continental shelf. *Nature Communications*, *8*(1), 15591. https://doi.org/10.1038/ncomms15591

Kusahara, K., & Hasumi, H. (2013). Modeling Antarctic ice shelf responses to future climate changes and impacts on the ocean. *Journal of Geophysical Research: Oceans*, *118*, 2454–2475. https://doi.org/10.1002/jgrc.20166

Kusahara, K., Hasumi, H., & Williams, G. D. (2011). Impact of the Mertz Glacier Tongue calving on dense water formation and export. *Nature Communications*, *2*(1), 159. https://doi.org/10.1038/ncomms1156

Kusahara, K., Williams, G. D., Tamura, T., Massom, R., & Hasumi, H. (2017). Dense Shelf Water spreading from Antarctic coastal polynyas to the deep Southern Ocean: A regional circumpolar model study. *Journal of Geophysical Research: Oceans*, *122*, 6238–6253. https://doi.org/10.1002/2017JC012911

Lago, V., & England, M. H. (2019). Projected slowdown of antarctic bottom water formation in response to amplified meltwater contributions. *Journal of Climate*, *32*(19), 6319–6335. https://doi.org/10.1175/JCLI-D-18-0622.1

Lambeck, K., Rouby, H., Purcell, A., Sun, Y., & Sambridge, M. (2014). Sea level and global ice volumes from the Last Glacial Maximum to the Holocene. *Proceedings of the National Academy of Sciences of the United States of America*, *111*(43), 15,296–15,303. https://doi.org/10.1073/pnas.1411762111

Langley, E. S., Leeson, A. A., Stokes, C. R., & Jamieson, S. S. R. (2016). Seasonal evolution of supraglacial lakes on an East Antarctic outlet glacier. *Geophysical Research Letters*, *43*, 8563–8571. https://doi.org/10.1002/2016GL069511

Langley, K., Kohler, J., Matsuoka, K., Sinisalo, A., Scambos, T., Neumann, T., et al. (2011). Recovery Lakes, East Antarctica: Radar assessment of sub-glacial water extent. *Geophysical Research Letters*, *38*, L05501. https://doi.org/10.1029/2010gl046094

Larour, E., Ivins, E. R., & Adhikari, S. (2017). Should coastal planners have concern over where land ice is melting? *Science Advances*, *3*(11), e1700537. https://doi.org/10.1126/sciadv.1700537

Larour, E., Seroussi, H., Adhikari, S., Ivins, E., Caron, L., Morlighem, M., & Schlegel, N. (2019). Slowdown in Antarctic mass loss from solid Earth and sea-level feedbacks. *Science*, *364*, eaav7908. https://doi.org/10.1126/science.aav7908

Larter, R. D., Anderson, J. B., Graham, A. G. C., Gohl, K., Hillenbrand, C. D., Jakobsson, M., et al. (2014). Reconstruction of changes in the Amundsen Sea and Bellingshausen Sea sector of the West Antarctic Ice Sheet since the Last Glacial Maximum. *Quaternary Science Reviews*, *100*, 55–86. https://doi.org/10.1016/J.QUASCIREV.2013.10.016

Larter, R. D., Graham, A. G. C., Hillenbrand, C. D., Smith, J. A., & Gales, J. A. (2012). Late Quaternary grounded ice extent in the Filchner Trough, Weddell Sea, Antarctica: New marine geophysical evidence. *Quaternary Science Reviews*, *53*(C), 111–122. https://doi.org/10.1016/j.quascirev.2012.08.006

Larter, R. D., Hogan, K. A., Hillenbrand, C.-D., Smith, J. A., Batchelor, C. L., Cartigny, M., et al. (2019). Subglacial hydrological control on flow of an Antarctic Peninsula palaeo-ice stream. *The Cryosphere*, *13*(6), 1583–1596. https://doi.org/10.5194/tc-13-1583-2019

Le Brocq, A. M., Payne, A. J., Siegert, M. J., & Alley, R. A. (2009). A subglacial water-flow model for West Antarctica. *Journal of Glaciology*, *55*(193), 879–888. https://doi.org/10.3189/002214309790152564

Le Brocq, A. M., Ross, N., Griggs, J., Bingham, R., Corr, H., Ferroccioli, F., et al. (2013). Evidence from ice shelves for channelized meltwater flow beneath the Antarctic Ice Sheet. *Nature Geoscience*, *6*(11), 945–948. https://doi.org/10.1038/ngeo1977

Lee, J. I., McKay, R. M., Golledge, N. R., Yoon, H. I., Yoo, K. C., Kim, H. J., & Hong, J. K. (2017). Widespread persistence of expanded East Antarctic glaciers in the southwest Ross Sea during the last deglaciation. *Geology*, *45*(5), 403–406. https://doi.org/10.1130/G38715.1

Leeman, J. R., Valdez, R. D., Alley, R. B., Anandakrishnan, S., & Saffer, D. M. (2016). Mechanical and hydrologic properties of Whillans Ice Stream till: Implications for basal strength and stick-slip failure. *Journal of Geophysical Research: Earth Surface*, *121*, 1295–1309. https://doi.org/10.1002/2016jf003863

Leguy, G. R., Asay-Davis, X. S., & Lipscomb, W. H. (2014). Parameterization of basal friction near grounding lines in a one-dimensional ice sheet model. *The Cryosphere*, *8*(4), 1239–1259. https://doi.org/10.5194/tc-8-1239-2014

LeMasurier, W. E., & Landis, C. A. (1996). Mantle-plume activity recorded by low-relief erosion surfaces in West Antarctica and New Zealand. *GSA Bulletin*, *108*(11), 1450–1466. https://doi.org/10.1130/0016-7606(1996)108<1450:MPARBL>2.3.CO;2
Lemieux, J. M., Sudicky, E. A., Peltier, W. R., & Tarasov, L. (2008). Dynamics of groundwater recharge and seepage over the Canadian landscape during the Wisconsinian glaciation. *Journal of Geophysical Research*, *113*, F01011. https://doi.org/10.1029/2007JF000838
Lenaerts, J. T. M., Lhermitte, S., Drews, R., Ligtenberg, S. R. M., Berger, S., Helm, V., et al. (2017). Meltwater produced by wind-albedo interaction stored in an East Antarctic ice shelf. *Nature Climate Change*, *7*(1), 58–62. https://doi.org/10.1038/nclimate3180
Lenaerts, J. T. M., Van Meijgaard, E., Van Den Broeke, M. R., Ligtenberg, S. R. M., Horwath, M., & Isaksson, E. (2013). Recent snowfall anomalies in Dronning Maud Land, East Antarctica, in a historical and future climate perspective. *Geophysical Research Letters*, *40*, 2684–2688. https://doi.org/10.1002/grl.50559
Leroux, S., Penduff, T., Bessières, L., Molines, J.-M., Brankart, J.-M., Sérazin, G., et al. (2018). Intrinsic and atmospherically forced variability of the AMOC: Insights from a large-ensemble ocean hindcast. *Journal of Climate*, *31*(3), 1183–1203. https://doi.org/10.1175/JCLI-D-17-0168.1
Leuliette, E., & Willis, J. (2011). Balancing the sea level budget. *Oceanography*, *24*(2), 122–129. https://doi.org/10.5670/oceanog.2011.32
Leventer, A., Domack, E., Dunbar, R., Pike, J., Stickley, C., Maddison, E., et al. (2006). Marine sediment record from the East Antarctic margin reveals dynamics of ice sheet recession. *GSA Today*, *16*(12), 4. https://doi.org/10.1130/GSAT01612A.1
Levermann, A., & Feldmann, J. (2019). Scaling of instability timescales of Antarctic outlet glaciers based on one-dimensional similitude analysis. *The Cryosphere*, *13*(6), 1621–1633. https://doi.org/10.5194/tc-13-1621-2019
Li, J., Jacka, J., & Budd, W. F. (1996). Deformation rates in combined compression and shear for ice which is initially isotropic and after the development of strong anisotropy. *Annals of Glaciology*, *23*, 247–252.
Li, X., Rignot, E., Mouginot, J., & Scheuchl, B. (2016). Ice flow dynamics and mass loss of Totten Glacier, East Antarctica, from 1989 to 2015. *Geophysical Research Letters*, *43*, 6366–6373. https://doi.org/10.1002/2016GL069173
Licht, K. J., & Hemming, S. R. (2017). Analysis of Antarctic glacigenic sediment provenance through geochemical and petrologic applications. *Quaternary Science Reviews*, *164*, 1–24. https://doi.org/10.1016/j.quascirev.2017.03.009
Lindeque, A., Martos Martin, Y. M., Gohl, K., & Maldonado, A. (2013). Deep-sea pre-glacial to glacial sedimentation in the Weddell Sea and southern Scotia Sea from a cross-basin seismic transect. *Marine Geology*, *336*, 61–83. https://doi.org/10.1016/j.margeo.2012.11.004
Lishman, B., Wadham, J., Drinkwater, B., Kendall, J.-M., Burrow, S., Hilton, G., & Craddock, I. (2013). Assessing the utility of acoustic communication for wireless sensors deployed beneath ice sheets. *Annals of Glaciology*, *54*(64), 124–134. https://doi.org/10.3189/2013AoG64A022
Lisiecki, L. E., & Raymo, M. E. (2005). A Pliocene-Pleistocene stack of 57 globally distributed benthic $\delta^{18}O$ records. *Paleoceanography*, *20*, PA1003. https://doi.org/10.1029/2004PA001071
Lisker, F., Wilson, C. J. L., & Gibson, H. J. (2007). Thermal history of the Vestfold Hills (East Antarctica) between Lambert rifting and Gondwana break-up, evidence from apatite fission track data. *Antarctic Science*, *19*(1), 97–106. https://doi.org/10.1017/S0954102007000144
Liu, C., Wang, Z., Cheng, C., Xia, R., Li, B., & Xie, Z. (2017). Modeling modified Circumpolar Deep Water intrusions onto the Prydz Bay continental shelf, East Antarctica. *Journal of Geophysical Research: Oceans*, *122*, 5198–5217. https://doi.org/10.1002/2016JC012336
Liu, Y., Moore, J. C., Cheng, X., Gladstone, R. M., Bassis, J. N., Liu, H., et al. (2015). Ocean-driven thinning enhances iceberg calving and retreat of Antarctic ice shelves. *Proceedings of the National Academy of Sciences of the United States of America*, *112*(11), 3263–3268. https://doi.org/10.1073/pnas.1415137112
Livingstone, S. J., Ó Cofaigh, C., Stokes, C. R., Hillenbrand, C. D., Vieli, A., & Jamieson, S. S. R. (2012). Antarctic palaeo-ice streams. *Earth-Science Reviews*, *111*(1–2), 90–128. https://doi.org/10.1016/j.earscirev.2011.10.003
Lliboutry, L. (1968). General theory of subglacial cavitation and sliding of temperate glaciers. *Journal of Glaciology*, *7*(49), 21–58. https://doi.org/10.3189/S0022143000020396
Loose, B., Naveira Garabato, A. C., Schlosser, P., Jenkins, W. J., Vaughan, D., & Heywood, K. J. (2018). Evidence of an active volcanic heat source beneath the Pine Island Glacier. *Nature Communications*, *9*(1), 2431. https://doi.org/10.1038/s41467-018-04421-3
Loose, B., Schlosser, P., Smethie, W. M., & Jacobs, S. (2009). An optimized estimate of glacial melt from the Ross Ice Shelf using noble gases, stable isotopes, and CFC transient tracers. *Journal of Geophysical Research*, *114*, C08007. https://doi.org/10.1029/2008JC005048
Lowe, A. L., & Anderson, J. B. (2002). Reconstruction of the West Antarctic ice sheet in Pine Island Bay during the last glacial maximum and its subsequent retreat history. *Quaternary Science Reviews*, *21*(16–17), 1879–1897. https://doi.org/10.1016/S0277-3791(02)00006-9
Lowry, D. P., Golledge, N. R., Bertler, N. A. N., Jones, R. S., McKay, R., & Stutz, J. (2020). Geologic controls on ice sheet sensitivity to deglacial climate forcing in the Ross Embayment, Antarctica. *Quaternary Science Advances*, *1*, 100002. https://doi.org/10.1016/j.qsa.2020.100002
Lowry, D. P., Golledge, N. R., Menviel, L., & Bertler, N. A. N. (2019). Deglacial evolution of regional Antarctic climate and Southern Ocean conditions in transient climate simulations. *Climate of the Past*, *15*(1), 189–215. https://doi.org/10.5194/cp-15-189-2019
Lüthi, D., le Floch, M., Bereiter, B., Blunier, T., Barnola, J. M., Siegenthaler, U., et al. (2008). High-resolution carbon dioxide concentration record 650,000–800,000 years before present. *Nature*, *453*(7193), 379–382. https://doi.org/10.1038/nature06949
Lynch, S., Batty, L., & Byrne, P. (2014). Environmental risk of metal mining contaminated river bank sediment at redox-transitional zones. *Minerals*, *4*(1), 52–73. https://doi.org/10.3390/min4010052
MacAyeal, D. R. (1987). *Ice-shelf backpressure: Form drag versus dynamic drag* (pp. 141–160). Dordrecht: Springer. https://doi.org/10.1007/978-94-009-3745-1_8
MacAyeal, D. R. (1989). Large-scale ice flow over a viscous basal sediment: Theory and application to ice stream B, Antarctica. *Journal of Geophysical Research*, *94*(134), 4071–4087.
MacAyeal, D. R. (1992a). Irregular oscillations of the West Antarctic ice sheet. *Nature*, *359*(6390), 29–32. https://doi.org/10.1038/359029a0
MacAyeal, D. R. (1992b). The basal stress distribution of ice stream E, Antarctica, inferred by control methods. *Journal of Geophysical Research*, *97*(B1), 595–603. https://doi.org/10.1029/91JB02454
MacAyeal, D. R., & Sergienko, O. V. (2013). The flexural dynamics of melting ice shelves. *Annals of Glaciology*, *54*(63), 1–10. https://doi.org/10.3189/2013AoG63A256
MacAyeal, D. R., Sergienko, O. V., & Banwell, A. F. (2015). A model of viscoelastic ice-shelf flexure. *Journal of Glaciology*, *61*(228), 635–645. https://doi.org/10.3189/2015JoG14J169
Mack, S. L., Dinniman, M. S., Klinck, J. M., McGillicuddy, D. J., & Padman, L. (2019). Modeling ocean eddies on Antarctica's cold water continental shelves and their effects on ice shelf basal melting. *Journal of Geophysical Research: Oceans*, *124*, 5067–5084. https://doi.org/10.1029/2018JC014688

Mackintosh, A., Golledge, N., Domack, E., Dunbar, R., Leventer, A., White, D., et al. (2011). Retreat of the East Antarctic ice sheet during the last glacial termination. *Nature Geoscience*, *4*(3), 195–202. https://doi.org/10.1038/ngeo1061

Mackintosh, A. N., Verleyen, E., O'Brien, P. E., White, D. A., Jones, R. S., McKay, R., et al. (2014). Retreat history of the East Antarctic Ice Sheet since the Last Glacial Maximum. *Quaternary Science Reviews*, *100*, 10–30. https://doi.org/10.1016/j.quascirev.2013.07.024

Mankoff, K. D., Jacobs, S. S., Tulaczyk, S. M., & Stammerjohn, S. E. (2012). The role of pine island glacier ice shelf basal channels in deep-water upwelling, polynyas and ocean circulation in pine island bay, antarctica. *Annals of Glaciology*, *53*(60), 123–128. https://doi.org/10.3189/2012AoG60A062

Marino, G., Rohling, E. J., Rodríguez-Sanz, L., Grant, K. M., Heslop, D., Roberts, A. P., et al. (2015). Bipolar seesaw control on last interglacial sea level. *Nature*, *522*(7555), 197–201. https://doi.org/10.1038/nature14499

Maritati, A., Aitken, A. R. A., Young, D. A., Roberts, J. L., Blankenship, D. D., & Siegert, M. J. (2016). The tectonic development and erosion of the Knox Subglacial Sedimentary Basin, East Antarctica. *Geophysical Research Letters*, *43*, 10,728–10,737. https://doi.org/10.1002/2016GL071063

Marshall, G. J., Thompson, D. W. J., & van den Broeke, M. R. (2017). The signature of Southern Hemisphere atmospheric circulation patterns in Antarctic precipitation. *Geophysical Research Letters*, *44*, 11,580–11,589. https://doi.org/10.1002/2017GL075998

Martín-Español, A., King, M. A., Zammit-Mangion, A., Andrews, S. B., Moore, P., & Bamber, J. L. (2016). An assessment of forward and inverse GIA solutions for Antarctica. *Journal of Geophysical Research: Solid Earth*, *121*, 6947–6965. https://doi.org/10.1002/2016JB013154

Martín-Español, A., Zammit-Mangion, A., Clarke, P. J., Flament, T., Helm, V., King, M. A., et al. (2016). Spatial and temporal Antarctic Ice Sheet mass trends, glacio-isostatic adjustment, and surface processes from a joint inversion of satellite altimeter, gravity, and GPS data. *Journal of Geophysical Research: Earth Surface*, *121*, 182–200. https://doi.org/10.1002/2015JF003550

Martínez-Botí, M. A., Foster, G. L., Chalk, T. B., Rohling, E. J., Sexton, P. F., Lunt, D. J., et al. (2015). Plio-Pleistocene climate sensitivity evaluated using high-resolution CO_2 records. *Nature*, *518*(7537), 49–54. https://doi.org/10.1038/nature14145

Martos, Y. M., Catalán, M., Jordan, T. A., Golynsky, A., Golynsky, D., Eagles, G., & Vaughan, D. G. (2017). Heat flux distribution of Antarctica unveiled. *Geophysical Research Letters*, *44*, 11,417–11,426. https://doi.org/10.1002/2017GL075609

Massom, R. A., Scambos, T. A., Bennetts, L. G., Reid, P., Squire, V. A., & Stammerjohn, S. E. (2018). Antarctic ice shelf disintegration triggered by sea ice loss and ocean swell. *Nature*, *558*(7710), 383–389. https://doi.org/10.1038/s41586-018-0212-1

Masson-Delmotte, V., Schulz, M., Abe-Ouchi, A., Beer, J., Ganopolski, A., González Rouco, J., et al. (2013). Information from paleoclimate archives. In T. F. Stocker et al. (Eds.), *Climate change 2013: The physical science basis. Contribution of Working Group I to the Fifth Assessment Report of the Intergovernmental Panel on Climate Change* (pp. 383–464).

Masson-Delmotte, V., Stenni, B., Blunier, T., Cattani, O., Chappellaz, J., Cheng, H., et al. (2010). Abrupt change of Antarctic moisture origin at the end of Termination II. *Proceedings of the National Academy of Sciences*, *107*(27), 12,091–12,094. https://doi.org/10.1073/pnas.0914536107

Matsuoka, K., Furukawa, T., Fujita, S., Maeno, H., Uratsuka, S., Naruse, R., & Watanabe, O. (2003). Crystal orientation fabrics within the Antarctic ice sheet revealed by a multipolarization plane and dual-frequency radar survey. *Journal of Geophysical Research*, *108*(B10), 2499. https://doi.org/10.1029/2003JB002425

Matsuoka, K., Power, D., Fujita, S., & Raymond, C. F. (2012). Rapid development of anisotropic ice-crystal-alignment fabrics inferred from englacial radar polarimetry, central West Antarctica. *Journal of Geophysical Research*, *117*, F03029. https://doi.org/10.1029/2012JF002440

Maule, C. F., Purucker, M. E., Olsen, N., & Mosegaard, K. (2005). Geophysics: Heat flux anomalies in Antarctica revealed by satellite magnetic data. *Science*, *309*(5733), 464–467. https://doi.org/10.1126/science.1106888

McConnochie, C. D., & Kerr, R. C. (2017). Testing a common ice-ocean parameterization with laboratory experiments. *Journal of Geophysical Research: Oceans*, *122*, 5905–5915. https://doi.org/10.1002/2017JC012918

McGlone, M. S., Turney, C. S. M., Wilmshurst, J. M., Renwick, J., & Pahnke, K. (2010). Divergent trends in land and ocean temperature in the Southern Ocean over the past 18,000 years. *Nature Geoscience*, *3*(9), 622–626. https://doi.org/10.1038/ngeo931

McIntosh, J. C., Garven, G., & Hanor, J. S. (2011). Impacts of Pleistocene glaciation on large-scale groundwater flow and salinity in the Michigan Basin. *Geofluids*, *11*(1), 18–33. https://doi.org/10.1111/j.1468-8123.2010.00303.x

McKay, N. P., Overpeck, J. T., & Otto-Bliesner, B. L. (2011). The role of ocean thermal expansion in Last Interglacial sea level rise. *Geophysical Research Letters*, *38*, L14605. https://doi.org/10.1029/2011GL048280

McKay, R., Golledge, N. R., Maas, S., Naish, T., Levy, R., Dunbar, G., & Kuhn, G. (2016). Antarctic marine ice-sheet retreat in the Ross Sea during the early Holocene. *Geology*, *44*(1), 7–10. https://doi.org/10.1130/G37315.1

McKay, R., Naish, T., Carter, L., Riesselman, C., Dunbar, R., Sjunneskog, C., et al. (2012). Antarctic and Southern Ocean influences on Late Pliocene global cooling. *Proceedings of the National Academy of Sciences*, *109*(17), 6423–6428. https://doi.org/10.1073/pnas.1112248109

McKay, R., Naish, T., Powell, R., Barrett, P., Scherer, R., Talarico, F., et al. (2012). Pleistocene variability of Antarctic Ice Sheet extent in the Ross Embayment. *Quaternary Science Reviews*, *34*, 93–112. https://doi.org/10.1016/j.quascirev.2011.12.012

McKay, R. M., Barrett, P. J., Levy, R. S., Naish, T. R., Golledge, N. R., & Pyne, A. (2016). Antarctic Cenozoic climate history from sedimentary records: ANDRILL and beyond. *Philosophical Transactions of the Royal Society A*, *374*(2059), 20140301. https://doi.org/10.1098/rsta.2014.0301

McKay, R. M., De Santis, L., Kulhanek, D. K., & Scientists, and the E. 374 (2019). Ross Sea West Antarctic Ice Sheet History. *Proceedings of the International Ocean Discovery Program, 374: College Station, TX (International Ocean Discovery Program)*, *374*(March). Retrieved from https://doi.org/10.14379/iodp.proc.374.2019

McMillan, M., Corr, H., Shepherd, A., Ridout, A., Laxon, S., & Cullen, R. (2013). Three-dimensional mapping by CryoSat-2 of subglacial lake volume changes. *Geophysical Research Letters*, *40*, 4321–4327. https://doi.org/10.1002/grl.50689

McMillan, M., Shepherd, A., Sundal, A., Briggs, K., Muir, A., Ridout, A., et al. (2014). Increased ice losses from Antarctica detected by CryoSat-2. *Geophysical Research Letters*, *41*, 3899–3905. https://doi.org/10.1002/2014GL060111

McMurtry, G. M., Tappin, D. R., Sedwick, P. N., Wilkinson, I., Fietzke, J., & Sellwood, B. (2007). Elevated marine deposits in Bermuda record a late Quaternary megatsunami. *Sedimentary Geology*, *200*(3), 155–165. https://doi.org/10.1016/j.sedgeo.2006.10.009

McPhee, M. G. (1981). An analytic similarity theory for the planetary boundary layer stabilized by surface buoyancy. *Boundary-Layer Meteorology*, *21*(3), 325–339. https://doi.org/10.1007/BF00119277

Menviel, L., Spence, P., & England, M. H. (2015). Contribution of enhanced Antarctic Bottom Water formation to Antarctic warm events and millennial-scale atmospheric CO_2 increase. *Earth and Planetary Science Letters*, *413*, 37–50. https://doi.org/10.1016/j.epsl.2014.12.050

Menviel, L., Timmermann, A., Timm, O. E., & Mouchet, A. (2010). Climate and biogeochemical response to a rapid melting of the West Antarctic Ice sheet during interglacials and implications for future climate. *Paleoceanography*, *25*, PA4231. https://doi.org/10.1029/2009PA001892

Mercer, J. H. (1978). West Antarctic ice sheet and CO_2 greenhouse effect: A threat of disaster. *Nature*, *271*(5643), 321–325. https://doi.org/10.1038/271321a0

Michaud, A. B., Skidmore, M. L., Mitchell, A. C., Vick-Majors, T. J., Barbante, C., Turetta, C., et al. (2016). Solute sources and geochemical processes in Subglacial Lake Whillans, West Antarctica. *Geology*, *44*(5), 347–350. https://doi.org/10.1130/G37639.1

Miles, B. W. J., Stokes, C. R., & Jamieson, S. S. R. (2016). Pan-ice-sheet glacier terminus change in East Antarctica reveals sensitivity of Wilkes Land to sea-ice changes. *Science Advances*, *2*(5), 7. https://doi.org/10.1126/sciadv.1501350

Miles, B. W. J., Stokes, C. R., & Jamieson, S. S. R. (2018). Velocity increases at Cook Glacier, East Antarctica, linked to ice shelf loss and a subglacial flood event. *The Cryosphere*, *12*(10), 3123–3136. https://doi.org/10.5194/tc-12-3123-2018

Millan, R., Rignot, E., Bernier, V., Morlighem, M., & Dutrieux, P. (2017). Bathymetry of the Amundsen Sea Embayment sector of West Antarctica from Operation IceBridge gravity and other data. *Geophysical Research Letters*, *44*, 1360–1368. https://doi.org/10.1002/2016GL072071

Miller, K. G., Wright, J. D., Browning, J. V., Kulpecz, A., Kominz, M., Naish, T. R., et al. (2012). High tide of the warm pliocene: Implications of global sea level for Antarctic deglaciation. *Geology*, *40*(5), 407–410. https://doi.org/10.1130/G32869.1

Milne, G. A., Davis, J. L., Mitrovica, J. X., Scherneck, H. G., Johansson, J. M., Vermeer, M., & Koivula, H. (2001). Space-geodetic constraints on glacial isostatic adjustment in Fennoscandia. *Science*, *291*(5512), 2381–2385.

Minzoni, R. T., Majewski, W., Anderson, J. B., Yokoyama, Y., Fernandez, R., & Jakobsson, M. (2017). Oceanographic influences on the stability of the Cosgrove Ice Shelf, Antarctica. *The Holocene*, *27*(11), 1645–1658. https://doi.org/10.1177/0959683617702226

Mitrovica, J. X., Gomez, N., Morrow, E., Hay, C., Latychev, K., & Tamisiea, M. E. (2011). On the robustness of predictions of sea level fingerprints. *Geophysical Journal International*, *187*(2), 729–742. https://doi.org/10.1111/j.1365-246X.2011.05090.x

Mitrovica, J. X., Hay, C. C., Kopp, R. E., Harig, C., & Latychev, K. (2017). Quantifying the Sensitivity of Sea Level Change in Coastal Localities to the Geometry of Polar Ice Mass Flux. *Journal of Climate*, *31*(9), 3701–3709. https://doi.org/10.1175/JCLI-D-17-0465.1

Mitrovica, J. X., Latychev, K., Tamisiea, M., & Schubert, G. (2009). Time variable gravity: Glacial isostatic adjustment. In T. A. Herring (Ed.), *Geodesy* (pp. 197–212). Amsterdam: Elsevier.

Mitrovica, J. X., Tamisiea, M. E., Davis, J. L., & Milne, G. A. (2001). Recent mass balance of polar ice sheets inferred from patterns of global sea-level change. *Nature*, *409*(6823), 1026–1029. https://doi.org/10.1038/35059054

Mitrovica, J. X., Wahr, J., Matsuyama, I., Paulson, A., & Tamisiea, M. E. (2006). Reanalysis of ancient eclipse, astronomic and geodetic data: A possible route to resolving the enigma of global sea-level rise. *Earth and Planetary Science Letters*, *243*(3–4), 390–399. https://doi.org/10.1016/j.epsl.2005.12.029

Moffat, C., Owens, B., & Beardsley, R. C. (2009). On the characteristics of Circumpolar Deep Water intrusions to the west Antarctic Peninsula Continental Shelf. *Journal of Geophysical Research*, *114*, C05017. https://doi.org/10.1029/2008JC004955

Mondal, M., Gayen, B., Griffiths, R. W., & Kerr, R. C. (2019). Ablation of sloping ice faces into polar seawater. *Journal of Fluid Mechanics*, *863*, 545–571. https://doi.org/10.1017/jfm.2018.970

Morlighem, M., Rignot, E., Binder, T., Blankenship, D., Drews, R., Eagles, G., et al. (2020). Deep glacial troughs and stabilizing ridges unveiled beneath the margins of the Antarctic ice sheet. *Nature Geoscience*, *13*(2), 132–137. https://doi.org/10.1038/s41561-019-0510-8

Morlighem, M., Rignot, E., Seroussi, H., Larour, E., Ben Dhia, H., & Aubry, D. (2010). Spatial patterns of basal drag inferred using control methods from a full-Stokes and simpler models for Pine Island Glacier, West Antarctica. *Geophysical Research Letters*, *37*, L14502. https://doi.org/10.1029/2010GL043853

Morlighem, M., Seroussi, H., Larour, E., & Rignot, E. (2013). Inversion of basal friction in Antarctica using exact and incomplete adjoints of a higher-order model. *Journal of Geophysical Research: Earth Surface*, *118*, 1746–1753. https://doi.org/10.1002/jgrf.20125

Morrison, A. K., England, M. H., & Hogg, A. M. C. (2015). Response of southern ocean convection and abyssal overturning to surface buoyancy perturbations. *Journal of Climate*, *28*(10), 4263–4278. https://doi.org/10.1175/JCLI-D-14-00110.1

Mouginot, J., Rignot, E., & Scheuchl, B. (2014). Sustained increase in ice discharge from the Amundsen Sea Embayment, West Antarctica, from 1973 to 2013. *Geophysical Research Letters*, *41*, 1576–1584. https://doi.org/10.1002/2013GL059069

Mueller, R. D., Padman, L., Dinniman, M. S., Erofeeva, S. Y., Fricker, H. A., & King, M. A. (2012). Impact of tide-topography interactions on basal melting of Larsen C Ice Shelf, Antarctica. *Journal of Geophysical Research*, *117*, C05005. https://doi.org/10.1029/2011JC007263

Muto, A., Peters, L. E., Gohl, K., Sasgen, I., Alley, R. B., Anandakrishnan, S., & Riverman, K. L. (2016). Subglacial bathymetry and sediment distribution beneath Pine Island Glacier ice shelf modeled using aerogravity and in situ geophysical data: New results. *Earth and Planetary Science Letters*, *433*, 63–75. https://doi.org/10.1016/j.epsl.2015.10.037

Naish, T., Powell, R., Levy, R., Wilson, G., Scherer, R., Talarico, F., et al. (2009). Obliquity-paced Pliocene West Antarctic ice sheet oscillations. *Nature*, *458*(7236), 322–328. https://doi.org/10.1038/nature07867

Nakayama, Y., Manucharyan, G., Zhang, H., Dutrieux, P., Torres, H. S., Klein, P., et al. (2019). Pathways of ocean heat towards Pine Island and Thwaites grounding lines. *Scientific Reports*, *9*(1), 16649. https://doi.org/10.1038/s41598-019-53190-6

Nakayama, Y., Schröder, M., & Hellmer, H. H. (2013). From circumpolar deep water to the glacial meltwater plume on the eastern Amundsen Shelf. *Deep-Sea Research Part I: Oceanographic Research Papers*, *77*, 50–62. https://doi.org/10.1016/j.dsr.2013.04.001

Nakayama, Y., Timmermann, R., Schröder, M., & Hellmer, H. H. (2014). On the difficulty of modeling Circumpolar Deep Water intrusions onto the Amundsen Sea continental shelf. *Ocean Modelling*, *84*, 26–34. https://doi.org/10.1016/j.ocemod.2014.09.007

Naveira Garabato, A. C., Forryan, A., Dutrieux, P., Brannigan, L., Biddle, L. C., Heywood, K. J., et al. (2017). Vigorous lateral export of the meltwater outflow from beneath an Antarctic ice shelf. *Nature*, *542*(7640), 219–222. https://doi.org/10.1038/nature20825

NEEM Community Members, N. community (2013). Eemian interglacial reconstructed from a Greenland folded ice core. *Nature*, *493*(7433), 489–494. https://doi.org/10.1038/nature11789

Nerlich, R., Clark, S. R., & Bunge, H. P. (2013). The Scotia Sea gateway: No outlet for Pacific mantle. *Tectonophysics*, *604*(Supplement C), 41–50. https://doi.org/10.1016/j.tecto.2012.08.023

Nicholls, K. W., & Østerhus, S. (2004). Interannual variability and ventilation timescales in the ocean cavity beneath Filchner-Ronne Ice Shelf, Antarctica. *Journal of Geophysical Research*, *109*, C04014. https://doi.org/10.1029/2003JC002149

Nicholls, K. W., Østerhus, S., Makinson, K., Gammelsrød, T., & Fahrbach, E. (2009). Ice-ocean processes over the continental shelf of the Southern Weddell Sea, Antarctica: A review. *Reviews of Geophysics*, *47*, RG3003. https://doi.org/10.1029/2007RG000250

Nichols, K. A., Goehring, B. M., Balco, G., Johnson, J. S., Hein, A. S., & Todd, C. (2019). New Last Glacial Maximum ice thickness constraints for the Weddell Sea Embayment. *Antarctica. Cryosphere*, *13*(11), 2935–2951. https://doi.org/10.5194/tc-13-2935-2019

Nicolas, J. P., Vogelmann, A. M., Scott, R. C., Wilson, A. B., Cadeddu, M. P., Bromwich, D. H., et al. (2017). January 2016 extensive summer melt in West Antarctica favoured by strong El Niño. *Nature Communications*, *8*(1), 15799. https://doi.org/10.1038/ncomms15799

Nield, G. A., Barletta, V. R., Bordoni, A., King, M. A., Whitehouse, P. L., Clarke, P. J., et al. (2014). Rapid bedrock uplift in the Antarctic Peninsula explained by viscoelastic response to recent ice unloading. *Earth and Planetary Science Letters*, *397*, 32–41. https://doi.org/10.1016/j.epsl.2014.04.019

Nield, G. A., Whitehouse, P. L., King, M. A., & Clarke, P. J. (2016). Glacial isostatic adjustment in response to changing Late Holocene behaviour of ice streams on the Siple Coast, West Antarctica. *Geophysical Journal International*, *205*(1), 1–21. https://doi.org/10.1093/gji/ggv532

Nield, G. A., Whitehouse, P. L., van der Wal, W., Blank, B., O'Donnell, J. P., & Stuart, G. W. (2018). The impact of lateral variations in lithospheric thickness on glacial isostatic adjustment in West Antarctica. *Geophysical Journal International*, *214*(2), 811–824. https://doi.org/10.1093/gji/ggy158

Ninnemann, U. S., Charles, C. D., & Hodell, D. A. (1999). In P. U. Clark, R. S. Webb, L. D. Keigwin (Eds.), *Mechanisms of global climate change at millennial time scales, Geophysical Monograph Series* (Vol. 112, pp. 99–112). Washington, DC: American Geophysical Union.

Nitsche, F. O., Jacobs, S. S., Larter, R. D., & Gohl, K. (2007). Bathymetry of the Amundsen Sea continental shelf: Implications for geology, oceanography, and glaciology. *Geochemistry, Geophysics, Geosystems*, *8*, Q10009. https://doi.org/10.1029/2007GC001694

Nitsche, F. O., Porter, D., Williams, G., Cougnon, E. A., Fraser, A. D., Correia, R., & Guerrero, R. (2017). Bathymetric control of warm ocean water access along the East Antarctic Margin. *Geophysical Research Letters*, *44*, 8936–8944. https://doi.org/10.1002/2017GL074433

North Greenland Ice Core Project members (2004). High-resolution record of Northern Hemisphere climate extending into the last interglacial period. *Nature*, *431*, 147–151. https://doi.org/10.1038/nature02805

Nowicki, S., & Seroussi, H. (2018). Projections of future sea level contributions from the greenland and antarctic ice sheets: Challenges beyond dynamical ice sheet modeling. *Oceanography*, *31*(2) Special Issue, 109–117. https://doi.org/10.5670/oceanog.2018.216

Nye, J. F. (1953). The flow law of ice from measurements in glacier tunnels, laboratory experiments and the Jungfraufirn borehole experiment. *Proceedings of the Royal Society of London. Series A. Mathematical and Physical Sciences*, *219*(1193), 477–489.

Nye, J. F. (1976). Water flow in glaciers: Jökulhlaups, tunnels and veins. *Journal of Glaciology*, *17*(76), 181–207. https://doi.org/10.1017/S002214300001354X

Ó Cofaigh, C., Davies, B. J., Livingstone, S. J., Smith, J. A., Johnson, J. S., Hocking, E. P., et al. (2014). Reconstruction of ice-sheet changes in the Antarctic Peninsula since the Last Glacial Maximum. *Quaternary Science Reviews*, *100*, 87–110. https://doi.org/10.1016/j.quascirev.2014.06.023

Ó Cofaigh, C., Dowdeswell, J. A., Evans, J., & Larter, R. D. (2008). Geological constraints on Antarctic palaeo-ice-stream retreat. *Earth Surface Processes and Landforms*, *33*(4), 513–525. https://doi.org/10.1002/esp.1669

Ó Cofaigh, C., Larter, R. D., Dowdeswell, J. A., Hillenbrand, C.-D., Pudsey, C. J., Evans, J., & Morris, P. (2005). Flow of the West Antarctic Ice Sheet on the continental margin of the Bellingshausen Sea at the Last Glacial Maximum. *Journal of Geophysical Research*, *110*, B11103. https://doi.org/10.1029/2005JB003619

Ó Cofaigh, C., Livingstone, S. J., & Dowdeswell, J. A. (2016). Mega-scale glacial lineations in Marguerite Trough, Antarctic Peninsula. *Geological Society Memoir*, *46*(1), 175–176. https://doi.org/10.1144/M46.72

O'Donnell, J. P., Selway, K., Nyblade, A. A., Brazier, R. A., Wiens, D. A., Anandakrishnan, S., et al. (2017). The uppermost mantle seismic velocity and viscosity structure of central West Antarctica. *Earth and Planetary Science Letters*, *472*, 38–49. https://doi.org/10.1016/j.epsl.2017.05.016

O'Kane, T. J., Matear, R. J., Chamberlain, M. A., Risbey, J. S., Sloyan, B. M., & Horenko, I. (2013). Decadal variability in an OGCM Southern Ocean: Intrinsic modes, forced modes and metastable states. *Ocean Modelling*, *69*, 1–21. https://doi.org/10.1016/J.OCEMOD.2013.04.009

O'Leary, M. J., Hearty, P. J., Thompson, W. G., Raymo, M. E., Mitrovica, J. X., & Webster, J. M. (2013). Ice sheet collapse following a prolonged period of stable sea level during the last interglacial. *Nature Geoscience*, *6*(9), 796–800. https://doi.org/10.1038/ngeo1890

Olson, S. L., & Hearty, P. J. (2009). A sustained +21 m sea-level highstand during MIS 11 (400 ka): Direct fossil and sedimentary evidence from Bermuda. *Quaternary Science Reviews*, *28*(3–4), 271–285. https://doi.org/10.1016/j.quascirev.2008.11.001

Oppenheimer, M., Glavovic, B., Hinkel, J., van de Wal, R., Magnan, A. K., Abd-Elgawad, A., et al. (2019). Sea level rise and implications for low lying islands, coasts and communities. *IPCC Special Report on the Ocean and Cryosphere in a Changing Climate*, *355*(6321), 126–129. https://doi.org/10.1126/science.aam6284

Orsi, A. H., Johnson, G. C., & Bullister, J. L. (1999). Circulation, mixing, and production of Antarctic Bottom Water. *Progress in Oceanography*, *43*(1), 55–109. https://doi.org/10.1016/S0079-6611(99)00004-X

Orszag-Sperber, F., Plaziat, J. C., Baltzer, F., & Purser, B. H. (2001). Gypsum salina-coral reef relationships during the Last Interglacial (Marine Isotopic Stage 5e) on the Egyptian Red Sea coast: A Quarternary analogue for Neogene marginal evaporites? *Sedimentary Geology*, *140*(1–2), 61–85. https://doi.org/10.1016/S0037-0738(00)00172-X

Otto-Bliesner, B. L., Rosenbloom, N., Stone, E. J., McKay, N. P., Lunt, D. J., Brady, E. C., & Overpeck, J. T. (2013). How warm was the last interglacial? New model-data comparisons. *Philosophical Transactions of the Royal Society A: Mathematical, Physical and Engineering Sciences*, *371*(2001), 20130097. https://doi.org/10.1098/rsta.2013.0097

Padman, L., Siegfried, M. R., & Fricker, H. A. (2018). Ocean tide influences on the Antarctic and Greenland ice sheets. *Reviews of Geophysics*, *56*, 142–184. https://doi.org/10.1002/2016RG000546

Pagani, M., Liu, Z., LaRiviere, J., & Ravelo, A. C. (2010). High Earth-system climate sensitivity determined from Pliocene carbon dioxide concentrations. *Nature Geoscience*, *3*(1), 27–30. https://doi.org/10.1038/ngeo724

Paillard, D., & Parrenin, F. (2004). The Antarctic ice sheet and the triggering of deglaciations. *Earth and Planetary Science Letters*, *227*(3–4), 263–271. https://doi.org/10.1016/j.epsl.2004.08.023

Paolo, F. S., Fricker, H. A., & Padman, L. (2015). Volume loss from Antarctic ice shelves is accelerating. *Science*, *348*(6232), 327–331. https://doi.org/10.1126/science.aaa0940

Paolo, F. S., Padman, L., Fricker, H. A., Adusumilli, S., Howard, S., & Siegfried, M. R. (2018). Response of Pacific-sector Antarctic ice shelves to the El Niño/Southern Oscillation. *Nature Geoscience*, *11*(2), 121–126. https://doi.org/10.1038/s41561-017-0033-0

Parizek, B. R., Christianson, K., Alley, R. B., Voytenko, D., Vaňková, I., Dixon, T. H., et al. (2019). Ice-cliff failure via retrogressive slumping. *Geology*, *47*(5), 449–452. https://doi.org/10.1130/G45880.1

Parizek, B. R., Christianson, K., Anandakrishnan, S., Alley, R. B., Walker, R. T., Edwards, R. A., et al. (2013). Dynamic (in)stability of Thwaites Glacier, West Antarctica. *Journal of Geophysical Research: Earth Surface*, *118*, 638–655. https://doi.org/10.1002/jgrf.20044

Parrenin, F., Cavitte, M. G. P., Blankenship, D. D., Chappellaz, J., Fischer, H., Gagliardini, O., et al. (2017). Is there 1.5 million-year old ice near Dome C, Antarctica? *The Cryosphere Discuss*, *2017*, 1–16. https://doi.org/10.5194/tc-2017-69

Patterson, M. O., McKay, R., Naish, T., Escutia, C., Jimenez-Espejo, F. J., & Raymo, M. E. (2014). Orbital forcing of the East Antarctic ice sheet during the Pliocene and Early Pleistocene. *Nature Geoscience*, *7*(11), 841–847. https://doi.org/10.1038/ngeo2273

Patton, H., Swift, D. A., Clark, C. D., Livingstone, S. J., & Cook, S. J. (2016). Distribution and characteristics of overdeepenings beneath the Greenland and Antarctic ice sheets: Implications for overdeepening origin and evolution. *Quaternary Science Reviews*, *148*, 128–145. https://doi.org/10.1016/j.quascirev.2016.07.012

Pattyn, F. (2010). Antarctic subglacial conditions inferred from a hybrid ice sheet/ice stream model. *Earth and Planetary Science Letters*, *295*(3–4), 451–461. https://doi.org/10.1016/j.epsl.2010.04.025

Pattyn, F. (2018). The paradigm shift in Antarctic ice sheet modelling. *Nature Communications*, *9*(1), 2728. https://doi.org/10.1038/s41467-018-05003-z

Pattyn, F., Favier, L., Sun, S., & Durand, G. (2017). Progress in numerical modeling of Antarctic ice-sheet dynamics. *Current Climate Change Reports*, *3*(3), 174–184. https://doi.org/10.1007/s40641-017-0069-7

Pattyn, F., Ritz, C., Hanna, E., Asay-Davis, X., DeConto, R., Durand, G., et al. (2018). The Greenland and Antarctic ice sheets under 1.5°C global warming. *Nature Climate Change*, *8*(12), 1053–1061. https://doi.org/10.1038/s41558-018-0305-8

Pauling, A. G., Bitz, C. M., Smith, I. J., & Langhorne, P. J. (2016). The response of the Southern Ocean and Antarctic sea ice to freshwater from ice shelves in an Earth system model. *Journal of Climate*, *29*(5), 1655–1672. https://doi.org/10.1175/JCLI-D-15-0501.1

Paxman, G. J. G., Jamieson, S. S. R., Ferraccioli, F., & Bentley, M. J. (2018). Bedrock erosion surfaces record former East Antarctic ice sheet extent. *Geophysical Research Letters*, *45*, 4114–4123. https://doi.org/10.1029/2018GL077268

Paxman, G. J. G., Jamieson, S. S. R., Hochmuth, K., Gohl, K., Bentley, M. J., Leitchenkov, G., & Ferraccioli, F. (2019). Reconstructions of Antarctic topography since the Eocene-Oligocene boundary. *Palaeogeography, Palaeoclimatology, Palaeoecology*, *535*(August), 109346. https://doi.org/10.1016/j.palaeo.2019.109346

Paxman, G. J. G., Watts, A. B., Ferraccioli, F., Jordan, T. A., Bell, R. E., Jamieson, S. S. R., & Finn, C. A. (2016). Erosion-driven uplift in the Gamburtsev Subglacial Mountains of East Antarctica. *Earth and Planetary Science Letters*, *452*, 1–14. https://doi.org/10.1016/j.epsl.2016.07.040

Payne, A. J., Vieli, A., Shepherd, A. P., Wingham, D. J., & Rignot, E. (2004). Recent dramatic thinning of largest West Antarctic ice stream triggered by oceans. *Geophysical Research Letters*, *31*, L23401. https://doi.org/10.1029/2004GL021284

Peck, V. L., Allen, C. S., Kender, S., McClymont, E. L., & Hodgson, D. A. (2015). Oceanographic variability on the West Antarctic Peninsula during the Holocene and the influence of upper circumpolar deep water. *Quaternary Science Reviews*, *119*, 54–65. https://doi.org/10.1016/J.QUASCIREV.2015.04.002

Pedro, J. B., Bostock, H. C., Bitz, C. M., He, F., Vandergoes, M. J., Steig, E. J., et al. (2016). The spatial extent and dynamics of the Antarctic Cold Reversal. *Nature Geoscience*, *9*(1), 51–55. https://doi.org/10.1038/ngeo2580

Pedro, J. B., Jochum, M., Buizert, C., He, F., Barker, S., & Rasmussen, S. O. (2018). Beyond the bipolar seesaw: Toward a process understanding of interhemispheric coupling. *Quaternary Science Reviews*, *192*, 27–46. https://doi.org/10.1016/J.QUASCIREV.2018.05.005

Pelle, T., Morlighem, M., & Bondzio, J. H. (2019). Brief communication: PICOP, a new ocean melt parameterization under ice shelves combining PICO and a plume model. *The Cryosphere*, *13*(3), 1043–1049. https://doi.org/10.5194/tc-13-1043-2019

Peltier, W. R. (2004). Global glacial isostasy and the surface of the ice-age Earth: The ICE-5G (VM2) model and GRACE. *Annual Review of Earth and Planetary Sciences*, *32*, 111–149. https://doi.org/10.1146/annurev.earth.32.082503.144359

Peltier, W. R., & Fairbanks, R. G. (2006). Global glacial ice volume and Last Glacial Maximum duration from an extended Barbados sea level record. *Quaternary Science Reviews*. https://doi.org/10.1016/j.quascirev.2006.04.010

Person, M., Bense, V., Cohen, D., & Banerjee, A. (2012). Models of ice-sheet hydrogeologic interactions: A review. *Geofluids*. https://doi.org/10.1111/j.1468-8123.2011.00360.x

Person, M., McIntosh, J., Bense, V., & Remenda, V. H. (2007). Pleistocene hydrology of North America: The role of ice sheets in reorganizing groundwater flow systems. *Reviews of Geophysics*, *45*, RG3007. https://doi.org/10.1029/2006rg000206

Petit, J. R., Jouzel, J., Raynaud, D., Barkov, N. I., Barnola, J. M., Basile, I., et al. (1999). Climate and atmospheric history of the past 420,000 years from the Vostok ice core, Antarctica. *Nature*, *399*(6735), 429–436. https://doi.org/10.1038/20859

Pettit, E. C., Thorsteinsson, T., Jacobson, H. F., & Waddington, E. D. (2007). The role of crystal fabric in flow near an ice divide. *Journal of Glaciology*, *53*(181), 277–288. https://doi.org/10.3189/172756507782202766

Petty, A. A., Feltham, D. L., & Holland, P. R. (2013). Impact of atmospheric forcing on Antarctic continental shelf water masses. *Journal of Physical Oceanography*, *43*(5), 920–940. https://doi.org/10.1175/JPO-D-12-0172.1

Petty, A. A., Holland, P. R., & Feltham, D. L. (2014). Sea ice and the ocean mixed layer over the Antarctic shelf seas. *The Cryosphere*, *8*(2), 761–783. https://doi.org/10.5194/tc-8-761-2014

Phillips, G., & Läufer, A. L. (2009). Brittle deformation relating to the Carboniferous-Cretaceous evolution of the Lambert Graben, East Antarctica: A precursor for Cenozoic relief development in an intraplate and glaciated region. *Tectonophysics*, *471*(3–4), 216–224. https://doi.org/10.1016/J.TECTO.2009.02.012

Phillips, H. A. (1998). Surface meltstreams on the Amery Ice Shelf, East Antarctica. *Annals of Glaciology*, *27*, 177–181. https://doi.org/10.3198/1998AoG27-1-177-181

Phipps, S. J., Fogwill, C. J., & Turney, C. S. M. (2016). Impacts of marine instability across the East Antarctic Ice Sheet on Southern Ocean dynamics. *The Cryosphere*, *10*(5), 2317–2328. https://doi.org/10.5194/tc-10-2317-2016

Picard, G., Domine, F., Krinner, G., Arnaud, L., & Lefebvre, E. (2012). Inhibition of the positive snow-albedo feedback by precipitation in interior Antarctica. *Nature Climate Change*, *2*(11), 795–798. https://doi.org/10.1038/nclimate1590

Picotti, S., Vuan, A., Carcione, J. M., Horgan, H. J., & Anandakrishnan, S. (2015). Anisotropy and crystalline fabric of Whillans Ice Stream (West Antarctica) inferred from multicomponent seismic data. *Journal of Geophysical Research: Solid Earth*, *120*, 4237–4262. https://doi.org/10.1002/2014JB011591

Placidi, L., Greve, R., Seddik, H., & Faria, S. H. (2010). Continuum-mechanical, anisotropic flow model, for polar ice masses, based on an anisotropic flow enhancement factor. *Continuum Mechanics and Thermodynamics*, *22*, 221–237. https://doi.org/10.1007/s00161-009-0126-0

Pollard, D., Chang, W., Haran, M., Applegate, P., & DeConto, R. (2016). Large ensemble modeling of the last deglacial retreat of the West Antarctic Ice Sheet: Comparison of simple and advanced statistical techniques. *Geoscientific Model Development*, *9*(5), 1697–1723. https://doi.org/10.5194/gmd-9-1697-2016

Pollard, D., & DeConto, R. M. (2009). Modelling West Antarctic ice sheet growth and collapse through the past five million years. *Nature*, *458*(7236), 329–332. https://doi.org/10.1038/nature07809

Pollard, D., & Deconto, R. M. (2012). Description of a hybrid ice sheet-shelf model, and application to Antarctica. *Geoscientific Model Development*, *5*(5), 1273–1295. https://doi.org/10.5194/gmd-5-1273-2012

Pollard, D., & DeConto, R. M. (2019). Continuous simulations over the last 40 million years with a coupled Antarctic ice sheet-sediment model. *Palaeogeography, Palaeoclimatology, Palaeoecology*, *537*(October 2019), 109374. https://doi.org/10.1016/J.PALAEO.2019.109374

Pollard, D., DeConto, R. M., & Alley, R. B. (2015). Potential Antarctic Ice Sheet retreat driven by hydrofracturing and ice cliff failure. *Earth and Planetary Science Letters*, *412*, 112–121. https://doi.org/10.1016/j.epsl.2014.12.035

Pollard, D., Gomez, N., & DeConto, R. M. (2017). Variations of the Antarctic Ice Sheet in a coupled ice sheet-Earth-sea level model: Sensitivity to viscoelastic Earth properties. *Journal of Geophysical Research: Earth Surface*, *122*, 2124–2138. https://doi.org/10.1002/2017JF004371

Powell, E., Gomez, N., Hay, C., Latychev, K., & Mitrovica, J. X. (2019). Viscous effects in the solid Earth response to modern Antarctic ice mass flux: Implications for geodetic studies of WAIS stability in a warming world. *Journal of Climate*, *33*(2), 443–459. https://doi.org/10.1175/JCLI-D-19-0479.1

Price, P. B., Nagornov, O. V., Bay, R., Chirkin, D., He, Y., Miocinovic, P., et al. (2002). Temperature profile for glacial ice at the South Pole: Implications for life in a nearby subglacial lake. *Proceedings of the National Academy of Sciences.*, *99*(12), 7844–7847. https://doi.org/10.1073/pnas.082238999

Pritchard, H. D., Arthern, R. J., Vaughan, D. G., & Edwards, L. A. (2009). Extensive dynamic thinning on the margins of the Greenland and Antarctic ice sheets: Supplemental. *Nature*, *461*(7266), 971–975. https://doi.org/10.1038/nature08471

Pritchard, H. D., Ligtenberg, S. R. M., Fricker, H. a., Vaughan, D. G., van den Broeke, M. R., & Padman, L. (2012). Antarctic ice-sheet loss driven by basal melting of ice shelves. *Nature*, *484*(7395), 502–505. https://doi.org/10.1038/nature10968

Pritchard, H. D., & Vaughan, D. G. (2007). Widespread acceleration of tidewater glaciers on the Antarctic Peninsula. *Journal of Geophysical Research*, *112*, F03S29. https://doi.org/10.1029/2006JF000597

Prothro, L. O., Majewski, W., Yokoyama, Y., Simkins, L. M., Anderson, J. B., Yamane, M., et al. (2020). Timing and pathways of East Antarctic Ice Sheet retreat. *Quaternary Science Reviews*, *230*, 106166. https://doi.org/10.1016/j.quascirev.2020.106166

Rack, W., & Rott, H. (2004). Pattern of retreat and disintegration of the Larsen B ice shelf, Antarctic Peninsula. *Annals of Glaciology*, *39*, 505–510. https://doi.org/10.3189/172756404781814005

Raphael, M. N. (2004). A zonal wave 3 index for the Southern Hemisphere. *Geophysical Research Letters*, *31*, L23212. https://doi.org/10.1029/2004GL020365

Raymo, M. E., & Mitrovica, J. X. (2012). Collapse of polar ice sheets during the stage 11 interglacial. *Nature*, *483*(7390), 453–456. https://doi.org/10.1038/nature10891

Raymo, M. E., Mitrovica, J. X., O'Leary, M. J., DeConto, R. M., & Hearty, P. J. (2011). Departures from eustasy in Pliocene sea-level records. *Nature Geoscience*, *4*(5), 328–332. https://doi.org/10.1038/ngeo1118

Reese, R., Albrecht, T., Mengel, M., Asay-Davis, X., & Winkelmann, R. (2018). Antarctic sub-shelf melt rates via PICO. *The Cryosphere*, *12*(6), 1969–1985. https://doi.org/10.5194/tc-12-1969-2018

Reese, R., Gudmundsson, G. H., Levermann, A., & Winkelmann, R. (2018). The far reach of ice-shelf thinning in Antarctica. *Nature Climate Change*, *8*(1), 53–57. https://doi.org/10.1038/s41558-017-0020-x

Richardson, G., Wadley, M. R., Heywood, K. J., Stevens, D. P., & Banks, H. T. (2005). Short-term climate response to a freshwater pulse in the Southern Ocean. *Geophysical Research Letters*, *32*, L03702. https://doi.org/10.1029/2004GL021586

Richter, A., Horwath, M., & Dietrich, R. (2016). Comment on Zwally and others (2015)—Mass gains of the Antarctic ice sheet exceed losses. *Journal of Glaciology*, *62*(233), 604–606. https://doi.org/10.1017/jog.2016.60

Rignot, E., Bamber, J. L., Van Den Broeke, M. R., Davis, C., Li, Y., Van De Berg, W. J., & Van Meijgaard, E. (2008). Recent Antarctic ice mass loss from radar interferometry and regional climate modelling. *Nature Geoscience*, *1*(2), 106–110. https://doi.org/10.1038/ngeo102

Rignot, E., Casassa, G., Gogineni, P., Krabill, W., Rivera, A., & Thomas, R. (2004). Accelerated ice discharge from the Antarctic Peninsula following the collapse of Larsen B ice shelf. *Geophysical Research Letters*, *31*, L18401. https://doi.org/10.1029/2004GL020697

Rignot, E., Jacobs, S., Mouginot, J., & Scheuchl, B. (2013). Ice-shelf melting around Antarctica. *Science*, *341*(6143), 266–270. https://doi.org/10.1126/science.1235798

Rignot, E., & Jacobs, S. S. (2002). Rapid bottom melting widespread near antarctic ice sheet grounding lines. *Science*, *296*(5575), 2020–2023. https://doi.org/10.1126/science.1070942

Rignot, E., Mouginot, J., Morlighem, M., Seroussi, H., & Scheuchl, B. (2014). Widespread, rapid grounding line retreat of Pine Island, Thwaites, Smith, and Kohler glaciers, West Antarctica, from 1992 to 2011. *Geophysical Research Letters*, *41*, 3502–3509. https://doi.org/10.1002/2014GL060140

Rignot, E., Mouginot, J., Scheuchl, B., van den Broeke, M., van Wessem, M. J., & Morlighem, M. (2019). Four decades of Antarctic Ice Sheet mass balance from 1979-2017. *Proceedings of the National Academy of Sciences of the United States of America*, *116*(4), 1095–1103. https://doi.org/10.1073/pnas.1812883116

Rintoul, S. R. (2018). The global influence of localized dynamics in the Southern Ocean. *Nature*, *558*(7709), 209–218. https://doi.org/10.1038/s41586-018-0182-3

Rintoul, S. R., Chown, S. L., DeConto, R. M., England, M. H., Fricker, H. A., Masson-Delmotte, V., et al. (2018). Erratum to: Choosing the future of Antarctica Nature, (2018), 558, 7709, (233-241), 10.1038/s41586-018-0173-4). *Nature*, *562*(7726), E5. https://doi.org/10.1038/s41586-018-0369-7

Rintoul, S. R., Silvano, A., Pena-Molino, B., Van Wijk, E., Rosenberg, M., Greenbaum, J. S., & Blankenship, D. D. (2016). Ocean heat drives rapid basal melt of the totten ice shelf. *Science Advances*, *2*(12), e1601610. https://doi.org/10.1126/sciadv.1601610

Rippin, D. M., Vaughan, D. G., & Corr, H. F. J. (2011). The basal roughness of Pine Island Glacier, West Antarctica. *Journal of Glaciology*, *57*(201), 67–76. https://doi.org/10.3189/002214311795306574

Ritz, C., Edwards, T. L., Durand, G., Payne, A. J., Peyaud, V., & Hindmarsh, R. C. A. (2015). Potential sea-level rise from Antarctic ice-sheet instability constrained by observations. *Nature*, *528*(7580), 115–118. https://doi.org/10.1038/nature16147

Riva, R. E. M., Gunter, B. C., Urban, T. J., Vermeersen, B. L. A., Lindenbergh, R. C., Helsen, M. M., et al. (2009). Glacial isostatic adjustment over Antarctica from combined ICESat and GRACE satellite data. *Earth and Planetary Science Letters*, *288*(3–4), 516–523. https://doi.org/10.1016/j.epsl.2009.10.013

Robel, A. A., & Banwell, A. F. (2019). A speed limit on ice shelf collapse through hydrofracture. *Geophysical Research Letters*, *46*, 12,092–12,100. https://doi.org/10.1029/2019GL084397

Robel, A. A., Schoof, C., & Tziperman, E. (2016). Persistence and variability of ice-stream grounding lines on retrograde bed slopes. *The Cryosphere*, *10*(4), 1883–1896. https://doi.org/10.5194/tc-10-1883-2016

Roberts, J., Galton-Fenzi, B. K., Paolo, F. S., Donnelly, C., Gwyther, D. E., Padman, L., et al. (2018). Ocean forced variability of Totten Glacier mass loss. *Geological Society Special Publication*, *461*(1), 175–186. https://doi.org/10.1144/SP461.6

Roberts, S. J., Hodgson, D. A., Sterken, M., Whitehouse, P. L., Verleyen, E., Vyverman, W., et al. (2011). Geological constraints on glacio-isostatic adjustment models of relative sea-level change during deglaciation of Prince Gustav Channel, Antarctic Peninsula. *Quaternary Science Reviews*, *30*(25–26), 3603–3617. https://doi.org/10.1016/j.quascirev.2011.09.009

Robinson, N. J., Stevens, C. L., & McPhee, M. G. (2017). Observations of amplified roughness from crystal accretion in the sub-ice ocean boundary layer. *Geophysical Research Letters*, *44*, 1814–1822. https://doi.org/10.1002/2016GL071491

Roemmich, D., Church, J., Gilson, J., Monselesan, D., Sutton, P., & Wijffels, S. (2015). Unabated planetary warming and its ocean structure since 2006. *Nature Climate Change*, *5*(3), 240–245. https://doi.org/10.1038/nclimate2513

Rohling, E. J., Grant, K., Bolshaw, M., Roberts, A. P., Siddall, M., Hemleben, C., & Kucera, M. (2009). Antarctic temperature and global sea level closely coupled over the past five glacial cycles. *Nature Geoscience*, *2*(7), 500–504. https://doi.org/10.1038/ngeo557

Rohling, E. J., Grant, K., Hemleben, C., Siddall, M., Hoogakker, B. A. A., Bolshaw, M., & Kucera, M. (2008). High rates of sea-level rise during the last interglacial period. *Nature Geoscience*, *1*(1), 38–42. https://doi.org/10.1038/ngeo.2007.28

Rohling, E. J., Haigh, I. D., Foster, G. L., Roberts, A. P., & Grant, K. M. (2013). A geological perspective on potential future sea-level rise. *Scientific Reports*, *3*(1), 3461. https://doi.org/10.1038/srep03461

Rohling, E. J., Hibbert, F. D., Grant, K. M., Galaasen, E. V., Irvalı, N., Kleiven, H. F., et al. (2019). Asynchronous Antarctic and Greenland ice-volume contributions to the last interglacial sea-level highstand. *Nature Communications*, *10*(1), 5040. https://doi.org/10.1038/s41467-019-12874-3

Rohling, E. J., Hibbert, F. D., Williams, F. H., Grant, K. M., Marino, G., Foster, G. L., et al. (2017). Differences between the last two glacial maxima and implications for ice-sheet, $\delta^{18}O$, and sea-level reconstructions. *Quaternary Science Reviews*, *176*, 1–28. https://doi.org/10.1016/j.quascirev.2017.09.009

Rohling, E. J., Marsh, R., Wells, N. C., Siddall, M., & Edwards, N. R. (2004). Similar meltwater contributions to glacial sea level changes from Antarctic and northern ice sheets. *Nature*, *430*(7003), 1016–1021. https://doi.org/10.1038/nature02859

Rose, K. C., Ferraccioli, F., Jamieson, S. S. R., Bell, R. E., Corr, H., Creyts, T. T., et al. (2013). Early East Antarctic Ice Sheet growth recorded in the landscape of the Gamburtsev Subglacial Mountains. *Earth and Planetary Science Letters*, *375*, 1–12. https://doi.org/10.1016/j.epsl.2013.03.053

Rosier, S. H. R., Hofstede, C., Brisbourne, A. M., Hattermann, T., Nicholls, K. W., Davis, P. E. D., et al. (2018). A new bathymetry for the southeastern Filchner-Ronne Ice Shelf: Implications for modern oceanographic processes and glacial history. *Journal of Geophysical Research: Oceans*, *123*, 4610–4623. https://doi.org/10.1029/2018JC013982

Röthlisberger, H. (1972). Water pressure in intra- and subglacial channels. *Journal of Glaciology*, *11*(62), 177–203. https://doi.org/10.1017/S0022143000022188

Rott, H., Skvarca, P., & Nagler, T. (1996). Rapid collapse of Northern Larsen Ice Shelf, Antarctica. *Science*, *271*(5250), 788–792. https://doi.org/10.1126/science.271.5250.788

Rovere, A., Raymo, M. E., Mitrovica, J. X., Hearty, P. J., O'Leary, M. J., & Inglis, J. D. (2014). The Mid-Pliocene sea-level conundrum: Glacial isostasy, eustasy and dynamic topography. *Earth and Planetary Science Letters*, *387*, 27–33. https://doi.org/10.1016/j.epsl.2013.10.030

Rowley, D. B., Forte, A. M., Moucha, R., Mitrovica, J. X., Simmons, N. A., & Grand, S. P. (2013). Dynamic topography change of the Eastern United States since 3 million years ago. *Science*, *340*(6140), 1560–1563. https://doi.org/10.1126/science.1229180

Salamatin, A. N., Lipenkov, V. Y., Barkov, N. I., Jouzel, J., Petit, J. R., & Raynaud, D. (1998). Ice core age dating and paleothermometer calibration based on isotope and temperature profiles from deep boreholes at Vostok Station (East Antarctica). *Journal of Geophysical Research*, *103*(D8), 8963–8977. https://doi.org/10.1029/97jd02253

Santoso, A., & England, M. H. (2008). Antarctic Bottom Water variability in a coupled climate model. *Journal of Physical Oceanography*, *38*(9), 1870–1893. https://doi.org/10.1175/2008JPO3741.1

Sasgen, I., Martín-Español, A., Horvath, A., Klemann, V., Petrie, E. J., Wouters, B., et al. (2017). Joint inversion estimate of regional glacial isostatic adjustment in Antarctica considering a lateral varying Earth structure (ESA STSE Project REGINA). *Geophysical Journal International*, *211*(3), 1534–1553. https://doi.org/10.1093/gji/ggx368

Scambos, T., & Shuman, C. (2016). Comment on "Mass gains of the Antarctic ice sheet exceed losses" by H. J. Zwally and others. *Journal of Glaciology*, *62*(233), 599–603. https://doi.org/10.1017/jog.2016.59

Scambos, T. A., Bohlander, J. A., Shuman, C. A., & Skvarca, P. (2004). Glacier acceleration and thinning after ice shelf collapse in the Larsen B embayment, Antarctica. *Geophysical Research Letters*, *31*, L18402. https://doi.org/10.1029/2004GL020670

Scambos, T. A., Hulbe, C., Fahnestock, M., & Bohlander, J. (2000). The link between climate warming and break-up of ice shelves in the Antarctic Peninsula. *Journal of Glaciology*, *46*(154), 516–530. https://doi.org/10.3189/172756500781833043

Scherer, R. P., Aldahan, A., Tulaczyk, S., Possnert, G., Engelhardt, H., & Kamb, B. (1998). Pleistocene collapse of the West Antarctic Ice Sheet. *Science*, *281*(5373), 82–85. https://doi.org/10.1126/science.281.5373.82

Scherer, R. P., Bohaty, S. M., Dunbar, R. B., Esper, O., Flores, J.-A., Gersonde, R., et al. (2008). Antarctic records of precession-paced insolation-driven warming during early Pleistocene Marine Isotope Stage 31. *Geophysical Research Letters*, *35*, L03505. https://doi.org/10.1029/2007GL032254

Scherer, R. P., DeConto, R. M., Pollard, D., & Alley, R. B. (2016). Windblown Pliocene diatoms and East Antarctic Ice Sheet retreat. *Nature Communications*, *7*(1), 12957. https://doi.org/10.1038/ncomms12957

Schlegel, N.-J., Seroussi, H., Schodlok, M. P., Larour, E. Y., Boening, C., Limonadi, D., et al. (2018). Exploration of Antarctic Ice Sheet 100-year contribution to sea level rise and associated model uncertainties using the ISSM framework. *The Cryosphere*, *12*(11), 3511–3534. https://doi.org/10.5194/tc-12-3511-2018

Schmeltz, M., Rignot, E., & MacAyeal, D. R. (2001). Ephemeral grounding as a signal of ice-shelf change. *Journal of Glaciology*, *47*(156), 71–77. https://doi.org/10.3189/172756501781832502

Schmidtko, S., Heywood, K. J., Thompson, A. F., & Aoki, S. (2014). Multidecadal warming of Antarctic waters. *Science*, *346*(6214), 1227–1231. https://doi.org/10.1126/science.1256117

Schmitt, J., Schneider, R., Elsig, J., Leuenberger, D., Lourantou, A., Chappellaz, J., et al. (2012). Carbon isotope constraints on the deglacial CO_2 rise from ice cores. *Science*, *336*(6082), 711–714. https://doi.org/10.1126/science.1217161

Schneider, D. P., & Steig, E. J. (2008). Ice cores record significant 1940s Antarctic warmth related to tropical climate variability. *Proceedings of the National Academy of Sciences of the United States of America*, *105*(34), 12,154–12,158. https://doi.org/10.1073/pnas.0803627105

Schneider Mor, A., Yam, R., Bianchi, C., Kunz-Pirrung, M., Gersonde, R., & Shemesh, A. (2012). Variable sequence of events during the past seven terminations in two deep-sea cores from the Southern Ocean. *Quaternary Research*, *77*(2), 317–325. https://doi.org/10.1016/j.yqres.2011.11.006

Schoof, C. (2005). The effect of cavitation on glacier sliding. *Proceedings of the Royal Society A: Mathematical, Physical and Engineering Sciences*, *461*(2055), 609–627. https://doi.org/10.1098/rspa.2004.1350

Schoof, C. (2007). Ice sheet grounding line dynamics: Steady states, stability, and hysteresis. *Journal of Geophysical Research*, *112*, F03S28. https://doi.org/10.1029/2006jf000664

Schoof, C. (2011). Marine ice sheet dynamics. Part 2. A Stokes flow contact problem. *Journal of Fluid Mechanics*, *679*, 122–155. https://doi.org/10.1017/jfm.2011.129

Schroeder, D. M., Blankenship, D. D., & Young, D. A. (2013). Evidence for a water system transition beneath Thwaites Glacier, West Antarctica. *Proceedings of the National Academy of Sciences*, *110*(30), 12,225–12,228. https://doi.org/10.1073/pnas.1302828110

Schroeder, D. M., Blankenship, D. D., Young, D. A., & Quartini, E. (2014). Evidence for elevated and spatially variable geothermal flux beneath the West Antarctic Ice Sheet. *Proceedings of the National Academy of Sciences*, *111*(25), 9070–9072. https://doi.org/10.1073/pnas.1405184111

Seddik, H., Greve, R., Zwinger, T., & Sugiyama, S. (2017). Regional modeling of the Shirase drainage basin, East Antarctica: Full Stokes vs. shallow ice dynamics. *The Cryosphere*, *11*(5), 2213–2229. https://doi.org/10.5194/tc-11-2213-2017

Seki, O., Foster, G. L., Schmidt, D. N., Mackensen, A., Kawamura, K., & Pancost, R. D. (2010). Alkenone and boron-based Pliocene pCO_2 records. *Earth and Planetary Science Letters*, *292*(1–2), 201–211. https://doi.org/10.1016/j.epsl.2010.01.037

Seroussi, H., & Morlighem, M. (2018). Representation of basal melting at the grounding line in ice flow models. *The Cryosphere*, *12*(10), 3085–3096. https://doi.org/10.5194/tc-12-3085-2018

Seroussi, H., Morlighem, M., Larour, E., Rignot, E., & Khazendar, A. (2014). Hydrostatic grounding line parameterization in ice sheet models. *The Cryosphere*, *8*(6), 2075–2087. https://doi.org/10.5194/tc-8-2075-2014

Seroussi, H., Nakayama, Y., Larour, E., Menemenlis, D., Morlighem, M., Rignot, E., & Khazendar, A. (2017). Continued retreat of Thwaites Glacier, West Antarctica, controlled by bed topography and ocean circulation. *Geophysical Research Letters*, *44*, 6191–6199. https://doi.org/10.1002/2017GL072910

Shapiro, N. M., & Ritzwoller, M. H. (2004). Inferring surface heat flux distributions guided by a global seismic model: Particular application to Antarctica. *Earth and Planetary Science Letters*, *223*(1–2), 213–224. https://doi.org/10.1016/j.epsl.2004.04.011

Shen, Q., Wang, H., Shum, C. K., Jiang, L., Hsu, H. T., & Dong, J. (2018). Recent high-resolution Antarctic ice velocity maps reveal increased mass loss in Wilkes Land, East Antarctica. *Scientific Reports*, *8*(1), 4477. https://doi.org/10.1038/s41598-018-22765-0

Shepherd, A., Gilbert, L., Muir, A. S., Konrad, H., McMillan, M., Slater, T., et al. (2019). Trends in Antarctic ice sheet elevation and mass. *Geophysical Research Letters*, *46*, 8174–8183. https://doi.org/10.1029/2019GL082182

Shepherd, A., Ivins, E. R., A, G., Barletta, V. R., Bentley, M. J., Bettadpur, S., et al. (2012). A reconciled estimate of ice-sheet mass balance. *Science*, *338*(6111), 1183–1189. https://doi.org/10.1126/science.1228102

Shtarkman, Y. M., Koçer, Z. A., Edgar, R., Veerapaneni, R. S., D'Elia, T., Morris, P. F., & Rogers, S. O. (2013). Subglacial Lake Vostok (Antarctica) accretion ice contains a diverse set of sequences from aquatic, marine and sediment-inhabiting bacteria and eukarya. *PLoS ONE*, *8*(7), e67221. https://doi.org/10.1371/journal.pone.0067221

Siddall, M., Rohling, E. J., Almogi-Labin, A., Hemleben, C., Meischner, D., Schmelzer, I., & Smeed, D. A. (2003). Sea-level fluctuations during the last glacial cycle. *Nature*, *423*(6942), 853–858. https://doi.org/10.1038/nature01690

Siegert, M., Ross, N., Corr, H., Kingslake, J., & Hindmarsh, R. (2013). Late Holocene ice-flow reconfiguration in the Weddell Sea sector of West Antarctica. *Quaternary Science Reviews*, *78*, 98–107. https://doi.org/10.1016/j.quascirev.2013.08.003

Siegert, M. J., Ellis-Evans, J. C., Tranter, M., Mayer, C., Petit, J. R., Salamatin, A., & Priscu, J. C. (2001). Physical, chemical and biological processes in Lake Vostok and other Antarctic subglacial lakes. *Nature*, *414*(6864), 603–609. https://doi.org/10.1038/414603a

Siegert, M. J., Kingslake, J., Ross, N., Whitehouse, P. L., Woodward, J., Jamieson, S. S. R., et al. (2019). Major ice sheet change in the Weddell Sea sector of West Antarctica over the last 5,000 years. *Reviews of Geophysics*, *57*, 1197–1223. https://doi.org/10.1029/2019RG000651

Siegert, M. J., Kulessa, B., Bougamont, M., Christoffersen, P., Key, K., Andersen, K. R., et al. (2017). Antarctic subglacial groundwater: A concept paper on its measurement and potential influence on ice flow. *Geological Society, London, Special Publications*, *461*(1), 197–213. https://doi.org/10.1144/SP461.8

Siegert, M. J., Priscu, J. C., Alekhina, I. A., Wadham, J. L., & Lyons, W. B. (2016). Antarctic subglacial lake exploration: First results and future plans. *Philosophical Transactions of the Royal Society A: Mathematical, Physical and Engineering Sciences*, *374*(2059), 20140466. https://doi.org/10.1098/rsta.2014.0466

Siegert, M. J., Taylor, J., & Payne, A. J. (2005). Spectral roughness of subglacial topography and implications for former ice-sheet dynamics in East Antarctica. *Global and Planetary Change*, *45*, 249–263. https://doi.org/10.1016/j.gloplacha.2004.09.008

Siegfried, M. R., Fricker, H. A., Roberts, M., Scambos, T. A., & Tulaczyk, S. (2014). A decade of West Antarctic subglacial lake interactions from combined ICESat and CryoSat-2 altimetry. *Geophysical Research Letters*, *41*, 891–898. https://doi.org/10.1002/2013gl058616

Silvano, A., Rintoul, S. R., Peña-Molino, B., Hobbs, W. R., Van Wijk, E., Aoki, S., et al. (2018). Freshening by glacial meltwater enhances melting of ice shelves and reduces formation of Antarctic Bottom Water. *Science Advances*, *4*(4), eaap9467. https://doi.org/10.1126/sciadv.aap9467

Silvano, A., Rintoul, S. R., Peña-Molino, B., & Williams, G. D. (2017). Distribution of water masses and meltwater on the continental shelf near the Totten and Moscow University ice shelves. *Journal of Geophysical Research: Oceans*, *122*, 2050–2068. https://doi.org/10.1002/2016JC012115

Simkins, L. M., Anderson, J. B., Greenwood, S. L., Gonnermann, H. M., Prothro, L. O., Halberstadt, A. R. W., et al. (2017). Anatomy of a meltwater drainage system beneath the ancestral East Antarctic ice sheet. *Nature Geoscience*, *10*(9), 691–697. https://doi.org/10.1038/ngeo3012

Simms, A. R., Whitehouse, P. L., Simkins, L. M., Nield, G., DeWitt, R., & Bentley, M. J. (2018). Late Holocene relative sea levels near Palmer Station, northern Antarctic Peninsula, strongly controlled by late Holocene ice-mass changes. *Quaternary Science Reviews*, *199*, 49–59. https://doi.org/10.1016/J.QUASCIREV.2018.09.017

Slater, D. A., Goldberg, D. N., Nienow, P. W., & Cowton, T. R. (2016). Scalings for submarine melting at tidewater glaciers from buoyant plume theory. *Journal of Physical Oceanography*, *46*(6), 1839–1855. https://doi.org/10.1175/JPO-D-15-0132.1

Slangen, A. B. A., Adloff, F., Jevrejeva, S., Leclercq, P. W., Marzeion, B., Wada, Y., & Winkelmann, R. (2017). A review of recent updates of sea-level projections at global and regional scales. *Surveys in Geophysics*, *38*(1), 385–406. https://doi.org/10.1007/s10712-016-9374-2

Small, D., Bentley, M. J., Jones, R. S., Pittard, M. L., & Whitehouse, P. L. (2019). Antarctic ice sheet palaeo-thinning rates from vertical transects of cosmogenic exposure ages. *Quaternary Science Reviews*, *206*, 65–80. https://doi.org/10.1016/J.QUASCIREV.2018.12.024

Smith, A. M., Bentley, C. R., Bingham, R. G., & Jordan, T. A. (2012). Rapid subglacial erosion beneath Pine Island Glacier, West Antarctica. *Geophysical Research Letters*, *39*, L12501. https://doi.org/10.1029/2012gl051651

Smith, A. M., & Murray, T. (2009). Bedform topography and basal conditions beneath a fast-flowing West Antarctic ice stream. *Quaternary Science Reviews*, *28*(7–8), 584–596. https://doi.org/10.1016/j.quascirev.2008.05.010

Smith, A. M., Murray, T., Nicholls, K. W., Makinson, K., Adalgeirsdóttir, G., Behar, A. E., & Vaughan, D. G. (2007). Rapid erosion, drumlin formation, and changing hydrology beneath an Antarctic ice stream. *Geology*, *35*(2), 127–130. https://doi.org/10.1130/G23036A.1

Smith, A. M., Woodward, J., Ross, N., Bentley, M. J., Hodgson, D. A., Siegert, M. J., & King, E. C. (2018). Evidence for the long-term sedimentary environment in an Antarctic subglacial lake. *Earth and Planetary Science Letters*, *504*, 139–151. https://doi.org/10.1016/j.epsl.2018.10.011

Smith, B. E., A, H., F., Joughin, I. R., & Tulaczyk, S. (2009). An inventory of active subglacial lakes in Antarctica detected by ICESat (2003–2008). *Journal of Glaciology*, *55*(192), 573–595.

Smith, B. E., Gourmelen, N., Huth, A., & Joughin, I. (2017). Connected subglacial lake drainage beneath Thwaites Glacier, West Antarctica. *The Cryosphere*, *11*(1), 451–467. https://doi.org/10.5194/tc-11-451-2017

Smith, D. A., Hofmann, E. E., Klinck, J. M., & Lascara, C. M. (1999). Hydrography and circulation of the West Antarctic Peninsula Continental Shelf. *Deep-Sea Research Part I: Oceanographic Research Papers*, *46*(6), 925–949. https://doi.org/10.1016/S0967-0637(98)00103-4

Smith, E. C., Baird, A. F., Kendall, J. M., Martín, C., White, R. S., Brisbourne, A. M., & Smith, A. M. (2017). Ice fabric in an Antarctic ice stream interpreted from seismic anisotropy. *Geophysical Research Letters*, *44*, 3710–3718. https://doi.org/10.1002/2016GL072093

Smith, J. A., Andersen, T. J., Shortt, M., Gaffney, A. M., Truffer, M., Stanton, T. P., et al. (2017). Sub-ice-shelf sediments record history of twentieth-century retreat of Pine Island Glacier. *Nature*, *541*(7635), 77–80. https://doi.org/10.1038/nature20136

Smith, J. A., Graham, A. G. C., Post, A. L., Hillenbrand, C. D., Bart, P. J., & Powell, R. D. (2019). The marine geological imprint of Antarctic ice shelves. *Nature Communications. NLM (Medline)*, *10*, 5635. https://doi.org/10.1038/s41467-019-13496-5

Smith, J. A., Hillenbrand, C. D., Kuhn, G., Klages, J. P., Graham, A. G. C., Larter, R. D., et al. (2014). New constraints on the timing of West Antarctic Ice Sheet retreat in the eastern Amundsen Sea since the Last Glacial Maximum. *Global and Planetary Change*, *122*, 224–237. https://doi.org/10.1016/j.gloplacha.2014.07.015

Smith, K. L., & Polvani, L. M. (2017). Spatial patterns of recent Antarctic surface temperature trends and the importance of natural variability: Lessons from multiple reconstructions and the CMIP5 models. *Climate Dynamics*, *48*(7–8), 2653–2670. https://doi.org/10.1007/s00382-016-3230-4

Snow, K., Goldberg, D. N., Holland, P. R., Jordan, J. R., Arthern, R. J., & Jenkins, A. (2017). The response of ice sheets to climate variability. *Geophysical Research Letters*, *44*, 11,878–11,885. https://doi.org/10.1002/2017GL075745

Snow, K., Hogg, A. M., Sloyan, B. M., & Downes, S. M. (2016). Sensitivity of Antarctic Bottom Water to changes in surface buoyancy fluxes. *Journal of Climate*, *29*(1), 313–330. https://doi.org/10.1175/JCLI-D-15-0467.1

Snow, K., Sloyan, B. M., Rintoul, S. R., Hogg, A. M. C., & Downes, S. M. (2016). Controls on circulation, cross-shelf exchange, and dense water formation in an Antarctic polynya. *Geophysical Research Letters*, *43*, 7089–7096. https://doi.org/10.1002/2016GL069479

Spasojevic, S., & Gurnis, M. (2012). Sea level and vertical motion of continents from dynamic Earth models since the late cretaceous. *AAPG Bulletin*, *96*(11), 2037–2064. https://doi.org/10.1306/03261211121

Spasojevic, S., Gurnis, M., & Sutherland, R. (2010). Inferring mantle properties with an evolving dynamic model of the Antarctica-New Zealand region from the Late Cretaceous. *Journal of Geophysical Research*, *115*, B05402. https://doi.org/10.1029/2009JB006612

Spector, P., Stone, J., Cowdery, S. G., Hall, B., Conway, H., & Bromley, G. (2017). Rapid early-Holocene deglaciation in the Ross Sea, Antarctica. *Geophysical Research Letters*, *44*, 7817–7825. https://doi.org/10.1002/2017GL074216

Spence, P., Griffies, S. M., England, M. H., Hogg, A. M. C., Saenko, O. A., & Jourdain, N. C. (2014). Rapid subsurface warming and circulation changes of Antarctic coastal waters by poleward shifting winds. *Geophysical Research Letters*, *41*, 4601–4610. https://doi.org/10.1002/2014GL060613

Spence, P., Holmes, R. M., Hogg, A. M. C., Griffies, S. M., Stewart, K. D., & England, M. H. (2017). Localized rapid warming of West Antarctic subsurface waters by remote winds. *Nature Climate Change*, *7*(8), 595–603. https://doi.org/10.1038/NCLIMATE3335

Sprenk, D., Weber, M. E., Kuhn, G., Rosén, P., Frank, M., Molina-Kescher, M., et al. (2013). Southern Ocean bioproductivity during the last glacial cycle—New detection method and decadal-scale insight from the Scotia Sea. *Geological Society, London, Special Publications*, *381*, 245–261. https://doi.org/10.1144/SP381.17

Stanford, J. D., Hemingway, R., Rohling, E. J., Challenor, P. G., Medina-Elizalde, M., & Lester, A. J. (2011). Sea-level probability for the last deglaciation: A statistical analysis of far-field records. *Global and Planetary Change*, *79*(3–4), 193–203. https://doi.org/10.1016/j.gloplacha.2010.11.002

Stanton, T. P., Shaw, W. J., Truffer, M., Corr, H. F. J., Peters, L. E., Riverman, K. L., et al. (2013). Channelized ice melting in the ocean boundary layer beneath Pine Island Glacier, Antarctica. *Science*, *341*(6151), 1236–1239. https://doi.org/10.1126/science.1239373

Stearns, L. A., Smith, B. E., & Hamilton, G. S. (2008). Increased flow speed on a large east antarctic outlet glacier caused by subglacial floods. *Nature Geoscience. Nature Publishing Group*, *1*(12), 827–831. https://doi.org/10.1038/ngeo356

Steig, E. J., Ding, Q., White, J. W. C., Küttel, M., Rupper, S. B., Neumann, T. A., et al. (2013). Recent climate and ice-sheet changes in West Antarctica compared with the past 2,000 years. *Nature Geoscience*, *6*(5), 372–375. https://doi.org/10.1038/ngeo1778

Steinberger, B. (2007). Effects of latent heat release at phase boundaries on flow in the Earth's mantle, phase boundary topography and dynamic topography at the Earth's surface. *Physics of the Earth and Planetary Interiors*, *164*(1–2), 2–20. https://doi.org/10.1016/j.pepi.2007.04.021

Steinemann, S. (1954). Results of preliminary experiments on the plasticity of ice crystals. *Journal of Glaciology*, *2*(16), 404–416. https://doi.org/10.3189/002214354793702533

Steinemann, S. (1958). Rèsultats expèrimentaux sur la dynamique de la glace et leurs corrèlations avec le mouvement et la pètrographie des glaciers. *International association of scientific hydrology*, *47*, 184–198.

Stern, A. A., Adcroft, A., Sergienko, O., & Marques, G. (2017). Modeling tabular icebergs submerged in the ocean. *Journal of Advances in Modeling Earth Systems*, *9*(4), 1948–1972. https://doi.org/10.1002/2017MS001002

Stevenson, S., Fox-Kemper, B., Jochum, M., Rajagopalan, B., & Yeager, S. G. (2010). ENSO Model validation using wavelet probability analysis. *Journal of Climate*, *23*(20), 5540–5547. https://doi.org/10.1175/2010JCLI3609.1

Stewart, A. L., Klocker, A., & Menemenlis, D. (2018). Circum-Antarctic shoreward heat transport derived from an eddy- and tide-resolving simulation. *Geophysical Research Letters*, *45*, 834–845. https://doi.org/10.1002/2017GL075677

Stewart, A. L., & Thompson, A. F. (2013). Connecting Antarctic cross-slope exchange with Southern Ocean overturning. *Journal of Physical Oceanography*, *43*(7), 1453–1471. https://doi.org/10.1175/JPO-D-12-0205.1

Stewart, A. L., & Thompson, A. F. (2015). Eddy-mediated transport of warm Circumpolar Deep Water across the Antarctic Shelf Break. *Geophysical Research Letters*, *42*, 432–440. https://doi.org/10.1002/2014GL062281

St-Laurent, P., Klinck, J. M., & Dinniman, M. S. (2013). On the role of coastal troughs in the circulation of warm circumpolar deep water on Antarctic shelves. *Journal of Physical Oceanography*, *43*(1), 51–64. https://doi.org/10.1175/JPO-D-11-0237.1

St-Laurent, P., Klinck, J. M., & Dinniman, M. S. (2015). Impact of local winter cooling on the melt of Pine Island Glacier, Antarctica. *Journal of Geophysical Research: Oceans*, *120*, 6718–6732. https://doi.org/10.1002/2015JC010709

Stokes, C. R., Sanderson, J. E., Miles, B. W. J., Jamieson, S. S. R., & Leeson, A. A. (2019). Widespread distribution of supraglacial lakes around the margin of the East Antarctic Ice Sheet. *Scientific Reports*, *9*(1), 1–14. https://doi.org/10.1038/s41598-019-50343-5

Stone, J. O., Balco, G. A., Sugden, D. E., Caffee, M. W., Sass, L. C., Cowdery, S. G., & Siddoway, C. (2003). Holocene deglaciation of Marie Byrd Land, West Antarctica. *Science*, *299*(5603), 99–102. https://doi.org/10.1126/science.1077998

Stouffer, R. J., Seidov, D., & Haupt, B. J. (2007). Climate response to external sources of freshwater: North Atlantic versus the Southern Ocean. *Journal of Climate*, *20*(3), 436–448. https://doi.org/10.1175/JCLI4015.1

Sugden, D., & Denton, G. (2004). Cenozoic landscape evolution of the Convoy Range to Mackay Glacier area, Transantartic Mountains: Onshore to offshore synthesis. *Bulletin of the Geological Society of America*, *116*(7), 840–857. https://doi.org/10.1130/B25356.1

Sugden, D. E., Denton, G. H., & Marchant, D. R. (1995). Landscape evolution of the Dry Valleys, Transantarctic Mountains: Tectonic implications. *Journal of Geophysical Research*, *100*(B6), 9949–9967. https://doi.org/10.1029/94JB02895

Sugden, D. E., Hein, A. S., Woodward, J., Marrero, S. M., Rodés, Á., Dunning, S. A., et al. (2017). The million-year evolution of the glacial trimline in the southernmost. *Earth and Planetary Science Letters*, *469*, 42–52. https://doi.org/10.1016/j.epsl.2017.04.006

Sugden, D. E., & Jamieson, S. S. R. (2018). The pre-glacial landscape of Antarctica. *Scottish Geographical Journal*, *134*(3–4), 203–223. https://doi.org/10.1080/14702541.2018.1535090

Sugden, D. E., Marchant, D. R., & Denton, G. H. (1993). The case for a stable East Antarctic ice sheet. *Geografiska Annaler, Series A*, *75 A*(4), 151–154.

Sun, S., Cornford, S. L., Liu, Y., & Moore, J. C. (2014). Dynamic response of Antarctic ice shelves to bedrock uncertainty. *The Cryosphere*, *8*(4), 1561–1576. https://doi.org/10.5194/tc-8-1561-2014

Swart, N. C., Gille, S. T., Fyfe, J. C., & Gillett, N. P. (2018). Recent Southern Ocean warming and freshening driven by greenhouse gas emissions and ozone depletion. *Nature Geoscience*, *11*(11), 836–841. https://doi.org/10.1038/s41561-018-0226-1

Swingedouw, D., Fichefet, T., Goosse, H., & Loutre, M. F. (2009). Impact of transient freshwater releases in the Southern Ocean on the AMOC and climate. *Climate Dynamics*, *33*(2–3), 365–381. https://doi.org/10.1007/s00382-008-0496-1

Talpe, M. J., Nerem, R. S., Forootan, E., Schmidt, M., Lemoine, F. G., Enderlin, E. M., & Landerer, F. W. (2017). Ice mass change in Greenland and Antarctica between 1993 and 2013 from satellite gravity measurements. *Journal of Geodesy*, *91*(11), 1283–1298. https://doi.org/10.1007/s00190-017-1025-y

Tamisiea, M. E., Hughes, C. W., Williams, S. D. P., & Bingley, R. M. (2014). Sea level: Measuring the bounding surfaces of the ocean. *Philosophical Transactions of the Royal Society A: Mathematical, Physical and Engineering Sciences*, *372*(2025), 20130336. https://doi.org/10.1098/rsta.2013.0336

Tamura, T., Ohshima, K. I., Fraser, A. D., & Williams, G. D. (2016). Sea ice production variability in Antarctic coastal polynyas. *Journal of Geophysical Research: Oceans*, *121*, 2967–2979. https://doi.org/10.1002/2015JC011537

Tapley, B. D., Bettadpur, S., Watkins, M., & Reigber, C. (2004). The Gravity Recovery and Climate Experiment: Mission overview and early results. *Geophysical Research Letters*, *31*, L09607. https://doi.org/10.1029/2004GL019920

Tedesco, M., & Monaghan, A. J. (2009). An updated Antarctic melt record through 2009 and its linkages to high-latitude and tropical climate variability. *Geophysical Research Letters*, *36*, L18502. https://doi.org/10.1029/2009GL039186

The IMBIE Team, Shepherd, A., Ivins, E., Rignot, E., Smith, B., Van Den Broeke, M., et al. (2018). Mass balance of the Antarctic Ice Sheet from 1992 to 2017. *Nature*, *558*(7709), 219–222. https://doi.org/10.1038/s41586-018-0179-y

The RAISED Consortium, Bentley, M. J., Ó Cofaigh, C., Anderson, J. B., Conway, H., Davies, B., et al. (2014). A community-based geological reconstruction of Antarctic Ice Sheet deglaciation since the Last Glacial Maximum. *Quaternary Science Reviews*, *100*, 1–9. https://doi.org/10.1016/j.quascirev.2014.06.025

Thoma, M., Determann, J., Grosfeld, K., Goeller, S., & Hellmer, H. H. (2015). Future sea-level rise due to projected ocean warming beneath the Filchner Ronne Ice Shelf: A coupled model study. *Earth and Planetary Science Letters*, *431*, 217–224. https://doi.org/10.1016/j.epsl.2015.09.013

Thoma, M., Jenkins, A., Holland, D., & Jacobs, S. (2008). Modelling Circumpolar Deep Water intrusions on the Amundsen Sea continental shelf, Antarctica. *Geophysical Research Letters*, *35*, L18602. https://doi.org/10.1029/2008GL034939

Thomas, I. D., King, M. A., Bentley, M. J., Whitehouse, P. L., Penna, N. T., Williams, S. D. P., et al. (2011). Widespread low rates of Antarctic glacial isostatic adjustment revealed by GPS observations. *Geophysical Research Letters*, *38*, L22302. https://doi.org/10.1029/2011GL049277

Thomas, R. H. (1979). The dynamics of marine ice sheets. *Journal of Glaciology*, *24*(90), 167–177. https://doi.org/10.1017/S0022143000014726

Thomas, R. H., & Bentley, C. R. (1978). A model for Holocene retreat of the West Antarctic Ice Sheet. *Quaternary Research*, *10*(2), 150–170. https://doi.org/10.1016/0033-5894(78)90098-4

Thompson, A. F., Stewart, A. L., Spence, P., & Heywood, K. J. (2018). The Antarctic slope current in a changing climate. *Reviews of Geophysics*, *56*, 741–770. https://doi.org/10.1029/2018RG000624

Thompson, D. W. J., Wallace, J. M., Thompson, D. W. J., & Wallace, J. M. (2000). Annular modes in the extratropical circulation. Part I: Month-to-month variability*. *Journal of Climate*, *13*(5), 1000–1016. https://doi.org/10.1175/1520-0442(2000)013<1000:AMITEC>2.0.CO;2

Thompson, W. G., Allen Curran, H., Wilson, M. A., & White, B. (2011). Sea-level oscillations during the last interglacial highstand recorded by Bahamas corals. *Nature Geoscience*, *4*(10), 684–687. https://doi.org/10.1038/ngeo1253

Thomson, S. N., Reiners, P. W., Hemming, S. R., & Gehrels, G. E. (2013). The contribution of glacial erosion to shaping the hidden landscape of East Antarctica. *Nature Geoscience*, *6*(3), 203–207. https://doi.org/10.1038/ngeo1722

Thorsteinsson, T. (2002). Fabric development with nearest-neighbour interaction and dynamic recrystallization. *Journal of Geophysical Research*, *107*(B1), 2014. https://doi.org/10.1029/2001JB000244

Thurnherr, A. M., Jacobs, S. S., Dutrieux, P., & Giulivi, C. F. (2014). Export and circulation of ice cavity water in Pine Island Bay, West Antarctica. *Journal of Geophysical Research: Oceans*, *119*, 1754–1764. https://doi.org/10.1002/2013JC009307

Timmermann, R., le Brocq, A., Deen, T., Domack, E., Dutrieux, P., Galton-Fenzi, B., et al. (2010). A consistent data set of Antarctic ice sheet topography, cavity geometry, and global bathymetry. *Earth System Science Data*, *2*(2), 261–273. https://doi.org/10.5194/essd-2-261-2010

Todd, C., Stone, J., Conway, H., Hall, B., & Bromley, G. (2010). Late Quaternary evolution of Reedy Glacier, Antarctica. *Quaternary Science Reviews*, *29*(11–12), 1328–1341. https://doi.org/10.1016/j.quascirev.2010.02.001

Toggweiler, J. R., Russell, J. L., & Carson, S. R. (2006). Midlatitude westerlies, atmospheric CO_2, and climate change during the ice ages. *Paleoceanography*, *21*, 01154. https://doi.org/10.1029/2005PA001154
Treverrow, A., Budd, W. F., Jacka, T. H., & Warner, R. C. (2012). The tertiary creep of polycrystalline ice: Experimental evidence for stress-dependent levels of strain-rate enhancement. *Journal of Glaciology*, *58*(208), 301–314. https://doi.org/10.3189/2012JoG11J149
Tsai, V. C., Stewart, A. L., & Thompson, A. F. (2015). Marine ice-sheet profiles and stability under Coulomb basal conditions. *Journal of Glaciology*, *61*(226), 205–215. https://doi.org/10.3189/2015JoG14J221
Tuckett, P. A., Ely, J. C., Sole, A. J., Livingstone, S. J., Davison, B. J., Melchior van Wessem, J., & Howard, J. (2019). Rapid accelerations of Antarctic Peninsula outlet glaciers driven by surface melt. *Nature Communications*, *10*(1), 4311. https://doi.org/10.1038/s41467-019-12039-2
Turner, J., Colwell, S. R., Marshall, G. J., Lachlan-Cope, T. A., Carleton, A. M., Jones, P. D., et al. (2005). Antarctic climate change during the last 50 years. *International Journal of Climatology*, *25*(3), 279–294. https://doi.org/10.1002/joc.1130
Turner, J., Lu, H., White, I., King, J. C., Phillips, T., Hosking, J. S., et al. (2016). Absence of 21st century warming on Antarctic Peninsula consistent with natural variability. *Nature*, *535*(7612), 411–415. https://doi.org/10.1038/nature18645
Turner, J., Orr, A., Gudmundsson, G. H., Jenkins, A., Bingham, R. G., Hillenbrand, C. D., & Bracegirdle, T. J. (2017). Atmosphere-ocean-ice interactions in the Amundsen Sea Embayment, West Antarctica. *Reviews of Geophysics*, *55*, 235–276. https://doi.org/10.1002/2016RG000532
Turney, C. S. M., Fogwill, C. J., Golledge, N. R., McKay, N. P., van Sebille, E., Jones, R. T., et al. (2020). Early Last Interglacial ocean warming drove substantial ice mass loss from Antarctica. *Proceedings of the National Academy of Sciences*, *117*(8), 3996–4006. https://doi.org/10.1073/PNAS.1902469117
Turney, C. S. M., & Jones, R. T. (2010). Does the Agulhas Current amplify global temperatures during super-interglacials? *Journal of Quaternary Science*, *25*(6), 839–843. https://doi.org/10.1002/jqs.1423
Turney, C. S. M., Jones, R. T., Phipps, S. J., Thomas, Z., Hogg, A., Kershaw, A. P., et al. (2017). Rapid global ocean-atmosphere response to Southern Ocean freshening during the last glacial. *Nature Communications*, *8*(1), 520–528. https://doi.org/10.1038/s41467-017-00577-6
Valletta, R. D., Willenbring, J. K., Passchier, S., & Elmi, C. (2018). ^{10} Be/^{9} Be ratios reflect Antarctic ice sheet freshwater discharge during Pliocene warming. *Paleoceanography and Paleoclimatology*, *33*, 934–944. https://doi.org/10.1029/2017PA003283
van den Broeke, M. (2005). Strong surface melting preceded collapse of Antarctic Peninsula ice shelf. *Geophysical Research Letters*, *32*, L12815. https://doi.org/10.1029/2005GL023247
van der Wal, W., Whitehouse, P. L., & Schrama, E. J. O. (2015). Effect of GIA models with 3D composite mantle viscosity on GRACE mass balance estimates for Antarctica. *Earth and Planetary Science Letters*, *414*, 134–143. https://doi.org/10.1016/j.epsl.2015.01.001
Van Liefferinge, B., & Pattyn, F. (2013). Using ice-flow models to evaluate potential sites of million year-old ice in Antarctica. *Climate of the Past*, *9*(5), 2335–2345. https://doi.org/10.5194/cp-9-2335-2013
Van Sebille, E., Spence, P., Mazloff, M. R., England, M. H., Rintoul, S. R., & Saenko, O. A. (2013). Abyssal connections of Antarctic Bottom Water in a Southern Ocean State Estimate. *Geophysical Research Letters*, *40*, 2177–2182. https://doi.org/10.1002/grl.50483
Vaughan, D. G. (2006). Recent trends in melting conditions on the Antarctic Peninsula and their implications for ice-sheet mass balance and sea level. *Arctic, Antarctic, and Alpine Research*, *38*(1), 147–152. https://doi.org/10.1657/1523-0430(2006)038[0147:RTIMCO]2.0.CO;2
Vaughan, D. G., & Arthern, R. (2007). Why is it hard to predict the future of ice sheets? *Science*, *315*(5818), 1503–1504. https://doi.org/10.1126/science.1141111
Vaughan, D. G., Barnes, D. K. A., Fretwell, P. T., & Bingham, R. G. (2011). Potential seaways across West Antarctica. *Geochemistry, Geophysics, Geosystems*, *12*, Q10004. https://doi.org/10.1029/2011GC003688
Vaughan, D. G., Corr, H. F. J., Bindschadler, R. A., Dutrieux, P., Gudmundsson, G. H., Jenkins, A., et al. (2012). Subglacial melt channels and fracture in the floating part of Pine Island Glacier, Antarctica. *Journal of Geophysical Research*, *117*, F03012. https://doi.org/10.1029/2012JF002360
van der Veen, C. J. (2007). Fracture propagation as means of rapidly transferring surface meltwater to the base of glaciers. *Geophysical Research Letters*, *34*, L01501. https://doi.org/10.1029/2006GL028385
Velicogna, I., Sutterley, T. C., & Van Den Broeke, M. R. (2014). Regional acceleration in ice mass loss from Greenland and Antarctica using GRACE time-variable gravity data. *Geophysical Research Letters*, *41*, 8130–8137. https://doi.org/10.1002/2014GL061052
Velicogna, I., & Wahr, J. (2006). Measurements of time-variable gravity show mass loss in Antarctica. *Science*, *311*(5768), 1754–1756. https://doi.org/10.1126/science.1123785
Vermeersen, L. L. A., & Schotman, H. H. A. (2009). Constraints on glacial isostatic adjustment from GOCE and sea level data. *Pure and Applied Geophysics*, *166*(8–9), 1261–1281. https://doi.org/10.1007/s00024-004-0503-3
Vernet, M., Geibert, W., Hoppema, M., Brown, P. J., Haas, C., Hellmer, H. H., et al. (2019). The Weddell Gyre, Southern Ocean: Present knowledge and future challenges. *Reviews of Geophysics*, *57*, 623–708. https://doi.org/10.1029/2018RG000604
Villa, G., Persico, D., Wise, S. W., & Gadaleta, A. (2012). Calcareous nannofossil evidence for Marine Isotope Stage 31 (1 Ma) in Core AND-1B, ANDRILL McMurdo Ice Shelf Project (Antarctica). *Global and Planetary Change*, *96–97*, 75–86. https://doi.org/10.1016/j.gloplacha.2009.12.003
Wåhlin, A. K., Kalén, O., Assmann, K. M., Darelius, E., Ha, H. K., Kim, T. W., & Lee, S. H. (2016). Subinertial oscillations on the Amundsen Sea Shelf, Antarctica. *Journal of Physical Oceanography*, *46*(9), 2573–2582. https://doi.org/10.1175/JPO-D-14-0257.1
Waibel, M. S., Hulbe, C. L., Jackson, C. S., & Martin, D. F. (2018). Rate of mass loss across the instability threshold for Thwaites Glacier determines rate of mass loss for entire basin. *Geophysical Research Letters*, *45*, 809–816. https://doi.org/10.1002/2017GL076470
Walker, R. T., Dupont, T. K., Parizek, B. R., & Alley, R. B. (2008). Effects of basal-melting distribution on the retreat of ice-shelf grounding lines. *Geophysical Research Letters*, *35*, L17503. https://doi.org/10.1029/2008GL034947
Wang, B., Sun, B., Martin, C., Ferraccioli, F., Steinhage, D., Cui, X., & Siegert, M. J. (2018). Summit of the East Antarctic Ice Sheet underlain by thick ice-crystal fabric layers linked to glacial–interglacial environmental change. *Geological Society, London, Special Publications*, *461*(1), 131–143. https://doi.org/10.1144/SP461.1
Wang, W., Li, J., & Zwally, H. J. (2012). Dynamic inland propagation of thinning due to ice loss at the margins of the Greenland ice sheet. *Journal of Glaciology*, *58*(210), 734–740. https://doi.org/10.3189/2012JoG11J187
Warrick, R., & Oerlemans, J. (1990). Sea level rise. Climate change: The IPCC scientific assessment.
WCRP Global Sea Level Budget Group (2018). Global sea-level budget 1993–present. *Earth System Science Data*, *10*(3), 1551–1590. https://doi.org/10.5194/essd-10-1551-2018
Webb, P. N., Harwood, D. M., McKelvey, B. C., Mercer, J. H., & Stott, L. D. (1984). Cenozoic marine sedimentation and ice-volume variation on the East Antarctic craton. *Geology*, *12*(5), 287. https://doi.org/10.1130/0091-7613(1984)12<287:CMSAIV>2.0.CO;2

Webber, B. G. M., Heywood, K. J., Stevens, D. P., Dutrieux, P., Abrahamsen, E. P., Jenkins, A., et al. (2017). Mechanisms driving variability in the ocean forcing of Pine Island Glacier. *Nature Communications*, *8*, 14507. https://doi.org/10.1038/ncomms14507
Weber, M. E., Clark, P. U., Kuhn, G., Timmermann, A., Sprenk, D., Gladstone, R., et al. (2014). Millennial-scale variability in Antarctic ice-sheet discharge during the last deglaciation. *Nature*, *510*(7503), 134–138. https://doi.org/10.1038/nature13397
Weber, M. E., Clark, P. U., Ricken, W., Mitrovica, J. X., Hostetler, S. W., & Kuhn, G. (2011). Interhemispheric ice-sheet synchronicity during the Last Glacial Maximum. *Science (New York, N.Y.)*, *334*(6060), 1265–1269. https://doi.org/10.1126/science.1209299
Weber, M. E., Raymo, M. E., Peck, V. L., Williams, T., and the Expedition 382 Scientists (2019). Expedition 382 Preliminary Report: Iceberg alley and subantarctic ice and ocean dynamics. *International Ocean Discovery Program*. https://doi.org/10.14379/iodp.pr.382.2019
Weertman, J. (1957). On the Sliding of Glaciers. *Journal of Glaciology*, *3*(21), 33–38. https://doi.org/10.3189/S0022143000024709
Weertman, J. (1972). General theory of water flow at the base of a glacier or ice sheet. *Reviews of Geophysics*, *10*(1), 287–333. https://doi.org/10.1029/RG010i001p00287
Weertman, J. (1974). Stability of the Junction of an Ice Sheet and an Ice Shelf. *Journal of Glaciology*, *13*(67), 3–11. https://doi.org/10.3189/S0022143000023327
Wells, A. J., & Worster, M. G. (2011). Melting and dissolving of a vertical solid surface with laminar compositional convection. *Journal of Fluid Mechanics*, *687*, 118–140. https://doi.org/10.1017/jfm.2011.322
Werder, M. A., Hewitt, I. J., Schoof, C. G., & Flowers, G. E. (2013). Modeling channelized and distributed subglacial drainage in two dimensions. *Journal of Geophysical Research: Earth Surface*, *118*, 2140–2158. https://doi.org/10.1002/jgrf.20146
Whitehead, J. M., Harwood, D. M., McKelvey, B. C., Hambrey, M. J., & McMinn, A. (2004). Diatom biostratigraphy of the Cenozoic glaciomarine Pagodroma Group, northern Prince Charles Mountains East Antarctica. *Australian Journal of Earth Sciences*, *51*(4), 521–547. https://doi.org/10.1111/j.1400-0952.2004.01072.x
Whitehouse, P. L., Bentley, M. J., & Le Brocq, A. M. (2012). A deglacial model for Antarctica: Geological constraints and glaciological modelling as a basis for a new model of Antarctic glacial isostatic adjustment. *Quaternary Science Reviews*, *32*(Supplement C), 1–24. https://doi.org/10.1016/j.quascirev.2011.11.016
Whitehouse, P. L., Bentley, M. J., Milne, G. A., King, M. A., & Thomas, I. D. (2012). A new glacial isostatic adjustment model for Antarctica: Calibrated and tested using observations of relative sea-level change and present-day uplift rates. *Geophysical Journal International*, *190*(3), 1464–1482. https://doi.org/10.1111/j.1365-246X.2012.05557.x
Whitehouse, P. L., Gomez, N., King, M. A., & Wiens, D. A. (2019). Solid Earth change and the evolution of the Antarctic Ice Sheet. *Nature Communications*, *10*(1), 503. https://doi.org/10.1038/s41467-018-08068-y
Williams, G. D., Herraiz-Borreguero, L., Roquet, F., Tamura, T., Ohshima, K. I., Fukamachi, Y., et al. (2016). The suppression of Antarctic bottom water formation by melting ice shelves in Prydz Bay. *Nature Communications*, *7*(1), 12577. https://doi.org/10.1038/ncomms12577
Williams, T., van de Flierdt, T., Hemming, S. R., Chung, E., Roy, M., & Goldstein, S. L. (2010). Evidence for iceberg armadas from East Antarctica in the Southern Ocean during the late Miocene and early Pliocene. *Earth and Planetary Science Letters*, *290*(3–4), 351–361. https://doi.org/10.1016/j.epsl.2009.12.031
Wilson, D. J., Bertram, R. A., Needham, E. F., van de Flierdt, T., Welsh, K. J., McKay, R. M., et al. (2018). Ice loss from the East Antarctic Ice Sheet during late Pleistocene interglacials. *Nature*, *561*(7723), 383–386. https://doi.org/10.1038/s41586-018-0501-8
Wilson, D. S., Jamieson, S. S. R., Barrett, P. J., Leitchenkov, G., Gohl, K., & Larter, R. D. (2012). Antarctic topography at the Eocene-Oligocene boundary. *Palaeogeography, Palaeoclimatology, Palaeoecology*, *335–336*, 24–34. https://doi.org/10.1016/j.palaeo.2011.05.028
Winkelmann, R., Levermann, A., Ridgwell, A., & Caldeira, K. (2015). Combustion of available fossil fuel resources sufficient to eliminate the Antarctic Ice Sheet. *Science Advances*, *1*(8), e1500589. https://doi.org/10.1126/sciadv.1500589
Winnick, M. J., & Caves, J. K. (2015). Oxygen isotope mass-balance constraints on Pliocene sea level and East Antarctic Ice Sheet stability. *Geology*, *43*(10), 879–882. https://doi.org/10.1130/G36999.1
Wise, M. G., Dowdeswell, J. A., Jakobsson, M., & Larter, R. D. (2017). Evidence of marine ice-cliff instability in Pine Island Bay from iceberg-keel plough marks. *Nature*, *550*(7677), 506–510. https://doi.org/10.1038/nature24458
Wobbe, F., Lindeque, A., & Gohl, K. (2014). Anomalous South Pacific lithosphere dynamics derived from new total sediment thickness estimates off the West Antarctic margin. *Global and Planetary Change*, *123*, 139–149. https://doi.org/10.1016/J.GLOPLACHA.2014.09.006
Wolff, E. W., Fischer, H., Fundel, F., Ruth, U., Twarloh, B., Littot, G. C., et al. (2006). Southern Ocean sea-ice extent, productivity and iron flux over the past eight glacial cycles. *Nature*, *440*(7083), 491–496. https://doi.org/10.1038/nature04614
Wolstencroft, M., King, M. A., Whitehouse, P. L., Bentley, M. J., Nield, G. A., King, E. C., et al. (2015). Uplift rates from a new high-density GPS network in Palmer Land indicate significant late Holocene ice loss in the southwestern Weddell Sea. *Geophysical Journal International*, *203*(1), 737–754. https://doi.org/10.1093/gji/ggv327
Woods, A. W. (1992). Melting and dissolving. *Journal of Fluid Mechanics*, *239*, 429–448. https://doi.org/10.1017/S0022112092004476
Wright, A. P., White, D. A., Gore, D. B., & Siegert, M. J. (2008). Chapter 12 Antarctica at the Last Glacial Maximum, Deglaciation and the Holocene. In F. Florindo & M. Siegert (Eds.), *Developments in Earth and Environmental Sciences* (Vol. 8, pp. 531–570). Elsevier. https://doi.org/10.1016/S1571-9197(08)00012-8
Wright, A. P., Young, D. A., Roberts, J. L., Schroeder, D. M., Bamber, J. L., Dowdeswell, J. A., et al. (2012). Evidence of a hydrological connection between the ice divide and ice sheet margin in the Aurora Subglacial Basin, East Antarctica. *Journal of Geophysical Research*, *117*, F01033. https://doi.org/10.1029/2011JF002066
van Wyk de Vries, M., Bingham, R. G., & Hein, A. S. (2017). A new volcanic province: An inventory of subglacial volcanoes in West Antarctica. *Geological Society, London, Special Publications*, *461*, 231–248. https://doi.org/10.1144/SP461.7
Yau, A. M., Bender, M. L., Robinson, A., & Brook, E. J. (2016). Reconstructing the last interglacial at Summit, Greenland: Insights from GISP2. *Proceedings of the National Academy of Sciences*, *113*(35), 9710–9715. https://doi.org/10.1073/PNAS.1524766113
Young, D. A., Wright, A. P., Roberts, J. L., Warner, R. C., Young, N. W., Greenbaum, J. S., et al. (2011). A dynamic early East Antarctic Ice Sheet suggested by ice-covered fjord landscapes. *Nature*, *474*(7349), 72–75. https://doi.org/10.1038/nature10114
Zhang, X., Thompson, A. F., Flexas, M. M., Roquet, F., & Bornemann, H. (2016). Circulation and meltwater distribution in the Bellingshausen Sea: From shelf break to coast. *Geophysical Research Letters*, *43*, 6402–6409. https://doi.org/10.1002/2016GL068998
Zhao, C., King, M., Watson, C. S., Barletta, V. R., Bordoni, A., Dell, M., & Whitehouse, P. L. (2017). Rapid ice unloading in the southern Antarctic Peninsula and its effect on bedrock uplift rates. *Earth and Planetary Science Letters*, *473*, 164–176. https://doi.org/10.1016/j.epsl.2017.06.002

Zheng, F., Li, J., Clark, R. T., & Nnamchi, H. C. (2013). Simulation and projection of the Southern Hemisphere annular mode in CMIP5 models. *Journal of Climate*, *26*(24), 9860–9879. https://doi.org/10.1175/JCLI-D-13-00204.1

Zoet, L. K., & Iverson, N. R. (2020). A slip law for glaciers on deformable beds. *Science*, *368*(6486), 76–78. https://doi.org/10.1126/science.aaz1183

Zwally, H. J., Li, J., Robbins, J. W., Saba, J. L., Yi, D., & Brenner, A. C. (2015). Mass gains of the Antarctic ice sheet exceed losses. *Journal of Glaciology*, *61*(230), 1019–1036. https://doi.org/10.3189/2015JoG15J071